

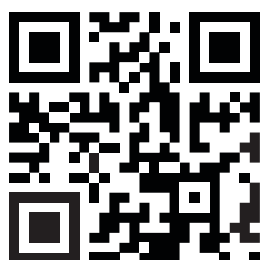


# PFMC-20

20TH INTERNATIONAL CONFERENCE ON  
PLASMA-FACING MATERIALS AND  
COMPONENTS FOR FUSION APPLICATIONS

LJUBLJANA, 19 – 23 May 2025

<https://pfmc20.com>



## BOOK OF ABSTRACTS



Jožef Stefan Institute, Ljubljana, Slovenia

20<sup>th</sup> International Conference on Plasma-Facing Materials and  
Components for Fusion Applications

Ljubljana, Slovenia  
19–23 May 2025

# Programme and Book of Abstracts

Organised by:  
**”Jožef Stefan” Institute**

Edited by:  
**Sabina Markelj, Petra Jenuš,  
and Klemen Bučar**

# Welcome

It is our great pleasure to welcome you to the **20<sup>th</sup> International Conference on Plasma-Facing Materials and Components for Fusion Applications**, which will take place from **19 to 23 May 2025** in the vibrant and historic city of **Ljubljana**, the capital of **Slovenia**. The conference venue is the elegant **Grand Hotel Union Eurostars**, located in the heart of the city.

This event brings together leading researchers and experts from across the globe to address the performance, resilience, and development of materials and components that interact directly with fusion plasma. These materials play a pivotal role in enabling the operation of future fusion devices and power plants.

During the conference, we will delve into essential topics such as thermal and particle load resistance, thermo-mechanical behaviour of materials, and the impact of neutron irradiation on material performance. These discussions will support ongoing efforts to optimise plasma-facing materials, from the atomic scale to full component integration. We hope that this conference will offer a valuable platform for exchanging ideas, presenting breakthroughs, and identifying key challenges in fusion materials research—an area central to the future of clean and sustainable energy.

We look forward to welcoming you to Ljubljana for a stimulating and productive week of scientific exchange, collaboration, and discovery.

## Scientific Programme Committee:

- Jan Coenen, FZJ, Juelich, Germany (Chair)
- Sebastijan Brezinsek, FZJ, Juelich, Germany
- Takeshi Hirai, ITER
- Thomas Schwarz-Selinger, MPG, Garching, Germany
- Robert Kolasinski, Sandia National Laboratory, Livermore, CA, USA
- Marianne Richou, CEA, Cadarache, France
- Guang-Hong Lu, Beihang University, Beihang, China
- Thomas Morgan, DIFFER, Eindhoven, The Netherlands
- Yasuhisa Oya, Shizuoka University, Shizuoka, Japan
- Daniel Primetzhofer, Uppsala University, Uppsala, Sweden
- Anna Widdowson, JET, UKAEA, Culham, UK

## Local Organising Committee:

- Sabina Markelj (chair)
- Petra Jenuš (co-chair)
- Andreja Šestan-Zavašnik
- Mitja Kelemen
- Esther Punzon-Quiorna
- Aljaž Ivekovič
- Klemen Bučar

## Sponsors



City of  
Ljubljana

## Venue

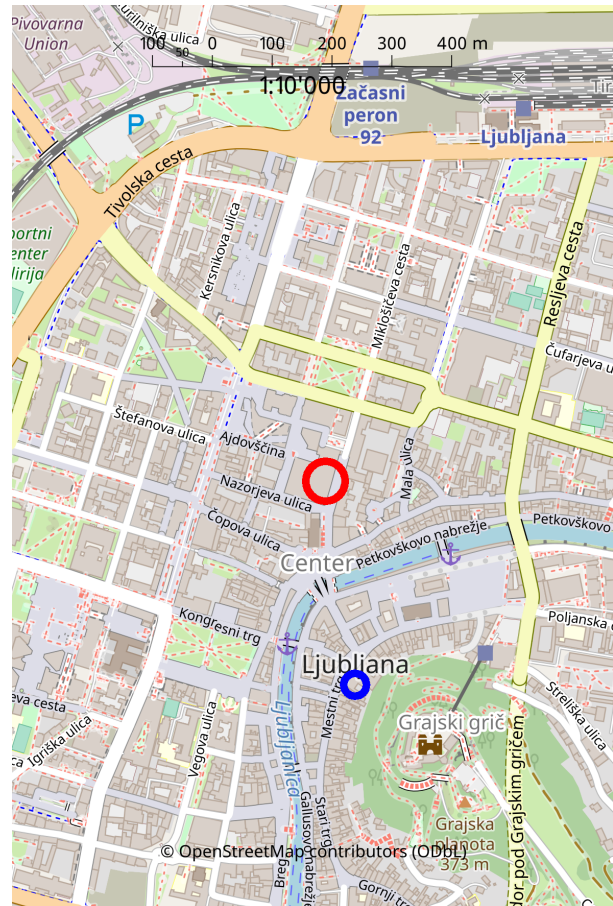
The venue for the conference is the *Union conference hall* within the *Grand Hotel Union Eurostars*, situated at Miklošičeva cesta 1, 1000 Ljubljana, Slovenia. It is marked with a red circle on the map in the right figure.

## Social events

**Welcome reception** will be held on Monday, 19 May 2025 in the lobby of the Ljubljana's Town Hall (Mestni trg 1, Ljubljana). It is marked with a blue circle on the map in the right figure.

**Gala dinner** will be organized on Thursday, 22 May 2025 in the Union Hotel.

**Excursions** described below will be organized on Wednesday, 21 May 2025.



**The town of Bled** has been known for over 1000 years. It is a breathtaking place that lies in the middle of the Julian Alps. The castle of Bled, which will be our first stop, has numerous collections, from the old-fashioned printing press, herbal gallery, chapel, and two tiny wine cellars, and a fascinating museum with stunning views of the area. After the castle tour we will go for a famous Bled cream cake *kremšnita* and have some free time in the center of Bled for coffee.

Embark on a **wine tasting journey** to Slovenia's Littoral Wine-Growing Region, renowned for districts like Gorizia Hills (Goriška brda), famous for Rebula and Merlot-Cabernet blends, and the Koper district, the warmest in Slovenia, known for Refosco and Malvazija grapes. This experience includes a visit to the Vina Koper winery, where you'll explore their magnificent cellar, learn about the creation of their world-class wines, and enjoy a tasting in a cosy atmosphere. Afterwards, you'll have free time to discover the historic charm and vibrant seaside atmosphere of Koper, a picturesque Slovenian port town with medieval Venetian palaces and a lively promenade.

Explore the **architectural splendors of Ljubljana**, a Central European jewel, on a guided walking tour starting from the Roman town of Emona and winding towards the old city. You'll discover Jože Plečnik's masterpiece, the National University Library, rich with hidden symbolism, and admire the scenic Ljubljanica river embankment with its many bridges, before visiting the City Square and St. Nicholas Cathedral. Then, choose your adventure: either ascend to Ljubljana Castle for breathtaking views, a coffee break, and a continued walk through the market, Prešeren Square, and Congress Square (Option 1), or embark on a delightful boat trip along the Ljubljanica River (Option 2).

# **DETAILED PROGRAMME**

# Oral Presentations – Invited and Regular Oral Lectures

Tuesday, 20 May 2025, 9:00–10:50

Location: lecture room

## Session 1: Fuel retention and removal

9:00 I-1	<b>Progress in the understanding of fuel retention and inventory management in the full-tungsten ITER</b>	36
	<p>Tom Wauters<sup>1</sup>, Remi Delaporthe–Mathurin<sup>2</sup>, Kaelyn Dunnell<sup>2</sup>, Etienne Hodille<sup>3</sup>, Stepan Krat<sup>4</sup>, Hao-Dong Liu<sup>5</sup>, Alberto Loarte<sup>1</sup>, Dmitry Matveev<sup>6</sup>, Jonathan Mougenot<sup>7</sup>, Richard Pitts<sup>1</sup>, Klaus Schmid<sup>8</sup></p> <p><sup>1</sup>ITER Organization, France; <sup>2</sup>Plasma Science and Fusion Center, MIT, United States; <sup>3</sup>CEA, IRFM, France; <sup>4</sup>National Research Nuclear University MEPhI, Russian Federation; <sup>5</sup>Institute of Plasma Physics, Chinese Academy of Sciences, China; <sup>6</sup>Forschungszentrum Jülich GmbH, Germany; <sup>7</sup>Université Sorbonne Paris Nord, CNRS, France; <sup>8</sup>Max-Planck-Institut für Plasmaphysik, Germany.</p>	
9:30 I-2	<b>First Demonstration of Laser Induced Breakdown Spectroscopy using Remote Handling for In-vessel Analysis of Tritiated and Activated JET Components</b>	37
	<p>Jari Likonen<sup>1</sup>, Salvatore Almagia<sup>2</sup>, Rahul Rayaprolu<sup>3</sup>, Rongxing Yi<sup>3</sup>, Ionut Jecu<sup>4</sup>, Gennady Sergienko<sup>3</sup>, Anna Widdowson<sup>4</sup>, Nick Jones<sup>4</sup>, Sahithya Atikukke<sup>5</sup>, Timo Dittmar<sup>3</sup>, Juuso Karhunen<sup>1</sup>, Pawel Gasior<sup>6</sup>, Christoph Kawan<sup>3</sup>, Marc Sackers<sup>3</sup>, Shweta Soni<sup>5</sup>, Erik Wüst<sup>3</sup>, Sebastijan Brezinsek<sup>3</sup>, Jelena Butikova<sup>7</sup>, Wojciech Gromelski<sup>6</sup>, Antti Hakola<sup>1</sup>, Indrek Jõgi<sup>8</sup>, Peeter Paris<sup>8</sup>, Jasper Ristkok<sup>8</sup>, Pavel Veis<sup>5</sup>, The UKAEA RACE Team<sup>9</sup></p> <p><sup>1</sup>VTT Technical Research Centre of Finland Ltd., Finland; <sup>2</sup>ENEA, Italy; <sup>3</sup>Forschungszentrum Jülich GmbH, Germany; <sup>4</sup>United Kingdom Atomic Energy Authority, Culham Campus, Abingdon, United Kingdom; <sup>5</sup>Comenius University, Slovakia; <sup>6</sup>Institute of Plasma Physics and Laser Microfusion, Poland; <sup>7</sup>University of Latvia, Institute of Solid State Physics, Latvia; <sup>8</sup>University of Tartu, Institute of Physics, Estonia; <sup>9</sup>UKAEA RACE Team, United Kingdom.</p>	
10:00 O-1	<b>Chemical analysis by Laser Induced Breakdown Spectroscopy of the poloidal cross-section of the JET divertor after its last D-T experimental campaign</b>	38
	<p>Salvatore Almagia<sup>1</sup>, Jari Likonen<sup>2</sup>, Antti Hakola<sup>2</sup>, Juuso Karhunen<sup>2</sup>, Sebastijan Brezinsek<sup>3</sup>, Gennady Sergienko<sup>3</sup>, Rahul Rayaprolu<sup>3</sup>, Rongxing Yi<sup>3</sup>, Timo Dittmar<sup>3</sup>, Christoph Kawan<sup>3</sup>, Marc Sackers<sup>3</sup>, Erik Wüst<sup>3</sup>, The UKAEA RACE Team<sup>4</sup>, Anna Widdowson<sup>4</sup>, Ionut Jecu<sup>4</sup>, Pavel Veis<sup>5</sup>, Sahithya Atikukke<sup>5</sup>, Shweta Soni<sup>5</sup>, Pawel Gasior<sup>6</sup>, Wojciech Gromelski<sup>6</sup>, Jelena Butikova<sup>7</sup>, Indrek Jõgi<sup>8</sup>, Peeter Paris<sup>8</sup>, Jasper Ristkok<sup>8</sup></p> <p><sup>1</sup>ENEA, Diagnostics and Metrology Laboratory, Italy; <sup>2</sup>VTT Technical Research Centre of Finland Ltd., Finland; <sup>3</sup>Forschungszentrum Jülich GmbH, Germany; <sup>4</sup>UKAEA, Culham Campus, Abingdon, United Kingdom; <sup>5</sup>Comenius University, Faculty of Math, Physics and Informatics, Slovakia; <sup>6</sup>Institute of Plasma Physics and Laser Microfusion, Poland; <sup>7</sup>Institute of Solid State Physics, University of Latvia, Latvia; <sup>8</sup>University of Tartu, Institute of Physics, Estonia.</p>	
10:25 O-2	<b>Depth-resolved deuterium retention profiles in displacement-damaged tungsten measured via laser-induced ablation quadrupole mass spectrometry</b>	39
	<p>Christoph Kawan<sup>1</sup>, Sebastijan Brezinsek<sup>1</sup>, Timo Dittmar<sup>1</sup>, Erik Wüst<sup>1</sup>, Thomas Schwarz–Selinger<sup>2</sup>, Liang Gao<sup>1</sup>, Christian Linsmeier<sup>1</sup></p> <p><sup>1</sup>Forschungszentrum Jülich GmbH, Germany; <sup>2</sup>Max-Planck-Institut für Plasmaphysik, Germany.</p>	

**Tuesday, 20 May 2025, 11:15–13:00**

*Location: lecture room*

## **Session 2: Erosion, re-deposition, mixing, and dust formation and Low-Z and liquid materials**

11:15 I–3	<b>Erosion of thin boron films at the linear plasma device PSI-2 during deuterium discharges: atomic and molecular spectroscopy of boron</b>	40
	<u>Marc Sackers</u> , Oleksandr Marchuk, Anne Houben, Eduard Warkentin, Marcin Rasinski, Sebastijan Brezinsek, Arkadi Kreter Forschungszentrum Jülich GmbH, Germany.	
11:45 O–3	<b>Improved material mixing model in ERO2.0: nonlinear effect of boron concentration on tungsten sputtering and influx from mixed tungsten-boron surfaces</b>	41
	Henri Kumpulainen <sup>1</sup> , Sebastijan Brezinsek <sup>1</sup> , Juri Romazanov <sup>1</sup> , Andreas Kirschner <sup>1</sup> , Christoph Baumann <sup>1</sup> , Klaus Schmid <sup>2</sup> <sup>1</sup> Forschungszentrum Jülich GmbH, Germany; <sup>2</sup> Max-Planck-Institut für Plasmaphysik, Germany.	
12:10 O–4	<b>Deuterium retention in sputter-deposited W-B layers: Implantation and in-situ ion beam analysis during annealing</b>	42
	<u>Daniel Gautam</u> <sup>1</sup> , Tuan Tran <sup>1</sup> , Martina Fellingner <sup>2</sup> , Friedrich Aumayr <sup>2</sup> , Marek Rubel <sup>3</sup> , Daniel Primetzhofer <sup>1</sup> , Eduardo Pitthan <sup>1</sup> <sup>1</sup> Uppsala University, Sweden; <sup>2</sup> TU Wien, Fusion@ÖAW, Vienna, Austria, Austria; <sup>3</sup> Uppsala University/KTH Royal Institute of Technology, Sweden.	
12:35 O–5	<b>Lifetimes of Boron layers on amorphous and crystalline tungsten under deuterium and impurity irradiation</b>	43
	<u>Udo von Toussaint</u> , Roland Preuss, Martin Balden, Karl Krieger, Klaus Schmid, Andreas Mutzke Max-Planck-Institut für Plasmaphysik, Germany.	

**Tuesday, 20 May 2025, 14:30–16:20**

*Location: lecture room*

## **Session 3: Neutron effects in plasma-facing materials**

14:30 I–4	<b>Neutron irradiation effects on PFC materials: an overview of EUROfusion programme</b>	44
	Dmitry Terentyev <sup>1</sup> , Michael Rieth <sup>2</sup> , Ermile Gaganidze <sup>2</sup> , Gerald Pintsuk <sup>3</sup> , Giacomo Aiello <sup>4</sup> , Michael Klimenkov <sup>2</sup> , Aleksandr Zinovev <sup>5</sup> , Shuhei Nogami <sup>6</sup> , Steffen Antusch <sup>2</sup> , Jan Coenen <sup>3</sup> , Petra Jenuš <sup>7</sup> , Koray Iroc <sup>5</sup> , Chao Yin <sup>8</sup> , Carmen Garcia Rosales <sup>9</sup> <sup>1</sup> Belgian Nuclear Research Center, Belgium; <sup>2</sup> KIT, Germany; <sup>3</sup> FZJ, Germany; <sup>4</sup> EUROfusion, Germany; <sup>5</sup> SCK CEN, Belgium; <sup>6</sup> ALMT, Japan; <sup>7</sup> JSI, Slovenia; <sup>8</sup> USTC, China; <sup>9</sup> CIET, Spain.	
15:00 I–5	<b>Modelling high dose irradiation damage in tungsten</b>	44
	<u>Max Boleininger</u> <sup>1</sup> , Daniel Mason <sup>1</sup> , Alexander Feichtmayer <sup>2</sup> , Luca Realì <sup>1</sup> , Sergei Dudarev <sup>1</sup> <sup>1</sup> UK Atomic Energy Authority, United Kingdom; <sup>2</sup> Technical University Munich, Germany.	

15:30 O-6	<b>Detection of defects and location of deuterium in displacement-damaged tungsten</b>	45
	Sabina Markelj <sup>1</sup> , Esther Punzón-Quijorna <sup>1</sup> , Mitja Kelemen <sup>1</sup> , Thomas Schwarz-Selinger <sup>2</sup> , Xin Jin <sup>3</sup> , Eryang Lu <sup>3</sup> , Flyura Djurabekova <sup>3</sup> , Kai Nordlund <sup>3</sup> , Janez Zavašnik <sup>1</sup> , Andreja Šestan Zavašnik <sup>1</sup> , Miguel L. Crespillo <sup>4</sup> , Gaston García López <sup>4</sup> , Rene Heller <sup>5</sup>	
	<sup>1</sup> Jožef Stefan Institute, Slovenia; <sup>2</sup> Max-Planck-Institut für Plasmaphysik, Germany; <sup>3</sup> University of Helsinki, Finland; <sup>4</sup> Center for Micro Analysis of Materials, Spain; <sup>5</sup> Helmholtz-Zentrum Dresden-Rossendorf, Germany.	
15:55 O-7	<b>Influence of the Presence of Deuterium on Damage Evolution in Tungsten</b>	46
	Zeqing Shen, Thomas Schwarz-Selinger, Mikhail Zibrov, Armin Manhard	
	Max Planck Institute for Plasma Physics, Germany.	

**Wednesday, 21 May 2025, 8:30-10:20**

*Location: lecture room*

## **Session 4: Boronisation and wall conditioning techniques**

8:30 I-6	<b>Effect of spatially non-uniform boronization on plasma restart in the full W environment of WEST</b>	47
	Alberto Gallo <sup>1</sup> , Mathilde Diez <sup>1</sup> , Etienne Hodille <sup>1</sup> , Eleonore Geulin <sup>1</sup> , Jonathan Gaspar <sup>2</sup> , Pierre Manas <sup>1</sup> , Paulo Puglia <sup>1</sup> , Nicolas Rivals <sup>1</sup> , Diana Sgrelli <sup>1</sup> , Regis Bisson <sup>3</sup> , Julien Denis <sup>1</sup> , Gabriele Gervasini <sup>4</sup> , Alex Thomas Grosjean <sup>5</sup> , Laura Laguardia <sup>4</sup> , Thierry Loarer <sup>1</sup> , Stefane Vartarian <sup>1</sup> , Tom Wauters <sup>6</sup> , Thierry Alarcon <sup>1</sup> , Viven Anzallo <sup>1</sup> , Eric Caprin <sup>1</sup> , Matthieu De Combarieu <sup>1</sup> , Philippe Moreau <sup>1</sup> , Francis-Pierre Pellissier <sup>1</sup> , Yann Corre <sup>1</sup> , Karl Krieger <sup>7</sup> , Anna Widdowson <sup>8</sup> , Emmanuelle Tsitrone <sup>1</sup> , Antti Hakola <sup>9</sup>	
	<sup>1</sup> CEA, IRFM, France; <sup>2</sup> CNRS, IUSTI, France; <sup>3</sup> CNRS, PIIM, France; <sup>4</sup> Istituto per la Scienza e Tecnologia dei Plasmi, CNR, Milano, Italy; <sup>5</sup> University of Tennessee Knoxville, United States; <sup>6</sup> ITER Organization, France; <sup>7</sup> Max-Planck-Institut für Plasmaphysik, Garching, Germany; <sup>8</sup> UKAEA, Culham Campus, Abingdon, United Kingdom; <sup>9</sup> VTT Technical Research Centre of Finland Ltd, Espoo, Finland.	
9:00 I-7	<b>Investigations on Boronization at tungsten ASDEX Upgrade</b>	48
	Volker Rohde, Karl Krieger, Andreas Redl, Tim-Oliver Hohmann, Joerg Hobrik, Seehon An	
	Max Planck Institute for Plasmaphysics, Germany.	
9:30 O-8	<b>Analysis of Boron-Hydrogen Interactions and Deuterium Retention for Fusion Applications</b>	48
	Aleksandr Afonin, Marco Minissale, Eric Salomon, Thierry Angot, Regis Bisson	
	Aix-Marseille University, CNRS, PIIM, France.	
9:55 O-9	<b>Sticking Coefficients of Boron Radicals</b>	49
	Matej Mayer, Torsten Bräuer, Dario Cipciar, Chandra Prakash Dhard, Carsten Killer, Dirk Naujoks, Ralf Steinwehr, Udo von Toussaint, Lilla Vano, Holger Viebke	
	Max-Planck-Institut für Plasmaphysik, Germany.	



Wednesday, 21 May 2025, 10:50–12:40

Location: lecture room

## Session 5: Technology and qualification of plasma-facing components and Erosion, re-deposition, mixing, and dust formation

10:50 I–8	<b>First insights into runaway electron (RE) damage induced to the JET divertor</b> 51 <u>Ionuț Jepu</u> <sup>1</sup> , Anna Widdowson <sup>1</sup> , Yevhen Zayachuk <sup>1</sup> , Cédric Reux <sup>2</sup> , Salvatore Almagia <sup>3</sup> , Rahul Rayaprolu <sup>4</sup> , Rongxing Yi <sup>4</sup> , Mirosław Zlobinski <sup>4</sup> , Jari Likonon <sup>5</sup> , Sebastijan Brezinsek <sup>4</sup> <sup>1</sup> UKAEA, Culham Campus, Abingdon, United Kingdom; <sup>2</sup> CEA, IRFM, France; <sup>3</sup> ENEA, Diagnostics and Metrology Laboratory, Italy; <sup>4</sup> Forschungszentrum Jülich GmbH, Germany; <sup>5</sup> VTT Technical Research Centre of Finland Ltd., Finland.
11:20 I–9	<b>Overview of the results achieved from the characterization program of the WEST plasma facing components (2018–2024)</b> 52 <u>Mathilde Diez</u> <sup>1</sup> , Martin Balden <sup>2</sup> , Elodie Bernard <sup>1</sup> , Iva Bogdanović Radović <sup>3</sup> , Yann Corre <sup>1</sup> , Alan Durif <sup>1</sup> , Elzbieta Fortuna-Zalesna <sup>4</sup> , Jonathan Gaspar <sup>5</sup> , Antti Hakola <sup>6</sup> , Indrek Jõgi <sup>7</sup> , Celine Martin <sup>8</sup> , Emmanuelle Tsitrone <sup>1</sup> , Marianne Richou <sup>1</sup> <sup>1</sup> CEA, IRFM, France; <sup>2</sup> IPP MPG, Germany; <sup>3</sup> Ruder Bošković Institute, Croatia; <sup>4</sup> Warsaw University of Technology, Poland; <sup>5</sup> CNRS, IUSTI, France; <sup>6</sup> VTT Technical Research Centre of Finland Ltd, Finland; <sup>7</sup> University of Tartu, Institute of Physics, Estonia; <sup>8</sup> Aix-Marseille Univ, CNRS, PIIM, France.
11:50 O–10	<b>Erosion and redeposition patterns on divertor tiles after exposure in the first operation phase of WEST</b> 53 <u>Martin Balden</u> <sup>1</sup> , Mathilde Diez <sup>2</sup> , Elodie Bernard <sup>2</sup> , Antti Hakola <sup>3</sup> , Matej Mayer <sup>1</sup> <sup>1</sup> Max-Planck-Institut für Plasmaphysik, Germany; <sup>2</sup> CEA, IRFM, France; <sup>3</sup> VTT Technical Research Centre of Finland Ltd., Finland.
12:15 O–11	<b>High heat flux testing of actively cooled graphite- and tungsten-armoured JT-60SA flat-tile divertor mock-ups</b> 54 <u>Daniel Dicks</u> <sup>1</sup> , Bernd Boeswirth <sup>1</sup> , Katja Hunger <sup>1</sup> , Henri Greuner <sup>1</sup> , Marianne Richou <sup>2</sup> , Johann Riesch <sup>1</sup> , Mehdi Firdaouss <sup>2</sup> , Valerio Tomarchio <sup>3</sup> , Rudolf Neu <sup>1</sup> <sup>1</sup> Max Planck Institute for Plasma Physics, Garching, Germany; <sup>2</sup> CEA-IRFM, F-13108 Saint Paul Lez Durance, France; <sup>3</sup> F4E Germany, Germany.

Thursday, 22 May 2025, 8:30–10:20

Location: lecture room

## Session 6: Erosion, re-deposition, mixing, and dust formation

8:30 I–10	<b>Measurements and modelling of charge-exchange neutral flux to the first wall on EAST</b> 55 <u>Rui Ding</u> Institute of Plasma Physics, HFIPS, Chinese Academy of Sciences, China.
9:00 I–11	<b>Ion-solid interaction for light ions in plasma-facing materials: Experimental corrections and their effects on simulation-based sputter yields</b> 56 <u>Eduardo Pittthan</u> <sup>1</sup> , Philipp M. Wolf <sup>1</sup> , Jila Shams-Latifi <sup>1</sup> , Martina Fellingner <sup>2</sup> , Friedrich Aumayr <sup>2</sup> , Daniel Primetzhofer <sup>1</sup> <sup>1</sup> Uppsala University, Sweden; <sup>2</sup> TU Wien, Fusion@ÖAW, Vienna, Austria, Austria.

9:30 O-12	<b>Modelling fuel retention in the W divertor during the D/H/D changeover experiment in WEST</b>	57
	<p><u>Etienne Hodille</u><sup>1</sup>, Davide Piccinelli<sup>1</sup>, Manon Bertoglio<sup>1</sup>, Thierry Loarer<sup>1</sup>, Julien Denis<sup>1</sup>, Guido Ciraolo<sup>1</sup>, Patrick Tamain<sup>1</sup>, Eleonore Geulin<sup>1</sup>, Alberto Gallo<sup>1</sup>, Stefane Vartarian<sup>1</sup>, Regis Bisson<sup>2</sup>, Bernard Pégourié<sup>1</sup>, Yann Anquetin<sup>3</sup>, Yann Corre<sup>1</sup>, Kaelyn Dunnell<sup>4</sup>, Tom Wauters<sup>5</sup></p> <p><sup>1</sup>CEA, IRFM, France; <sup>2</sup>CNRS, PIIM, France; <sup>3</sup>Aix-Marseille Univ, CNRS, IUSTI, France; <sup>4</sup>Plasma Science and Fusion Center, MIT, United States; <sup>5</sup>ITER Organization, France.</p>	
9:55 O-13	<b>ERO2.0 study of erosion and deposition on ITER diagnostic mirrors assuming different material mixes</b>	58
	<p><u>Sebastian Rode</u><sup>1</sup>, Sebastijan Brezinsek<sup>1</sup>, Andreas Kirschner<sup>1</sup>, Lucas Moser<sup>2</sup>, Richard Pitts<sup>2</sup>, Juri Romazanov<sup>1</sup>, Alexis Terra<sup>1</sup>, Tom Wauters<sup>2</sup>, Sven Wiesen<sup>3</sup></p> <p><sup>1</sup>Forschungszentrum Jülich GmbH, Germany; <sup>2</sup>ITER Organization, France; <sup>3</sup>DIFFER – Dutch Institute for Fundamental Energy Research, Netherlands.</p>	

*Thursday, 22 May 2025, 10:50–12:40*

*Location: lecture room*

## **Session 7: Tungsten, tungsten alloys, and advanced steels**

10:50 I-12	<b>Tungsten Alloys with Enhanced Stability and Manufacturability Through Integrated Alloy Design and Microstructural Engineering</b>	59
	<p><u>Jason Trelewicz</u><sup>1</sup>, Ian McCue<sup>2</sup>, Nicholas Olynik<sup>1</sup>, Sean Mascarenhas<sup>1</sup>, David Sprouster<sup>1</sup>, Hyeji Kim<sup>2</sup>, Samuel Price<sup>2</sup>, Tim Graening<sup>3</sup>, Travis Gray<sup>3</sup>, Christopher Ledford<sup>3</sup>, Julio Rojas<sup>3</sup>, Michael Kirka<sup>3</sup></p> <p><sup>1</sup>Stony Brook University, United States; <sup>2</sup>Northwestern University, United States; <sup>3</sup>Oak Ridge National Laboratory, United States.</p>	
11:20 I-13	<b>Advanced Tungsten Based Materials for Plasma Facing Components</b>	60
	<p><u>Shuhei Nogami</u></p> <p>ALMT, Japan.</p>	
11:50 O-14	<b>Recent development on upscaling functionally graded W/EUROFER coating for the DEMO First Wall application</b>	61
	<p><u>Ashwini Kumar Mishra</u><sup>1</sup>, Thilo Grammes<sup>1</sup>, Arkadi Kreter<sup>2</sup>, Marcin Rasinski<sup>2</sup>, Jan Coenen<sup>3</sup>, Jarir Aktaa<sup>1</sup></p> <p><sup>1</sup>Karlsruhe Institute of Technology (KIT), Germany; <sup>2</sup>Forschungszentrum Jülich GmbH, Germany; <sup>3</sup>FZJ, Germany.</p>	
12:15 O-15	<b>Development and Testing of a Novel FAST-Diffusion Bonding Process for Joining Eurofer97 Steel to Tungsten in Plasma Facing Components</b>	61
	<p><u>Daniel Wilkison</u>, Patrick Grant, Enzo Liotti</p> <p>Department of Materials University of Oxford, United Kingdom.</p>	

Thursday, 22 May 2025, 14:20–16:40

Location: lecture room

## Session 8: Fuel retention and removal

- 14:20  
I–14
- In situ Measurement of H, D, T Retention in the JET Tungsten Divertor Components – Lessons Learned for the ITER LID-QMS Diagnostic** 63
- Miroslaw Zlobinski<sup>1</sup>, Gennady Sergienko<sup>1</sup>, Ionuț Jecu<sup>2</sup>, Chris Rowley<sup>2</sup>, Anna Widdowson<sup>2</sup>, Rob Ellis<sup>2</sup>, Domagoj Kos<sup>2</sup>, Ivor Coffey<sup>3</sup>, Martin Fortune<sup>2</sup>, David Kinna<sup>2</sup>, Misha Beldishevski<sup>2</sup>, Laura Laguardia<sup>4</sup>, Gabriele Gervasini<sup>4</sup>, Andreas Krimmer<sup>1</sup>, Horst Toni Lambertz<sup>1</sup>, Alexis Terra<sup>1</sup>, Alexander Huber<sup>1</sup>, Sebastian Brezinsek<sup>1</sup>, Timo Dittmar<sup>1</sup>, Meike Flebbe<sup>1</sup>, Rongxing Yi<sup>1</sup>, Rahul Rayaprolu<sup>1</sup>, Sebastian Frieze<sup>1</sup>, Philippe Mertens<sup>1</sup>, Ilia Ivashov<sup>1</sup>, Yuri Krasikov<sup>1</sup>, Krzysztof Młynczak<sup>1</sup>, Jochen Assmann<sup>1</sup>, David Castaño Bardawil<sup>1</sup>, Michael Schrader<sup>1</sup>, Philip Andrew<sup>5</sup>, Xi Jiang<sup>5</sup>, João Figueiredo<sup>6</sup>, Peter Blatchford<sup>2</sup>, Scott Silburn<sup>2</sup>, Emmanuelle Tsitrone<sup>7</sup>, Emmanuel Joffrin<sup>7</sup>, Karl Krieger<sup>8</sup>, Yann Corre<sup>7</sup>, Antti Hakola<sup>9</sup>, Jari Likonen<sup>9</sup>, The EUROFUSION TOKAMAK EXPLOITATION Team<sup>10</sup>, The JET CONTRIBUTORS Team<sup>11</sup>
- <sup>1</sup>Forschungszentrum Jülich GmbH, Jülich, Germany; <sup>2</sup>UKAEA, Culham Campus, Abingdon, United Kingdom; <sup>3</sup>Queen's University Belfast, Belfast, Northern Ireland, United Kingdom; <sup>4</sup>Istituto per la Scienza e Tecnologia dei Plasmi, CNR, Milano, Italy; <sup>5</sup>ITER Organization, St-Paul-lez-Durance, France; <sup>6</sup>EUROfusion Programme Management Unit, Garching, Germany; <sup>7</sup>CEA, Institute for Research on Fusion by Magnetic confinement, St-Paul-lez-Durance, France; <sup>8</sup>Max-Planck-Institut für Plasmaphysik, Garching, Germany; <sup>9</sup>VTT Technical Research Centre of Finland Ltd, Espoo, Finland; <sup>10</sup>See the author list of E. Joffrin et al., Nuclear Fusion 64 (2024) 11, doi:10.1088/1741-4326/ad2be4, Germany; <sup>11</sup>See the author list of C.F. Maggi et al., Nuclear Fusion 64 (2024) 11, doi:10.1088/1741-4326/ad3e16, United Kingdom.
- 14:45  
I–15
- Femtosecond laser-induced ablation – quadrupole mass spectroscopy for depth- and lateral profiling of helium and hydrogen-isotopes in fusion materials** 64
- Steffen Mittelmann, Benedikt Buchner, Udo von Toussaint, Matej Mayer, Andreas Theodorou, Thomas Dürbeck, Wolfgang Jacob, Thomas Schwarz-Selinger
- Max Planck Institute for Plasma Physics, Germany.
- 15:15  
I–16
- Tritium containing plasma-facing materials from fusion reactors: research needs, capabilities and limitations in tritium studies** 65
- Miyuki Yajima<sup>1</sup>, Yuji Hatano<sup>2</sup>, Yasuhisa Oya<sup>3</sup>, Teppei Otsuka<sup>4</sup>, Yuji Torikai<sup>5</sup>, Suguru Masuzaki<sup>1</sup>, Masayuki Tokitani<sup>1</sup>, Mitsutaka Miyamoto<sup>6</sup>, Yui Obata<sup>5</sup>, Nobuyuki Asakura<sup>7</sup>, Hirofumi Nakamura<sup>7</sup>, Takumi Hayashi<sup>7</sup>, Kanetsugu Isobe<sup>7</sup>, Dai Hamaguchi<sup>7</sup>, Hiroyasu Tanigawa<sup>7</sup>, Kim Jaehwan<sup>7</sup>, Yutaka Sugimoto<sup>7</sup>, Takashi Nozawa<sup>7</sup>, Anna Widdowson<sup>8</sup>, Marek Rubel<sup>9</sup>, Jari Likonen<sup>10</sup>
- <sup>1</sup>National Institute for Fusion Science, Japan; <sup>2</sup>Tohoku University, Japan; <sup>3</sup>Shizuoka University, Japan; <sup>4</sup>Kindai University, Japan; <sup>5</sup>Ibaraki University, Japan; <sup>6</sup>Shimane University, Japan; <sup>7</sup>National Institute for Quantum Science and Technology, Japan; <sup>8</sup>UKAEA, Culham Campus, Abingdon, United Kingdom; <sup>9</sup>Uppsala University/KTH Royal Institute of Technology, Sweden; <sup>10</sup>VTT Technical Research Centre of Finland Ltd, Espoo, Finland.
- 15:45  
O–16
- Depth profiling of tritium in bulk tungsten divertor tiles from JET with metal walls: tritium quantification and surface decontamination** 66
- Yuji Torikai<sup>1</sup>, Yui Obata<sup>1</sup>, Kazuaki Kasai<sup>1</sup>, Rion Nishida<sup>1</sup>, Senzai Oono<sup>1</sup>, Kazuma Mizobuchi<sup>1</sup>, Naoko Ashikawa<sup>2</sup>, Atushi Owada<sup>3</sup>, Suguru Masuzaki<sup>4</sup>, Miyuki Yajima<sup>4</sup>, Kanetsugu Isobe<sup>3</sup>, Takumi Hayashi<sup>3</sup>, Hirofumi Nakamura<sup>3</sup>, Yutaka Sugimoto<sup>3</sup>, Marek Rubel<sup>5</sup>, Anna Widdowson<sup>6</sup>
- <sup>1</sup>Ibaraki University, Japan; <sup>2</sup>Kyoto Fusioneering, Japan; <sup>3</sup>National Institute for Quantum Science and Technology, Japan; <sup>4</sup>National Institute for Fusion Science, Japan; <sup>5</sup>Uppsala University/KTH Royal Institute of Technology, Sweden; <sup>6</sup>UKAEA, Culham Campus, Abingdon, United Kingdom.

16:10 O-17	<b>Low Hydrogen Isotope Retention and High Irradiation Resistance in Columnar-Grained Tungsten Prepared via Chemical Vapor Deposition</b>	67
	<p><u>Yue Yuan</u><sup>1</sup>, Hanqing Wang<sup>1</sup>, Ting Wang<sup>1</sup>, Yiwen Sun<sup>1</sup>, Hao Yin<sup>1</sup>, Mi Liu<sup>1</sup>, Hao Wang<sup>1</sup>, Ying Qin<sup>1</sup>, Long Cheng<sup>1</sup>, Fan Feng<sup>2</sup>, Zhe Chen<sup>2</sup>, Youyun Lian<sup>2</sup>, Binyou Yan<sup>3</sup>, Arkadi Kreter<sup>4</sup>, Guang-Hong Lu<sup>1</sup></p> <p><sup>1</sup>Beihang University, China; <sup>2</sup>Southwestern Institute of Physics, China; <sup>3</sup>Xiamen Tungsten Co., Ltd., China; <sup>4</sup>Forschungszentrum Jülich GmbH, Germany.</p>	

**Friday, 23 May 2025, 9:00-11:15**

*Location: lecture room*

## **Session 9: Tungsten, tungsten alloys, and advanced steels and Technology and qualification of plasma-facing components**

9:00 O-18	<b>Response of fibre-reinforced tungsten composites exposed to ELM-like transient events</b>	68
	<p><u>Tyler Ray</u><sup>1</sup>, Jack Johnson<sup>1</sup>, Matthew Halloran<sup>1</sup>, Jitendra Tripathi<sup>1</sup>, Marius Wirtz<sup>2</sup>, Jan Coenen<sup>3</sup>, Ahmed Hassanain<sup>1</sup></p> <p><sup>1</sup>Purdue University, United States; <sup>2</sup>Forschungszentrum Jülich GmbH, Germany; <sup>3</sup>FZJ, Germany.</p>	
9:25 I-17	<b>Plasma facing and high heat flux material development and down-selection process within the European fusion materials program</b>	69
	<p><u>Gerald Pintsuk</u><sup>1</sup>, Giacomo Aiello<sup>2</sup>, Marius Wirtz<sup>3</sup></p> <p><sup>1</sup>FZJ, Germany; <sup>2</sup>EUROfusion, Germany; <sup>3</sup>Forschungszentrum Juelich GmbH, Germany.</p>	
9:55 I-18	<b>Design development of inertially cooled tungsten first wall for ITER Start of Research Operation</b>	69
	<p><u>Lei Chen</u></p> <p>ITER Organization, France.</p>	
10:25 O-19	<b>CFEDR and its PFMC progress</b>	70
	<p><u>Jiangang Li</u>, Rui Ding, Tiejun Xu, Xuebin Peng</p> <p>Institute of Plasma Physics, Chinese Academy of Sciences, China.</p>	
10:50 O-20	<b>Overview of Advanced Plasma-Facing Materials Testing for Fusion Pilot Plants at DIII-D</b>	71
	<p><u>Jonathan Coburn</u><sup>1</sup>, Florian Effenberg<sup>2</sup>, Mary Alice Cusentino<sup>1</sup>, Chase Hargrove<sup>3</sup>, Mykola Ialovega<sup>4</sup>, Maria Cunha<sup>5</sup>, Lauren Nuckols<sup>6</sup>, Žana Popović<sup>7</sup>, Shawn Zamperini<sup>7</sup>, Tyler Abrams<sup>7</sup>, Dmitry Rudakov<sup>8</sup></p> <p><sup>1</sup>Sandia National Laboratories, United States; <sup>2</sup>Princeton Plasma Physics Laboratory, United States; <sup>3</sup>Pennsylvania State University, United States; <sup>4</sup>University of Wisconsin-Madison, United States; <sup>5</sup>Dutch Institute for Fundamental Energy Research, Netherlands; <sup>6</sup>Oak Ridge National Laboratory, United States; <sup>7</sup>General Atomics, United States; <sup>8</sup>University of California San Diego, United States.</p>	

Friday, 23 May 2025, 11:40–13:35

Location: lecture room

## Session 10: Tungsten, tungsten alloys, and advanced steels and Neutron effects in plasma-facing materials

- |               |  |    |
|---------------|--|----|
| 11:40<br>O-21 | <p><b>Performance study of fully dense tungsten fiber-reinforced tungsten composites for plasma facing material</b></p> <p><u>Juan Du</u><sup>1</sup>, Tianyu Zhao<sup>1</sup>, Pan Wen<sup>1</sup>, Fan Feng<sup>1</sup>, Jun Tang<sup>2</sup>, Chen Jiming<sup>1</sup>, Xiang Liu<sup>1</sup>, Qiang Tao<sup>3</sup>, Zhaodong Liu<sup>3</sup>, Fanya Jin<sup>1</sup>, Yiran Mao<sup>4</sup>, Jan Coenen<sup>5</sup>, Christian Linsmeier<sup>4</sup></p> <p><sup>1</sup>Southwestern Institute of Physics, Chengdu, China; <sup>2</sup>Institute of Nuclear Science and Technology, Sichuan University, Chengdu, China; <sup>3</sup>Synergetic Extreme Condition User Facility, Jilin University, Changchun, China; <sup>4</sup>Forschungszentrum Jülich GmbH, Germany; <sup>5</sup>FZJ, Germany.</p> | 72 |
| 12:05<br>I-19 | <p><b>Studying the influence of redeposited tungsten and EUROFER97 layers on deuterium retention in plasma-facing materials</b></p> <p>Martina Fellingner<sup>1</sup>, Eduardo Pitthan<sup>2</sup>, Daniel Gautam<sup>2</sup>, Daniel Primetzhofer<sup>2</sup>, Friedrich Aumayr<sup>1</sup></p> <p><sup>1</sup>TU Wien, Fusion@ÖAW, Austria; <sup>2</sup>Uppsala University, Sweden.</p>  | 73 |
| 12:35<br>I-20 | <p><b>Molecular Dynamics Modeling and Experimental Assessment of Helium Bubble Growth, Surface Morphology Evolution, and Displacement Damage Effects in Multi-Component Alloys</b></p> <p>Mary Alice Cusentino<sup>1</sup>, Megan McCarthy<sup>1</sup>, Katie Karl<sup>2</sup>, Shane Evans<sup>3</sup>, Eric Lang<sup>3</sup>, Guddi Suman<sup>1</sup>, Rico Treadwell<sup>1</sup>, Matt Baldwin<sup>4</sup>, Tyler Abrams<sup>5</sup>, Jonathan Coburn<sup>1</sup></p> <p><sup>1</sup>Sandia National Laboratories, United States; <sup>2</sup>University of Tennessee, United States; <sup>3</sup>University of New Mexico, United States; <sup>4</sup>University of San Diego, United States; <sup>5</sup>General Atomics, United States.</p>  | 73 |
| 13:05<br>I-21 | <p><b>Evolution and recovery of the irradiation-induced defect populations and thermal diffusivity in post self-ion irradiated, isochronal annealed tungsten</b></p> <p>Brandon Schwendeman<sup>1</sup>, Michael Simmonds<sup>1</sup>, Sicong He<sup>2</sup>, Gabriel Gorelick<sup>2</sup>, Thomas Schwarz-Selinger<sup>3</sup>, Matt Baldwin<sup>1</sup>, Jaime Marian<sup>2</sup>, George Tynan<sup>1</sup></p> <p><sup>1</sup>University of California San Diego, United States; <sup>2</sup>Materials Science and Engineering Department, University of California Los Angeles, United States; <sup>3</sup>Max-Planck-Institut für Plasmaphysik, Germany.</p>  | 74 |

## Poster Presentations

Tuesday, 20 May 2025, 16:30–18:30

Location: foyer

Poster session

### TOPIC: Boronisation and wall conditioning techniques

- |       |   |    |
|-------|---|----|
| POA-1 | <p><b>Study of spectral features and depth distributions of boron layers on tungsten substrates by ps-LIBS in a vacuum environment</b></p> <p>Huace Wu<sup>1</sup>, Rongxing Yi<sup>2</sup>, Anne Houben<sup>2</sup>, Sebastijan Brezinsek<sup>2</sup>, Marcin Rasinski<sup>2</sup>, Cong Li<sup>1</sup>, Genady Sergienko<sup>2</sup>, Timo Dittmar<sup>2</sup>, Hongbin Ding<sup>1</sup></p> <p><sup>1</sup>Dalian University of Technology, China; <sup>2</sup>Forschungszentrum Jülich GmbH, Germany.</p>   | 77 |
| POA-2 | <p><b>Diffusion of Ne in boron and borides</b></p> <p>Daniel Gautam<sup>1</sup>, Eduardo Pitthan<sup>1</sup>, Marek Rubel<sup>2</sup>, Daniel Primetzhofer<sup>1</sup></p> <p><sup>1</sup>Uppsala University, Sweden; <sup>2</sup>Uppsala University and KTH Royal Institute of Technology, Sweden.</p>   | 77 |
| POA-3 | <p><b>Reduction of Impurity from First Wall with Boron Powder Dropping in LHD</b></p> <p>Suguru Masuzaki<sup>1</sup>, Tetsutaro Oishi<sup>2</sup>, Tomoko Kawate<sup>1</sup>, Mamoru Shoji<sup>1</sup>, Federico Nespoli<sup>3</sup>, Robert Lunsford<sup>3</sup>, Motoshi Goto<sup>1</sup>, Miyuki Yajima<sup>1</sup>, Masayuki Tokitani<sup>1</sup>, Gen Motojima<sup>1</sup>, Erik Gilson<sup>3</sup>, Alexander Nagy<sup>3</sup>, Novimir Pablant<sup>3</sup>, Tomohiro Morisaki<sup>1</sup></p> <p><sup>1</sup>National Institute for Fusion Science, Japan; <sup>2</sup>Tohoku University, Japan; <sup>3</sup>Princeton Plasma Physics Laboratory, United States.</p> | 78 |
| POA-4 | <p><b>Engineering Research &amp; Development of Wall Conditioning Systems at HL-3</b></p> <p>Chengzhi Cao, Yi Hu, Yanfeng Xie, Jun Zhou, Xiangmei Huang, HL-3 Team</p> <p>Southwestern Institute of Physics, China.</p>   | 79 |
| POA-6 | <p><b>Influence of Deuterium Gas during Tungsten / Boron Film Deposition</b></p> <p>Laurent Marot<sup>1</sup>, Matej Mayer<sup>2</sup>, Thomas Morgan<sup>3</sup>, Tomás Sousa<sup>1</sup>, Nicolò Lopopolo<sup>1</sup>, Ernst Meyer<sup>1</sup></p> <p><sup>1</sup>Department of Physics, University of Basel, Switzerland; <sup>2</sup>Max-Planck-Institut für Plasmaphysik, Germany; <sup>3</sup>Dutch Institute for Fundamental Energy Research, Netherlands.</p>   | 79 |

### TOPIC: Neutron effects in plasma-facing materials

- |       |   |    |
|-------|---|----|
| POA-7 | <p><b>Defect evolution in tungsten at high-temperature as a function of damage dose</b></p> <p>Andreja Šestan Zavašnik<sup>1</sup>, Janez Zavašnik<sup>1</sup>, Sabina Markelj<sup>1</sup>, Nejc Parkelj<sup>1</sup>, Miha Sajovic<sup>1</sup>, Srečo Škapin<sup>1</sup>, Thomas Schwarz-Selinger<sup>2</sup></p> <p><sup>1</sup>Jožef Stefan Institute, Slovenia; <sup>2</sup>Max-Planck-Institut für Plasmaphysik, Germany.</p> | 80 |
|-------|---|----|

POA-8	<b>Status of the UCSD POSEIDON facility: An experiment for the study of simulated burning-plasma-material-interaction</b>	81
	<u>Matt Baldwin</u> , Daisuke Nishijima, Marlene Patino, Brandon Schwendeman, Michael Simmonds, Anže Založnik, George Tynan University of California San Diego, United States.	
POA-9	<b>Machine-learning force fields for hydrogen and vacancy complex in tungsten</b>	81
	<u>Yuki Noguchi</u> <sup>1</sup> , Daiji Kato <sup>2</sup> <sup>1</sup> Kyushu University, Japan; <sup>2</sup> National Institute for Fusion Science, Japan.	
POA-10	<b>A New Experimental System for Studying Defects and Deuterium Lattice Location in Tungsten Crystals by Ion Beam Methods</b>	82
	<u>Esther Punzón-Quijorna</u> , Mitja Kelemen, Roberto Galende-Pérez, Primož Vavpetič, Primož Pelicon, Sabina Markelj Jožef Stefan Institute, Slovenia.	
POA-11	<b>Atomic-Scale Investigation of Re/Os Precipitation in Neutron-Irradiated Tungsten Using Atom Probe Tomography: Validation of FISPACT-II Nuclear Data</b>	83
	<u>Iuliia Ipatova</u> <sup>1</sup> , Mark Gilbert <sup>1</sup> , Dmitry Terentyev <sup>2</sup> , Christina Hofer <sup>3</sup> , Ryo Shibahara <sup>4</sup> , Kazuhiro Kurano <sup>4</sup> , Kazutoshi Inoue <sup>4</sup> <sup>1</sup> UK Atomic Energy Authority (UKAEA), United Kingdom; <sup>2</sup> Belgian Nuclear Research Center, Belgium; <sup>3</sup> University of Oxford, Department of Materials, United Kingdom; <sup>4</sup> Institute for Materials Research, Tohoku University, Japan.	

## TOPIC: Technology and qualification of plasma-facing components

POA-12	<b>Ablation characteristics of fusion materials in preparation for local profiling of helium and hydrogen-isotopes with a novel laser ablation experiment</b>	84
	<u>Benedikt Buchner</u> , Steffen Mittelmann, Udo von Toussaint Max Planck Institute for Plasma Physics, Germany.	
POA-13	<b>Qualification activities of the first DTT divertor</b>	85
	<u>Selanna Roccella</u> <sup>1</sup> , Davide Caprini <sup>1</sup> , Marco Cerocchi <sup>1</sup> , Francesco Crea <sup>1</sup> , Riccardo De Luca <sup>1</sup> , Francesco Giorgetti <sup>1</sup> , Pierdomenico Lorusso <sup>1</sup> , Annunziata Satriano <sup>1</sup> , Luigi Verdini <sup>1</sup> , Domanico Marzullo <sup>2</sup> , Gian Mario Polli <sup>3</sup> , Hélène Roche <sup>4</sup> , Nicolas Vignal <sup>4</sup> , Marianne Richou <sup>4</sup> , Henri Greuner <sup>5</sup> , Johann Riesch <sup>5</sup> , Bernd Boeswirth <sup>5</sup> , Katja Hunger <sup>5</sup> , Rudolf Neu <sup>5</sup> <sup>1</sup> ENEA, Nuclear Department, Italy; <sup>2</sup> University of Trieste, Italy; <sup>3</sup> DTT S.C. a r.l., Frascati, Italy; <sup>4</sup> CEA, IRFM, France; <sup>5</sup> Max Planck Institute for Plasma Physics, Germany.	
POA-14	<b>Effect of bending and heat treatment on CuCrZr/316L interface for flat-type divertor target by explosive welding</b>	86
	<u>Siqing Feng</u> <sup>1</sup> , Xuebing Peng <sup>2</sup> , Peng Liu <sup>2</sup> <sup>1</sup> Anhui Vocational And Technical College, China; <sup>2</sup> Institute of Plasma Physics, Hefei Institutes of Physical Science, China.	





POA-25	<b>Studies of runaway electron impact on plasma facing surfaces in the DIII-D tokamak</b> Dmitry Rudakov <sup>1</sup> , Eric Hollmann <sup>1</sup> , Claudio Marini <sup>1</sup> , Erick Martinez-Loran <sup>1</sup> , Matthew Beidler <sup>2</sup> , Jeffrey Herfindal <sup>2</sup> , Daisuke Shiraki <sup>2</sup> , Yueqiang Liu <sup>3</sup> , Igor Bykov <sup>3</sup> , Andrey Lvovsky <sup>3</sup> , Charles Lasnier <sup>4</sup> , Jun Ren <sup>5</sup> , Svetlana Ratynskaia <sup>6</sup> , Panagiotis Tolas <sup>6</sup> , Richard Pitts <sup>7</sup> <sup>1</sup> University of California San Diego, United States; <sup>2</sup> Oak Ridge National Laboratory, TN, United States; <sup>3</sup> General Atomics, San Diego, CA, United States; <sup>4</sup> Lawrence Livermore National Laboratory, Livermore, CA, United States; <sup>5</sup> University of Tennessee, Knoxville, United States; <sup>6</sup> KTH Royal Institute of Technology, Sweden; <sup>7</sup> ITER Organization, France.	92
POA-28	<b>Erosion and Modification of Tungsten Surfaces Under Sequential Steady-State and High Heat Fluxes Transient Plasma Impacts</b> Vadym Makhlai <sup>1</sup> , Igor Garkusha <sup>1</sup> , Yuliia Volkova <sup>1</sup> , Stanislav Herashchenko <sup>1</sup> , Yurii Petrov <sup>1</sup> , Dmytro Yelisyeyev <sup>1</sup> , Pavel Shevchuk <sup>1</sup> , Thomas Morgan <sup>2</sup> <sup>1</sup> National Science Center 'Kharkiv Institute of Physics and Technology', Institute of Plasma Physics, Ukraine; <sup>2</sup> Dutch Institute for Fundamental Energy Research, Netherlands.	93
POA-29	<b>The influence of H plasma implantation on the low-cycle thermal fatigue cracking of plasma-facing tungsten in EU DEMO</b> James Hargreaves <sup>1</sup> , Jeong-Ha You <sup>2</sup> , Francesca Maviglia <sup>3</sup> , Jordy Vernimmen <sup>1</sup> , John Scholten <sup>1</sup> , Thomas Morgan <sup>1</sup> <sup>1</sup> Dutch Institute for Fundamental Energy Research, Netherlands; <sup>2</sup> Max Planck Institute for Plasma Physics, Germany; <sup>3</sup> Eurofusion PMU, Germany.	94
POA-30	<b>Tungsten based composites and heavy alloys exposed to ELM-y H-mode plasmas in the DIII-D tokamak</b> Žana Popović <sup>1</sup> , Tyler Abrams <sup>1</sup> , Zachary Bergstrom <sup>1</sup> , Jonathan Coburn <sup>2</sup> , Florian Effenberg <sup>3</sup> , Tatsuya Hinoki <sup>4</sup> , Ryan Hood <sup>2</sup> , Carlos Monton <sup>1</sup> , Rudolf Neu <sup>5</sup> , Jun Ren <sup>6</sup> , Johann Riesch <sup>5</sup> , Dmitry Rudakov <sup>7</sup> , Ruben Santana <sup>1</sup> , Cedric Tsui <sup>2</sup> <sup>1</sup> General Atomics, United States; <sup>2</sup> Sandia National Laboratories, United States; <sup>3</sup> Princeton Plasma Physics Laboratory, United States; <sup>4</sup> Kyoto University, Kyoto, Japan; <sup>5</sup> Max Planck Institute for Plasma Physics, Germany; <sup>6</sup> University of Tennessee, Knoxville, United States; <sup>7</sup> University of California San Diego, United States.	95
POA-32	<b>MatDB4Fusion: A new initiative to collect, merge, and leverage material properties data</b> Philipp Lied <sup>1</sup> , Giacomo Aiello <sup>2</sup> , Zachary Bergstrom <sup>3</sup> , Arunodaya Bhattacharya <sup>4</sup> , Daniel Clark <sup>5</sup> , Thomas Davis <sup>6</sup> , Mark Gilbert <sup>7</sup> , Michael Gorley <sup>7</sup> , Cory Hamelin <sup>7</sup> , Jim Pickles <sup>8</sup> , Gerald Pintsuk <sup>9</sup> , Andrew Sowder <sup>10</sup> , Sehila Gonzalez <sup>11</sup> <sup>1</sup> FusionCatalyst, Germany; <sup>2</sup> EUROfusion, Germany; <sup>3</sup> General Atomics, United States; <sup>4</sup> University of Birmingham, United Kingdom; <sup>5</sup> Type One Energy Group, United States; <sup>6</sup> Oxford Sigma, United Kingdom; <sup>7</sup> UK Atomic Energy Authority (UKAEA), United Kingdom; <sup>8</sup> Tokamak Energy, United Kingdom; <sup>9</sup> Forschungszentrum Jülich GmbH, Germany; <sup>10</sup> Electric Power Research Institute (EPRI), United States; <sup>11</sup> Clean Air Task Force (CATF), United States.	96
POA-33	<b>First wall simulated W-EUROFER mock-up characterization under HHF DEMO relevant conditions</b> Javier de Prado <sup>1</sup> , Ignacio Izaguirre <sup>1</sup> , Daniel Dorow-Gerspach <sup>2</sup> , Emanuele Cacciotti <sup>3</sup> , Francesco Crea <sup>3</sup> , María Sánchez <sup>1</sup> , Riccardo De Luca <sup>3</sup> , Marius Wirtz <sup>2</sup> <sup>1</sup> Universidad Rey Juan Carlos, Spain; <sup>2</sup> Forschungszentrum Jülich GmbH, Germany; <sup>3</sup> ENEA, Nuclear Department, Italy.	97

POA-34	<b>Heat Flux Test of the Small Thermal Shielding Mockups for the ITER Electron Cyclotron Heating Window Shielding Block</b> Chen Yanyu <sup>1</sup> , Wang Pinghuai <sup>1</sup> , Chen Jiming <sup>1</sup> , Zhang Fu <sup>2</sup> , Wang Kun <sup>3</sup> , Li Qian <sup>1</sup> , Wei Zhengxing <sup>1</sup> <sup>1</sup> Southwestern Institute of Physics, China; <sup>2</sup> International Thermonuclear Experimental Reactor, France; <sup>3</sup> ITER CNDA, China.	98
POA-36	<b>A novel approach to studying divertor gap heat loads</b> Miha Radež <sup>1</sup> , Jernej Kovačič <sup>2</sup> , Matic Brank <sup>2</sup> , Stefan Costea <sup>2</sup> , Leon Bogdanovič <sup>2</sup> , Tomaž Gyergyek <sup>3</sup> , Leon Kos <sup>2</sup> <sup>1</sup> University of Ljubljana, Faculty of Mathematics and Physics, Slovenia; <sup>2</sup> University of Ljubljana, Faculty of Mechanical Engineering, Slovenia; <sup>3</sup> University of Ljubljana, Faculty of Electrical Engineering, Slovenia.	98
POA-37	<b>Helium bubbles at grain boundaries in low-energy helium plasma exposed tungsten: Atomic-scale characteristics and evolution kinetics</b> Yu Li, Yi-Wen Zhu, Guangnan Luo, Haishan Zhou Institute of Plasma Physics, Chinese Academy of Sciences, China.	99
POA-39	<b>SALAMANDER: Advanced Multiphysics Simulation for Fusion Energy Systems</b> Pierre-Clément Simon <sup>1</sup> , Casey Icenhour <sup>1</sup> , Guillaume Giudicelli <sup>1</sup> , Logan Harbour <sup>1</sup> , Lin Yang <sup>1</sup> , Derek Gaston <sup>1</sup> , Masashi Shimada <sup>1</sup> , Grayson Gall <sup>2</sup> , Amanda Lietz <sup>2</sup> , Mahmoud Eltawila <sup>3</sup> , April Novak <sup>3</sup> , Trevor Franklin <sup>4</sup> , Lane Carasik <sup>4</sup> , Helen Brooks <sup>5</sup> <sup>1</sup> Idaho National Laboratory, United States; <sup>2</sup> NCSU, United States; <sup>3</sup> UIUC, United States; <sup>4</sup> VCU, United States; <sup>5</sup> UKAEA, United Kingdom.	100
POA-40	<b>Primary and secondary metallic PFC damage induced by RE dissipation in FTU</b> Marco De Angeli <sup>1</sup> , Panagiotis Tolias <sup>2</sup> , Svetlana Ratynskaia <sup>2</sup> , Dario Ripamonti <sup>3</sup> , Giorgio Maddaluno <sup>4</sup> , Giambattista Daminelli <sup>3</sup> , Elzbieta Fortuna-Zalesna <sup>5</sup> , Witold Zielinski <sup>5</sup> <sup>1</sup> Institute for Plasma Science and Technology, CNR, Italy; <sup>2</sup> KTH Royal Institute of Technology, Sweden; <sup>3</sup> Institute of Condensed Matter Chemistry and Energy Technologies, CNR, Italy; <sup>4</sup> ENEA, C.R. Frascati, Italy; <sup>5</sup> Warsaw University of Technology, Poland.	100

## TOPIC: Fuel retention and removal

POA-41	<b>Comparison between discrete and continuous energy formalisms used to model multi-level kinetic hydrogen trapping in PFM</b> Sokay Chroeun, Jonathan Mougenot, Yann Charles, Monique Gaspérini Université Sorbonne Paris Nord, CNRS, LSPM, France.	101
POA-42	<b>A code-comparison to establish a common-ground for component-level transport codes</b> Gabriele Ferrero <sup>1</sup> , Etienne Hodille <sup>2</sup> , Raffaella Testoni <sup>1</sup> <sup>1</sup> Politecnico di Torino, Dipartimento di Energia, Italy; <sup>2</sup> CEA, IRFM, France.	102
POA-43	<b>Diffusion of H atoms at the W/Cu interface: a kinetic model based on DFT data</b> Yovany Silva-Solis <sup>1</sup> , Julien Denis <sup>2</sup> , Etienne Hodille <sup>2</sup> , Yves Ferro <sup>1</sup> <sup>1</sup> Aix-Marseille University, CNRS, PIIM, France; <sup>2</sup> CEA, IRFM, France.	103

- POA-44 **LIBS for in-situ characterisation of JET plasma facing components: autoencoder-based spectral data processing** 103  
Paweł Gqsior<sup>1</sup>, Damian Sokulski<sup>1</sup>, Salvatore Almaviva<sup>2</sup>, Juuso Karhunen<sup>3</sup>, Jari Likonen<sup>3</sup>, Shweta Soni<sup>4</sup>, Sahithya Atikukke<sup>4</sup>, Pavel Veis<sup>4</sup>, Sanath Shetty<sup>5</sup>, Matej Veis<sup>5</sup>, Jelena Butikova<sup>6</sup>, Sebastian Brezinsek<sup>7</sup>, Rongxing Yi<sup>7</sup>, Ionuț Jecu<sup>8</sup>, Indrek Jõgi<sup>9</sup>, Jasper Ristkok<sup>9</sup>, Peeter Paris<sup>9</sup>, Corneliu Porosnicu<sup>10</sup>  
<sup>1</sup>Institute of Plasma Physics and Laser Microfusion, Poland; <sup>2</sup>ENEA, Diagnostics and Metrology Laboratory, Italy; <sup>3</sup>VTT Technical Research Centre of Finland Ltd, Finland; <sup>4</sup>Comenius University, Faculty of Math, Physics and Informatics, Slovakia; <sup>5</sup>Department of Experimental Physics, FMPI, Comenius Univ, Slovakia; <sup>6</sup>Institute of Solid State Physics, University of Latvia, Latvia; <sup>7</sup>Forschungszentrum Jülich GmbH, Germany; <sup>8</sup>UKAEA, Culham Campus, Abingdon, United Kingdom; <sup>9</sup>University of Tartu, Institute of Physics, Estonia; <sup>10</sup>INFLPR 409, Magurele, Romania.
- POA-45 **Deuterium retention in different tungsten-based alloys measured by LIBS, NRA and TDS** 104  
Mauricio Gago<sup>1</sup>, Bernhard Unterberg<sup>1</sup>, Steffen Antusch<sup>2</sup>, Anne Houben<sup>1</sup>, Alexander Klein<sup>2</sup>, Arkadi Kreter<sup>1</sup>, Sören Möller<sup>1</sup>, Michael Rieth<sup>2</sup>, Gennady Sergienko<sup>1</sup>, Marius Wirtz<sup>1</sup>, Rongxing Yi<sup>1</sup>, Christian Linsmeier<sup>1</sup>  
<sup>1</sup>Forschungszentrum Jülich GmbH, Germany; <sup>2</sup>Karlsruhe Institute of Technology, Germany.
- POA-46 **Oxidation of tungsten and its implications to tritium retention in decommissioning, maintenance and accident scenarios in future devices** 105  
Eric Prestat<sup>1</sup>, Rongri Li<sup>2</sup>, Guillermo Alvarez-Diaz<sup>2</sup>, Imogen Haydon<sup>1</sup>, Livia Cupertino Malheiros<sup>2</sup>, Emilio Martinez-Paneda<sup>2</sup>, Mark Gilbert<sup>1</sup>  
<sup>1</sup>UK Atomic Energy Authority (UKAEA), United Kingdom; <sup>2</sup>Imperial College London, United Kingdom.
- POA-47 **Comparison of D Retention for Advanced Plasma Facing Materials by D plasma exposure or D ion implantation** 106  
Yasuhiro Oya<sup>1</sup>, Yuzuka Hoshino<sup>1</sup>, Shingo Okumura<sup>1</sup>, Ayumu Hayakawa<sup>1</sup>, Kenshiro Miura<sup>1</sup>, Fei Sun<sup>2</sup>, Suguru Masuzaki<sup>3</sup>, Makoto Oyaizu<sup>4</sup>, Robert Kolasinski<sup>5</sup>, Chase Taylor<sup>6</sup>, Teppei Otsuka<sup>7</sup>, Yuji Hatano<sup>8</sup>, Masashi Shimada<sup>6</sup>, Hao Yu<sup>8</sup>, Ryuta Kasada<sup>8</sup>, Akira Hasegawa<sup>8</sup>  
<sup>1</sup>Shizuoka University, Japan; <sup>2</sup>Hefei University of Technology, China; <sup>3</sup>National Institute for Fusion Science, Japan; <sup>4</sup>National Institutes for Quantum Science and Technology, Japan; <sup>5</sup>Sandia National Laboratories, United States; <sup>6</sup>Idaho National Laboratory, United States; <sup>7</sup>Kindai University, Japan; <sup>8</sup>Tohoku University, Japan.
- POA-48 **Evidence of helium trapping in the lower divertor targets of WEST after the 2018–2020 campaigns based on TOF ERDA and TEM analysis** 107  
Iva Bogdanović Radović<sup>1</sup>, Zdravko Siketić<sup>1</sup>, Mathilde Diez<sup>2</sup>, Elodie Bernard<sup>2</sup>, Emmanuelle Tsitrone<sup>2</sup>, Antti Hakola<sup>3</sup>, Tomi Vuoriheimo<sup>4</sup>, Celine Martin<sup>5</sup>, Martiane Cabie<sup>6</sup>, Thomas Neisius<sup>6</sup>  
<sup>1</sup>Ruder Bošković Institute, Croatia; <sup>2</sup>CEA, IRFM, France; <sup>3</sup>VTT Technical Research Centre of Finland Ltd, Finland; <sup>4</sup>Department of Physics, University of Helsinki, Finland; <sup>5</sup>Aix-Marseille Univ, CNRS, PIIM, France; <sup>6</sup>Aix-Marseille Univ, CNRS, CP2M, France.
- POA-51 **Investigating Tritium Retention in tungsten coated plasma facing components from the divertor region of the Joint European Torus (JET)** 107  
Anete Stine Teimane<sup>1</sup>, Elina Pajuste<sup>1</sup>, Liga Avotina<sup>1</sup>, Matiss Sondars<sup>1</sup>, Jari Likonen<sup>2</sup>, Anna Widdowson<sup>3</sup>  
<sup>1</sup>Institute of Chemical Physics, University of Latvia, Latvia; <sup>2</sup>VTT Technical Research Centre of Finland Ltd, Finland; <sup>3</sup>UKAEA, Culham Campus, United Kingdom.

POA-53	<b>Novel dynamic deuterium transport measurements using Upgraded Pilot-PSI</b> <u>Cas Robben<sup>1</sup></u> , Jort Kesteren <sup>1</sup> , Remco Timmer <sup>1</sup> , Wim Arnoldbik <sup>2</sup> , Maria Cunha <sup>1</sup> , Beata Tyburska-Pueschel <sup>1</sup> , Thomas Morgan <sup>1</sup> <sup>1</sup> Dutch Institute for Fundamental Energy Research, Netherlands; <sup>2</sup> Detect99, Netherlands.	108
POA-55	<b>Evaluation of the boronization effect on fuel retention in WEST long pulses</b> <u>Laura Laguardia<sup>1</sup></u> , Gabriele Gervasini <sup>1</sup> , Eleonore Geulin <sup>2</sup> , Alberto Gallo <sup>2</sup> , Regis Bisson <sup>3</sup> , Yann Corre <sup>2</sup> , Julien Denis <sup>2</sup> , Corinne Desgranges <sup>2</sup> , Annika Ekedahl <sup>2</sup> , Nicolas Fedorczak <sup>2</sup> , Jonathan Gaspar <sup>4</sup> , Alex Thomas Grosjean <sup>5</sup> , Etienne Hodille <sup>2</sup> , Antti Hakola <sup>6</sup> , Thierry Loarer <sup>2</sup> , Karl Krieger <sup>7</sup> , Pierre Manas <sup>2</sup> , Philippe Moreau <sup>2</sup> , Emmanuelle Tsitrone <sup>2</sup> , Stefane Vartarian <sup>2</sup> , Anna Widdowson <sup>8</sup> , Tom Wauters <sup>9</sup> <sup>1</sup> Istituto per la Scienza e Tecnologia dei Plasmi, CNR, Milano, Italy; <sup>2</sup> CEA, IRFM, France; <sup>3</sup> CNRS, PIIM, France; <sup>4</sup> CNRS, IUSTI, France; <sup>5</sup> University of Tennessee Knoxville, United States; <sup>6</sup> VTT Technical Research Centre of Finland Ltd, Finland; <sup>7</sup> Max-Planck-Institut für Plasmaphysik, Germany; <sup>8</sup> UKAEA, Culham Campus, Abingdon, United Kingdom; <sup>9</sup> ITER Organization, France.	109
POA-56	<b>Hydrogen Retention in Plasma-Facing Components: Parameter Study</b> <u>Mikhail Lavrentiev<sup>1</sup></u> , Dinusha Jayasundara <sup>1</sup> , Tez Orr <sup>1</sup> , Celyn Sammons <sup>2</sup> <sup>1</sup> United Kingdom Atomic Energy Authority (UKAEA), United Kingdom; <sup>2</sup> UKAEA and University of Manchester, United Kingdom.	110
POA-59	<b>A calibration method for water signals during thermal desorption spectroscopy of deuterium from tungsten</b> <u>Thomas Schwarz-Selinger</u> , Maximilian Brucker Max Planck Institut for Plasma Physics, Germany.	110
POA-60	<b>Progress in laser-based surface analysis techniques for fusion applications – from laboratory experiments to reactor-class diagnostics</b> <u>Sebastijan Brezinsek</u> Forschungszentrum Jülich GmbH, Germany.	111
POA-61	<b>Analysis of hydrogen transport and trapping in SS316L</b> <u>Floriane Montupet-Leblond<sup>1</sup></u> , Etienne Hodille <sup>1</sup> , Mickaël Payet <sup>1</sup> , Elodie Bernard <sup>1</sup> , Dominique Vrel <sup>2</sup> , Frédéric Miserque <sup>3</sup> , Christian Grisolia <sup>1</sup> <sup>1</sup> CEA, IRFM, France; <sup>2</sup> LSPM, CNRS, France; <sup>3</sup> CEA, SCCME, France.	112

## TOPIC: Erosion, re-deposition, mixing, and dust formation

POA-62	<b>The Interplay of Ion Impact Angle and Energy on Mixed-Material Surface Concentrations in a DIII-D Tungsten Divertor</b> <u>Alec Cacheris<sup>1</sup></u> , Tyler Abrams <sup>2</sup> , Davis Easley <sup>3</sup> , Daisuke Shiraki <sup>3</sup> , Robert Wilcox <sup>3</sup> , Jeffrey Herfindal <sup>3</sup> , David Christian Donovan <sup>1</sup> <sup>1</sup> University of Tennessee at Knoxville, United States; <sup>2</sup> General Atomics, United States; <sup>3</sup> Oak Ridge National Laboratory, United States.	113
POA-63	<b>Dust-Plasma Interaction Studies in the STOR-M Tokamak</b> <u>Nathan Nelson</u> , Lenaïc Couëdel, Chijin Xiao University of Saskatchewan, Canada.	113

POA-64	<b>Analysis and Modelling of the Relationship Between WI, WII, and WIII Emission Signals and Tungsten Net Erosion in the DIII-D Divertor</b> Luca Cappelli <sup>1</sup> , Jerome Guterl <sup>2</sup> , Tyler Abrams <sup>2</sup> , Ulises Losada <sup>3</sup> , Žana Popović <sup>2</sup> , Zachary Bergstrom <sup>2</sup> <sup>1</sup> ORAU, United States; <sup>2</sup> General Atomics, United States; <sup>3</sup> Auburn University, United States.	114
POA-65	<b>Ex-situ LIBS study for the determination of boron content in WEST divertor tiles after the 2019 campaign</b> Indrek Jõgi <sup>1</sup> , Peeter Paris <sup>1</sup> , Marta Malin Muru <sup>1</sup> , Elodie Bernard <sup>2</sup> , Mathilde Diez <sup>2</sup> , Emmanuelle Tsitrone <sup>2</sup> , Jari Likonen <sup>3</sup> , Antti Hakola <sup>3</sup> , Eduard Grigore <sup>4</sup> <sup>1</sup> University of Tartu, Institute of Physics, Estonia; <sup>2</sup> CEA, IRFM, France; <sup>3</sup> VTT Technical Research Centre of Finland Ltd., Finland; <sup>4</sup> Acasa Institutul National pentru Fizica Laserilor, Plasmei si Radiatiei, Romania.	115
POA-66	<b>Modeling of erosion/deposition patterns observed during WEST high-fluence campaign</b> Alexis Huart <sup>1</sup> , Guido Ciraolo <sup>1</sup> , Yann Corre <sup>1</sup> , Nicolas Rivals <sup>1</sup> , Wojciech Gromelski <sup>2</sup> , Jamie Gunn <sup>1</sup> , Nicolas Fedorczak <sup>1</sup> , Mathilde Diez <sup>1</sup> , Jonathan Gerardin <sup>1</sup> , Alex Thomas Grosjean <sup>3</sup> , Christophe Guillemaut <sup>1</sup> , Juri Romazanov <sup>4</sup> <sup>1</sup> CEA, IRFM, France; <sup>2</sup> IFPILM, Poland; <sup>3</sup> University of Tennessee Knoxville, United States; <sup>4</sup> Forschungszentrum Jülich GmbH, Germany.	116
POA-67	<b>Study on the influence of ELM and ELM-control methods on WD sputtering in EAST</b> Qing Zhang, Fang Ding Institute of Plasma Physics, HFIPS, Chinese Academy of Sciences, China.	117
POA-68	<b>Mixing and enrichment effects on low- and high-Z impurities from W carbides as PFMs</b> Tatyana Sizyuk <sup>1</sup> , Tyler Abrams <sup>2</sup> , Gregory Sinclair <sup>2</sup> , Ahmed Hassanein <sup>3</sup> <sup>1</sup> Argonne National Laboratory, Lemont, United States; <sup>2</sup> General Atomics, San Diego, United States; <sup>3</sup> Purdue University, West Lafayette, United States.	117
POA-69	<b>Thick deposited tungsten layer growth and characterization using Magnum-PSI</b> Thomas Morgan <sup>1</sup> , Luc Bouwmeester <sup>2</sup> , Marcin Rasinski <sup>3</sup> , Erwin Zoethout <sup>1</sup> , Jort Kesteren <sup>1</sup> , Cas Robben <sup>1</sup> , Beata Tyburska-Pueschel <sup>1</sup> , Vairavel Mathayan <sup>1</sup> , Lambert van Breemen <sup>1</sup> , David Dellasega <sup>4</sup> , Matteo Passoni <sup>4</sup> , Luigi Bana <sup>4</sup> , Nora Lecis <sup>4</sup> <sup>1</sup> Dutch Institute for Fundamental Energy Research, Netherlands; <sup>2</sup> Eindhoven University of Technology, Netherlands; <sup>3</sup> Forschungszentrum Jülich GmbH, Germany; <sup>4</sup> Politecnico di Milano, Italy.	118
POA-70	<b>Theoretical modelling of a non-hydrogenic plasma-wall interaction experiment in the GyM linear device</b> Carlo Tuccari <sup>1</sup> , Gabriele Alberti <sup>1</sup> , Fabio Mombelli <sup>1</sup> , Matteo Passoni <sup>1</sup> , Andrea Uccello <sup>2</sup> , Anna Cremona <sup>2</sup> , Matteo Pedroni <sup>2</sup> , Juri Romazanov <sup>3</sup> <sup>1</sup> Dipartimento di Energia, Politecnico di Milano, Milan, Italy; <sup>2</sup> Istituto per la Scienza e Tecnologia dei Plasmi, CNR, Milano, Italy; <sup>3</sup> Forschungszentrum Jülich GmbH, Germany.	119

POA-71	<b>Evaluation of erosion and deposition in JA DEMO divertor and the effects of tungsten impurities</b> Makoto Oya <sup>1</sup> , Kazuo Hoshino <sup>2</sup> , Nobuyuki Asakura <sup>3</sup> , Yoshiteru Sakamoto <sup>3</sup> , Noriyasu Ohno <sup>4</sup> , Kazuaki Hanada <sup>1</sup> <sup>1</sup> Kyushu University, Japan; <sup>2</sup> Keio University, Japan; <sup>3</sup> National Institutes for Quantum Science and Technology, Japan; <sup>4</sup> Nagoya University, Japan.	120
POA-72	<b>Overview of Material Balance and Dust Production in JET Beryllium – Tungsten Wall from Post-Mortem Analysis Studies</b> Anna Widdowson <sup>1</sup> , Charlie Ayres <sup>1</sup> , Joe Banks <sup>1</sup> , Aleksandra Baron-Wiechec <sup>2</sup> , Sebastijan Brezinsek <sup>3</sup> , Matthews Clancy <sup>1</sup> , Paul Coad <sup>1</sup> , Elzbieta Fortuna-Zalesna <sup>4</sup> , Kalle Heinola <sup>5</sup> , Matt Hook <sup>1</sup> , Ilona Karnowska-Peterski <sup>1</sup> , Ionuț Jecu <sup>1</sup> , Jari Likonen <sup>6</sup> , Marek Rubel <sup>7</sup> <sup>1</sup> United Kingdom Atomic Energy Authority (UKAEA), United Kingdom; <sup>2</sup> Guangdong Technion – Israel Institute of Technology, China; <sup>3</sup> Forschungszentrum Jülich GmbH, Germany; <sup>4</sup> Warsaw University of Technology, Poland; <sup>5</sup> IAEA, Austria; <sup>6</sup> VTT Technical Research Centre of Finland Ltd, Espoo, Finland; <sup>7</sup> Uppsala University and KTH Royal Institute of Technology, Sweden.	121
POA-73	<b>Elemental analysis of divertor marker tiles exposed during the 2018 (C3), 2019 (C4) and 2020 (C5) WEST campaigns</b> Rodrigo Mateus <sup>1</sup> , Norberto Catarino <sup>1</sup> , Eduardo Alves <sup>1</sup> , Elodie Bernard <sup>2</sup> , Mathilde Diez <sup>2</sup> , Emmanuelle Tsitrone <sup>2</sup> , Jari Likonen <sup>3</sup> , Antti Hakola <sup>3</sup> <sup>1</sup> IPFN, Instituto Superior Técnico, Universidade de Lisboa, Portugal; <sup>2</sup> CEA, IRFM, France; <sup>3</sup> VTT Technical Research Centre of Finland Ltd, Finland.	122
POA-74	<b>The influence of nitrogen seeding on beryllium erosion by hydrogen plasma</b> Timo Dittmar <sup>1</sup> , Dmitriy Borodin <sup>1</sup> , Sebastijan Brezinsek <sup>1</sup> , Ewa Pawelec <sup>2</sup> , Antti Hakola <sup>3</sup> , Karl Krieger <sup>4</sup> , Scott Silburn <sup>5</sup> , Emmanuelle Tsitrone <sup>6</sup> , Anna Widdowson <sup>5</sup> <sup>1</sup> Forschungszentrum Jülich GmbH, Germany; <sup>2</sup> Institute of Physics, University of Opole, Poland; <sup>3</sup> VTT Technical Research Centre of Finland Ltd, Finland; <sup>4</sup> Max-Planck-Institut für Plasmaphysik, Germany; <sup>5</sup> UKAEA, Culham Campus, United Kingdom; <sup>6</sup> CEA, IRFM, France.	122
POA-75	<b>Radio frequency plasma cleaning for Core Plasma Thomson Scattering diagnostic mirrors</b> Youpeng Wang <sup>1</sup> , Artem Dmitriev <sup>1</sup> , Laurent Marot <sup>1</sup> , Paul Hirt <sup>1</sup> , Tomás Sousa <sup>1</sup> , Maitane Amarika <sup>2</sup> , Gorka Beaskoetxea <sup>2</sup> , Aitor Marco <sup>2</sup> , Ulrich Walach <sup>3</sup> , Laura Sanchez <sup>3</sup> , Jordi Puig <sup>4</sup> , Ernst Meyer <sup>1</sup> <sup>1</sup> University of Basel, Switzerland; <sup>2</sup> IDOM Consulting, Engineering, Architecture S.A.U., Spain; <sup>3</sup> Fusion for Energy (F4E), Spain; <sup>4</sup> ATG Europe, Spain.	123
POA-76	<b>Suppression of impurity release on the low field side tungsten limiter in EAST long-pulse discharges</b> Fang Ding, Rui Ding, Haishan Zhou Institute of Plasma Physics, HFIPS, Chinese Academy of Sciences, China.	124
POA-77	<b>Erosion behavior of porous boron and boron-tungsten layers exposed to deuterium plasma in the GyM linear device</b> Andrea Uccello <sup>1</sup> , Federico Gaspari <sup>2</sup> , Davide Orecchia <sup>2</sup> , Matteo Pedroni <sup>1</sup> , Irene Casiraghi <sup>1</sup> , Daria Ricci <sup>1</sup> , Natale Rispoli <sup>1</sup> , Jimmy Scionti <sup>1</sup> , David Dellasega <sup>2</sup> , Matteo Passoni <sup>2</sup> , Valeria Russo <sup>2</sup> , Fabio Subba <sup>3</sup> , Alessio Villa <sup>3</sup> , Alessandro Maffini <sup>2</sup> <sup>1</sup> Istituto per la Scienza e Tecnologia dei Plasmi, CNR, Italy; <sup>2</sup> Politecnico di Milano, Italy; <sup>3</sup> NEMO Group, Dipartimento di Energia, Politecnico di Torino, Italy.	125

## TOPIC: Tungsten, tungsten alloys, and advanced steels

- |        |  |     |
|--------|--|-----|
| POA-78 | <p><b>Tungsten-diamond composite for plasma-facing materials</b></p> <p>Shaokai Tang<sup>1</sup>, Thomas Morgan<sup>2</sup>, Nicu Scarisoreanu<sup>3</sup>, Beata Tyburska-Pueschel<sup>2</sup>, Jort Kesteren<sup>2</sup>, Maria Cunha<sup>2</sup>, Paul Mummery<sup>1</sup>, Aneeqa Khan<sup>1</sup></p> <p><sup>1</sup>The University of Manchester, United Kingdom; <sup>2</sup>Dutch Institute for Fundamental Energy Research, Netherlands; <sup>3</sup>National Institute for Laser, Plasma and Radiation Physics, Romania.</p>   | 126 |
| POA-79 | <p><b>Advancements in the design of a W-based coating as protective barrier for liquid Sn-based divertor</b></p> <p>Davide Vavassori<sup>1</sup>, Luigi Bana<sup>1</sup>, Marco Bugatti<sup>1</sup>, Matteo Iafrati<sup>2</sup>, Matteo Passoni<sup>1</sup>, David Dellasega<sup>1</sup></p> <p><sup>1</sup>Politecnico di Milano, Italy; <sup>2</sup>ENEA, Frascati, Italy.</p>   | 127 |
| POA-81 | <p><b>Inverse finite element based methodology applied to ITER grade tungsten: a model for mini-flat tensile specimens</b></p> <p>Francisco Miranda<sup>1</sup>, Aleksandr Zinovev<sup>2</sup>, David Bermudez Parra<sup>3</sup>, Alexander Bakaev<sup>2</sup>, Dmitry Terentyev<sup>4</sup>, Kim Verbeken<sup>5</sup>, Thomas Pardoen<sup>6</sup></p> <p><sup>1</sup>Université Catholique de Louvain, Louvain-la-Neuve. Belgian Nuclear Research Centre SCKCEN, Mol., Belgium; <sup>2</sup>Belgian Nuclear Research Centre SCKCEN, Mol., Belgium; <sup>3</sup>Belgian Nuclear Research Centre SCKCEN, Belgium and Universidad Politécnica de Madrid, Spain; <sup>4</sup>Belgian Nuclear Research Centre SCKCEN, Mol. Ghent University, Department of Materials, Textiles and Chemical Engineering, Ghent, Belgium; <sup>5</sup>Ghent University, Department of Materials, Textiles and Chemical Engineering, Ghent, Belgium; <sup>6</sup>Université Catholique de Louvain, Louvain-la-Neuve. WEL Research Institute, Wavre, Belgium.</p> | 128 |
| POA-82 | <p><b>Effect of baseplate preheating on the crack formation of W-W2C during Laser Powder Bed Fusion</b></p> <p>Aljaž Iveković<sup>1</sup>, Črtomir Donik<sup>2</sup>, Irena Paulin<sup>2</sup>, Petra Jenuš<sup>1</sup></p> <p><sup>1</sup>Jožef Stefan Institute, Slovenia; <sup>2</sup>Institute of Metals and Technology, Slovenia.</p>   | 129 |
| POA-83 | <p><b>Predicting irradiation hardening and microstructural evolution in ion-irradiated Eurofer97: a nanoindentation study supported by CPFEM and TEM</b></p> <p>Tymofii Khvan, Katarzyna Mulewska, Łukasz Kurpaska, Witold Chromiński, Michał Stróżyk</p> <p>National Centre for Nuclear Research, Poland.</p>   | 130 |
| POA-84 | <p><b>Brazeability study of W2C-reinforced tungsten alloy to EUROFER for first wall application in DEMO fusion reactor</b></p> <p>Ignacio Izaguirre<sup>1</sup>, Javier de Prado<sup>1</sup>, Maria Sánchez<sup>1</sup>, Aljaž Iveković<sup>2</sup>, Petra Jenuš<sup>2</sup>, Alejandro Ureña<sup>1</sup></p> <p><sup>1</sup>Universidad Rey Juan Carlos, Spain; <sup>2</sup>Jožef Stefan Institute, Slovenia.</p>   | 130 |
| POA-85 | <p><b>Comparative study of mechanical properties of W-Cu composites with Diamond TPMS geometries</b></p> <p>Diana Knyzhnykova<sup>1</sup>, Petra Jenuš<sup>1</sup>, Saša Novak<sup>1</sup>, Irena Paulin<sup>2</sup>, Borut Žužek<sup>2</sup>, Nejc Novak<sup>3</sup>, Robert Lürbke<sup>4</sup>, Alexander Von Mueller<sup>4</sup>, Rudolf Neu<sup>4</sup>, Aljaž Iveković<sup>1</sup></p> <p><sup>1</sup>Jožef Stefan Institute, Slovenia; <sup>2</sup>Institute of Metals and Technology, Slovenia; <sup>3</sup>University of Maribor, Faculty of Mechanical Engineering, Slovenia; <sup>4</sup>Max Planck Institute for Plasma Physics, Germany.</p>   | 131 |

POA-86	<b>Temperature-dependent grain boundary permeation in tungsten investigated by hydrogenography</b> <u>Fahrudin Delic</u> , Armin Manhard, Udo von Toussaint Max Planck Institute for Plasma Physics, Germany.	132
POA-87	<b>An experimental assessment of interatomic potentials for fusion-relevant ion-solid combinations</b> <u>Philipp M. Wolf</u> , Eduardo Pitthan, Daniel Primetzhofer Uppsala University, Sweden.	133
POA-88	<b>Helium irradiation induced the crystallographic orientation change of tungsten via grain rotation</b> <u>Cuncai Fan</u> Zhejiang University, China.	133
POA-89	<b>Influence of the addition of Fe on the CrTaVW medium entropy alloy for Nuclear Fusion applications</b> Ricardo Martins <sup>1</sup> , Vasco Valadares <sup>1</sup> , Bernardo Monteiro <sup>1</sup> , António P.Gonçalves <sup>2</sup> , José B.Correia <sup>3</sup> , Andrei Galatanu <sup>4</sup> , Elena Tejado <sup>5</sup> , José Y.Pastor <sup>5</sup> , Marta Dias <sup>1</sup> <sup>1</sup> Instituto de Plasmas e Fusão Nuclear (IPFN), Universidade de Lisboa, Portugal; <sup>2</sup> C2TN, Instituto Superior Técnico, Universidade de Lisboa, Portugal; <sup>3</sup> Laboratório Nacional de Energia e Geologia (LNEG), Portugal; <sup>4</sup> National Institute of Materials Physics, Romania; <sup>5</sup> Universidad Politecnica de Madrid, Spain.	134
POA-90	<b>Structural and mechanical characterization of functionally graded W/EUROFER coatings for fusion applications</b> <u>Siyu Zhang</u> , Ashwini Kumar Mishra, Jarir Aktaa Karlsruhe Institute of Technology (KIT), Germany.	135
POA-91	<b>Assessing the Viability of Tungsten/Silicon Carbide Plasma Facing Components</b> <u>Zachary Bergstrom</u> , Ruben Santana, Žana Popović, Carlos Monton, Tyler Abrams General Atomics, United States.	136
POA-92	<b>Study of degradation of tungsten-based materials for fusion reactors by thermal load testing</b> <u>Ester Duchková</u> <sup>1</sup> , Ondřej Čížek <sup>2</sup> , Michal Hájíček <sup>2</sup> , Petr Havlík <sup>3</sup> , Jiří Matějčíček <sup>4</sup> , Mark Murtazin <sup>1</sup> , Matěj Peterka <sup>4</sup> , Roman Petráš <sup>1</sup> , Ladislav Vála <sup>1</sup> , Jiří Zýka <sup>2</sup> <sup>1</sup> Research Centre Řež, Czech Republic; <sup>2</sup> UJP PRAHA a.s., Prague, Czech Republic; <sup>3</sup> Faculty of Mechanical Engineering, Brno University of Technology, Czech Republic; <sup>4</sup> Institute of Plasma Physics of the Czech Academy of Sciences, Czech Republic.	136
POA-93	<b>Hydrogen retention in tungsten at ELM-relevant energies</b> <u>Sophie Towell</u> <sup>1</sup> , Mikhail Lavrentiev <sup>2</sup> <sup>1</sup> University of Oxford, United Kingdom; <sup>2</sup> United Kingdom Atomic Energy Authority (UKAEA), United Kingdom.	137
POA-96	<b>In-situ Measurement of Helium-Induced Surface Modification in Tungsten using Advanced Characterization Techniques</b> <u>Robert Kolasinski</u> , Feng-Jen Chang, Jonathan Coburn, Antonio Cruz Sandia National Laboratories, United States.	138



POA-97	<b>Effect of deuterium on defect evolution in tungsten</b> <u>Fredric Granberg</u> <sup>1</sup> , Victor Lindblad <sup>1</sup> , Jintong Wu <sup>1</sup> , Daniel Mason <sup>2</sup> <sup>1</sup> Department of Physics, University of Helsinki, Finland; <sup>2</sup> UK Atomic Energy Authority, United Kingdom.	139
POA-98	<b>High-dose long-time defect evolution in tungsten studied by atomistically informed Object Kinetic Monte Carlo simulations</b> <u>Jintong Wu</u> <sup>1</sup> , Juan-Pablo Balbuena <sup>2</sup> , Zhiwei Hu <sup>3</sup> , Ville Jantunen <sup>1</sup> , Marie-France Barthe <sup>3</sup> , Maria Jose Caturla <sup>4</sup> , Fredric Granberg <sup>1</sup> <sup>1</sup> University of Helsinki, Finland; <sup>2</sup> Universidad de Alcala, Spain; <sup>3</sup> University of Orleans, France; <sup>4</sup> Universidad de Alicante, Spain.	139
POA-99	<b>ITER EU First Wall Panel CuCrZr cooling rate study</b> Margherita Sardo <sup>1</sup> , Samuli Heikkinen <sup>2</sup> , Jose Miguel Pacheco Cansino <sup>2</sup> , Marta Freitas <sup>3</sup> , Nuno A. Marques <sup>3</sup> , Sergio A. Reis <sup>3</sup> , Monica Mendes Reis <sup>3</sup> <sup>1</sup> ATG Europe, Italy; <sup>2</sup> Fusion for Energy, Spain; <sup>3</sup> Instituto de Soldadura e Qualidade (ISQ), Portugal.	140

Thursday, 22 May 2025, 16:45–18:45

Location: foyer

Poster session

## TOPIC: Fusion devices and edge plasma physics

- POB-1 **Plasma performance and qualification of optical plasma diagnostics at the JULE-PSI linear plasma generator** 142  
Michael Reinhart, Rahul Rayaprolu, Dirk Nicolai, Marc Sackers, Gennady Sergienko, Arkadi Kreter, Sebastijan Brezinsek, Bernhard Unterberg, Christian Linsmeier  
Forschungszentrum Jülich GmbH, Germany.
- POB-2 **The DIII-D Full Wall Change-Out Project: High-Level Options and Key Research Considerations** 143  
Tyler Abrams<sup>1</sup>, Florian Effenberg<sup>2</sup>, Andrea Garofalo<sup>1</sup>, Suk-Ho Hong<sup>1</sup>, Adam McLean<sup>3</sup>, Christopher Murphy<sup>1</sup>, Craig Petty<sup>1</sup>, Karl Schultz<sup>1</sup>, Morgan Shafer<sup>4</sup>, Gregory Sinclair<sup>1</sup>, Theresa Wilks<sup>5</sup>  
<sup>1</sup>General Atomics, United States; <sup>2</sup>Princeton Plasma Physics Laboratory, Princeton, United States; <sup>3</sup>Lawrence Livermore National Laboratory, United States; <sup>4</sup>Oak Ridge National Laboratory, United States; <sup>5</sup>Massachusetts Institute of Technology, United States.
- POB-4 **SOLPS-ITER modelling of a deuterium plasma discharge in the GyM linear plasma device** 143  
Alessio Villa<sup>1</sup>, Andrea Uccello<sup>2</sup>, Fabio Subba<sup>1</sup>, Matteo Passoni<sup>3</sup>, Irene Casiraghi<sup>2</sup>, Giuseppe Francesco Nallo<sup>1</sup>, Fabio Mombelli<sup>3</sup>, Alessandro Maffini<sup>3</sup>  
<sup>1</sup>NEMO Group, Dipartimento di Energia, Politecnico di Torino, Italy; <sup>2</sup>Istituto per la Scienza e Tecnologia dei Plasmi, CNR, Italy; <sup>3</sup>Dipartimento di Energia, Politecnico di Milano, Italy.
- POB-5 **Plasma modelling with SOLPS-ITER to support the design of the new high-density BiGyM linear plasma device** 144  
Irene Casiraghi<sup>1</sup>, Jimmy Scionti<sup>1</sup>, William Bin<sup>1</sup>, Stefano Cipelli<sup>2</sup>, Daria Ricci<sup>1</sup>, Marcelo Baquero-Ruiz<sup>3</sup>, Ivo Furno<sup>3</sup>, Lyes Kadi<sup>3</sup>, Philippe Guittienne<sup>3</sup>, Christine Stollberg<sup>3</sup>, Renat Karimov<sup>3</sup>, Elena Tonello<sup>3</sup>, Andrea Uccello<sup>1</sup>  
<sup>1</sup>Istituto per la Scienza e Tecnologia dei Plasmi, CNR, Milano, Italy; <sup>2</sup>CRF – Università degli Studi di Padova, Padova, Italy; <sup>3</sup>Swiss Plasma Center (SPC) – EPFL, Lausanne, Switzerland.
- POB-6 **Impact of nitrogen seeding on edge plasma transport on CFETR X-divertor with EMC3-EIRENE modelling** 145  
Tian Xie<sup>1</sup>, Yujian Wang<sup>1</sup>, Hang Li<sup>2</sup>, Wei Zhang<sup>3</sup>, Dezhen Wang<sup>4</sup>  
<sup>1</sup>Northeast Agricultural University, China; <sup>2</sup>College of Physics and Optoelectronic Engineering, Shenzhen University, China; <sup>3</sup>Institute of Plasma Physics, Chinese Academy of Sciences, China; <sup>4</sup>School of Physics, Dalian University of Technology, China.
- POB-7 **LH Power and core line integrated density impact on impurity sources and W prompt redeposition for various plasma shapes in WEST** 146  
Alex Thomas Grosjean<sup>1</sup>, David Christian Donovan<sup>1</sup>, Pascal Devynck<sup>2</sup>, Nicolas Fedorczak<sup>2</sup>, Louis Fevre<sup>3</sup>, Jonathan Gerardin<sup>2</sup>, Jamie Gunn<sup>2</sup>, Christophe Guillemaut<sup>2</sup>, Benoit Guillermin<sup>2</sup>, Curtis A. Johnson<sup>4</sup>, Christopher C. Klepper<sup>4</sup>, Sean Robert Kosslow<sup>1</sup>, Brian Putra<sup>1</sup>, Nicolas Rivals<sup>2</sup>, Ezekial A. Unterberg<sup>4</sup>  
<sup>1</sup>University of Tennessee Knoxville, United States; <sup>2</sup>CEA, IRFM, France; <sup>3</sup>Institut Jean Lamour IJL, Université de Lorraine, France; <sup>4</sup>Oak Ridge National Laboratory, United States.

POB-9	<b>Deuterated ammonia formation, emission and dissociation in a nitrogen-seeded, Ohmic JET low-recycling plasma</b>	147
	Roni Mäenpää <sup>1</sup> , Mathias Groth <sup>1</sup> , Henri Kumpulainen <sup>2</sup> , Andrew Meigs <sup>3</sup> , Ewa Pawelec <sup>4</sup> , Detlev Reiter <sup>5</sup> , Juri Romazanov <sup>2</sup> , Anthony Shaw <sup>3</sup> , Sebastijan Brezinsek <sup>2</sup>	
	<sup>1</sup> Aalto University, Finland; <sup>2</sup> Forschungszentrum Jülich GmbH, Germany; <sup>3</sup> UKAEA, United Kingdom; <sup>4</sup> Institute of Physics, University of Opole, Poland; <sup>5</sup> Institute for Laser and Plasma Physics, Heinrich-Heine-University, Germany.	
POB-10	<b>Advantages of highly radiating plasma in negative triangularity for a stable plasma material interface</b>	148
	Livia Casali <sup>1</sup> , David Eldon <sup>2</sup> , Tomas Odstroil <sup>2</sup> , Ray Mattes <sup>1</sup> , Austin Welsh <sup>1</sup>	
	<sup>1</sup> University of Tennessee, Knoxville, United States; <sup>2</sup> General Atomics, United States.	
POB-11	<b>Thermal modelling of ITER castellated fingers with phase change using control volume finite element method</b>	148
	Matic Brank, Gregor Simic, Jernej Kovacic, Stefan Costea, Leon Bogdanovič, Miha Radež, Leon Kos	
	University of Ljubljana, Faculty of Mechanical Engineering, Slovenia.	

## TOPIC: Technology and qualification of plasma-facing components

POB-12	<b>In-vessel and depth-resolved hydrogen isotope composition analysis in JET by LIBS operated on a remote handling arm</b>	149
	Rongxing Yi <sup>1</sup> , Rahul Rayaprolu <sup>1</sup> , Jari Likonen <sup>2</sup> , Salvatore Almariva <sup>3</sup> , Ionuț Jecu <sup>4</sup> , Gennady Sergienko <sup>1</sup> , Anna Widdowson <sup>4</sup> , Sahithya Atikukke <sup>5</sup> , Timo Dittmar <sup>1</sup> , Juuso Karhunen <sup>2</sup> , Pawel Gasior <sup>6</sup> , Marc Sackers <sup>1</sup> , Shweta Soni <sup>5</sup> , Erik Wüst <sup>1</sup> , Jelena Butikova <sup>7</sup> , Wojciech Gromelski <sup>6</sup> , Antti Hakola <sup>2</sup> , Indrek Jõgi <sup>8</sup> , Peeter Paris <sup>8</sup> , Jasper Ristkok <sup>8</sup> , Pavel Veis <sup>5</sup> , Sebastijan Brezinsek <sup>1</sup> , The UKAEA RACE Team <sup>4</sup>	
	<sup>1</sup> Forschungszentrum Jülich GmbH, Germany; <sup>2</sup> VTT Technical Research Centre of Finland Ltd, Finland; <sup>3</sup> ENEA, Diagnostics and Metrology Laboratory, Italy; <sup>4</sup> UKAEA, Culham Campus, United Kingdom; <sup>5</sup> Comenius University, Faculty of Math, Physics and Informatics, Slovakia; <sup>6</sup> Institute of Plasma Physics and Laser Microfusion, Poland; <sup>7</sup> Institute of Solid State Physics, University of Latvia, Latvia; <sup>8</sup> University of Tartu, Institute of Physics, Estonia.	
POB-13	<b>Current Status of High Heat Flux Testing at the HELCZA facility</b>	150
	Ladislav Vála, Richard Jílek, Tomáš Kubásek, Lukáš Toupal	
	Research Centre Řež (CVR), Czech Republic.	
POB-16	<b>Different tungsten structure divertor performance on EAST</b>	151
	Damao Yao	
	Institute of Plasma Physics, Hefei Institutes of Physical Science, Chinese Academy of Science, China.	
POB-17	<b>Interfacial mechanical properties of multilayer structures for high heat flux components of divertor</b>	151
	Qianqian Lin, Lei Cao, Damao Yao	
	Institute of Plasma Physics, Hefei Institutes of Physical Science, Chinese Academy of Sciences, China.	

POB-18	<b>Structure design and brazing technologies for HFS first wall on the NBI shine-through area of the EAST device</b> <u>Xianke Yang<sup>1</sup>, Damao Yao<sup>2</sup>, Lei Yin<sup>2</sup></u> <sup>1</sup> University of Science and Technology of China, China; <sup>2</sup> Institute of Plasma Physics, Hefei Institutes of Physical Science, Chinese Academy of Science, China.	152
POB-20	<b>Qualification activities of thermally sprayed W-coated small-scale steel mock-ups of the DTT first wall modules</b> <u>Maurizio Furno Palumbo<sup>1</sup>, Gabriele De Sano<sup>2</sup>, Riccardo De Luca<sup>3</sup>, Matteo Iafrati<sup>3</sup>, Paolo Innocente<sup>4</sup>, Laura Laguardia<sup>5</sup>, Damiano Paoletti<sup>2</sup>, Gian Mario Polli<sup>2</sup>, Bruno Riccardi<sup>2</sup>, Selanna Roccella<sup>3</sup>, Rudolf Neu<sup>6</sup>, Bradute-Eugen Ghidersa<sup>7</sup></u> <sup>1</sup> ENEA, Department of Fusion and Technology for Nuclear Safety and Security, Italy; <sup>2</sup> DTT S.c.a.r.l., Italy; <sup>3</sup> ENEA, Nuclear Department, Frascati, Italy; <sup>4</sup> CNR, Padova, Italy; <sup>5</sup> Istituto per la Scienza e Tecnologia dei Plasmi, CNR, Milano, Italy; <sup>6</sup> Max Planck Institute for Plasma Physics, Germany; <sup>7</sup> Karlsruhe Institute of Technology (KIT), Germany.	153
POB-23	<b>Engineering Overview of the Upgrade KSTAR Divertor System</b> <u>Sungjin Kwon<sup>1</sup>, Soo-Hyeon Park<sup>1</sup>, Yong Bok Chang<sup>1</sup>, Nak Hyong Song<sup>1</sup>, Hong-Tack Kim<sup>1</sup>, Sang Woo Kwag<sup>1</sup>, Hyung Ho Lee<sup>1</sup>, Jong Man Lee<sup>2</sup>, Hwnag Rae Cho<sup>2</sup>, Do Yoon Kim<sup>2</sup>, Soocheol Shin<sup>3</sup>, Henri Greuner<sup>4</sup>, Bernd Boeswirth<sup>4</sup></u> <sup>1</sup> Korea Institute of Fusion Energy, Korea, Republic of; <sup>2</sup> Vitzrotech Co. Ltd., Korea, Republic of; <sup>3</sup> Tae Sung S&E Inc., Korea, Republic of; <sup>4</sup> Max Planck Institute for Plasma Physics, Germany.	153
POB-24	<b>Experimental and numerical study on ratcheting effects of CuCrZr as heat sink in divertor monoblock</b> <u>Peng Liu</u> Institute of Plasma Physics, Hefei Institutes of Physical Science, China.	154
POB-25	<b>Manufacturing and high heat flux testing of advanced target mock-ups for the EU-DEMO Divertor target</b> <u>Pierdomenico Lorusso<sup>1</sup>, Selanna Roccella<sup>1</sup>, Mariano Di Bartolomeo<sup>1</sup>, Emanuele Cacciotti<sup>1</sup>, Marco Cerocchi<sup>1</sup>, Riccardo De Luca<sup>1</sup>, Luigi Verdini<sup>1</sup>, Katja Hunger<sup>2</sup>, Patrick Junghanns<sup>2</sup>, Alexander Von Mueller<sup>2</sup>, Henri Greuner<sup>2</sup>, Johann Riesch<sup>2</sup>, Jeong-Ha You<sup>2</sup></u> <sup>1</sup> ENEA, Nuclear Department, Frascati, Italy; <sup>2</sup> Max Planck Institute for Plasma Physics, Germany.	155
POB-26	<b>Tungsten Coating Options for Plasma-Facing Surfaces of an inertially cooled ITER First Wall</b> <u>Takeshi Hirai, Lei Chen, Franck Dechelette, Frederic Escourbiac, Ryan Hunt</u> ITER Organization, France.	155
POB-28	<b>A Blanket Component Test Facility at General Atomics to Advance Fusion Technologies</b> <u>Giacomo Dose, Brian Grierson, Paul Beharrell, Kenneth Khumthong, Bruce Lombardo, Panto Mitjaticovic, Nikolai Norausky, Mark Tillack, David Weisberg</u> General Atomics, United States.	156

## TOPIC: Low-Z and liquid materials

- POB-29 **Linear Stability of Liquid Metal Free-Surface Flows on Inclined and Cylindrical Substrates: Effects of Transverse Magnetic Fields** 157  
 Simone Mingozzi<sup>1</sup>, Eric Favre<sup>2</sup>, Ricardo Puente<sup>2</sup>, Thomas Morgan<sup>3</sup>, Alessandro Tassone<sup>4</sup>  
<sup>1</sup>Renaissance Fusion and Technical University of Eindhoven, France; <sup>2</sup>Renaissance Fusion, France; <sup>3</sup>Dutch Institute for Fundamental Energy Research, Netherlands; <sup>4</sup>Sapienza University of Rome, Italy.
- POB-30 **EMC3-EIRENE simulations of boron transport in wall conditioning experiments on EAST upgraded divertor** 157  
 Yan Qin<sup>1</sup>, Tian Xie<sup>1</sup>, Guizhong Zuo<sup>2</sup>, Wei Zhang<sup>2</sup>, Jiansheng Hu<sup>2</sup>, Yühe Feng<sup>3</sup>  
<sup>1</sup>Northeast Agricultural University, China; <sup>2</sup>Institute of Plasma Physics, Chinese Academy of Sciences, China; <sup>3</sup>Max-Planck-Institut für Plasmaphysik, Germany.
- POB-31 **Initial physics assessment of liquid lithium divertor for the DIII-D tokamak** 158  
 Gregory Sinclair, Tyler Abrams, Giacomo Dose  
 General Atomics, San Diego, United States.
- POB-32 **SOLPS-ITER Predictions for Upstream Impurity Concentration Dependence on Deuterium Recycling in the Spherical Tokamak Advanced Reactor (STAR)** 158  
 Eric Emdee, Thomas Brown, Robert Goldston, Andrei Khodak, Rajesh Maingi, Jonathan Menard  
 Princeton Plasma Physics Laboratory, United States.
- POB-33 **Impact of boron injection location on divertor heat flux in EAST wall conditioning experiments with EMC3-EIRENE modelling** 159  
 Baizeng Li<sup>1</sup>, Tian Xie<sup>1</sup>, Guizhong Zuo<sup>2</sup>, Wei Zhang<sup>2</sup>, Jiansheng Hu<sup>2</sup>, Yühe Feng<sup>3</sup>, Dezhen Wang<sup>4</sup>  
<sup>1</sup>Northeast Agricultural University, China; <sup>2</sup>Institute of Plasma Physics, Chinese Academy of Sciences, China; <sup>3</sup>Max-Planck-Institut für Plasmaphysik, Germany; <sup>4</sup>School of Physics, Dalian University of Technology, China.

## TOPIC: Materials under extreme thermal and particle loads

- POB-38 **Thermal shock resistance of a tungsten-diamond composite under extreme transient heat loads** 160  
 Christophe Guillemaut<sup>1</sup>, Marianne Richou<sup>1</sup>, Mathilde Diez<sup>1</sup>, Steven Lisgo<sup>2</sup>, Martiane Cabie<sup>3</sup>, Alan Durif<sup>1</sup>, Laurent Gallais<sup>4</sup>, Jean-Laurent Gardarein<sup>5</sup>, Jonathan Gaspar<sup>6</sup>, Benoit Guillermin<sup>1</sup>, Jamie Gunn<sup>1</sup>, Celine Martin<sup>5</sup>, Marco Minissale<sup>5</sup>, Gregory de Temmerman<sup>7</sup>  
<sup>1</sup>CEA, IRFM, France; <sup>2</sup>Independent Researcher, Canada; <sup>3</sup>Aix-Marseille Univ, CNRS, CP2M, France; <sup>4</sup>Aix-Marseille University, CNRS, Centrale Marseille, Institut Fresnel, France; <sup>5</sup>Aix-Marseille University, CNRS, PIIM, France; <sup>6</sup>CNRS, IUSTI, France; <sup>7</sup>Zenon Research, France.

POB-39	<b>Innovative STEAM Heat Shield for Ultra-High Heat Flux in Tokamak Divertors</b> <u>Jan Horacek</u> <sup>1</sup> , Vaclav Sedmidubsky <sup>2</sup> , Anna Horacek <sup>2</sup> , Jan Prevratil <sup>1</sup> , Maria Reji <sup>1</sup> , Tomas Plechacek <sup>2</sup> , Marek Janata <sup>1</sup> , Zdenek Kutilek <sup>1</sup> , Lukas Sedlacek <sup>1</sup> , Michal Bousek <sup>1</sup> , Tomas Romsy <sup>3</sup> , Pavel Zacha <sup>3</sup> , Zdenek Vesely <sup>4</sup> , Matej Hruska <sup>4</sup> , Jan Hruby <sup>5</sup> , Matěj Peterka <sup>1</sup> , Slavomir Entler <sup>1</sup> <sup>1</sup> Institute of Plasma Physics, Czech Academy of Sciences, Czech Republic; <sup>2</sup> Faculty of Nuclear Sciences, Czech Technical University, Czech Republic; <sup>3</sup> Faculty of Mechanical Engineering, Czech Technical University, Czech Republic; <sup>4</sup> New Technologies Research Centre, University of West Bohemia, Czech Republic; <sup>5</sup> Institute of Thermomechanics, Czech Academy of Sciences, Czech Republic.	161
POB-40	<b>Thermal analysis of the W/Cu flat-type component as the lower divertor target in EAST</b> <u>Junling Chen</u> , Dahuan Zhu, Chunyu He, Binfu Gao, Wenxue Fu, Rui Ding Institute of Plasma Physics, Chinese Academy of Sciences, China.	161
POB-43	<b>Thermal fatigue study of different advanced tungsten materials at a wide Gaussian power density distribution at the OLMAT high heat flux facility</b> Daniel Alegre <sup>1</sup> , Pablo Fernández-Mayo <sup>1</sup> , David Tafalla <sup>1</sup> , Alfonso De Castro <sup>1</sup> , Jesus G. Manchon <sup>1</sup> , Sophie Shick <sup>1</sup> , Carmen Garcia Rosales <sup>2</sup> , Elisa Sal <sup>2</sup> , Marius Wirtz <sup>3</sup> , Jan Coenen <sup>3</sup> , Yiran Mao <sup>3</sup> , Eider Oyarzabal <sup>1</sup> , The OLMAT Team <sup>1</sup> <sup>1</sup> Laboratorio Nacional de Fusion, CIEMAT, Spain; <sup>2</sup> Ceit Technology Center (Centro de Estudios e Investigaciones Técnicas), Spain; <sup>3</sup> Forschungszentrum Jülich GmbH, Germany.	162
POB-44	<b>Optical Spectroscopy as a diagnostic tool at the high heat flux test facility GLADIS</b> <u>Hans Maier</u> <sup>1</sup> , Henri Greuner <sup>1</sup> , Johann Riesch <sup>1</sup> , Bernd Boeswirth <sup>1</sup> , Rudolf Neu <sup>1</sup> , Adam Kuang <sup>2</sup> , Jason Trelewicz <sup>3</sup> <sup>1</sup> Max Planck Institute for Plasma Physics, Germany; <sup>2</sup> Commonwealth Fusion Systems, MA, United States; <sup>3</sup> Stony Brook University, NY, United States.	163
POB-45	<b>Development of inhomogeneous high heat flux loading pattern for mimicking loading conditions of plasma-facing materials in tokamaks</b> <u>Daniel Dorow-Gerspach</u> <sup>1</sup> , Renaud Dejarnac <sup>2</sup> , Gerald Pintsuk <sup>1</sup> , Marius Wirtz <sup>1</sup> , Christian Linsmeier <sup>1</sup> <sup>1</sup> Forschungszentrum Jülich GmbH, Germany; <sup>2</sup> Institute of Plasma Physics of the Czech Academy of Sciences, Czech Republic.	163
POB-46	<b>Mechanical and Microstructural Characterization of Structural Materials for Nuclear Applications with Inverse Finite Element Analysis</b> <u>David Bermudez Parra</u> <sup>1</sup> , Dmitry Terentyev <sup>2</sup> , David Garoz <sup>3</sup> <sup>1</sup> Belgian Nuclear Research Centre SCKCEN, Belgium, and Universidad Politécnica de Madrid, Spain; <sup>2</sup> Belgian Nuclear Research Centre SCKCEN, and Ghent University, Belgium; <sup>3</sup> Escuela Técnica Superior de Ingenieros Industriales, UPM, Spain.	164
POB-47	<b>Investigating heat flux behavior and power dissipation in the Shape and Volume Rise divertor of DIII-D</b> <u>Jun Ren</u> <sup>1</sup> , Robert Wilcox <sup>2</sup> , Huiqian Wang <sup>3</sup> , Ryan Hood <sup>4</sup> , Cedric Tsui <sup>4</sup> , Morgan Shafer <sup>2</sup> , Suk-Ho Hong <sup>3</sup> , David Christian Donovan <sup>1</sup> <sup>1</sup> University of Tennessee, Knoxville, United States; <sup>2</sup> Oak Ridge National Laboratory, United States; <sup>3</sup> General Atomics, United States; <sup>4</sup> Sandia National Laboratories, Livermore, United States.	165

POB-48	<b>Performance of recrystallized and molten Tungsten surfaces under fusion relevant loads</b>	166
	<u>Marius Wirtz</u> , Mauricio Gago, Gerald Pintsuk, Bernhard Unterberg Forschungszentrum Jülich GmbH, Germany.	
POB-49	<b>Design challenges for the COMPASS Upgrade closed tungsten divertor</b>	166
	<u>Mikulas Durovec</u> <sup>1</sup> , Renaud Dejarnac <sup>1</sup> , Petr Vondracek <sup>1</sup> , Philippe Chappuis <sup>2</sup> , David Sestak <sup>1</sup> <sup>1</sup> Institute of Plasma Physics of the Czech Academy of Sciences, Czech Republic; <sup>2</sup> CHAPS Engineering, France.	
POB-50	<b>High Heat Flux Testing of Erosion Markers: Electrical Resistivity and Alumina Diffusion in Tungsten via Four-Point Probe</b>	167
	<u>Amelia Deleau</u> <sup>1</sup> , Caroline Hernandez <sup>1</sup> , Anastasios Skarlatos <sup>2</sup> , Zarel Valdez-Nava <sup>3</sup> , David Malec <sup>3</sup> <sup>1</sup> CEA, IRFM, France; <sup>2</sup> Cea Saclay laboratoire DIGITEO, France; <sup>3</sup> Université Toulouse Paul Sabatier, France.	
POB-51	<b>Modelling of RE induced damage of BN tiles of WEST inner limiter</b>	168
	<u>Tommaso Rizzi</u> <sup>1</sup> , Svetlana Ratynskaia <sup>1</sup> , Panagiotis Tolias <sup>1</sup> , Yann Corre <sup>2</sup> , Mathilde Diez <sup>2</sup> , Mehdi Firdaouss <sup>2</sup> , Jonathan Gerardin <sup>2</sup> , Raphael Mitteau <sup>2</sup> , Cédric Reux <sup>2</sup> <sup>1</sup> KTH Royal Institute of Technology, Sweden; <sup>2</sup> CEA, IRFM, France.	
POB-52	<b>JT-60SA Divertor: Combining Advanced Simulation and Additive Manufacturing to propose an Enhanced Design for a Tungsten Actively Cooled Divertor</b>	169
	<u>Diogo Dias Aleixo</u> <sup>1</sup> , Mehdi Firdaouss <sup>1</sup> , Thierry Baffie <sup>2</sup> , Pierre-Eric Frayssines <sup>2</sup> , Hervé Gleyzes <sup>2</sup> , Pierre Lechevalier <sup>1</sup> , Alizée Thomas <sup>2</sup> , Valerio Tomarchio <sup>3</sup> , Marianne Richou <sup>1</sup> <sup>1</sup> CEA, IRFM, France; <sup>2</sup> Université Grenoble Alpes, France; <sup>3</sup> F4E, Germany.	
POB-53	<b>Melting threshold at toroidal gaps of ITER divertor monoblocks under repetitive ELM transients</b>	170
	<u>Konstantinos Paschalidis</u> <sup>1</sup> , Svetlana Ratynskaia <sup>1</sup> , Panagiotis Tolias <sup>1</sup> , Richard Pitts <sup>2</sup> <sup>1</sup> KTH Royal Institute of Technology, Sweden; <sup>2</sup> ITER Organization, France.	

## TOPIC: Fuel retention and removal

POB-54	<b>ps Laser Induced Breakdown Spectroscopy and Mass Spectrometry - Deuterium depth resolution, removal fraction and uncertainties</b>	170
	<u>Sören Möller</u> <sup>1</sup> , <u>Christoph Kawan</u> <sup>1</sup> , Arkadi Kreter <sup>1</sup> , Gennady Sergienko <sup>1</sup> , Marcin Rasinski <sup>1</sup> , Erik Wüst <sup>1</sup> , Sebastijan Brezinsek <sup>1</sup> , Eduard Grigore <sup>2</sup> <sup>1</sup> Forschungszentrum Jülich GmbH, Germany; <sup>2</sup> Acasa Institutul National pentru Fizica Laserilor, Plasmei si Radiatiei, Romania.	
POB-55	<b>Deuterium Uptake and Isotope Exchange in Tungsten Displacement-damaged at High Temperature</b>	171
	<u>Laurin Hess</u> , Thomas Schwarz-Selinger Max Planck Institute for Plasma Physics, Germany.	
POB-56	<b>Deuterium Retention in Boron-Based Codesposits</b>	172
	<u>James Davis</u> , Hikaru Tanaka, Steven Theriault, Eric Nicholson University of Toronto, Canada.	

POB-59	<b>Hydrogen isotope interaction in laboratory boron layers</b> <u>Eduard Warkentin</u> , Anne Houben, Marcin Rasinski, Hans Rudolf Koslowski, Timo Dittmar, Arkadi Kreter, Bernhard Unterberg, Christian Linsmeier Forschungszentrum Jülich GmbH, Germany.	173
POB-60	<b>Fuel imbalance and accumulation of protium in a fusion power reactor</b> <u>Yuri Igitchkanov</u> , Thomas Giegerich Karlsruhe Institute of Technology, Germany.	173
POB-61	<b>Dynamics of Deuterium Retention in Tungsten and Deposited Boron Thin Films During Plasma Exposure Using In-Operando Nuclear Reaction Analysis in DIONISOS</b> <u>Joey Demiane</u> <sup>1</sup> , Camila Lopez Perez <sup>2</sup> , Kevin Woller <sup>1</sup> <sup>1</sup> MIT – PSFC, United States; <sup>2</sup> Ken and Mary Alice Lindquist Department of Nuclear Engineering, Pennsylvania State University, United States.	174
POB-62	<b>The effect of surface-near helium on deuterium retention in EUROFER</b> <u>Sabina Markelj</u> <sup>1</sup> , Thomas Schwarz-Selinger <sup>2</sup> , Janez Zavašnik <sup>1</sup> , Andreja Šestan Zavašnik <sup>1</sup> <sup>1</sup> Jožef Stefan Institute, Slovenia; <sup>2</sup> Max-Planck-Institut für Plasmaphysik, Germany.	174
POB-63	<b>A critical overview of ion beam methods for the determination of H isotopes in reactor materials: depth profiling and micro-beam analysis aspects</b> <u>Marek Rubel</u> <sup>1</sup> , Laura Dittrich <sup>1</sup> , Sunwoo Moon <sup>1</sup> , Per Petersson <sup>1</sup> , Eduardo Pitthan <sup>2</sup> , Daniel Primetzhofer <sup>2</sup> , Anna Widdowson <sup>3</sup> <sup>1</sup> KTH Royal Institute of Technology, Sweden; <sup>2</sup> Uppsala University, Sweden; <sup>3</sup> UKAEA, Culham Campus, Abingdon, United Kingdom.	175

## TOPIC: Erosion, re-deposition, mixing, and dust formation

POB-64	<b>Application of the ERO2.0 Code to Plasma-Material Interaction Studies in GyM and BiGyM Devices</b> <u>Francesco Cani</u> , Irene Casiraghi, Anna Cremona, Daria Ricci, Laura Laguardia, Andrea Uccello Istituto per la Scienza e Tecnologia dei Plasmi, CNR, Milano, Italy.	176
POB-66	<b>Modelling of boron dust with the MIGRAINE code</b> <u>Lorenzo Boccaccia</u> , Panagiotis Tolas, Svetlana Ratynskaia, Ladislav Vignitchouk KTH Royal Institute of Technology, Sweden.	177
POB-67	<b>Examination of plasma-induced surface morphology using spectroscopic ellipsometry</b> <u>Daisuke Nishijima</u> <sup>1</sup> , Mitsutaka Miyamoto <sup>2</sup> , Matt Baldwin <sup>1</sup> , George Tynan <sup>1</sup> <sup>1</sup> University of California San Diego, United States; <sup>2</sup> Shimane University, Japan.	177
POB-68	<b>Sputtering of Tungsten Surfaces by Different Ion Types: A Molecular Dynamics Simulation Approach</b> <u>Faith Kporha</u> , Fredric Granberg University of Helsinki, Finland.	178



POB-70	<b>Comparison of methods for erosion/redeposition measurements of plasma-facing components in fusion devices</b> <u>Caroline Hernandez</u> , Amelia Deleau, Mathilde Diez, Etienne Delmas, Mehdi Firdaouss, Marianne Richou CEA, IRFM, France.	179
POB-71	<b>Tungsten erosion and injection investigations in the stellarator Wendelstein 7-X during OP2.2</b> <u>Chandra Prakash Dhard</u> <sup>1</sup> , Sebastijan Brezinsek <sup>2</sup> , René Bussiahn <sup>1</sup> , Birger Buttenschön <sup>1</sup> , Dario Cipciar <sup>1</sup> , David Ennis <sup>3</sup> , Joris Fellingner <sup>1</sup> , Erik Flom <sup>4</sup> , Tomasz Fornal <sup>5</sup> , Yu Gao <sup>1</sup> , Isabel Garcia-Cortés <sup>6</sup> , Dorothea Gradic <sup>1</sup> , Tomas Gonda <sup>3</sup> , Carsten Killer <sup>1</sup> , Alexander Knieps <sup>2</sup> , Petra Kornejew <sup>1</sup> , David Kriete <sup>3</sup> , Maciej Krychowiak <sup>1</sup> , Oleksandr Marchuk <sup>2</sup> , Andreas Langenberg <sup>1</sup> , Kieran Joseph McCarthy <sup>6</sup> , Daniel Medina-Roque <sup>6</sup> , Dirk Naujoks <sup>1</sup> , Novimir Pablant <sup>7</sup> , Arun Pandey <sup>1</sup> , Mohammad Foisal Siddiki <sup>8</sup> , Lukasz Syrocki <sup>5</sup> , Naoki Tamura <sup>1</sup> , Sebastian Thiede <sup>1</sup> , Thomas Wegner <sup>1</sup> , The W7-X Team <sup>1</sup> <sup>1</sup> Max Planck Institute for Plasma Physics, Germany; <sup>2</sup> Forschungszentrum Jülich GmbH, Germany; <sup>3</sup> Auburn University, AL, United States; <sup>4</sup> Thea Energy, Kearny, United States; <sup>5</sup> Institute of Plasma Physics and Laser Microfusion, Poland; <sup>6</sup> Laboratorio Nacional de Fusión, CIEMAT, Spain; <sup>7</sup> Princeton Plasma Physics Laboratory, United States; <sup>8</sup> University of Wisconsin-Madison, United States.	180
POB-73	<b>Progress on ELM and inter-ELM tungsten erosion &amp; re-deposition measurements in the DIII-D tokamak using ultraviolet spectroscopy</b> <u>Ulises Losada</u> <sup>1</sup> , David Ennis <sup>1</sup> , Stuart Loch <sup>1</sup> , Dane van Tol <sup>1</sup> , Tyler Abrams <sup>2</sup> , Adam McLean <sup>3</sup> , Gilson Ronchi <sup>4</sup> , Dmitry Rudakov <sup>5</sup> , William Wampler <sup>6</sup> , David Kriete <sup>1</sup> <sup>1</sup> Auburn University, AL, United States; <sup>2</sup> General Atomics, United States; <sup>3</sup> Lawrence Livermore National Laboratory, United States; <sup>4</sup> Oak Ridge National Laboratories, TN, United States; <sup>5</sup> University of California San Diego, United States; <sup>6</sup> Sandia National Laboratories, NM, United States.	181
POB-74	<b>Insulator thickness dependence on RF sheath-induced sputtering</b> <u>Gayatri Dhamale</u> <sup>1</sup> , Marlene Patino <sup>2</sup> , James Myra <sup>3</sup> , Matt Baldwin <sup>2</sup> , George Tynan <sup>2</sup> , Juergen Rapp <sup>1</sup> <sup>1</sup> Oak Ridge National Laboratory, United States; <sup>2</sup> University of California San Diego, United States; <sup>3</sup> Lodestar Research Corporation, United States.	182
POB-75	<b>Effects of surface roughness on sputter yield of Mo under laboratory and tokamak conditions</b> <u>Mitja Kelemen</u> <sup>1</sup> , Sabina Markelj <sup>1</sup> , Karl Krieger <sup>2</sup> , Thomas Schwarz-Selinger <sup>2</sup> , Espedito Vassallo <sup>3</sup> , David Dellasega <sup>4</sup> , Matteo Passoni <sup>4</sup> , Antti Hakola <sup>5</sup> , Martin Balden <sup>2</sup> , Andreas Mutzke <sup>2</sup> , Primož Pelicon <sup>1</sup> , Rok Zaplotnik <sup>1</sup> , The ASDEX UPGRADE Team <sup>6</sup> , The EUROfusion Tokamak Exploitation Team <sup>7</sup> <sup>1</sup> Jožef Stefan Institute, Slovenia; <sup>2</sup> Max Planck Institute for Plasma Physics, Germany; <sup>3</sup> Istituto per la Scienza e Tecnologia dei Plasmi, CNR, Italy; <sup>4</sup> Politecnico di Milano, Italy; <sup>5</sup> VTT Technical Research Centre of Finland Ltd, Espoo, Finland; <sup>6</sup> see author list of H. Zohm et al, 2024 Nucl. Fusion 64 112001, Germany; <sup>7</sup> see author list of E. Joffrin et al 2024 Nucl. Fusion 64 112019, Germany.	182
POB-76	<b>Plasma-chemical mechanism of surface destruction of the diagnostic system components inside EAST vacuum vessel</b> <u>Lidia Lobanova</u> , Shouxin Wang, Hui Lian, Xiaoqian Cui, Jihui Chen, Rong Yan, Ling Zhang, Viktor Afanas'ev, Haiqing Liu Institute of Plasma Physics, Chinese Academy of Sciences, China.	183
POB-77	<b>ERO2.0 modelling of divertor marker erosion in ASDEX Upgrade L-mode</b> <u>Samuli Saari</u> <sup>1</sup> , Antti Hakola <sup>1</sup> , Juuso Karhunen <sup>1</sup> , Martin Balden <sup>2</sup> , Christoph Baumann <sup>2</sup> , Aaro Järvinen <sup>1</sup> , Karl Krieger <sup>2</sup> , Henri Kumpulainen <sup>2</sup> , Jari Likonen <sup>1</sup> , Juri Romazanov <sup>2</sup> <sup>1</sup> VTT Technical Research Centre of Finland, Finland; <sup>2</sup> Forschungszentrum Jülich GmbH, Germany.	184

POB-78	<b>First Coupling of SOLEDGE3X-QLKNN10D: Integrated W Modelling Accounting for Neoclassical Effects</b>	185
--------	---	-----

Naren Varadarajan, Guido Ciraolo, Hugo Bufferand, Pierre Manas, Luca Cappelli, Nicolas Rivals, Patrick Tamain, Srikanth Sureshkumar, Ludovica de Gianni, Virginia Quadri, Nicolas Fedorczak  
CEA, IRFM, France.

POB-79	<b>Evolution of elemental depth profiles on co-deposited layers at the divertor region of the WEST tokamak during its Phase 1 operations</b>	185
--------	--	-----

Antti Hakola<sup>1</sup>, Jari Likonon<sup>1</sup>, Tomi Vuoriheimo<sup>2</sup>, Eduard Grigore<sup>3</sup>, Indrek Jõgi<sup>4</sup>, Peeter Paris<sup>4</sup>, Elodie Bernard<sup>5</sup>, Mathilde Diez<sup>5</sup>, Emmanuelle Tsitrone<sup>5</sup>

<sup>1</sup>VTT Technical Research Centre of Finland Ltd, Finland; <sup>2</sup>Department of Physics, University of Helsinki, Finland; <sup>3</sup>Acasa Institutul National pentru Fizica Laserilor, Plasmei si Radiatiei, Romania; <sup>4</sup>University of Tartu, Institute of Physics, Estonia; <sup>5</sup>CEA, IRFM, France.

## TOPIC: Tungsten, tungsten alloys, and advanced steels

POB-80	<b>Impact of helium plasma implantation on tungsten softening approach- ing detached plasma conditions at the divertor region</b>	186
--------	---	-----

Anthony Flament<sup>1</sup>, Maxime Lemetais<sup>2</sup>, Alan Durif<sup>1</sup>, Federica Pappalardo<sup>3</sup>, Marco Minissale<sup>3</sup>, Laurent Gallais<sup>3</sup>, Guillaume Kermouche<sup>2</sup>, Marianne Richou<sup>1</sup>

<sup>1</sup>CEA, IRFM, France; <sup>2</sup>Mines Saint-Etienne, CNRS UMR 5307 LGF, France; <sup>3</sup>Aix-Marseille Université, CNRS, PIIM, France.

POB-81	<b>Thermophysical and thermomechanical properties of Tungsten-based (W-Ti-Ta-Cr-V) High-Entropy Alloys</b>	187
--------	--	-----

Zori Harutyunyan

Imperial College London, United Kingdom.

POB-82	<b>Impact of Phase Decomposition on Performance of SMART Tungsten- Based Alloys for a First Wall of DEMO</b>	188
--------	--	-----

Duc Nguyen-Manh<sup>1</sup>, Eric Prestat<sup>1</sup>, Mark Gilbert<sup>1</sup>, Damian Sobieraj<sup>2</sup>, Jan Wrobel<sup>2</sup>, Jie Chen<sup>3</sup>, Andrey Litnovsky<sup>3</sup>

<sup>1</sup>United Kingdom Atomic Energy Authority (UKAEA), United Kingdom; <sup>2</sup>Warsaw University of Technology, Poland; <sup>3</sup>Forschungszentrum Jülich GmbH, Germany.

POB-83	<b>First attempts for industrialization of tungsten fiber-reinforced tungsten composites</b>	189
--------	--	-----

Yiran Mao<sup>1</sup>, Ute Wilkinson<sup>2</sup>, Jan Coenen<sup>1</sup>, Daniel Wilkinson<sup>2</sup>, Johann Riesch<sup>3</sup>, Christian Linsmeier<sup>1</sup>

<sup>1</sup>Forschungszentrum Jülich GmbH, Germany; <sup>2</sup>Dr. Fritsch Sondermaschinen GmbH, Germany; <sup>3</sup>Max Planck Institute for Plasma Physics, Germany.

POB-84	<b>Recent Advances in Tungsten Fiber-Reinforced Composites for Fusion Reactor Applications</b>	189
--------	--	-----

Jan Coenen<sup>1</sup>, Yiran Mao<sup>1</sup>, Alexander Lau<sup>1</sup>, Rui Shu<sup>1</sup>, Juan Du<sup>2</sup>, Johann Riesch<sup>3</sup>, Christian Linsmeier<sup>1</sup>

<sup>1</sup>Forschungszentrum Jülich GmbH, Germany; <sup>2</sup>Southwestern Institute of Physics, Chengdu, China; <sup>3</sup>Max Planck Institute for Plasma Physics, Germany.

POB-85	<b>Evaluation of hydrogen isotopes desorption dynamics for tungsten rhenium alloy</b> <u>Yuzuka Hoshino</u> <sup>1</sup> , Robert Kolasinski <sup>2</sup> , Yasuhisa Oya <sup>1</sup> <sup>1</sup> Shizuoka University, Japan; <sup>2</sup> Sandia National Laboratories, United States.	190
POB-88	<b>Evidence for sputtering of D and O adsorbed on W(110) by a D<sub>2</sub><sup>+</sup> ion beam</b> <u>Latournerie Matthieu</u> , Thierry Angot, Eric Salomon, Marco Minissale, Regis Bisson Aix-Marseille Université, CNRS, PIIM, France.	191
POB-89	<b>Applications of a newly developed tungsten-boron potential</b> <u>Nima Fakhrai Mofrad</u> , Antoine Clement, Andrea Sand Aalto University, Finland.	192
POB-90	<b>Development of W<sub>2</sub>C-reinforced W for a plasma-facing armour material</b> <u>Petra Jenuš</u> <sup>1</sup> , Sabina Markelj <sup>1</sup> , Anže Abram <sup>1</sup> , Andreja Šestan Zavašnik <sup>1</sup> , Aleksander Učakar <sup>1</sup> , Andrei Galatanu <sup>2</sup> , Magdalena Galatanu <sup>2</sup> , Elena Tejado <sup>3</sup> , José Y.Pastor <sup>3</sup> , Marius Wirtz <sup>4</sup> , Gerald Pintsuk <sup>4</sup> , Aljaž Iveković <sup>1</sup> <sup>1</sup> Jožef Stefan Institute, Slovenia; <sup>2</sup> 4 National Institute of Materials Physics, Romania; <sup>3</sup> Departamento de Ciencia de Materiales-CIME, ETSI Caminos, Canales y Puertos, Universidad Politecnica de Madrid, Spain; <sup>4</sup> Forschungszentrum Jülich GmbH, Germany.	192
POB-91	<b>Manufacturing of Potassium-doped Tungsten ITER-type monoblock PFC mock-up for the high heat flux test</b> <u>Eunnam Bang</u> <sup>1</sup> , Hyoung Chan Kim <sup>1</sup> , Jeongseok Kim <sup>2</sup> , Heung Nam Han <sup>2</sup> <sup>1</sup> Korea Institute of Fusion Energy (KFE), Korea, Republic of; <sup>2</sup> Seoul National University (SNU), Korea, Republic of.	193
POB-92	<b>Growth of deuterium supersaturated surface layer with increasing ion flux and fluence in plasma-exposed tungsten</b> <u>Anže Založnik</u> <sup>1</sup> , Witold Chromiński <sup>2</sup> , Łukasz Ciupiński <sup>2</sup> , Thomas Schwarz-Selinger <sup>3</sup> , Daisuke Nishijima <sup>1</sup> , Marlene Patino <sup>1</sup> , Michael Simmonds <sup>1</sup> , Matt Baldwin <sup>1</sup> , George Tynan <sup>1</sup> <sup>1</sup> University of California San Diego, United States; <sup>2</sup> Faculty of Materials Science and Engineering, Warsaw University of Technology, Poland; <sup>3</sup> Max-Planck-Institut für Plasmaphysik, Germany.	194
POB-93	<b>Defect production in tungsten under sub-threshold energy irradiation: Role of hydrogen and surface effects</b> Hao-Xuan Huang, Yuhao Li, Hongbo Zhou, <u>Guang-Hong Lu</u> Beihang University, China.	195
POB-94	<b>Synergy of helium ion irradiation and thermal annealing in tungsten: a combined effort of experiment and simulation</b> Jiaguan Peng <sup>1</sup> , <u>Long Cheng</u> <sup>1</sup> , Hongxian Xie <sup>2</sup> , Xiuli Zhu <sup>3</sup> , Xiancai Meng <sup>4</sup> , Yuhao Li <sup>1</sup> , Linyun Liang <sup>1</sup> , Sijie Hao <sup>1</sup> , Zheng Wang <sup>1</sup> , Yue Yuan <sup>1</sup> , Hongbo Zhou <sup>1</sup> , Guang-Hong Lu <sup>1</sup> <sup>1</sup> Beihang University, China; <sup>2</sup> Hebei University of Technology, China; <sup>3</sup> North China Electric Power University, China; <sup>4</sup> Institute of Plasma Physics, Chinese Academy of Sciences, China.	196
POB-95	<b>Fatigue Crack Propagation in Plasma Facing Materials – A case study on ITER grade Tungsten</b> <u>Stefan Wurster</u> <sup>1</sup> , Michael Pegritz <sup>1</sup> , Reinhard Pippan <sup>1</sup> , Anton Hohenwarter <sup>2</sup> <sup>1</sup> Erich Schmid Institute of Materials Science, Austrian Academy of Sciences, Austria; <sup>2</sup> Department of Materials Science, Chair of Materials Physics, Montanuniversität Leoben, Austria.	196

POB-96	<b>Development of Functionally Graded Copper-Tungsten Composite Coatings Through Collaboration Between IPP Prague and IPP Greifswald</b> <u>Jakub Klecka</u> <sup>1</sup> , Joris Fellingner <sup>2</sup> , Frantisek Lukac <sup>1</sup> , Petr Kralicek <sup>1</sup> , Jonas Dudik <sup>1</sup> <sup>1</sup> Institute of Plasma Physics of the Czech Academy of Sciences, Czech Republic; <sup>2</sup> Max Planck Institute for Plasma Physics, Germany.	197
POB-97	<b>Interaction of molten fluoride salts with tungsten-coated structural materials</b> <u>Luigi Bana</u> <sup>1</sup> , Davide Vavassori <sup>1</sup> , Nayoung Kim <sup>2</sup> , Weiyue Zhou <sup>2</sup> , Michael Short <sup>2</sup> , David Dellasega <sup>1</sup> , Matteo Passoni <sup>1</sup> <sup>1</sup> Politecnico di Milano, Italy; <sup>2</sup> Department of Nuclear Science and Engineering, Massachusetts Institute of Technology, United States.	198
POB-98	<b>Nanosecond laser ablation modelling applied to LIBS diagnostics</b> Stefano Cipelli <sup>1</sup> , Domenico Aceto <sup>2</sup> , Paolo Francesco Ambrico <sup>2</sup> , Irene Casiraghi <sup>3</sup> , Anna Cremona <sup>3</sup> , Olga De Pascale <sup>2</sup> , Giorgio DiLecce <sup>2</sup> , Arshad Hussain <sup>4</sup> , Laura Laguardia <sup>3</sup> , Matteo Pedroni <sup>3</sup> , Daria Ricci <sup>3</sup> , Dario Ripamonti <sup>5</sup> , Jimmy Scionti <sup>3</sup> , Andrea Uccello <sup>3</sup> <sup>1</sup> CRF – Università degli Studi di Padova, Padova, Italy; <sup>2</sup> Institute for Plasma Science and Technology, CNR, Bari, Italy; <sup>3</sup> Istituto per la Scienza e Tecnologia dei Plasmi, CNR, Milano, Italy; <sup>4</sup> Fusion Research Center, University of Padua, Italy; <sup>5</sup> Institute of Condensed Matter Chemistry and Energy Technologies, CNR, Milan, Italy.	199
POB-99	<b>Detailed analysis of helium and hydrogen isotopes in bubbles formed in tungsten by STEM-EELS</b> <u>Mitsutaka Miyamoto</u> <sup>1</sup> , Shinsuke Okubo <sup>1</sup> , Mitsutaka Haruta <sup>2</sup> <sup>1</sup> Shimane University, Japan; <sup>2</sup> Kyoto University, Japan.	200
POB-100	<b>Development of Eurofer97 steel powder for additive manufacturing of fusion components</b> <u>Xinjiang Hao</u> , Adam Hunt Globus Metal Powders Ltd, United Kingdom.	201

**INVITED  
AND  
REGULAR  
ORAL  
LECTURES'  
ABSTRACTS**

## Session 1: Fuel retention and removal

20 May, 9:00 – 10:50

I-1

### Progress in the understanding of fuel retention and inventory management in the full-tungsten ITER

Tom Wauters<sup>1</sup>, Remi Delaporthe-Mathurin<sup>2</sup>, Kaelyn Dunnell<sup>2</sup>, Etienne Hodille<sup>3</sup>, Stepan Krat<sup>4</sup>, Hao-Dong Liu<sup>5</sup>, Alberto Loarte<sup>1</sup>, Dmitry Matveev<sup>6</sup>, Jonathan Mougenot<sup>7</sup>, Richard Pitts<sup>1</sup>, Klaus Schmid<sup>8</sup>

<sup>1</sup>ITER Organization, France; <sup>2</sup>Plasma Science and Fusion Center, MIT, United States; <sup>3</sup>CEA, IRFM, France; <sup>4</sup>National Research Nuclear University MEPhI, Russian Federation; <sup>5</sup>Institute of Plasma Physics, Chinese Academy of Sciences, China; <sup>6</sup>Forschungszentrum Jülich GmbH, Germany; <sup>7</sup>Universite Sorbonne Paris Nord, CNRS, France; <sup>8</sup>Max-Planck-Institut für Plasmaphysik, Germany.

Fuel inventory management in ITER's new baseline is significantly influenced by the transition from beryllium (Be) to tungsten (W) as the first wall material, alongside the implementation of a diborane Glow Discharge Conditioning (GDC) boronization system. Boron (B) replaces the gettering function of Be, aiming to lower impurity influx and mitigate risks associated with achieving  $Q = 10$ . The primary factor driving tritium (T) inventory buildup in the re-baseline is retention in B deposits. This talk discusses the analysis conducted to define the ITER fuel recovery strategy, with a focus on hydrogen retention, B layer dynamics, and fuel removal methods. A recent review of hydrogen retention in laboratory B layers has been extended with magnetron sputtered layer results, confirming that ITER's conservative inventory estimate (0.5 H,D,T/B) remains valid. Updated WalIDYN3D simulations of B layer erosion and migration with improved description of thin layers confirm that boronization cycles in ITER last up to two weeks, with the possibility of longer intervals being feasible. Strong deposition is initially observed at the divertor baffles where up to 2.8 microns of B accumulate per boronization cycle.

Baking at temperatures up to 240°C, applied between campaigns, is ineffective for thick B layers (>10 microns) which accumulate through multiple boronization cycles. Tokamak plasmas with Raised Inner Strike Points (RISP) are effective in recovering fuel from thin layers on the inner divertor target due to strong heating by plasma, and can be applied before a new boronization layer is deposited. Ion Cyclotron Wall Conditioning (ICWC) depletes T from the near-surface layers of both W and B (~100 nm) within a pulse sequence of ~20 minutes at a 15% duty cycle. ICWC effectively controls the T content in subsequent tokamak plasmas and is planned to be applied in combination with RISP plasmas to minimize redeposition during RISP pulses.

T permeation to the water coolant loops occurs predominantly during baking periods. Whilst it is low through W PFCs unless they are exposed to very high temperatures, significant permeation can occur through stainless steel 316L. A parametric study on plasma-driven permeation in ITER-like conditions, including different material parameters, baking conditions and barrier coatings is being undertaken to improve understanding of means to mitigate permeation risks in ITER.

The Hydrogen Inventory Simulations for PFCs (HISP) tool is being developed to evaluate the dynamic T inventory alongside fuel removal strategies, comparing different scenarios using RISP, ICWC, GDC, and baking. First results suggest that an inventory reduction of up to 70–80% may be achievable compared to the estimated worst case fuel retention scenario in the absence of any active fuel recovery strategy.

## **First Demonstration of Laser Induced Breakdown Spectroscopy using Remote Handling for In-vessel Analysis of Tritiated and Activated JET Components**

Jari Likonen<sup>1</sup>, Salvatore Almagia<sup>2</sup>, Rahul Rayaprolu<sup>3</sup>, Rongxing Yi<sup>3</sup>, Ionut Jecu<sup>4</sup>, Gennady Sergienko<sup>3</sup>, Anna Widdowson<sup>4</sup>, Nick Jones<sup>4</sup>, Sahithya Atikukke<sup>5</sup>, Timo Dittmar<sup>3</sup>, Juuso Karhunen<sup>1</sup>, Pawel Gasior<sup>6</sup>, Christoph Kawan<sup>3</sup>, Marc Sackers<sup>3</sup>, Shweta Soni<sup>5</sup>, Erik Wüst<sup>3</sup>, Sebastijan Brezinsek<sup>3</sup>, Jelena Butikova<sup>7</sup>, Wojciech Gromelski<sup>6</sup>, Antti Hakola<sup>1</sup>, Indrek Jõgi<sup>8</sup>, Peeter Paris<sup>8</sup>, Jasper Ristkok<sup>8</sup>, Pavel Veis<sup>5</sup>, The UKAEA RACE Team<sup>9</sup>

<sup>1</sup>VTT Technical Research Centre of Finland Ltd., Finland; <sup>2</sup>ENEA, Italy; <sup>3</sup>Forschungszentrum Jülich GmbH, Germany; <sup>4</sup>United Kingdom Atomic Energy Authority, Culham Campus, Abingdon, United Kingdom; <sup>5</sup>Comenius University, Slovakia; <sup>6</sup>Institute of Plasma Physics and Laser Microfusion, Poland; <sup>7</sup>University of Latvia, Institute of Solid State Physics, Latvia; <sup>8</sup>University of Tartu, Institute of Physics, Estonia; <sup>9</sup>UKAEA RACE Team, United Kingdom.

The feasibility of laser-induced breakdown spectroscopy (LIBS) for measuring fuel retention was demonstrated for the first time in a tokamak operating with tritium using a remotely controlled in situ application in JET. In JET and future fusion reactors such as ITER and DEMO, thick co-deposited layers will be formed at the inner wall during extended plasma operations. Experiments in present-day fusion devices indicate that these layers consist of eroded plasma facing materials, various impurities and plasma fuel species like deuterium and tritium. Accumulation of radioactive tritium in the reactor vacuum vessel is a particularly critical safety issue requiring active monitoring. LIBS is one of the few techniques available for monitoring the tritium content and the composition of co-deposited layers during maintenance breaks [1]. This paper will provide an overview of the LIBS experiment that was performed post DTE3 campaign, and D and H cleanup at JET in October 2024.

Prior to the LIBS experiment at JET, preliminary test measurements were performed at VTT using the LIBS tool developed at ENEA and optimized by FZJ. The tool consisted of the LIBS enclosure equipped with a sub-nanosecond Nd:YAG laser and focusing optics, which was connected via a 20 m optical fibre to an Echelle type spectrometer with wide spectral range (260–760 nm). Samples, including from JET limiters and divertor, were characterised for calibration-free LIBS and for calibration of the ablation rate. The final setup of the JET LIBS tool consisted of a high resolution Littrow spectrometer for separation of the hydrogen isotopic lines, an Echelle spectrometer and photomultipliers. The LIBS enclosure was mounted onto the MASCOT robot which was remotely operated from a dedicated control room by the UKAEA remote handling team. During the LIBS experiment at JET ~840 locations on the main wall and the divertor were analysed successfully. The high spatial accuracy of the MASCOT manipulator was also demonstrated by analysing single castellations on the limiter tiles. Validation of results will take place with future ex-situ LIBS measurements and post-mortem analysis on JET tiles.

[1] H.J. Van Der Meiden et al, Monitoring of tritium and impurities in the first wall of fusion devices using a LIBS based diagnostic, Nucl. Fusion. 61 (2021) 125001.

## **Chemical analysis by Laser Induced Breakdown Spectroscopy of the poloidal cross-section of the JET divertor after its last D-T experimental campaign**

Salvatore Almagia<sup>1</sup>, Jari Likonen<sup>2</sup>, Antti Hakola<sup>2</sup>, Juuso Karhunen<sup>2</sup>, Sebastijan Brezinsek<sup>3</sup>, Gennady Sergienko<sup>3</sup>, Rahul Rayaprolu<sup>3</sup>, Rongxing Yi<sup>3</sup>, Timo Dittmar<sup>3</sup>, Christoph Kawan<sup>3</sup>, Marc Sackers<sup>3</sup>, Erik Wüst<sup>3</sup>, The UKAEA RACE Team<sup>4</sup>, Anna Widdowson<sup>4</sup>, Ionuț Jecu<sup>4</sup>, Pavel Veis<sup>5</sup>, Sahithya Atikukke<sup>5</sup>, Shweta Soni<sup>5</sup>, Paweł Gąsior<sup>6</sup>, Wojciech Gromelski<sup>6</sup>, Jelena Butikova<sup>7</sup>, Indrek Jõgi<sup>8</sup>, Peeter Paris<sup>8</sup>, Jasper Ristkok<sup>8</sup>

<sup>1</sup>ENEA, Diagnostics and Metrology Laboratory, Italy; <sup>2</sup>VTT Technical Research Centre of Finland Ltd., Finland; <sup>3</sup>Forschungszentrum Jülich GmbH, Germany; <sup>4</sup>UKAEA, Culham Campus, Abingdon, United Kingdom; <sup>5</sup>Comenius University, Faculty of Math, Physics and Informatics, Slovakia; <sup>6</sup>Institute of Plasma Physics and Laser Microfusion, Poland; <sup>7</sup>Institute of Solid State Physics, University of Latvia, Latvia; <sup>8</sup>University of Tartu, Institute of Physics, Estonia.

Following the last JET D-T experimental campaign, ended in late 2023, in the framework of a close collaboration between several EUROFUSION partners and UKAEA, it was possible to design and carry out a measurement campaign by using the Laser-Induced-Breakdown Spectroscopy (LIBS) technique [1]. For the first time, in-situ material characterization of the first wall (FW) part of the JET tokamak was conducted without requiring any manipulation or removal of plasma facing components. One particular attention was given to the divertor area, where the most evident phenomena of redeposition of the material eroded by the FW, implantation and co-deposition of the unburned D-T fuel are expected [2,3]. Several points of the divertor were sampled with a dedicated number of laser shots and the resulting LIBS spectra were recorded in the UV-VIS spectral range (250–750 nm) by using an Echelle spectrometer.

This contribution presents the main results of the data analysis, focusing the study on the poloidal cross-section of the JET divertor. The LIBS spectra have highlighted the redeposition on the divertor surface of Be, coming from the JET FW components, together with residual traces of Hydrogen isotopes and possibly, Oxygen. The structure of the divertor elements, consisting of both W bulk and W-coated Carbon fibre composites (CFC), with Mo interlayers has also been observed. Moreover, by performing a depth profile analysis on Be-coated elements of known thickness, the average ablation rate was estimated to be around 160 nm per laser pulse.

To estimate the residual content of Hydrogen isotopes, a calibration free [4] (CF) analysis will be applied to the spectral signal of the T-alpha/D-alpha/H-alpha lines (656–656.3 nm). CF technique is based on the knowledge of the plasma parameters, like electron temperature and density and can give quantitative results by looking at the intensities of the emission lines obtained by the experimental data. CF does not require calibration samples [4] and is more reliable when many emission lines of the detected elements are recorded in a broad spectral range, as in the case of the present data.

[1] L.J. Radziemski, D. A. Cremers, Handbook of laser-induced breakdown spectroscopy. (2006) New York: John Wiley. ISBN 0-470-09299-8.

[2] S. Brezinsek, et al., Nucl. Fusion 55 (2015) 063021 (10pp).

[3] A. Widdowson, et al., Phys. Scr. (2021) 96 124075

[4] Z. Hu, D. Zhang, W. Wang, et al, TrAC Trend. Anal. Chem. 152, 116618 (2022).



## **Depth-resolved deuterium retention profiles in displacement-damaged tungsten measured via laser-induced ablation quadrupole mass spectrometry**

Christoph Kawan<sup>1</sup>, Sebastijan Brezinsek<sup>1</sup>, Timo Dittmar<sup>1</sup>, Erik Wüst<sup>1</sup>, Thomas Schwarz-Selinger<sup>2</sup>, Liang Gao<sup>1</sup>, Christian Linsmeier<sup>1</sup>

<sup>1</sup>Forschungszentrum Jülich GmbH, Germany; <sup>2</sup>Max-Planck-Institut für Plasmaphysik, Germany.

Tungsten (W) is the front-runner candidate for use as plasma-facing material in future deuterium-tritium (D-T) fusion reactors due to its favorable properties, such as low sputtering yield, low chemical reactivity, high melting point, and low intrinsic fuel retention. However, the highly energetic neutrons from DT fusion reactions cause displacement-damage in the W lattice, enhancing fuel atom retention. This has an impact on the tritium cycle requirements and safety. Therefore, diagnostics are required to quantify the D and T content in the plasma-facing and structural materials. Laser-induced ablation quadrupole mass spectrometry (LIA-QMS) is a promising method for quantifying fuel content with good depth resolution. LIA-QMS can be simultaneously applied with laser-induced breakdown spectroscopy (LIBS). Combining both techniques could provide the high depth resolution of LIBS with the calibration capabilities of LIA-QMS. This study compares pico-second LIA-QMS D profiles with LIBS as well as nuclear reaction analysis (NRA) with <sup>3</sup>He on displacement-damaged W samples which act as a proxy for fusion neutron damage. A set of similarly 10.8 MeV W<sup>3+</sup> irradiated ITER-grade W samples from PLANSEE was gently loaded with D from a low-temperature plasma at 370 K without further damage. The D concentration was varied by vacuum annealing of the samples at different temperatures after the D loading. Recording HD and D<sub>2</sub> with a 10:1 ratio for the total amount of D release, LIA-QMS shows a higher sensitivity (< 0.1 atu nm average ablation rate (AAR)) than LIBS. While LIBS provides a depth profile with 15 nm AAR, LIA-QMS requires a signal generated by using ~ 45 nm AAR, which is achieved by integrating over three laser shots of 15 nm AAR each. Qualitatively, LIA-QMS can reproduce the NRA depth profiles with the lowest AAR of 45 nm. Quantitatively, the D content differs by a factor of ~ 3 in the current setup. The laser-induced crater surface stays relatively flat for up to 4 μm until the roughness exceeds 30% of the crater depth.

## Session 2: Erosion, re-deposition, mixing, and dust formation and Low-Z and liquid materials

20 May, 11:15 – 13:00

I-3

### **Erosion of thin boron films at the linear plasma device PSI-2 during deuterium discharges: atomic and molecular spectroscopy of boron**

Marc Sackers, Oleksandr Marchuk, Anne Houben, Eduard Warkentin, Marcin Rasinski, Sebastijan Brezinsek, Arkadi Kreter

Forschungszentrum Jülich GmbH, Germany.

Boronization of tungsten is one of the solutions providing successful ignition of the deuterium plasma in ITER, but the erosion behavior in deuterium plasmas of thin B layers (~100 nm thickness) requires detailed investigation. In this case, both chemical and physical sputtering significantly contribute to the erosion of the boron layers.

To address the lack of experimental data, we deposited ~130 nm boron layer thickness onto polished tungsten samples via magnetron sputtering and exposed these to deuterium plasmas in the linear plasma device PSI-2. A reciprocating probe estimated the peak flux of deuterium ions onto the sample as  $4 \times 10^{21} \text{ m}^{-2} \text{ s}^{-1}$ . Biasing the target to 43 V (floating), 60 V, 80 V, and 100 V allowed for controlling the impact energy of the deuterons. Complete removal of the boron layers occurred after roughly 150 s to 170 s at floating potential and 80 V bias. For partial erosion (70 s of the plasma exposure), focused ion beam/scanning electron microscopy (FIB/SEM) provided post-mortem layer thickness measurements to estimate erosion rates and compare them with theoretical data.

We used optical emission spectroscopy (OES) to monitor time-resolved physical and chemical erosion. An Acton 750 imaging spectrometer tracked physical erosion by capturing two resonant B I lines at 250 nm with a time resolution of 10 s. Simultaneously, two Littrow spectrometers observed chemical erosion by measuring the 432.8 nm BD Q-branch of the A-X+ system in the spectral orders  $m=2$  and  $m=56$  with a temporal resolution of 10 s and 60 s, respectively. Due to the strong oxygen-gettering properties of boron, a four-channel Avantes spectrometer (298 nm to 889 nm, integration time of 0.2 s) detected the prominent O I lines at 777 nm and 844 nm, with their  $1/e$  decay times around 9 s.

Our findings demonstrate that OES is a reliable operando diagnostic for studying the erosion of thin boron layers under controlled conditions in PSI-2. During the deuterium discharges in the linear plasma device, we observed a clear transition from the deposited boron layer (~130 nm) to the underlying polished tungsten substrate. These measurements will contribute to refining modeling predictions for the lifetime of boron coatings in ITER.

## **Improved material mixing model in ERO2.0: nonlinear effect of boron concentration on tungsten sputtering and influx from mixed tungsten-boron surfaces**

Henri Kumpulainen<sup>1</sup>, Sebastijan Brezinsek<sup>1</sup>, Juri Romazanov<sup>1</sup>, Andreas Kirschner<sup>1</sup>, Christoph Baumann<sup>1</sup>, Klaus Schmid<sup>2</sup>

<sup>1</sup>Forschungszentrum Jülich GmbH, Germany; <sup>2</sup>Max-Planck-Institut für Plasmaphysik, Germany.

SDTrimSP [1] simulations indicate that incorporating a low-Z material, such as B, into a W surface reduces the surface binding energy and the impact energy threshold for W sputtering. For D projectiles, a surface mix of 90% W and 10% B results in a more than doubled W sputtering rate compared to a pure-W surface at impact energies below 270 eV. However, the W sputtering rate at impact energies above 600 eV decreases with increasing B due to a reduced W concentration. Increasing the B surface concentration also increases the initial energy of the sputtered B and W atoms by up to 30% due to weaker surface binding.

The material mixing model [2] in the ERO2.0 [3] code has been upgraded such that the sputtering and reflection yields for each particle species are no longer linearly interpolated from pure-material SDTrimSP yields, but include nonlinear effects of the surface concentration. A database of sputtering yields and energy-angular distributions of the sputtered particles has been compiled from new SDTrimSP simulations for surface material combinations of W mixed with D, Be, or B. The studied projectile species include H, D, T, He, Be, B, Ne, Ar, and W. The energy and angular distributions of particles sputtered from the mixed-material surfaces are described in ERO2.0 using parametrized analytic expressions fitted to SDTrimSP data. These analytic expressions are more robust to statistical noise than tabulated data, particularly for low sputtering yields during detached divertor operation.

The first ERO2.0 simulations using the mixed-material sputtering yields in validated tokamak plasma conditions predict that adding, as an example, a 10% boron surface concentration to the JET W divertor components would increase the total W influx into the confined plasma by 6% in attached L-mode and by 2% in a type-I ELMy H-mode scenario, assuming the incident particle fluxes on surfaces remain unchanged.

### **Acknowledgments**

This work is financially supported by a research grant awarded by the Finnish Cultural Foundation. This work has been carried out within the framework of the Contract for the Operation of the JET Facilities and has received funding from the European Union's Horizon 2020 research and innovation programme. The views and opinions expressed herein do not necessarily reflect those of the European Commission.

[1] A.Mutzke et al., SDTrimSP Version 6.00, IPP Report 2019-02 (2019)

[2] M. Navarro et al., 24th PSI conference (2021)

[3] J. Romazanov et al., Physica Scripta T170, 014018 (2017)

## Deuterium retention in sputter-deposited W-B layers: Implantation and in-situ ion beam analysis during annealing

Daniel Gautam<sup>1</sup>, Tuan Tran<sup>1</sup>, Martina Fellinger<sup>2</sup>, Friedrich Aumayr<sup>2</sup>, Marek Rubel<sup>3</sup>, Daniel Primetzhofer<sup>1</sup>, Eduardo Pitthan<sup>1</sup>

<sup>1</sup>Uppsala University, Sweden; <sup>2</sup>TU Wien, Fusion@ÖAW, Vienna, Austria, Austria; <sup>3</sup>Uppsala University/KTH Royal Institute of Technology, Sweden.

Tungsten (W) is one of the main materials considered for Plasma Facing Components (PFC) in magnetic confinement fusion devices, due to its comparably low sputter yield and low retention of deuterium (D) and tritium (T), among other favorable properties [1]. It may be necessary to coat the W wall with boron (B) in a process known as boronization, to reduce the partial pressure of low-Z impurities like oxygen and water [2]. However, this procedure may result in the formation of W-B mixtures due to continuous redeposition steps from plasma wall interactions.

Properties such as fuel retention and oxygen gettering might differ between the W-B mixtures and W. To better understand the behavior of these materials and consequences of their presence in fusion devices, we investigated D retention in W-B films with different stoichiometries. The films were grown on silicon substrates by means of magnetron sputter deposition. Thin-films of unmixed W and B were also grown for comparison. After pre-characterization, the layers were subjected to deuterium implantation (1 keV D<sub>2</sub><sup>+</sup>) followed by in-situ analysis. Specifically, the compositions of the films were determined with Time-of-Flight Elastic Recoil Detection Analysis (ToF-ERDA) and depth profiles were obtained in-situ by simultaneous Elastic Recoil Detection Analysis (ERDA) and Rutherford Backscattering (RBS) measurements using a primary beam of 2 MeV He<sup>+</sup> ions.

The samples were annealed to 600°C and in-situ ion beam analysis measurements were performed on all samples before, during and after the annealing process. The concentration of B in the films led to significant differences in D retention. After annealing, the lowest amount of retained D was seen for a W-to-B ratio of 2:1, with an areal density of  $8 \times 10^{13}$  D/cm<sup>2</sup>, having close to three times lower retention than unmixed W. The bare B film showed the highest retention with an areal density of around  $1 \times 10^{17}$  D/cm<sup>2</sup>, after annealing to 600°C. Ex-situ analysis was performed to characterize the changes in surface structure of the films before and after implantation/annealing. Significant morphological modifications due to implantation/annealing steps were observed, such as W surface enrichment (B-rich films), and crack formation (W-rich films).

[1] V. Philipps, J. Nucl. Mater. 415 (2011)

[2] K. Schmid, T. Wauters, Nucl. Mater. Energy 41 (2024)

## Lifetimes of Boron layers on amorphous and crystalline tungsten under deuterium and impurity irradiation

Udo von Toussaint, Roland Preuss, Martin Balden, Karl Krieger, Klaus Schmid, Andreas Mutzke  
Max-Planck-Institut für Plasmaphysik, Germany.

The most prominent aspect of the recent ITER reconfiguration, the switch from beryllium to tungsten for the blanket first wall armour, is also the most challenging modification in terms of impact on the ITER Research Plan [1]. A higher tungsten source means higher potential W-contamination of the plasma. It can thus be an obstacle to reliable plasma start-up which, in most tokamaks including ITER, is performed by establishing the plasma in a configuration that is in direct contact with the main chamber walls. Wall-conditioning via Boronisation has been suggested to reduce the tungsten impurity concentration in the plasma and has been applied successfully in several mid-size tokamak devices such as ASDEX-Upgrade [2]. Key parameters influencing the performance are the lifetime of the boron layers on top of the tungsten first wall surfaces and their effective surface coverage. Since the relative importance of these two factors is still a matter of debate [3] we address both using the binary collision code family SDTrimSP. The lifetime of a given boron layer is determined by the incident flux of deuterium atoms and the sputter yield of boron by deuterium. The sputter yield is a nonlinear function of the thickness of the boron layer as well as of the energy and angular distribution of the impinging deuterium atoms. It also depends on the material structure of the tungsten substrate and the surface topology. Here we investigate in detail using static and dynamic simulations with SDTrimSP 7.03 how the sputter yield depends on the deuterium impact angle, impact energy and tungsten solid-state structure. The simulation results reveal that the common but often unrealistic assumption of a fully amorphous tungsten substrate consistently yield a too pessimistic picture of the lifetime of thin ( $O(\text{deuterium range})$ ) boron layers. For the main W crystal orientations of ITER grade tungsten the lifetime for these layers is typically 40% – 100% larger compared to the amorphous case. A similar picture emerges if the boron layer surface coverage of corrugated surfaces (i.e. technical surfaces with 1D grooves) is simulated using SDTrimSP-2D. Even small surface corrugations (e.g. sinusoidal groove profiles with a root mean square roughness of 7.5 nm) yield a significantly reduced depletion rate (by a factor of 5 and more) of the boron surface coverage compared to the case of an atomistically flat surface. The addition of heavier impurities such as oxygen or neon to the incident flux change the quantitative results but do not alter the qualitative conclusions. Therefore, the kinetic simulation results (i.e. without considering potential effects of boron chemistry) suggest that boron deposits will have a longer lifetime than predicted by from 1D simulations based on the assumption of a flat, amorphous tungsten substrate.

[1] R. Pitts, presentation at E2M-workshop, Kloster Seeon (2024), <https://www.iter.org/node/20687/iter-and-asdex-upgrade-monastic-quiet>

[2] K. Krieger, M. Balden, A. Bortolon et al, Nucl. Mat. Energy 34 (2024) 101374

[3] V. Rohde, R. Dux, A. Kallenbach et al, J. Nucl. Mat. 363–364 (2007) 1369–1374

## Session 3: Neutron effects in plasma-facing materials

20 May, 14:30 – 16:20

I-4

### Neutron irradiation effects on PFC materials: an overview of EUROfusion programme

Dmitry Terentyev<sup>1</sup>, Michael Rieth<sup>2</sup>, Ermile Gaganidze<sup>2</sup>, Gerald Pintsuk<sup>3</sup>, Giacomo Aiello<sup>4</sup>, Michael Klimenkov<sup>2</sup>, Aleksandr Zinovev<sup>5</sup>, Shuhei Nogami<sup>6</sup>, Steffen Antusch<sup>2</sup>, Jan Coenen<sup>3</sup>, Petra Jenuš<sup>7</sup>, Koray Iroc<sup>5</sup>, Chao Yin<sup>8</sup>, Carmen Garcia Rosales<sup>9</sup>

<sup>1</sup>Belgian Nuclear Research Center, Belgium; <sup>2</sup>KIT, Germany; <sup>3</sup>FZJ, Germany; <sup>4</sup>EUROfusion, Germany; <sup>5</sup>SCK CEN, Belgium; <sup>6</sup>ALMT, Japan; <sup>7</sup>JSI, Slovenia; <sup>8</sup>USTC, China; <sup>9</sup>CIET, Spain.

The EUROfusion Consortium is an association of Laboratories across 28 European countries in charge of implementing the European Roadmap to Fusion Electricity. Development and qualification of neutron tolerant materials is one of the missions on the Roadmap, with neutron irradiation and subsequent post irradiation examination representing a key challenge as it requires substantial time and financial resources, expertise in dealing with nuclear materials and long-term vision for the codification of the results into reactor design codes. In this talk we provide an overview of the EUROfusion contribution to the investigation of the neutron irradiation effects in plasma-facing materials (PFC). The presentation summarizes the main results and lessons learned over the 2018–2024 period, and it is sub-divided into four sections covering: (i) commercial ITER-specification tungsten; (ii) advanced tungsten grades achieved by alloying or innovative production methods; (iii) advanced copper-based heat sink materials; (iv) W-Cu joints. The effects of neutron irradiation are assessed in terms of the modification of mechanical properties, and supported by microstructural investigations to explain and interpret the obtained results. The corresponding irradiation matrix for the development of the Material Property Handbook (MPH) is presented and discussed. Currently existing gaps in the MPH and outlook for the actions to cover these gaps are discussed as well.

I-5

### Modelling high dose irradiation damage in tungsten

Max Boleininger<sup>1</sup>, Daniel Mason<sup>1</sup>, Alexander Feichtmayer<sup>2</sup>, Luca Realì<sup>1</sup>, Sergei Dudarev<sup>1</sup>

<sup>1</sup>UK Atomic Energy Authority, United Kingdom; <sup>2</sup>Technical University Munich, Germany.

The realisation of economically viable fusion reactors requires the development of comprehensive materials models spanning the parameter space of simultaneous thermal, mechanical, and radiation loads. As materials data for such conditions is scarce, there is a clear benefit in simulating materials behaviour in silico from first principles: if we can accurately simulate how the microstructure in a metal evolves under irradiation, we may attempt to derive engineering-relevant properties from it.

Here, we present the molecular dynamics (MD) method as a powerful tool for generating high-dose irradiation microstructure in tungsten from first principles, predicting materials properties such as thermal conductivity [1], deuterium retention [2], lattice strains [3], and stress relaxation [4] consistent with experimental findings. We will discuss the principles, capabilities, and limitations of the method in reference to the aforementioned predictions, and list the steps involved in performing a typical irradiation damage simulation.

We demonstrate how MD can be used to build a virtual representation, or “digital shadow”, of an experiment to predict the outcome before the actual experiment is performed [4]. While

the scope of the fusion materials challenge is far broader than the examples presented here, we show that it is possible to derive predictions from first principles in a previously unexplored regime, and to validate them by a carefully tailored experiment.

- [1] D.R. Mason et al., Phys. Rev. Mater 5:12, 125407 (2021)
- [2] M. Boleininger et al., Sci. Rep. 13:1, 1684 (2023)
- [3] D.R. Mason et al., PRL 125:22, 225503 (2020)
- [4] A. Feichtmayer et al., Commun. Mater. 5:1, 218 (2024)

O-6

### **Detection of defects and location of deuterium in displacement-damaged tungsten**

Sabina Markelj<sup>1</sup>, Esther Punzón-Quijorna<sup>1</sup>, Mitja Kelemen<sup>1</sup>, Thomas Schwarz-Selinger<sup>2</sup>, Xin Jin<sup>3</sup>, Eryang Lu<sup>3</sup>, Flyura Djurabekova<sup>3</sup>, Kai Nordlund<sup>3</sup>, Janez Zavašnik<sup>1</sup>, Andreja Šestan Zavašnik<sup>1</sup>, Miguel L. Crespillo<sup>4</sup>, Gaston García López<sup>4</sup>, Rene Heller<sup>5</sup>

<sup>1</sup>Jožef Stefan Institute, Slovenia; <sup>2</sup>Max-Planck-Institut für Plasmaphysik, Germany; <sup>3</sup>University of Helsinki, Finland; <sup>4</sup>Center for Micro Analysis of Materials, Spain; <sup>5</sup>Helmholtz-Zentrum Dresden-Rossendorf, Germany.

Due to its advantageous characteristics, tungsten (W) is the main plasma-facing material candidate for future fusion reactors. However, in a future nuclear environment, the W crystal lattice will be heavily altered due to defects caused by 14 MeV neutrons from the D-T fusion reaction, affecting the physical properties of the material. To examine defects created in the W lattice, we utilized Rutherford backscattering spectrometry in channeling configuration (RBS-C), a well-established method for studying lattice disorder and defect evolution induced by irradiation. To quantify the disorder, the change in the ion yield of light ions backscattered along a specific crystallographic direction is measured [1]. Moreover, when combining nuclear reaction analysis in channeling configuration (NRA-C) with RBS-C utilizing D(3He,p)4He nuclear reaction, we can gain insights into the location of trapped D in displacement-damaged W. To study the defects and trapping of D, we irradiated W (111) and (100) single crystals (SC) with 10.8 MeV W ions at two different doses (0.02 and 0.2 dpa) and temperatures (300 and 800 K). Our goal was to create samples, with either dominantly single vacancies, small vacancy clusters or large vacancy clusters [2]. This was later on also confirmed by positron annihilation spectroscopy on our samples. The transmission electron microscopy (TEM) analysis of W (111) SC revealed dislocation lines and loops of different sizes, depending on the irradiation dose and temperature. Multi-energy RBS-C spectra analysis along the  $\langle 111 \rangle$  direction unveiled distinct ion yield responses for each sample [3]. For the first time for W, we employed molecular dynamics (MD) simulations of overlapping cascades as input for the RBSADEC code [4], to simulate the RBS-C spectra. The simulated spectra agreed remarkably well with the experiment for the lower dose sample, but showed discrepancies for the high-dose-irradiated sample, attributed to the presence of large dislocation lines observed by TEM, which cannot be formed in finite-size MD cells [3]. New simulation results with larger MD cell and different MD potential for the high dose and high-temperature samples will be discussed. Irradiated and with D plasma decorated W (100) SCs were used to perform NRA-C and RBS-C using a 0.8 MeV 3He probing beam and study the D location in the tungsten lattice. The maximum NRA signal was detected in the  $\langle 100 \rangle$  axial and in the (110) planar channels [5]. The interpretation of the spectra with the RBSADEC code [4], recently upgraded to simulate the NRA-C signal, will also be discussed.

- [1] Feldman et al., Academic Press, San Diego, (1982), pp. 88–116
- [2] Hu et al. J. Nucl. Mater. 556, 153175 (2021)
- [3] Markelj et al, Acta Materialia 263 (2024) 119499
- [4] Zhang et al. Phys. Rev. E 94, 043319 (2016).
- [5] Markelj et al. Nucl. Mater. Energ 39 (2024) 101630

O-7

## **Influence of the Presence of Deuterium on Damage Evolution in Tungsten**

Zeqing Shen, Thomas Schwarz-Selinger, Mikhail Zibrov, Armin Manhard

Max Planck Institute for Plasma Physics, Germany.

The influence of the presence of deuterium (D) on damage evolution at elevated temperatures was studied for self-ion irradiated tungsten (W). W samples were irradiated by 20.3 MeV W ions at room temperature to the peak damage dose of 0.23 dpa and loaded with a low-temperature D plasma at 370 K to decorate the created defects. Low energy ( $< 5$  eV/D) and low flux ( $5.6 \times 10^{19}$  D m<sup>-2</sup>s<sup>-1</sup>) was used to make sure plasma exposure does not create additional defects. Afterward, samples were heated during plasma loading at four different temperatures, ranging from 470 K to 770 K. The appropriate annealing time was calculated applying the rate equation modelling code TESSIM-X. For accurate quantitative comparison, annealing experiments at each temperature were carried out also in vacuum. Nuclear reaction analysis (NRA) with <sup>3</sup>He was used to determine the D depth profile and thermal desorption spectroscopy (TDS) was used to measure the total retention and de-trapping energy of D.

Both vacuum annealing and plasma annealing exhibit a decrease in D retention with increasing annealing temperature. Decorating all samples after annealing again with the same D plasma allows to differentiate between the effects caused by thermal de-trapping and defect evolution. Combined with results from plasma-annealed samples without D reloading, it is found that most of the decrease in D retention during annealing is due to thermal de-trapping, and only a small portion is due to defect evolution. The presence of D during annealing has a small stabilizing effect on the defects. The results differ from the plasma annealing results reported in [1] but align with the vacuum annealing results in [2]. All TDS spectra can be described consistently with six different traps with energies of 1.05–1.10 eV, 1.25–1.28 eV, 1.39–1.46 eV, 1.72–1.74 eV, 1.94 eV for the defects created by the W irradiation within the first 2 μm, and 1.18 eV for the intrinsic defects. The fitting results show that defects with a lower de-trapping energy for D are more prone to thermal annealing, while those with a higher de-trapping energy for D remain more stable. Consistent with [2] the trap with the highest de-trapping energy for D is not affected up to 770 K. The trap with the lowest de-trapping energy for D starts to decrease in density already above 470 K.

[1] M.J. Simmonds et al., Nucl. Fusion 62 036012 (2022)

[2] M. Pečovnik et al., Nucl. Fusion 60 106028 (2020)



## Session 4: Boronisation and wall conditioning techniques

21 May, 8:30 – 10:20

I-6

### Effect of spatially non-uniform boronization on plasma restart in the full W environment of WEST

Alberto Gallo<sup>1</sup>, Mathilde Diez<sup>1</sup>, Etienne Hodille<sup>1</sup>, Eleonore Geulin<sup>1</sup>, Jonathan Gaspar<sup>2</sup>, Pierre Manas<sup>1</sup>, Paulo Puglia<sup>1</sup>, Nicolas Rivals<sup>1</sup>, Diana Sgrelli<sup>1</sup>, Regis Bisson<sup>3</sup>, Julien Denis<sup>1</sup>, Gabriele Gervasini<sup>4</sup>, Alex Thomas Grosjean<sup>5</sup>, Laura Laguardia<sup>4</sup>, Thierry Loarer<sup>1</sup>, Stefane Vartarian<sup>1</sup>, Tom Wauters<sup>6</sup>, Thierry Alarcon<sup>1</sup>, Viven Anzallo<sup>1</sup>, Eric Caprin<sup>1</sup>, Matthieu De Combarieu<sup>1</sup>, Philippe Moreau<sup>1</sup>, Francis-Pierre Pellissier<sup>1</sup>, Yann Corre<sup>1</sup>, Karl Krieger<sup>7</sup>, Anna Widdowson<sup>8</sup>, Emmanuelle Tsitrone<sup>1</sup>, Antti Hakola<sup>9</sup>

<sup>1</sup>CEA, IRFM, France; <sup>2</sup>CNRS, IUSTI, France; <sup>3</sup>CNRS, PIIM, France; <sup>4</sup>Istituto per la Scienza e Tecnologia dei Plasmi, CNR, Milano, Italy; <sup>5</sup>University of Tennessee Knoxville, United States; <sup>6</sup>ITER Organization, France; <sup>7</sup>Max-Planck-Institut für Plasmaphysik, Garching, Germany; <sup>8</sup>UKAEA, Culham Campus, Abingdon, United Kingdom; <sup>9</sup>VTT Technical Research Centre of Finland Ltd, Espoo, Finland.

The recent ITER re-baseline with the adoption of a full-W wall calls for mandatory boronization studies. Among existing W machines, the W Environment Steady-state Tokamak (WEST) offers a unique opportunity to study boronization effects on wall retention and plasma conditions thanks to its routine minute-long pulses and ITER grade, actively cooled divertor. In spring 2024, we carried out the first ever WEST experiment dedicated to boronization by repeating a sequence of identically programmed pulses before and after a boronization. In pulses after boronization, we initially observed a factor of 2 higher wall retention that vanishes after  $\sim 100$  s of plasma. On the other hand, throughout the whole post-boronization session ( $\sim 10$  min of plasma), we measured a 20% lower radiated power, lower effective charge and lower UV line intensity for most impurities including oxygen, while keeping the same central electron density and temperature as well as same divertor regime as before boronization. In fall 2024, for the first time in five years, we attempted to restart plasma operations without boronization after a vent and after reinstalling W limiter tiles (replaced by BN tiles from 2020 to mid-2024). In 2 days of operation corresponding to  $\sim 60$  limiter pulses, we reached a maximum pulse length of 1.5 s and a maximum current of 600 kA. Plasmas were cold and dense, mostly detached from the inboard limiter and dominated by light impurities with radiated fractions close to unity and no particular sign of runaway electrons. We then carried out the first WEST boronization utilizing only 3 out of 6 diborane injection points, to study the effect of non-uniform B layers expected in ITER due to its toroidally asymmetric boronization system. Repeatable ohmic limiter pulses of 10 s were immediately achieved with a factor of 4 reduction of the oxygen signal from UV spectroscopy and radiated fractions between 50% and 70%. In the remainder of the campaign, we achieved 422 pulses corresponding to about 2 hours of cumulated plasma time and 12.5 GJ of cumulated injected/extracted energy over 5 weeks of operation without any further glow discharge boronization. These efforts culminated in a new record long pulse for WEST, which lasted for 824 s with 1.93 GJ of injected/extracted energy. Despite these successes, towards the end of the campaign, wall conditions started to show signs of degradation that would have made a new boronization desirable, should the experiments have continued further.

### Investigations on Boronization at tungsten ASDEX Upgrade

Volker Rohde, Karl Krieger, Andreas Redl, Tim-Oliver Hohmann, Joerg Hobrik, Seehon An

Max Planck Institute for Plasmaphysics, Germany.

Conditioning of the plasma-facing surfaces (PFSs) in fusion devices is essential for reliable plasma operation. In ASDEX Upgrade (AUG), boronization by a glow discharge in He with 10% of deuterated diborane is used as standard wall conditioning technique. Recently the PFSs in ITER were changed to full tungsten, which triggered strong interest in wall conditioning techniques currently used at full metal fusion devices.

Analysis of the existing data from AUG were presented at the recent PSI conference [1]. To fill the knowledge gaps, new diagnostics such as witness samples, quartz microbalance monitors (QMB) and manipulator systems were installed or activated.

During the last vent a new upper divertor was installed at AUG. This opportunity was used to remove all deposited layers from the PFSs. AUG was restarted without boronization coating to document the role of boronization on plasma start up after a vent. It turned out that it was not possible to gather useful discharges in this configuration. After boronization, plasma restart was immediately achieved.

QMBs are used to measure the layer thickness during the coating process. This allows collecting data for different glow anode configurations without venting AUG. A code was developed to estimate the position and number of anodes required for boronization of ITER [2]. To benchmark this code a coating with only 2 active anodes was performed in AUG. From the QMB data, a reduction of a factor of two of the layer thickness at a position close to a non-active anode was found, in qualitative agreement with the simulations, although the layers are much thicker than predicted.

Samples made of different materials exposed during the boronization were used to confirm the deposition. As the layers react with air, they were dismantled under nitrogen atmosphere and measured by ion beam techniques with air exposure <5min. Up to 75% of the boron input was found, indicating almost homogeneous deposition. The samples were exposed 24h to air and analysed again. Typically, 10% less boron was found for one boronization, whereas a second sample set proved to be more stable.

This work is supported by Commonwealth Fusion systems.

[1] V.Rohde et al., PSI 24, NME, submitted

[2] T.Wauters et al., PSI 24, NME, submitted

### Analysis of Boron-Hydrogen Interactions and Deuterium Retention for Fusion Applications

Aleksandr Afonin, Marco Minissale, Eric Salomon, Thierry Angot, Regis Bisson

Aix-Marseille University, CNRS, PIIM, France.

Plasma-facing component boronization reduces the impurities coming from the walls of the tokamak and improves the performance of plasma experiments. Understanding how boron interacts with fusion fuels (deuterium and tritium) is important for nuclear safety and plasma detachment requirements, given the radioactivity of tritium, the possible production of diborane and potential impurity effects on recycling. The present work provides new experimental data for a better understanding of the boron-hydrogen interaction.

An amorphous boron sample (99.9 wt.% purity) was exposed to a beam of deuterium ions ( $D_2^+$ ) with 250 eV/D at room temperature. Deuterium retention was evaluated using temperature-programmed desorption (TPD) with a temperature ramp of 1 K/s and a maximum temperature of 1350 K. The TPD spectra were measured for various deuterium-containing molecules, including possible products of diborane ionization. The sample surface composition was additionally characterized by X-ray photoelectron spectroscopy (XPS).

Implanted deuterium ions desorb mainly as  $D_2$  and  $HD$  (73% of  $D$ ) and partly as  $D_2O$  and  $HDO$  (27% of  $D$ ). Given the line-of-sight geometry of our TPD setup, the branching ratio for diborane products was estimated to be 0.04% relative to the main products of desorption. We conclude the absence of diborane production under the present experimental conditions.

TPD measurements show two desorption components. The first one is a low-temperature broad peak (400–600 K), similar to previous observations on boron polycrystals [1]. The second component appears at a much higher temperature (>1220 K). It is narrower, has a higher intensity and interestingly, the position of its maximum depends on the absolute amount of deuterium retained.

XPS measurements were performed after heating the sample to 1023 K to remove most of the impurities, after irradiation by the 250 eV/D ions at room temperature, and again after heating to 1023 K to remove deuterium. The  $B_{1s}$  and  $O_{1s}$  peaks show identical behaviour:  $D_2$  irradiation shifted energy levels by 1.2 eV towards higher binding energy. Heating the sample after irradiation shifted back the peak energy by 0.4 eV towards lower binding energy, likely due to the remaining presence of deuterium in the sample given the high-temperature desorption peak of  $\sim 1200$  K.

[1] Y. Oya et al., J. Nucl. Mater. 329–333, 870–873 (2004)

O-9

### **Sticking Coefficients of Boron Radicals**

Matej Mayer, Torsten Bräuer, Dario Cipciar, Chandra Prakash Dhard, Carsten Killer, Dirk Naujoks, Ralf Steinwehr, Udo von Toussaint, Lilla Vano, Holger Viebke

Max-Planck-Institut für Plasmaphysik, Germany.

The recent decision of ITER to start plasma operation with a full tungsten wall necessitates implementing a wall conditioning method for gettering impurities, especially oxygen and water molecules, for obtaining efficient plasma start-up [1]. Regular boronizations using a glow discharge in  $B_2H_6$  gas diluted in He are foreseen in order to coat the wall with a thin layer of boron [1], which acts as getter.  $B_2H_6$  molecules are dissociated in the glow-discharge plasma into atoms and radicals, which finally stick to the walls. Simulation calculations predict a non-uniform distribution of boron over the whole inner wall, with thicker layers close to the discharge electrodes and thinner layers further away [1]. However, these predictions depend crucially on the assumptions about the sticking coefficients of the boron radicals. Unfortunately, these sticking coefficients are not known, thus rendering these predictions quite uncertain. Therefore a proper design of the ITER boronization system urgently requires experimental data on the sticking coefficients of boron radicals.

We used the cavity technique [2] in order to determine the effective sticking coefficient of boron radicals during an individual boronization in the stellarator Wendelstein 7-X (W7-X). A cavity is a small box made from silicon wafers with an entrance slit facing the glow-discharge plasma. The analysis of the lateral distribution of boron on the bottom and top inner surfaces

allows determining the effective sticking coefficient of boron radicals.

Two cavities were exposed during an individual boronization in W7-X using the multi-purpose manipulator. The cavities were exposed at about the position of the inner wall. The boron distributions on the inner surfaces of the cavities were measured using Nuclear Reaction Analysis (NRA) with 3 MeV incident  $^3\text{He}$  ions. Multiple peaks from the  $^{10}\text{B}(^3\text{He},\text{px})^{12}\text{C}$  and  $^{11}\text{B}(^3\text{He},\text{px})^{13}\text{C}$  reactions were used for quantifying the amount of boron. Two detectors with a combined solid angle of about 110 msr were used simultaneously – this very large solid angle provides the necessary sensitivity for the very thin deposited boron layers. The distribution of boron inside the cavities was simulated using a Monte-Carlo program [2] and compared to the experimental distributions. The mean effective sticking coefficient of boron radicals created by the applied boronization plasma was in the range 0.4 – 0.5.

[1] A. Loarte et al., Initial evaluations in support of the new ITER baseline and Research Plan, ITER Technical Report ITR-24-004 (2024).

[2] S. Krat et al., Hydrocarbon film deposition inside cavity samples in remote areas of the JET divertor during the 1999–2001 and 2005–2009 campaigns, J. Nucl. Mater. 463 (2015) 822.

## Session 5: Technology and qualification of plasma-facing components and Erosion, re-deposition, mixing, and dust formation

21 May, 10:50 – 12:40

I-8

### First insights into runaway electron (RE) damage induced to the JET divertor

Ionuț Jecu<sup>1</sup>, Anna Widdowson<sup>1</sup>, Yevhen Zayachuk<sup>1</sup>, Cédric Reux<sup>2</sup>, Salvatore Almaviva<sup>3</sup>, Rahul Rayaprolu<sup>4</sup>, Rongxing Yi<sup>4</sup>, Mirosław Zlobinski<sup>4</sup>, Jari Likonen<sup>5</sup>, Sebastijan Brezinsek<sup>4</sup>

<sup>1</sup>UKAEA, Culham Campus, Abingdon, United Kingdom; <sup>2</sup>CEA, IRFM, France; <sup>3</sup>ENEA, Diagnostics and Metrology Laboratory, Italy; <sup>4</sup>Forschungszentrum Jülich GmbH, Germany; <sup>5</sup>VTT Technical Research Centre of Finland Ltd., Finland.

High energetic runaway electrons (REs) triggered due to plasma disruptions in tokamak reactors pose significant challenges due to their potential damage of the plasma-facing components (PFCs). Previous studies on the Joint European Torus (JET) device have highlighted the RE interaction with PFCs during an induced disruption, mainly on the beryllium (Be) main chamber components [1]. Due to the significant risks REs posed to the integrity of the PFCs and the overall functionality of the reactor, studies on REs in JET were limited in number, and mainly focused on the main chamber components, while RE-induced damage to the divertor were left unexplored – until now.

During the final operational days of JET, in December 2023, dedicated experimental sessions were conducted to investigate the impact of REs also on the divertor PFCs, including their triggering mechanisms, a deeper understanding of the physics behind these events and improved observation of the resulting damage. Artificially triggered REs using argon (Ar) massive gas injection (MGI) were controlled and pushed towards the divertor interacting with the apron of Tile 1. For the first time, this study presents evidence of RE effects in the JET divertor, the RE-induced damage to the tungsten-coated carbon fibre composite (W-CFC) tiles. High-resolution photography, performed in 2024, following the end of JET operations, offered a unique and detailed visual representation of the destruction. The photographic survey revealed that the damage is not toroidally uniform: in some regions, parts of the W coating on the inner divertor tiles (Tile 1) was entirely removed, while in others, the tiles appeared intact. This observation aligns with prior findings of non-uniformity of the RE-induced damage to the JET main wall, highlighting the localized nature of RE interactions with the main chamber PFCs [2].

To further characterize the damage, LID-QMS (Laser-Induced Desorption-Quadrupole Mass Spectrometry) was performed on one of the damaged tiles, focusing on fuel retention in both damaged and undamaged areas. Results revealed notable differences in fuel retention between these regions. LIBS (Laser-Induced Breakdown Spectroscopy) was also performed in similar regions to investigate the material composition of the damaged areas and their surroundings, providing complementary insights into the erosion and fuel removal mechanisms.

[1] I. Jecu Nucl. Fusion 64 (2024) 106047 (15pp)

[2] C. Reux et al Nucl. Fusion 55 093013 (2015)

\*See the author list of Maggi, C. F., & JET Contributors (2024) Overview of T and D-T results in JET with ITER-like Wall Nuclear Fusion, 64 (112012) <https://doi.org/10.1088/1741-4326/AD3E16>

## Overview of the results achieved from the characterization program of the WEST plasma facing components (2018-2024)

Mathilde Diez<sup>1</sup>, Martin Balden<sup>2</sup>, Elodie Bernard<sup>1</sup>, Iva Bogdanović Radović<sup>3</sup>, Yann Corre<sup>1</sup>, Alan Durif<sup>1</sup>, Elzbieta Fortuna-Zalesna<sup>4</sup>, Jonathan Gaspar<sup>5</sup>, Antti Hakola<sup>6</sup>, Indrek Jõgi<sup>7</sup>, Celine Martin<sup>8</sup>, Emmanuelle Tsitrone<sup>1</sup>, Marianne Richou<sup>1</sup>

<sup>1</sup>CEA, IRFM, France; <sup>2</sup>IPP MPG, Germany; <sup>3</sup>Ruder Bošković Institute, Croatia; <sup>4</sup>Warsaw University of Technology, Poland; <sup>5</sup>CNRS, IUSTI, France; <sup>6</sup>VTT Technical Research Centre of Finland Ltd, Finland; <sup>7</sup>University of Tartu, Institute of Physics, Estonia; <sup>8</sup>Aix-Marseille Univ, CNRS, PIIM, France.

This contribution summarizes the main results related to fuel retention, material migration and tungsten cracking, after the first phase (2018-2020) and the start of the second phase (2022-2024) of WEST operation. The results are based on post-exposure analyses of several plasma facing components and on analysis of plasma edge conditions during operation. More specifically, the presentation will report the following findings:

- Erosion was investigated using 2 types of lower divertor components: W-coated graphite tiles installed during phase 1 of WEST and bulk W ITER-grade PFUs with fiducials on their surface installed during phase 2. For the same plasma conditions (5h of plasma in attached regime,  $T_e=20$  eV) they both follow the same erosion pattern along the ripple, e.g. the modulation of the angle of incidence. A global maximum tungsten erosion of about  $8\ \mu\text{m}$  is observed in both cases, which is in a good agreement with ERO simulations.
- In 2019, a dedicated helium campaign was carried out to investigate He-W interactions (45 min, He fluence  $> 10^{24}$  He/m<sup>2</sup>) [1]. The characterization of W-coated graphite tiles and bulk W ITER-grade PFUs shows that helium is implanted in erosion-dominant areas, with maximal concentrations of 10-12 at.% and 7-8 at.% in the outer and inner strike points respectively. A more detailed TEM analysis showed the presence of nanobubbles on the first 10 nm of the plasma-exposed surface. Similar subsurface cavities were also observed on single crystalline W samples installed on the reciprocating collector probe during this helium campaign [2].
- Thanks to the protection of the toroidal bevel, and in contrast to phase 1, no cracks were observed on the leading edges and in the magnetically shadowed part of the monoblocks. However, a crack network was observed on the top surface of the monoblocks, in plasma-exposed area around typical position of outer strike point (MB26-28). A strong correlation appears between the ripple modulation and the presence/density of these cracks. A characterization is on going to better evaluate the cracks depth and potential consequences on power exhaust capability, as well as better evaluate the role of manufacturing and machining in the crack formation.

[1] E.Tsitrone et al., Nucl. Fusion 62, 076028 (2022)

[2] B. Wirth, IAEA, 2024

## **Erosion and redeposition patterns on divertor tiles after exposure in the first operation phase of WEST**

Martin Balden<sup>1</sup>, Mathilde Diez<sup>2</sup>, Elodie Bernard<sup>2</sup>, Antti Hakola<sup>3</sup>, Matej Mayer<sup>1</sup>

<sup>1</sup>Max-Planck-Institut für Plasmaphysik, Germany; <sup>2</sup>CEA, IRFM, France; <sup>3</sup>VTT Technical Research Centre of Finland Ltd., Finland.

This contribution summarizes the results obtained from ion beam analyses (RBS and NRA) and scanning electron microscopy (SEM assisted with FIB cutting and EDX) on entire W-coated graphite divertor tiles exposed during the 1st operational phase of WEST (2017–2021) with campaigns C1 to C5.

The WEST project is devoted to test tungsten (W) divertor components for ITER and their performance in an integrated tokamak environment. During the 1st phase, the predominant fraction of the lower divertor consisted of inertially cooled graphite tiles coated with ~13 µm W on top of ~3 µm molybdenum (Mo) allowing to study the W erosion by measuring the remaining layer thickness, while from the 2nd phase on, the complete lower divertor is equipped with water-cooled ITER-like bulk W components. After 2018 (C3) and 2019 (C4), some tiles were removed for analyses. These tiles were selected from toroidal positions with the highest heat and particle loads. This toroidal variation in loads along the inner and outer strike line is originated by the pronounced magnetic field ripple. After 2020 (C5), a large number of coated graphite tiles got available for analyses allowing to study the effect of the ripple.

Erosion and deposition patterns for tiles exposed until the end of C5, i.e., after about 7.5 h of plasma, are compared to those for tiles removed after C3 (2.5 h of plasma) and C4 (6 h of plasma), which are published in [1–2]. Very thick deposits exceeding 50 µm after C5 are observed on the high field side of the inner strike line. These deposits peel off on the sub-millimeter length scale, probably triggered by arcing. The area fraction altered by delamination exceeds 25%.

The toroidal W erosion pattern regarding the ripple, but also on each individual tile was analyzed additional to the poloidal width of the strike lines. A maximum tungsten erosion of about 15 µm is observed on a very restricted area of several mm<sup>2</sup>. There erosion reaches on microscopic areas the graphite. The erosion follows the ripple and is stronger pronounced at the outer strike line with a variation by nearly one order of magnitude. The total erosion is only about 20% higher at the outer than at the inner strike line. This assessment of the total W erosion in the divertor will be discussed.

[1] M.Balden et al., Phys.Scripta 96, 124020 (2021)

[2] M.Diez et al., Nucl.Mater.Energy 34, 101399 (2023)

## High heat flux testing of actively cooled graphite- and tungsten-armoured JT-60SA flat-tile divertor mock-ups

Daniel Dickes<sup>1</sup>, Bernd Boeswirth<sup>1</sup>, Katja Hunger<sup>1</sup>, Henri Greuner<sup>1</sup>, Marianne Richou<sup>2</sup>, Johann Riesch<sup>1</sup>, Mehdi Firdaouss<sup>2</sup>, Valerio Tomarchio<sup>3</sup>, Rudolf Neu<sup>1</sup>

<sup>1</sup>Max Planck Institute for Plasma Physics, Garching, Germany; <sup>2</sup>CEA-IRFM, F-13108 Saint Paul Lez Durance, France;

<sup>3</sup>F4E Germany, Germany.

JT-60SA is a fusion experiment built within the “Broader Approach Agreement” between the European Union and Japan, aiming to complement the ITER fusion reactor project [1]. The JT-60SA experiment is a superconducting tokamak, initially planned to have an operation phase with actively cooled carbon plasma-facing components followed by an operation phase with tungsten plasma-facing components [2]. Under this assumption, Fusion for Energy and EUROfusion worked on a series of actively cooled test divertor mock-ups [3]. The first test mock-ups consisted of armour tiles, which were either made of graphite (C) or tungsten (W), and an actively cooled heat sink made of a Titanium–Zirconium–Molybdenum (TZM) alloy, with Copper–Chromium–Zirconium alloy being discussed as an alternative [3].

Three actively cooled TZM-based mock-ups with C and W armour tiles were tested in the GLADIS [4] high heat flux (HHF) test facility. Following a pre-characterization, the mock-ups were exposed to a series of HHF screening tests with heat loads of up to 15 MW/m<sup>2</sup>, followed by cyclic loading. The cyclic loading was performed at an incident heat flux of 10 MW/m<sup>2</sup> for a pulse length of 10 s. While the W-armoured mock-up exhibited a water leakage in the TZM heat-sink material already during the screening test series, the C-armoured mock-ups could be tested for a minimum of 150 cycles and more. After HHF testing, the mock-ups were subjected to a microscopy analysis, indicating crack formation in selected W and C armour tiles. In this contribution, we report and discuss these HHF tests and the post-exposure characterisation results in detail, also considering non-destructive thermal contact resistance SATIR tests [3].

### References:

- [1] JT-60SA website, [www.jt60sa.org/wp/governance/](http://www.jt60sa.org/wp/governance/), accessed 11.12.2024
- [2] Y. Kamada et al., Nucl. Fusion 62 042002 (2022)
- [3] S. Garitta et al., Fusion Engineering and Design 199, 114133 (2024)
- [4] H. Greuner et al., Fusion Engineering and Design 75–79, 345–350 (2005)



## Session 6: Erosion, re-deposition, mixing, and dust formation

22 May, 8:30 – 10:20

I-10

### Measurements and modelling of charge-exchange neutral flux to the first wall on EAST

Rui Ding

Institute of Plasma Physics, HFIPS, Chinese Academy of Sciences, China.

In future fusion reactors such as ITER and DEMO, the charge-exchange neutrals (CXN) flux to the first wall will be increased by several orders of magnitude compared to the present tokamaks. CXN-induced erosion will play an important role on the lifetime of first wall materials, the core plasma confinement, and the overall fuel retention, especially in magnetically shadowed regions where plasma ions cannot reach. To make reliable numerical predictions for future devices, it is essential to know the generation mechanism of CXN, and also the fluxes, energy and angular distributions of the CXN on the first wall. Recent experiments on EAST reveal the dependence of CXN flux to the first wall on different plasma conditions, which help to elucidate the key physics of CXN production and transport with the help of edge simulations using the grids extended to the first wall.

A low-energy neutral particle analyzer (LENPA) diagnostic system has been developed on EAST to measure the CXN flux to the outer wall in the energy range of 20–3000 eV [1]. Recent measurements show that the energy distribution of CXN flux strongly depends on the heating power, plasma density, fueling method and wall condition. Higher heating power leads to higher flux of both low and high energy CXNs. During plasma density ramp up experiments, lower energy CXN flux (<150 eV) increases, while higher energy CXN flux decreases. Improving fueling depth and wall conditioning can decrease the CXN flux to the first wall, which is related to the edge neutral pressure.

New EIRENE diagnostic options have been developed in SOLPS-ITER code to model the LENPA measured CXN spectrum. Based on the computational grid fully extended to the wall, simulations reproduce the measured edge plasma profiles, and obtain the CXN energy spectrum matching well with the LENPA diagnostic (differences are within 40%). The dependency of the CXN energy spectrum on the heating power, plasma density, fueling, and wall condition are reproduced by simulations. The source and loss of CXN with different energy are elucidated in detail for the first time. Based on the source analysis, the energy spectrum shape has been well explained and verified by experiments. The loss processes of CXN in flight pathway is dominated by charge exchange, and also impacted by ionization. The loss fraction increases with particle energy. These results are valuable for understanding CXN behavior and prediction of its induced first wall erosion in future fusion reactors.

[1] N.X. Liu, R. Ding, L. Mu, et al., Nucl. Mater. Energy 33, 101258 (2022)

## **Ion-solid interaction for light ions in plasma-facing materials: Experimental corrections and their effects on simulation-based sputter yields**

Eduardo Pitthan<sup>1</sup>, Philipp M. Wolf<sup>1</sup>, Jila Shams-Latifi<sup>1</sup>, Martina Fellinger<sup>2</sup>, Friedrich Aumayr<sup>2</sup>, Daniel Primetzhofer<sup>1</sup>

<sup>1</sup>Uppsala University, Sweden; <sup>2</sup>TU Wien, Fusion@ÖAW, Vienna, Austria, Austria.

Sputtering, defect formation, and particle implantation due to plasma-wall interactions (PWI) are key processes that must be understood for operation of future fusion reactors with minimum maintenance [1]. In these processes, fundamental quantities in ion-solid interactions such as the specific energy deposition of plasma species in wall materials or the interaction potentials between ions and wall species play significant roles. Despite being important input variables for modelling erosion and implantation, such quantities are often insufficiently known: For example, there are no available experimental datasets for interatomic potentials for slow light ions in tungsten (W). In addition, the influence of these quantities on plasma-wall related parameters such as sputtering yields remains to be investigated.

This contribution summarizes recent experimental studies of these fundamental quantities. In particular, electronic energy losses and short-range repulsive potentials of impacting light plasma species (H, D, and He) in candidates for plasma-facing materials of next-generation fusion devices (W, Fe, and EUROFER97) are evaluated experimentally. For that, ions with a wide range of energies (sub-keV to multiple MeV) [2] and different targets (bulk samples, pre-irradiated and damaged materials, and deposited thin films) are used. The experimental results [3,4] are compared to currently available semi-empirical and theoretical models, and quantitative corrections are extracted. From our results, discrepancies up to 60% were identified in comparison to commonly used semi-empirical models.

The sensitivity of statistical quantities such as sputtering yields on the magnitude of the aforementioned parameters is furthermore tested with simulation codes based on the binary collision approximation. The simulated values are compared to experimentally obtained ones using a high sensitivity quartz crystal microbalance and discrepancies are discussed. Our recent results thus not only provide necessary datasets for these fundamental quantities but also directly enhance the understanding on how these values influence ion-solid interaction relevant for future fusion reactors.

[1] S. Brezinsek et al., Nucl. Fusion. 57, 116041 (2017)

[2] P. Ström and D. Primetzhofer, J. Instrum. 17, P04011 (2022)

[3] J. Shams-Latifi, E. Pitthan, P. M. Wolf, and D. Primetzhofer, Nucl. Mater. Energy 36 (2023)

[4] J. Shams-Latifi, E. Pitthan, and D. Primetzhofer, Radiat. Phys. Chem. 224 (2024)

## Modelling fuel retention in the W divertor during the D/H/D changeover experiment in WEST

Etienne Hodille<sup>1</sup>, Davide Piccinelli<sup>1</sup>, Manon Bertoglio<sup>1</sup>, Thierry Loarer<sup>1</sup>, Julien Denis<sup>1</sup>, Guido Ciraolo<sup>1</sup>, Patrick Tamain<sup>1</sup>, Eleonore Geulin<sup>1</sup>, Alberto Gallo<sup>1</sup>, Stefane Vartarian<sup>1</sup>, Regis Bisson<sup>2</sup>, Bernard Pégourié<sup>1</sup>, Yann Anquetin<sup>3</sup>, Yann Corre<sup>1</sup>, Kaelyn Dunnell<sup>4</sup>, Tom Wauters<sup>5</sup>

<sup>1</sup>CEA, IRFM, France; <sup>2</sup>CNRS, PIIM, France; <sup>3</sup>Aix-Marseille Univ, CNRS, IUSTI, France; <sup>4</sup>Plasma Science and Fusion Center, MIT, United States; <sup>5</sup>ITER Organization, France.

The retention, outgassing and removal of hydrogen isotopes (HIs) in the plasma facing components are key issues for the development of fusion reactors. The WEST divertor is made of the same actively cooled tungsten (W) monoblock technology as in ITER. Thus, the investigation of fuel retention, outgassing and removal in the WEST divertor is key to estimate the tritium inventory in the ITER divertor.

During the C7 WEST campaign (February 2023), a D/H/D changeover experiment was performed in WEST to investigate isotopic exchange as a possible technique of fuel removal. The session of about 40 pulses was divided in 3: the first 6 pulses were fuelled by puffing D2, the next 17 pulses by puffing H2, and the last 16 pulses by puffing D2.

This study concerns the modelling of the D/H retention in the WEST W divertor during this D/H/D changeover experiment using the MHIMS code. A pure W divertor is considered with a MHIMS model parametrized with laboratory experiment [2]. After validating the background plasma calculated by SOLEDGE3X-EIRENE [3] with the Langmuir Probe data in the divertor, the H/D implantation properties (fluxes, energies, angle of incidence) are given as input to MHIMS. Finally, the outgassing fluxes of the MHIMS simulations are transformed into partial pressures of H2, HD and D2 [4,5] and compared to the mass spectrometer signal during the waiting phase between each pulse of the changeover session.

The outgassing fluxes calculated by MHIMS and the one measured in WEST after the discharges shows similar  $t^{-\alpha}$  exponential decay with  $\alpha$  around 0.8 in the simulations and 1.0 in the experiment. However, the pressure given by the outgassing from the divertor only is about 5 times lower than the experimentally observed pressure, suggesting outgassing from other components less exposed to the plasma contributes to the total vacuum pressure. Regarding the dynamics of the calculated H and D inventory, they follow the sequence of the changeover as the plasma and the divertor implants and recycles fuel particles. However, during the H plasmas, the H isotopic ratio in the plasma grows up to 0.7 while it stays below 0.6 in the material. Indeed, the analysis of the H/D depth profiles shows that the 17 H plasmas are able to remove the D up to the first 100 nm while 700 s of cumulated H plasma exposure is not enough to reach D trapped deeper. Thus, the changeover is an efficient tool to recover hydrogen isotopes but focused near the plasma-exposed surface.

Acknowledgements: EUROfusion, ANR Platon.

Additional authors: WEST TEAM and the EUROfusion Tokamak Exploitation Team.

[1] E. A. Hodille et al, Nucl. Fusion 64 (2024) 046022

[2] J. Roth et al, J. Nucl. Mater 432 (2013) 341 – 347

[3] H. Bufferand et al, Nucl. Fusion 61 (2021) 116052

[4] J. Denis et al, Nucl. Mater. Energ. 19 (2019) 550–557

[5] F. Cursi et al, Submitted to Nuclear Fusion (2025)

## **ERO2.0 study of erosion and deposition on ITER diagnostic mirrors assuming different material mixes**

Sebastian Rode<sup>1</sup>, Sebastijan Brezinsek<sup>1</sup>, Andreas Kirschner<sup>1</sup>, Lucas Moser<sup>2</sup>, Richard Pitts<sup>2</sup>, Juri Romazanov<sup>1</sup>, Alexis Terra<sup>1</sup>, Tom Wauters<sup>2</sup>, Sven Wiesen<sup>3</sup>

<sup>1</sup>Forschungszentrum Jülich GmbH, Germany; <sup>2</sup>ITER Organization, France; <sup>3</sup>DIFFER – Dutch Institute for Fundamental Energy Research, Netherlands.

Optical diagnostics hold a critical role in the operation of experimental fusion devices. In ITER, diagnostic apertures are located in the Diagnostic First Wall (DFW) of the Equatorial and Upper Port Plugs (EPP, UPP). The apertures serve as entry points to mirror systems of optical diagnostics, such as the Visible and Infrared Wide Angle Viewing Systems. Impacting particle fluxes, e.g. energetic Charge-Exchange Neutral (CXN) hydrogen isotopes or sputtered wall material, can affect the quality of the mirror systems by deposition and erosion on the plasma-facing metallic mirrors, i.e. the First Mirrors (FMs).

In this study, the particle fluxes into the diagnostic ports and apertures of the UPP and EPP cut-outs in ITER were simulated with the Monte-Carlo transport code ERO2.0. A full 3D treatment of the particle transport in a validated multi-stage simulation workflow [1] was applied, evaluating the fluxes over the full expected ITER pre-fusion and fusion power operation times [2]. Changes in the elemental composition of the stainless steel (simplified to pure iron) port surfaces were described by a Homogeneous Mixing Model. This ERO2.0 study presents predictive modelling as part of the recent ITER re-baselining activities [3] and assesses different material assumptions: full-tungsten (W) ITER, an infinitely boronized ITER representing the worst-case scenario fluxes into the ports from boron coatings put down on the First Wall by regular boronizations, and a comparison to the originally planned material mix with a beryllium (Be) First Wall and W divertor.

The key findings of this study are very favourable for the FM performance: the erosion and deposition on the FMs at the end of the envisaged ITER operational time are negligible in the centre of the FMs in both ports, featuring less than 5 nm deposition of impurities, and ~10 nm erosion of the metallic mirror surface in all cases. Sputtering is caused nearly exclusively by the CXN, which means that the assumed DFW material does not significantly affect the FM erosion. Concerning additional deposition of material from outside the aperture on the mirrors, the boronized ITER performs slightly better than a clean Be/W ITER, while a pristine full-W ITER is expected to have the lowest additional deposition.

## **Session 7: Tungsten, tungsten alloys, and advanced steels**

**22 May, 10:50 – 12:40**

I-12

### **Tungsten Alloys with Enhanced Stability and Manufacturability Through Integrated Alloy Design and Microstructural Engineering**

Jason Trelewicz<sup>1</sup>, Ian McCue<sup>2</sup>, Nicholas Olynik<sup>1</sup>, Sean Mascarenhas<sup>1</sup>, David Sprouster<sup>1</sup>, Hyeji Kim<sup>2</sup>, Samuel Price<sup>2</sup>, Tim Graening<sup>3</sup>, Travis Gray<sup>3</sup>, Christopher Ledford<sup>3</sup>, Julio Rojas<sup>3</sup>, Michael Kirka<sup>3</sup>

<sup>1</sup>Stony Brook University, United States; <sup>2</sup>Northwestern University, United States; <sup>3</sup>Oak Ridge National Laboratory, United States.

Of the many significant materials challenges for future fusion reactors, the susceptibility of tungsten to recrystallization above 1200°C and its stability under thermal transients continues to plague the development of stable divertor armor. Additionally, the need for geometrically complex components to control strike point interactions has driven interest in laser additively manufactured (AM) tungsten, which suffers from cracking during solidification. In this presentation, two computationally designed tungsten alloys are introduced for addressing the intrinsic limitations of unalloyed tungsten in terms of thermal stability and manufacturability. The first material is a grain boundary stabilized ultrafine grained W-Ti-Cr alloy. Constructed using computational thermodynamics, alloy design maps are used to identify compositional complexities that stabilize fine-grained microstructures via synergistic thermodynamic and kinetic mechanisms. The resulting W-Ti-Cr (>95 wt.% W) compositions are synthesized through high energy ball milling and field assisted sintering with stable microstructures demonstrated up to 1500°C, well above the common recrystallization point for unalloyed tungsten.

The second W-Ti-Fe (>96 wt.% W) alloy was developed through a CALPHAD-based alloy design strategy to fabricate laser AM tungsten materials free of process cracking and with improved fracture properties. Microstructures are first contrasted with pure laser AM tungsten and demonstrate an effective “crack-healing” mechanism attributed to the presence of a solute-rich phase during solidification, which simultaneously enhances the alloy’s capacity for plastic strain accumulation relative to pure laser AM tungsten. A second comparison is made with tungsten processed through electron beam (e-beam) melting. Densities are reported up to 99.98% with process parameter – texture correlations identified. Mini tensile test samples extracted in build and perpendicular directions were tested up to 800°C and revealed exceptional strength and ductility, but unsurprisingly anisotropic properties. A reduction of preheat temperature and accelerated build times were achieved by using a W-3Re alloy, which are contrasted to the laser AM W-Ti-Fe alloys in terms of microstructure and properties. Collectively, we show that all these novel classes of tungsten alloys provide a basis for enhancing plasma facing armor performance relative to unalloyed tungsten in terms of thermal stability and manufacturability.

**Advanced Tungsten Based Materials for Plasma Facing Components**Shuhei Nogami

ALMT, Japan.

Tungsten (W) will be used as plasma facing material (PFM) in fusion reactors after ITER. However, in order to maintain the integrity of the material even during long-term operation under high heat loads, it is necessary to overcome issues such as the low temperature brittleness and recrystallization embrittlement of W. To overcome these issues, the development of modified W based materials has been promoted in Japan using a powder metallurgy technology in cooperation with universities, national institutes, and companies. The main methods applied for the modification were the second phase dispersion and solid solution alloying, which involved the control of grains and grain boundary characteristics. In particular, the effects of doping with potassium bubbles (K-doping) and lanthanum (La) oxide particles, and alloying with rhenium (Re) and tantalum (Ta) were evaluated. As a result, the ductile-to-brittle transition temperature (DBTT), recrystallization resistance, and resistance to high heat flux (HHF), which might be the dominant factors for the operating temperature range and lifetime of plasma facing components (PFCs), were improved compared to pure W, and a certain effect was successfully observed.

Even in the modified W based materials that have been improved through the above-mentioned methods, most DBTT is still higher than room temperature. Considering the maintenance of PFCs during the operation period and the increase in DBTT caused by neutron irradiation, further improvement is desirable. As one candidate solution, W matrix composites reinforced with W wires (Wf/W composites) is being developed. A.L.M.T. Corp. has been providing W narrow wires as mass-produced products for many years. It has also been shown that the recrystallization resistance and strength of W wires can be improved by K-doping. Possibility of application of the W narrow wires to composite materials will be presented in this talk.

In addition to the above-mentioned development of monolithic and composite materials, recent progress on the development for future fusion, e.g., advanced W powders for additive manufacturing (AM) and W based materials for radiation shielding, will be presented.

Acknowledgements: The author would like to express my gratitude for the great cooperation of Professor Emeritus Akira Hasegawa and his team at Tohoku University, Dr. Michael Rieth and his team at Karlsruhe Institute of Technology (KIT), Dr. Gerald Pintsuk, Dr. Jan Coenen, Dr. Marius Wirtz and their team at Forschungszentrum Juelich (FZJ), Dr. Dmitry Terentyev and his team at SCKCEN, Dr. Yutai Kato and his team at Oak Ridge National Laboratory (ORNL), and finally, many colleagues at A.L.M.T. Corp.

O-14

### **Recent development on upscaling functionally graded W/EUROFER coating for the DEMO First Wall application**

Ashwini Kumar Mishra<sup>1</sup>, Thilo Grammes<sup>1</sup>, Arkadi Kreter<sup>2</sup>, Marcin Rasinski<sup>2</sup>, Jan Coenen<sup>3</sup>, Jarir Aktaa<sup>1</sup>

<sup>1</sup>Karlsruhe Institute of Technology (KIT), Germany; <sup>2</sup>Forschungszentrum Jülich GmbH, Germany; <sup>3</sup>FZJ, Germany.

A functionally graded W/EUROFER coating has been planned as a protective layer for the structural material EUROFER of the DEMO First Wall. Tungsten has high thermal conductivity, high melting temperature, high sputtering resistance, and low neutron activation which makes it a suitable candidate for a protective layer over steel. The coefficient of thermal expansion mismatch between W and steel generates high thermal stress during the deposition and fusion applications, which can lead to failure/delamination of coatings. A functionally graded W/EUROFER layer has been introduced between top-coat W and steel substrate to solve this problem.

This work shows a recent development of functionally graded W/EUROFER coating over the First Wall relevant flat and curve structures of steel. A functionally graded W/EUROFER coating was deposited by a low-pressure plasma spraying process over the large flat and curved steel structure and the quality of the coating was evaluated. A phased array ultrasonic method was developed to evaluate the interface properties of the coating. Furthermore, structural and mechanical characterizations of these coatings were performed using cross-sectional images by scanning electron microscope and indentations. The performance of functionally graded W/EUROFER coating in fusion-relevant plasma exposure conditions was also evaluated using the linear plasma device PSI-2. The first set of experiments was performed by exposing the coating to Ne plasma to determine the sputtering of the coating as compared to bulk tungsten. The second set of experiments was performed by exposing it to deuterium plasma to evaluate the deuterium retention properties of coating as compared to bulk tungsten.

Castellation of coating was introduced as an additional method to further reduce the thermal stresses in the coatings. Finite element simulations were performed to determine the optimized castellation. Castellation of the straight coated sample was performed which shows the reduction in bending after castellation indicating the reduction in residual stresses. Afterwards, a thermal fatigue test was performed on the castellated sample and no crack/delamination was found till 5000 cycles which shows a successful castellation of coatings.

O-15

### **Development and Testing of a Novel FAST-Diffusion Bonding Process for Joining Eurofer97 Steel to Tungsten in Plasma Facing Components**

Daniel Wilkison, Patrick Grant, Enzo Liotti

Department of Materials University of Oxford, United Kingdom.

Manufacturing plasma-facing components for nuclear fusion reactors involves joining an armour material with a structural material used in the vacuum vessel. Tungsten (W) is a strong candidate for the armour material due to its high melting point, excellent thermal conductivity, low vapour pressure, low tritium retention, and high resistance to sputtering. For structural materials, low-activation steels like EUROFER 97 (E97) are favoured for their superior mechanical properties. However, joining W to E97 is challenging due to significant mismatch in their melting points, thermal expansion rates, and the formation of brittle intermetallic phases. To address these issues, approaches such as interlayers, functionally graded layers, and dense vertical crack coatings have been developed and have shown partial success on small-scale

joints. Recently, V. Ganesh et al. [1] compared these approaches to direct diffusion bonding of W to E97 performed with field-assisted sintering technique (FAST), also known as spark plasma sintering (SPS). The FAST diffusion bonding method produced joints capable of withstanding higher heat loads than joints produced with interlayers or functionally graded layers. However, the reason why FAST diffusion bonding can overcome the stress created by thermal expansion mismatch and produce W-E97 joints with excellent resistance to thermal cycling remains unknown.

To answer this question, this work identifies the key mechanisms underlying FAST diffusion bonding that address the challenges of W-E97 joining. These mechanisms are first analysed with finite element modelling and then validated through a comparative study using the Magnum PSI facility at the Dutch Institute for Fundamental Energy Research. The joints are subjected to fusion-relevant thermal conditions and cyclic heat loads produced by hydrogen plasma. Finally, we demonstrate the suitability of FAST diffusion bonding for joining other dissimilar material systems, including W-CuCrZr joints. Together with the Dr. Fritsch Group, we demonstrated the scalability of FAST diffusion bonding by producing tiles as large as 10 cm × 10 cm with excellent bonding strength using industry-scale FAST machines.

[1] V. Ganesh, D. Dorow-Gerspach, M. Bram, C. Linsmeier, J. Matejicek, M. Vilemova, *Energies* 16, 3664 (2023).



## Session 8: Fuel retention and removal

22 May, 14:20 – 16:40

I-14

### **In situ Measurement of H, D, T Retention in the JET Tungsten Divertor Components – Lessons Learned for the ITER LID-QMS Diagnostic**

Mirosław Zlobinski<sup>1</sup>, Gennady Sergienko<sup>1</sup>, Ionuț Jecu<sup>2</sup>, Chris Rowley<sup>2</sup>, Anna Widdowson<sup>2</sup>, Rob Ellis<sup>2</sup>, Domagoj Kos<sup>2</sup>, Ivor Coffey<sup>3</sup>, Martin Fortune<sup>2</sup>, David Kinna<sup>2</sup>, Misha Beldishevski<sup>2</sup>, Laura Laguardia<sup>4</sup>, Gabriele Gervasini<sup>4</sup>, Andreas Krimmer<sup>1</sup>, Horst Toni Lambertz<sup>1</sup>, Alexis Terra<sup>1</sup>, Alexander Huber<sup>1</sup>, Sebastian Brezinsek<sup>1</sup>, Timo Dittmar<sup>1</sup>, Meike Flebbe<sup>1</sup>, Rongxing Yi<sup>1</sup>, Rahul Rayaprolu<sup>1</sup>, Sebastian Frieze<sup>1</sup>, Philippe Mertens<sup>1</sup>, Ilia Ivashov<sup>1</sup>, Yury Krasikov<sup>1</sup>, Krzysztof Młynczak<sup>1</sup>, Jochen Assmann<sup>1</sup>, David Castaño Bardawil<sup>1</sup>, Michael Schrader<sup>1</sup>, Philip Andrew<sup>5</sup>, Xi Jiang<sup>5</sup>, João Figueiredo<sup>6</sup>, Peter Blatchford<sup>2</sup>, Scott Silburn<sup>2</sup>, Emmanuelle Tsitrone<sup>7</sup>, Emmanuel Joffrin<sup>7</sup>, Karl Krieger<sup>8</sup>, Yann Corre<sup>7</sup>, Antti Hakola<sup>9</sup>, Jari Likonen<sup>9</sup>, The EUROFUSION TOKAMAK EXPLOITATION Team<sup>10</sup>, The JET CONTRIBUTORS Team<sup>11</sup>

<sup>1</sup>Forschungszentrum Jülich GmbH, Jülich, Germany; <sup>2</sup>UKAEA, Culham Campus, Abingdon, United Kingdom; <sup>3</sup>Queen's University Belfast, Belfast, Northern Ireland, United Kingdom; <sup>4</sup>Istituto per la Scienza e Tecnologia dei Plasmi, CNR, Milano, Italy; <sup>5</sup>ITER Organization, St-Paul-lez-Durance, France; <sup>6</sup>EUROfusion Programme Management Unit, Garching, Germany; <sup>7</sup>CEA, Institute for Research on Fusion by Magnetic confinement, St-Paul-lez-Durance, France; <sup>8</sup>Max-Planck-Institut für Plasmaphysik, Garching, Germany; <sup>9</sup>VTT Technical Research Centre of Finland Ltd, Espoo, Finland; <sup>10</sup>See the author list of E. Joffrin et al., Nuclear Fusion 64 (2024) 11, doi:10.1088/1741-4326/ad2be4, Germany; <sup>11</sup>See the author list of C.F. Maggi et al., Nuclear Fusion 64 (2024) 11, doi:10.1088/1741-4326/ad3e16, United Kingdom.

It is important to monitor the retention of hydrogen isotopes at PFCs with respect to tritium due to radiation safety, w.r.t. the fusion fuel (D, T) due to the fuel cycle and for all hydrogen isotopes due to their material degradation effect. In 2023 a new in situ retention diagnostic has been installed on JET [1] and its first quantitative results will be presented here.

The diagnostic relies on Laser-Induced Desorption that thermally releases retained gases and their detection by Quadrupole Mass Spectrometry – thus called LID-QMS. The detection limit was so low that we detected the long-term D retention from each individual laser spot of 3 mm diameter along the whole poloidal scan of the upper inner divertor of JET. Then, during the DT campaign even the low T amount of one week of DT operation was detected due to a fast laser raster mode. This allowed to monitor the T retention every week and after the DT campaign the T depletion due to different T removal techniques was observed by repetitive LID-QMS measurements. Hence, this diagnostic not only allows direct access to retention physics and identification of high retention areas, but also the assessment of T removal techniques.

Therefore, LID-QMS is already under design as Tritium Monitor Diagnostic for ITER benefitting from the lessons learned at JET. Similarities and differences to the application at JET will be shown and new challenges at ITER will be discussed.

[1] M. Zlobinski, et al. Nucl. Fusion 64, 086031 (2024), doi:10.1088/1741-4326/ad52a5

## **Femtosecond laser-induced ablation – quadrupole mass spectroscopy for depth- and lateral profiling of helium and hydrogen-isotopes in fusion materials**

Steffen Mittelmann, Benedikt Buchner, Udo von Toussaint, Matej Mayer, Andreas Theodorou, Thomas Dürbeck, Wolfgang Jacob, Thomas Schwarz-Selinger

Max Planck Institute for Plasma Physics, Germany.

We present our new instrumentation LAMA (Laser Ablation Mass Analysis) using femto-second pulsed Laser Induced Ablation (fs-LIA) in combination with a Quadrupole Mass Spectrometer (QMS) for the simultaneous detection of helium (He) and hydrogen (H) isotopes in relevant materials used in fusion devices. Our study highlights the importance of using sub-picosecond laser pulses for an accurate depth-resolved detection of gaseous species trapped in metallic substrates. Notably, our experiment is the first to demonstrate the feasibility of fs-LIA-QMS, as previous pioneer experiments have only used picosecond and nanosecond laser pulses [1, 2, 3]. These pulse durations are not sufficient to achieve the required depth resolution due to heat affected diffusion and desorption of the gaseous species.

Our fs-LIA-QMS experiment detected deuterium (D) and He in tungsten (W) and EUROFER steel samples with depth resolution better than 20 nm or high lateral resolution better than 20  $\mu$ m. In order to achieve this, we developed a deconvolution algorithm that takes into account the crater shape and the ablation rate, allowing us to gain more reliable depth-resolved information. Depending on the configuration and possible size of ablation area, a detection limit of less than 0.02 at.% concentration per ablated layer is achieved with the presented device. This is tested using displacement-damaged W samples decorated with D and He-implanted W and EUROFER samples.

The fs-LIA-QMS technique offers the potential for high depth and lateral resolution, making it an attractive tool for the investigation of plasma-facing components in future fusion devices. This can in many cases enable the detailed characterization of the distribution of impurities in these materials, which is crucial for the development of next-generation fusion reactors.

We compare our fs-LIA-QMS results quantitatively with Nuclear Reaction Analysis (NRA) and Thermal Desorption Spectroscopy (TDS) data, demonstrating the accuracy and reliability of the fs-LIA-QMS technique. Furthermore, we discuss future applications and necessary developments to make the fs-LIA-QMS technique a reliable depth and laterally resolved method.

[1] O.S. Medvedev, et al., Nuclear Materials and Energy, 41, 101829 (2024)

[2] G. Shaw, et al., Phys. Scr., 2020, 014029 (2020)

[3] J. Oelmann, et al., Spectrochimica Acta Part B: Atomic Spectroscopy, 2018, 144 (2018)

### **Tritium containing plasma-facing materials from fusion reactors: research needs, capabilities and limitations in tritium studies**

Miyuki Yajima<sup>1</sup>, Yuji Hatano<sup>2</sup>, Yasuhisa Oya<sup>3</sup>, Teppei Otsuka<sup>4</sup>, Yuji Torikai<sup>5</sup>, Suguru Masuzaki<sup>1</sup>, Masayuki Tokitani<sup>1</sup>, Mitsutaka Miyamoto<sup>6</sup>, Yui Obata<sup>5</sup>, Nobuyuki Asakura<sup>7</sup>, Hirofumi Nakamura<sup>7</sup>, Takumi Hayashi<sup>7</sup>, Kanetsugu Isobe<sup>7</sup>, Dai Hamaguchi<sup>7</sup>, Hiroyasu Tanigawa<sup>7</sup>, Kim Jaehwan<sup>7</sup>, Yutaka Sugimoto<sup>7</sup>, Takashi Nozawa<sup>7</sup>, Anna Widdowson<sup>8</sup>, Marek Rubel<sup>9</sup>, Jari Likonen<sup>10</sup>

<sup>1</sup>National Institute for Fusion Science, Japan; <sup>2</sup>Tohoku University, Japan; <sup>3</sup>Shizuoka University, Japan; <sup>4</sup>Kindai University, Japan; <sup>5</sup>Ibaraki University, Japan; <sup>6</sup>Shimane University, Japan; <sup>7</sup>National Institute for Quantum Science and Technology, Japan; <sup>8</sup>UKAEA, Culham Campus, Abingdon, United Kingdom; <sup>9</sup>Uppsala University/KTH Royal Institute of Technology, Sweden; <sup>10</sup>VTT Technical Research Centre of Finland Ltd, Espoo, Finland.

Fueling a fusion reactor with heavy hydrogen isotopes (D and T) involves a whole spectrum of safety measures connected with the presence of T and material activation by neutron fluxes. This – in turn – implies the need for relevant material handling and research facilities to ensure as detailed as possible characterization of in-vessel components, erosion – deposition probes and dust retrieved from a reactor. In this sense, the examination of materials from the Joint European Torus (JET) is the most demanding because of T and Be presence [1].

In the following, the Material R&D Facility at the International Fusion Energy Research Centre (IFERC) is introduced and results of specific T analyses are presented. Equipment in the controlled area (restricted access) comprises microscopes (electron and optical) and electron microprobes, material cutting devices, set-ups for X-ray and radiography, X-ray photoelectron spectrometer, chemical laboratory used e.g. for etching, equipment for thermal desorption and full combustion, optical spectrometers, liquid scintillation counters, precision balance etc.

Studies have been performed for a range of materials from JET with metal (Be and W) walls after three D2-fueled campaigns with T originating from  $D+D \rightarrow T$  (1 MeV) + H (3 MeV) in the case of divertor and limiter tiles, and also from earlier DTE1 experiments in the case of vacuumed dust. An overview from the ten year cooperation will summarise how the range of analysis techniques have provided comprehensive T results for JET retention studies including [2–5]:

- Global T distribution on wall components.
- Limiters: the highest T levels, up to 0.3 kBq cm<sup>-2</sup>, found in outer poloidal limiters.
- Divertor: the majority of T detected in the surface region of divertor tiles, with areal activities in the range 0.5–12 kBq cm<sup>-2</sup>.
- Tritium in dust is associated mainly with the presence of carbon particles being a legacy from the JET-C operation. The T level in C –based particles is over 100 times greater than in Be- and W-based objects.
- New procedures combining chemical etching with radiographic techniques were developed and tested to determine T levels in bulk W.

In addition to the results coming from IFERC, the work has provided relevant personnel training to form the basis for working with heavily contaminated materials coming first from JET after full D-T campaigns 2022 & 2023, and then from the next-step devices.

[1] A. Widdowson et al., Phys. Scr. T167 (2016) 014057./ [2] M. Tokitani et al., Phys. Scr. T171 (2020) 014010./ [3] T.Otsuka et al., Nucl. Mater. Energy 17 (2018) 279–83. / [4] S. E. Lee et al., Nucl. Fusion 63 (2023) 046023./ [5] Y. Torikai et al., Nucl. Fusion 64 (2024) 016032.

## Depth profiling of tritium in bulk tungsten divertor tiles from JET with metal walls: tritium quantification and surface decontamination

Yuji Torikai<sup>1</sup>, Yui Obata<sup>1</sup>, Kazuaki Kasai<sup>1</sup>, Rion Nishida<sup>1</sup>, Senzai Oono<sup>1</sup>, Kazuma Mizobuchi<sup>1</sup>, Naoko Ashikawa<sup>2</sup>, Atushi Owada<sup>3</sup>, Suguru Masuzaki<sup>4</sup>, Miyuki Yajima<sup>4</sup>, Kanetsugu Isobe<sup>3</sup>, Takumi Hayashi<sup>3</sup>, Hirofumi Nakamura<sup>3</sup>, Yutaka Sugimoto<sup>3</sup>, Marek Rubel<sup>5</sup>, Anna Widdowson<sup>6</sup>

<sup>1</sup>Ibaraki University, Japan; <sup>2</sup>Kyoto Fusioneering, Japan; <sup>3</sup>National Institute for Quantum Science and Technology, Japan; <sup>4</sup>National Institute for Fusion Science, Japan; <sup>5</sup>Uppsala University/KTH Royal Institute of Technology, Sweden; <sup>6</sup>UKAEA, Culham Campus, Abingdon, United Kingdom.

Quantification of tritium (T) in bulk tungsten (W) is foreseen to be a challenging point in the determination of fuel balance and retention rate in a reactor with metal plasma-facing components (PFC). This calls for the development and testing of laboratory procedures to determine T on the surface and in the bulk of tiles, i.e. depth profiling.

Bulk W divertor tiles, especially Tile 5 lamella, retrieved from JET with metal walls after consecutive D2-fueled campaigns is the most relevant material for such studies which constitute an entry point for future T analyses in the JET divertor after DT campaigns, and materials from next step reactor-class machines. Therefore, JET samples cut from heavily plasma-loaded Stack C were chosen to accomplish lateral and in-depth T mapping. The procedure is based on: (i) chemical etching of W, (ii) T determination on the W surface and in the etchant after consecutive experimental steps [1]. The overall approach involves radiography, W weight loss measurements, liquid scintillography counting and microscopy. Masking techniques enable T profiles to be obtained separately for the plasma-facing surface (PFS) and side surfaces located in poloidal gaps between adjacent lamellae (ion and electron drift sides), and stacks in the divertor module (toroidal gap). Measurements were performed on samples after three JET operating periods spanning 2011–2016. A brief summary of the results are:

- Depth resolution is 0.2–0.3 m, but for practical reasons each etching step is 0.8–1.5 m.
- Results clearly show that following the D2-fueled shots one deals with the implantation of the non-confined 1 MeV T from the D–D reaction, and with the deposition of re-eroded T, i.e. species that entered a regular material migration regime.
- On the PFS the maximum T content is detected at a depth of around 2 m thus indicating high energy T implantation.
- In the poloidal gaps there is a 1–2 mm wide belt of high T content from the PFS. This is followed by a continuum of a lower T level further into the gap.
- The results demonstrate the use of etching as a surface decontamination method for post exposure handling of components, for example, during decommissioning.

Detailed results will be given together with a discussion of advantages/limitations of the method, and with plans for dealing with samples from DT campaigns.

[1] Y. Torikai et al., Fusion Sci. Tech. 54 (2008) 515

## Low Hydrogen Isotope Retention and High Irradiation Resistance in Columnar-Grained Tungsten Prepared via Chemical Vapor Deposition

Yue Yuan<sup>1</sup>, Hanqing Wang<sup>1</sup>, Ting Wang<sup>1</sup>, Yiwen Sun<sup>1</sup>, Hao Yin<sup>1</sup>, Mi Liu<sup>1</sup>, Hao Wang<sup>1</sup>, Ying Qin<sup>1</sup>, Long Cheng<sup>1</sup>, Fan Feng<sup>2</sup>, Zhe Chen<sup>2</sup>, Youyun Lian<sup>2</sup>, Binyou Yan<sup>3</sup>, Arkadi Kreter<sup>4</sup>, Guang-Hong Lu<sup>1</sup>

<sup>1</sup>Beihang University, China; <sup>2</sup>Southwestern Institute of Physics, China; <sup>3</sup>Xiamen Tungsten Co., Ltd., China; <sup>4</sup>Forschungszentrum Jülich GmbH, Germany.

With its advantages of high density, ultra-high purity (>99.99997%), and ease of preparing into complex geometries, chemical vapor deposited tungsten (CVD-W) stands out as a promising candidate for plasma-facing materials (PFMs) in future fusion devices. Atmospheric pressure CVD was employed to fabricate millimeter-thick columnar-grained W materials. The exposed surface, oriented perpendicular to the growth direction (GD), exhibits radial grain sizes ranging from 15 to 50  $\mu\text{m}$  and a strong [001] preferential grain orientation ([001] GD). The columnar grains feature an aspect ratio as high as 20. This study systematically reports the exceptional low hydrogen isotope retention and high irradiation resistance of CVD-W under various irradiation and thermal loading conditions.

Low-energy deuterium (D) plasma exposures were performed at  $\sim 500$  K over a wide fluence range (1024 – 1027 D m<sup>-2</sup>, up to 30 h). The results demonstrate that surface blistering in CVD-W is significantly suppressed by its [001] preferential grain orientation, with the blister area ratio being only 10% of that observed in ITER-like W. The total D retention in CVD-W was only 12 – 30% of that in ITER-like W. Simulations using the rate equation code indicate that D retention in tungsten is primarily governed by dislocation defects induced by D-induced surface blistering. Additionally, plasma-driven permeation (PDP) experiments revealed that vertical grain boundaries in CVD-W enhance the outward transport of D, further reducing D retention. Sequential irradiation experiments, involving pre-damage by 7 MeV tungsten ions (up to 2 dpa) followed by exposure to pure D or D+5% He mixed plasma, demonstrated that D retention in CVD-W was significantly lower than that in ITER-like W, amounting to 38% and 82% of the total, respectively. This highlights the superior low hydrogen retention of CVD-W even under synergistic high-energy heavy ion and low-energy plasma irradiation conditions. Additionally, a combination of extensive Transmission Electron Microscopy (TEM) defect analysis and nanoindentation tests confirmed that after 6 MeV copper ion irradiation at various temperatures up to 973 K, the irradiation defect populations and hardness of as-irradiated CVD-W were comparable to those of ITER-like W, indicating that CVD-W exhibits competitive resistance to displacement damage.

Moreover, the remarkable structural thermal stability of CVD-W was demonstrated in annealing experiments, where no obvious grain growth or loss of the columnar grain structure was observed after annealing at 2173 K for 3 h. Furthermore, under simulated ELM-like thermal shock conditions (duration: 1 ms, 100 pulses), CVD-W demonstrated a significantly higher cracking threshold (0.33 – 0.44 GW m<sup>-2</sup>) compared to ITER-like W (0.19 – 0.33 GW m<sup>-2</sup>), confirming its superior resistance to thermal shock cracking.

In conclusion, the results from this comprehensive study highlight the excellent performance of CVD-W, relative to ITER-like W, in terms of low hydrogen isotope retention, high resistance to hydrogen-induced blistering, high-temperature microstructural stability, resistance to displacement damage and thermal shock.

## Session 9: Tungsten, tungsten alloys, and advanced steels and Technology and qualification of plasma-facing components

23 May, 9:00 – 11:15

O-18

### Response of fibre-reinforced tungsten composites exposed to ELM-like transient events

Tyler Ray<sup>1</sup>, Jack Johnson<sup>1</sup>, Matthew Halloran<sup>1</sup>, Jitendra Tripathi<sup>1</sup>, Marius Wirtz<sup>2</sup>, Jan Coenen<sup>3</sup>, Ahmed Hassanein<sup>1</sup>

<sup>1</sup>Purdue University, United States; <sup>2</sup>Forschungszentrum Jülich GmbH, Germany; <sup>3</sup>FZJ, Germany.

Fibre-reinforced tungsten (Wf/W) composites exploit the extrinsic toughening mechanism of drawn fibres embedded in a W matrix. The fibres have superior tensile strength and can deflect cracks formed in the weaker W matrix alongside ductile deformation. Wf/W retains Wf/W ~95% of the thermal diffusivity of polycrystalline W, similar sputtering resistance, and more favourable mechanical properties [1]. Previous thermal shock studies performance conducted at room temperature indicated similar thresholds to uniform polycrystalline W, in which catastrophic melting occurred when exposed to a single 1.6 GWm<sup>-2</sup> transient heat load over 2 ms [2]. This work expands current research by introducing full ELM-like fusion events simulated via. steady-state heating, applied transient heat loading, and dual ion beam irradiations (He<sup>+</sup> and D<sup>+</sup>). Experiments were conducted at the Center for Materials Under eXtreme Environments (CMUXE) using the Ultra-High Flux Irradiation (UHFI-II) vacuum chamber. The UHFI-II is equipped with two broad beam end hall type ion sources which for these studies operated at 100 eV, just below the sputtering threshold for He<sup>+</sup> bombardment on W. Steady state heat loading was varied from simulated reactor startup conditions of RT to steady state temperatures of 450 °C and 850 °C. Simulated transients were applied to samples using a pulsed millisecond Nd:YAG laser orthogonal to the sample surface. Experiments were performed for one-hour testing with transient heat loadings in the 1-30 Hz frequency range, 0.2-2 ms pulse duration, resulting in a heat flux factors (HFF) ranging 10-50 MJm<sup>-2</sup>s<sup>-1</sup>/2 primarily at 850 °C.

Reactor-relevant ion loading (10:90|He<sup>+</sup>:D<sup>+</sup>) yielded increased surface bubbles at 450 °C compared to He only loading which led to enhanced erosion during transient heating studies. Cracking was observed on all Wf/W samples exposed to HFFs greater than 20 MJm<sup>-2</sup>s<sup>-1</sup>/2 while analysis of lower HFFs is underway. The W fibres were effective in deflecting cracks, with minor fibre cracking observed at higher HFFs. At HFF greater than 40 MJm<sup>-2</sup>s<sup>-1</sup>/2, significant cracking, melting, and recrystallization was observed. Crack depth analysis and testing are underway on W samples fabricated similarly to the Wf/W without fibre integration. This study aims to measure the cracking threshold, effectiveness of fibre addition to crack propagation, and overall effectiveness of Wf/W composites as potential plasma facing materials.

Acknowledgements:

This work was supported by the US DOE (FES) DE-SC0022993

[1] Y. Mao, J. W. Coenen, S. Sistla, et al., Phys. Scripta T171 014030 (2020)

[2] Y. Mao, J. W. Coenen, A. Terra, et al., Nucl. Fusion 62 106029 (2022)

## **Plasma facing and high heat flux material development and down-selection process within the European fusion materials program**

Gerald Pintsuk<sup>1</sup>, Giacomo Aiello<sup>2</sup>, Marius Wirtz<sup>3</sup>

<sup>1</sup>FZJ, Germany; <sup>2</sup>EUROfusion, Germany; <sup>3</sup>Forschungszentrum Juelich GmbH, Germany.

Material development for future fusion devices has a decades-long history in Europe, initiated under EURATOM through the EFDA collaborative agreement and further developed in the framework of the EUROfusion Consortium. One particular topic thereby is the development of advanced plasma facing and heat sink materials, which should allow extending the operational regime and the lifetime of in-vessel components as well as tackle safety concerns in case of accidental scenarios with regard to the baseline materials tungsten and CuCrZr.

While the primary focus in the European framework program FP8 was still on the optimization of the material concepts including chemical composition, manufacturing technology and material design, progressing into the conceptual design for DEMO the focus shifted towards industrial upscaling and technological implementation of the materials in the actual component design, which inevitably includes also qualification at operationally relevant neutron fluences. The progress thereby is, amongst others, monitored via assessment of the material technology readiness level of the individual materials, which also includes the identification of showstoppers leading to either modifications of the material / material concept or to discarding the material completely.

In this down-selection process, which is a necessity with regard to available manpower and financial resources and which require a variety of material data to take a sound decision, on the one hand a multitude of materials and fabrication processes have been discarded. This includes amongst others powder injection molding for plasma facing materials, SiC-fiber reinforced tungsten, TiC- and Y<sub>2</sub>O<sub>3</sub> particle reinforced tungsten, quaternary Cu-alloys. On the other hand, several materials and technologies are still part of the selection process for DEMO, which are self-passivating tungsten alloys for First Wall applications and K-doped as well as WC-reinforced tungsten materials as plasma facing material and W-fiber and -particle reinforced Cu-alloys as well as ODS-Cu (Y<sub>2</sub>O<sub>3</sub>) as heatsink. On top of that additive manufacturing technologies for both, tungsten and Cu-based structures, are assessed for in-situ repair as well as alternative and complex shaped design concepts as well as prospective material concepts for a fusion reactor that are yet on a low maturity level.

The history as well as the actual status of this development and down-selection process will be presented and an outlook on the final decision on the most promising concepts for the engineering design given.

## **Design development of inertially cooled tungsten first wall for ITER Start of Research Operation**

Lei Chen

ITER Organization, France.

The revised ITER Research Plan accompanying the 2024 re-baseline includes a new "Start of Research Operation" (SRO) phase, replacing the First Plasma and Pre-Fusion Power Operation phases of the 2016 Baseline [1]. A key feature of the new baseline is the switch from beryllium to tungsten (W) first wall (FW) armour [2]. To avoid the risk of damaging the complex, water-cooled panels while learning to avoid/mitigate disruptions and runaway electrons, an inertially

cooled, temporary first wall (TFW) will be fitted to the blanket shield blocks for SRO only. This contribution focuses on the design of this TFW, which is constrained by the demands of the two principal SRO scenario objectives: deuterium H-mode plasmas at half plasma current and toroidal field (7.5 MA, 2.65 T) and hydrogen L-mode discharges at full field and current (15 MA, 5.3 T).

Mimicking the final, actively cooled FW (for DT operation) in material, geometry, and interfaces, two design concepts are under development, to be deployed at different locations on the FW dictated by local plasma thermal loads: a heavy design with bulk W mechanically connected to stainless steel (SS) support, and a light design with W coating on SS. The TFW panel is segmented into W bulk or coated tiles bolted to a steel frame with partial slitting, or with fully separate fingers to ensure proper management of thermal loads and electromagnetic stresses.

Given the limited industrial experience with W coatings on SS in tokamak environments, a detailed coating qualification plan is underway. This includes high heat flux testing using an electron beam facility, and exposure of coated samples across reasonably large surface areas in a tokamak with ITER-relevant plasma loading conditions. The hydrogen transport code MHIMS [3] is employed to analyze outgassing from the inertially cooled TFW SS components throughout the SRO campaign, using average temperature evolutions of TFW panel designs obtained from ANSYS, with heat loads for the 15 MA/5.3 T L-mode discharge. Results indicate that the inter-pulse hydrogen pressure is affected by outgassing and provides insights for optimizing the SRO pulse plan to mitigate its effect.

[1] P. Barabaschi et al., 33rd Symposium on Fusion Technology (SOFT) (2024)

[2] R. A. Pitts et al., Nuclear Materials and Energy 42 (2025) 101854

[3] E. Hodille et al., J. Nucl. Mater. 467 (2015) 424

O-19

### **CFEDR and its PFMC progress**

Jiangang Li, Rui Ding, Tiejun Xu, Xuebin Peng

Institute of Plasma Physics, Chinese Academy of Sciences, China.

The Chinese Fusion Engineering DEMO Reactor (CFEDR) is the next device for the Chinese magnetic confinement fusion (MCF) program which aims the early demonstration of tokamak DEMO reactor in China. CFEDR will be operated either hybrid or steady-state operation scenarios of fusion power over 1 GW. The progress of CFEDR based on CFETR is briefly introduced in this talk.

Plasma facing material and components are the key issues of CFEDR. W alloy was chosen for both first wall and divertor material. Design of CFEDR first wall together with breeding blanket and its R&D will be presented. The details of the first prototype divertor module will be given in detail, including the design of divertor, material development, manufacture and full power testing up to 15MW/m<sup>2</sup> heat load.

[1]. Chan V. et al 2015 Nucl. Fusion 55 023017

[2] Yuanxi Wan, J.Li, Y.Liu et al., Nuclear Fusion 57 (2017)102009

[3] Y Q Yang et al, 2021 Plasma Phys. Control. Fusion 63 025015



## Overview of Advanced Plasma-Facing Materials Testing for Fusion Pilot Plants at DIII-D

Jonathan Coburn<sup>1</sup>, Florian Effenberg<sup>2</sup>, Mary Alice Cusentino<sup>1</sup>, Chase Hargrove<sup>3</sup>, Mykola Ialovega<sup>4</sup>, Maria Cunha<sup>5</sup>, Lauren Nuckols<sup>6</sup>, Žana Popović<sup>7</sup>, Shawn Zamperini<sup>7</sup>, Tyler Abrams<sup>7</sup>, Dmitry Rudakov<sup>8</sup>

<sup>1</sup>Sandia National Laboratories, United States; <sup>2</sup>Princeton Plasma Physics Laboratory, United States; <sup>3</sup>Pennsylvania State University, United States; <sup>4</sup>University of Wisconsin-Madison, United States; <sup>5</sup>Dutch Institute for Fundamental Energy Research, Netherlands; <sup>6</sup>Oak Ridge National Laboratory, United States; <sup>7</sup>General Atomics, United States; <sup>8</sup>University of California San Diego, United States.

A total of 17 novel plasma-facing materials (PFMs) from 8 institutions have been successfully tested at the DIII-D National Fusion Facility as a part of the ongoing, two-year FPP Candidate Materials Thrust. This effort coordinates exposure and down-selection of promising PFMs through testing at DIII-D in an integrated, reactor-like environment. The first year of experiments were completed across 3.5 run days utilizing the Divertor Materials Evaluation System (DiMES). The materials included varieties of tungsten (W) (alloys, fibers, dispersoids), W capillary porous structures (CPS) with liquid lithium (Li), thermal spray W coatings, ultra-high temperature ceramics (UHTCs) and silicon carbides (SiC) (CVD, coatings, fibers), analyzed pre- and post-experiment via SEM, EDS, and confocal microscopy. Repeatable reference discharges were developed to ensure uniformity between experiments, including a new strike-point rastering/sweeping scenario to provide more uniform heat/particle flux across DiMES during ELMy H-mode discharges:  $q_{(\perp, inter-ELM)} \approx 2 \text{ MW/m}^2$ ,  $q_{(\perp, intra-ELM)} \approx 6 \text{ MW/m}^2$ ,  $f_{ELM} \approx 40 \text{ Hz}$ . Various DiMES and sample geometries were used to achieve FPP relevant heat/particle fluxes, including samples angled 10–15° towards the incident plasma flux and heated DiMES up to 500 °C. Experiments revealed superior surface morphology (low surface defects, high density), compositional stability, thermal response, and crack resistance compared to PFMs previously tested at DIII-D.

The first exposure of liquid Li CPS in a tokamak successfully demonstrated uniform emission of Li vapor and suppression of Li droplets in H-mode with the sample pre-heated to 350 °C, while without pre-heating droplet ejection was observed. Dispersoid-strengthened W with 1 wt% TaC, TiC, and ZrC exposed to H-mode using 10° angled samples showed cracking and dispersoid ejection for all varieties except TiC, providing a clear down-selection. UHTC materials TiB<sub>2</sub> and ZrB<sub>2</sub> showed minimal degradation under L-mode exposure. SiC fiber composites showed microscopic cracking and arcing along edges, while CVD SiC remained pristine. Thermal plasma spray W and SiC demonstrated granular material ejection during ELMy H-mode but survived with no macroscopic delamination. Additional W-based alloys were stress tested in H mode, including Ni-based W Heavy Alloys (WHAs), WfSiCf/W, and functionally-graded W/SiC. 10° angled WHAs displayed edge melting and cracking and heavy redeposition.

Sandia is managed and operated by NTESS under DOE NNSA contract DE NA0003525. Work also supported by US DOE under DE-AC02-09CH11466, DE FC02-04ER54698, DE-SC00210005, DE-FG02-07ER54917, DE-SC0014664, DE-AR0001258, DE-SC0020284, and UW-Madison Dept of NEEP discretionary funding.

## Session 10: Tungsten, tungsten alloys, and advanced steels and Neutron effects in plasma-facing materials

23 May, 11:40 – 13:35

O-21

### Performance study of fully dense tungsten fiber-reinforced tungsten composites for plasma facing material

Juan Du<sup>1</sup>, Tianyu Zhao<sup>1</sup>, Pan Wen<sup>1</sup>, Fan Feng<sup>1</sup>, Jun Tang<sup>2</sup>, Chen Jiming<sup>1</sup>, Xiang Liu<sup>1</sup>, Qiang Tao<sup>3</sup>, Zhaodong Liu<sup>3</sup>, Fanya Jin<sup>1</sup>, Yiran Mao<sup>4</sup>, Jan Coenen<sup>5</sup>, Christian Linsmeier<sup>4</sup>

<sup>1</sup>Southwestern Institute of Physics, Chengdu, China; <sup>2</sup>Institute of Nuclear Science and Technology, Sichuan University, Chengdu, China; <sup>3</sup>Synergetic Extreme Condition User Facility, Jilin University, Changchun, China; <sup>4</sup>Forschungszentrum Jülich GmbH, Germany; <sup>5</sup>FZJ, Germany.

Tungsten is the most promising plasma-facing material for future fusion reactors due to its high melting point. However, one major concern is its brittleness even at elevated temperatures. By incorporating tungsten fibers, its toughness and strength can be enhanced while maintaining high-temperature performance. In this study, fully dense tungsten-based composites reinforced with three-dimensional tungsten fibers were prepared in large sizes (diameter > 60 mm) through an innovative multi-step high-temperature, high-pressure sintering process. High heat flux test results indicate that the tungsten fiber-reinforced tungsten (Wf/Wm) composites have superior thermal shock fatigue resistance ( $>0.55 \text{ GW/m}^2$ ) under transient heat events resembling edge-localized modes (ELMs) compared to most tungsten grades.

To investigate the feasibility of the Wf/Wm composites, we evaluated their performance under application environments. The mechanical properties were assessed through high-temperature tensile tests up to  $1000^\circ\text{C}$ . A three-point bending test in a scanning electron microscope showed that cracks propagate along the interface between the fiber and matrix, which ensures the effect of pseudo-toughness. Heavy ion ( $7.5 \text{ MeV W}^2$ ) bombardment was employed to simulate displacement damage (up to 5 dpa) caused by neutron irradiation, followed by high-density deuterium plasma irradiation (flux of  $10^{22} \text{ D m}^{-2}\text{s}^{-1}$  @ 500 K, fluence of  $2 \times 10^{26} \text{ D m}^{-2}$ ). The sputtering resistance of the composite materials under displacement damage conditions and the retention of deuterium in the composite materials were detected using thermal desorption spectroscopy. Finally, the crack thresholds of the composite materials after pre-damage and deuterium plasma irradiation were tested using a high thermal load device to evaluate their resistance to thermal shock. The results indicate that, compared to ITER-grade tungsten, the fully dense tungsten fiber-reinforced tungsten composite exhibits twice the fracture toughness; it has five times lower deuterium retention than the CVD Wf/Wm composite due to its high density; its superior performance under transient thermal loads is attributed to the pseudo-toughness mechanism. This study provides the latest research progress on Wf/Wm composites developed in China.

## **Studying the influence of redeposited tungsten and EUROFER97 layers on deuterium retention in plasma-facing materials**

Martina Fellingner<sup>1</sup>, Eduardo Pitthan<sup>2</sup>, Daniel Gautam<sup>2</sup>, Daniel Primetzhofer<sup>2</sup>, Friedrich Aumayr<sup>1</sup>

<sup>1</sup>TU Wien, Fusion@ÖAW, Austria; <sup>2</sup>Uppsala University, Sweden.

Retention of hydrogen isotopes in plasma-facing materials is critical for the efficiency and safety of nuclear fusion reactors. While macroscopic retention in operational devices can be quantified using post-mortem analysis [1] or global gas balance [2], laboratory experiments are necessary to understand the microscopic mechanisms governing retention of hydrogen isotopes in first wall materials [3]. In realistic reactor conditions, where erosion, redeposition, implantation and outgassing occur simultaneously, it is furthermore important to investigate potential synergistic effects of these coupled processes under laboratory conditions.

In this study, we investigated deuterium (D) retention underneath redeposited material layers, to more closely mimic reactor conditions and gain more insight into realistic scenarios. Using Ion Beam Analysis (IBA) techniques, specifically Rutherford Backscattering Spectrometry (RBS) and Elastic Recoil Detection Analysis (ERDA), we quantified the amount of D retained in tungsten (W) and EUROFER97 during in-situ annealing. Via magnetron sputter deposition we grew approximately 200 nm thick W and EUROFER97 layers, which were exposed to 1 keV D<sub>2</sub><sup>+</sup> irradiation. The D-loaded samples were subsequently coated ex-situ with approximately 15 nm thick W or EUROFER97 layers. Furthermore, they were annealed to 500°C. Bare D-loaded layers without additional coating were also studied as reference samples. This allowed us to compare the outgassing characteristics of D-implanted bare materials to D-implanted coated layer systems, simulating possible redeposition effects in a reactor environment.

We observed that redeposited W can act as a diffusion barrier, preventing D from outgassing, a phenomenon not observed for redeposited EUROFER97. These findings highlight the critical role of redeposited layers on D retention in fusion devices. We will present our recent results and discuss their broader implications for fusion reactor operation.

[1] K. Heinola et al., J. Nucl. Mater. 463 (2015)

[2] S. Brezinsek et al., Nucl. Fusion 53 (2013)

[3] E. A. Hodille et al., Nucl. Fusion 57 (2017)

## **Molecular Dynamics Modeling and Experimental Assessment of Helium Bubble Growth, Surface Morphology Evolution, and Displacement Damage Effects in Multi-Component Alloys**

Mary Alice Cusentino<sup>1</sup>, Megan McCarthy<sup>1</sup>, Katie Karl<sup>2</sup>, Shane Evans<sup>3</sup>, Eric Lang<sup>3</sup>, Guddi Suman<sup>1</sup>, Rico Treadwell<sup>1</sup>, Matt Baldwin<sup>4</sup>, Tyler Abrams<sup>5</sup>, Jonathan Coburn<sup>1</sup>

<sup>1</sup>Sandia National Laboratories, United States; <sup>2</sup>University of Tennessee, United States; <sup>3</sup>University of New Mexico, United States; <sup>4</sup>University of San Diego, United States; <sup>5</sup>General Atomics, United States.

Tungsten is currently a leading candidate material for the divertor component of future fusion reactors due to its favorable properties including high melting temperature, good thermal conductivity, and low sputtering yield. Despite these favorable properties, tungsten suffers from a high ductile-to-brittle transition temperature and a low recrystallization temperature. In addition, tungsten is also prone to microstructural damage from plasma exposure such as helium bubble and fuzz formation. This limits the use of pure tungsten as a plasma-facing

material. However, alloying tungsten with other refractory metals is one way to alleviate these issues. Adding elements like Re, Ta, Ti, etc. have been shown to improve the mechanical properties of tungsten. In particular, high entropy alloys (HEAs) have shown promising properties like improved radiation tolerance. However, the role between composition and material properties is not well understood.

This talk will focus on how chemical composition affects the response of multi-component alloys (including varying amounts of W, Nb, Ta, Mo, Ti, Cr) to a fusion-relevant environment. MD simulations, using machine learning interatomic potentials, were used to identify compositions that improve the resiliency of these materials to plasma exposure and displacement damage. We simulated a range of compositions where different elements were systematically enriched or depleted over a range of 5 and 50 at%. Based on this work, we found Mo and W both served to reduce helium bubble size, whereas incorporation of Ta and W provided better resistance to displacement damage. Materials with optimized compositions were fabricated and exposed to high-flux He plasmas in the PISCES-A device at UCSD. Postmortem scanning transmission electron microscopy (STEM) and energy dispersive x-ray spectroscopy (EDS) of He-induced nanotendrils revealed that non-uniform compositional regions within the material. Compositions consistent with enhanced He bubble growth matched predictions from the MD modelling. In addition, complimentary experimental work involving exposure of specimens to divertor plasmas at DIII-D were recently completed. Post-mortem characterization and modelling of these materials is underway and will emphasize surface morphology evolution and preferential sputtering.

SNL is managed and operated by NTESS under DOE NNSA contract DE-NA0003525. Additional support for this work was performed under contract number DE-FC02-04ER54698.

I-21

### **Evolution and recovery of the irradiation-induced defect populations and thermal diffusivity in post self-ion irradiated, isochronal annealed tungsten**

Brandon Schwendeman<sup>1</sup>, Michael Simmonds<sup>1</sup>, Sicong He<sup>2</sup>, Gabriel Gorelick<sup>2</sup>, Thomas Schwarz-Selinger<sup>3</sup>, Matt Baldwin<sup>1</sup>, Jaime Marian<sup>2</sup>, George Tynan<sup>1</sup>

<sup>1</sup>University of California San Diego, United States; <sup>2</sup>Materials Science and Engineering Department, University of California Los Angeles, United States; <sup>3</sup>Max-Planck-Institut für Plasmaphysik, Germany.

Experimental X-ray diffuse scattering (XRDS) measurements and simulations are used to determine the densities of small, transmission electron microscopy “invisible” defects in non-saturated, self-ion irradiated, bulk tungsten (W) at room temperature. Novel defect scattering cross-section calculations are used to analyze laboratory based, “integral” XRDS measurements of irradiated W single crystals and determine separate densities and size distributions for the interstitial and vacancy-type dislocation loop populations. The evolution and recovery of these defect populations as a function of increasing isochronal annealing temperatures post irradiation are measured experimentally and initial comparisons are made to stochastic cluster dynamics simulation predictions of the irradiation-induced defect densities and size distributions upon annealing. The degradation of the thermal diffusivity associated with the measured and modeled defect populations is predicted with both a simple kinetic electron transport model and raytracing Monte Carlo modeling of electron dynamics for W crystals containing defects. These predictions are compared with experimental Transient Grating Spectroscopy

(TGS) measurements of the post-irradiation degradation of the thermal diffusivity of the same W single crystals and the subsequent recovery with increasing annealing temperatures.

This work was supported by the US Department of Energy (Cooperative Agreement No. DE-SC0022528). The authors acknowledge the use of facilities and instrumentation at the UC Irvine Materials Research Institute (IMRI) which is supported in part by the National Science Foundation through the UC Irvine Materials Research Science and Engineering Center (grant No. DMR-2011967).

**POSTER  
ABSTRACTS**

## Poster session PO-A (Tuesday)

20 May, 16:30 – 18:30

POA-1

### **Study of spectral features and depth distributions of boron layers on tungsten substrates by ps-LIBS in a vacuum environment**

Huace Wu<sup>1</sup>, Rongxing Yi<sup>2</sup>, Anne Houben<sup>2</sup>, Sebastijan Brezinsek<sup>2</sup>, Marcin Rasinski<sup>2</sup>, Cong Li<sup>1</sup>, Gennady Sergienko<sup>2</sup>, Timo Dittmar<sup>2</sup>, Hongbin Ding<sup>1</sup>

<sup>1</sup>Dalian University of Technology, China; <sup>2</sup>Forschungszentrum Jülich GmbH, Germany.

Boronization is used in present-devices as wall condition technique due to its effectiveness in reducing oxygen and other impurities in the vessel as well as improving plasma performance. The technique is also currently under consideration as wall conditioning method for the proposed full-tungsten (W) wall of the ITER. However, the impact of the deposited Boron (B) layer thickness, and its homogeneity after the boronization process is uncertain as well as knowledge about the layer lifetime and improved conditions.

In this study, an approach of the picosecond-laser-induced breakdown spectroscopy (ps-LIBS) is investigated to analyze the depth distribution of B-films on W-substrates in a vacuum environment. At first, based on the dynamic behaviour of the plasma in a vacuum, the appropriate spectral lines and acquisition settings for B and W were determined. Sequentially, the depth distribution of two types of B-films on W-substrates with the thicknesses of 130 nm and 260 nm were measured under different laser spot sizes (diameter:142-1518  $\mu\text{m}$ ). The measured average ablation rate of ps-LIBS shows a notable decrease with increasing laser spot size. The spectral lines of B II and W I exhibit distinct intensity distributions under different spot sizes due to the different excitation thresholds of the B II and W I. The interface between B-films and W-substrates, as well as the thickness of the B-films, were determined using the normalized intensity and intensity ratio method, respectively. The results from ps-LIBS measurements regarding the depth are in good agreement with those obtained through the FIB-SEM and EDS. Finally, the B-films with a range of different thickness (10-150 nm) on the W-substrates were used to establish quantitative curve and obtain the LOD. The results of LIBS detection of two samples after boronization in W7-X device are consistent with the quantitative curve. These initial findings verify the feasibility to characterize the thickness and uniformity of thin B films in the order of 100 nm and below on W-substrates using ps-LIBS.

POA-2

### **Diffusion of Ne in boron and borides**

Daniel Gautam<sup>1</sup>, Eduardo Pitthan<sup>1</sup>, Marek Rubel<sup>2</sup>, Daniel Primetzhofer<sup>1</sup>

<sup>1</sup>Uppsala University, Sweden; <sup>2</sup>Uppsala University and KTH Royal Institute of Technology, Sweden.

Neon is considered to be used in gas injections necessary for edge cooling and disruption mitigation in magnetic confinement fusion devices [1]. For devices with a full tungsten wall, boronization is critical for successful upstart. Thus, Ne can be expected to interact with boron and boron compounds, potentially altering their properties.

We here investigate how Ne introduced in boron and borides is diffusing at elevated temperatures. We prepare boron and tungstenboride thin films using magnetron sputtering. Ion implantation is employed to introduce characteristic Ne-profiles. Annealing of samples during

and after implantation enhances diffusion of Ne in the films. Subsequent Time-of-Flight Elastic Recoil Analysis reveals the resulting Ne-profiles, providing information on diffusion and trapping of Ne. Complementary characterization using microscopy is performed.

[1] J. Mailloux and JET Contributors, Nucl. Fusion 62 (2022) 042026

POA-3

### **Reduction of Impurity from First Wall with Boron Powder Dropping in LHD**

Suguru Masuzaki<sup>1</sup>, Tetsutaro Oishi<sup>2</sup>, Tomoko Kawate<sup>1</sup>, Mamoru Shoji<sup>1</sup>, Federico Nespoli<sup>3</sup>, Robert Lunsford<sup>3</sup>, Motoshi Goto<sup>1</sup>, Miyuki Yajima<sup>1</sup>, Masayuki Tokitani<sup>1</sup>, Gen Motojima<sup>1</sup>, Erik Gilson<sup>3</sup>, Alexander Nagy<sup>3</sup>, Novimir Pablant<sup>3</sup>, Tomohiro Morisaki<sup>1</sup>

<sup>1</sup>National Institute for Fusion Science, Japan; <sup>2</sup>Tohoku University, Japan; <sup>3</sup>Princeton Plasma Physics Laboratory, United States.

Boron powder-dropping experiments have been conducted in the Large Helical Device (LHD) for real-time wall conditioning [1-3] and plasma transport studies [4,5]. It has been observed that introducing boron powder reduces the optical emission of iron, a component of stainless steel which is the first wall material. In long-duration discharges with ICRF heating, where iron emission significantly contributes to radiative loss, the boron powder-dropping helps prevent the termination of discharge caused by radiative collapse. This study investigates the effect of boron powder-dropping on iron emissions.

An impurity powder dropper (IPD) developed by PPPL has been installed on a top port of LHD. The B powder particles for the IPD have a nominal diameter of 150  $\mu\text{m}$  in this study. Boron powder falls freely into plasma, where it is ablated and ionized, resulting in deposits on the plasma-facing surfaces. Results of numerical simulations suggest that boron deposits on divertor tiles, made of graphite, and a limited area on first wall, made of stainless steel type 316, close to plasma [6].

Optical emissions from boron and intrinsic impurities such as oxygen, carbon, and iron have been measured by EUV/VUV spectroscopy [7]. Emission intensities from these impurities decrease with the boron powder-dropping. It has been observed that the behavior of FeXVI differs from that of OV and CIII: The time response of FeXVI to the boron emission, BV, from the powder-dropping is faster than that of OV and CIII. The intensity of FeXVI returns to the pre-powder-dropping intensity when BV intensity drops, whereas OV and CIII have a longer time to return to the pre-powder-dropping intensity [3]. To understand the behavior of iron, the time-evolutions of the emission intensity of iron across low and high charge states have been analyzed.

This presentation will indicate and discuss the results of the analysis and possible models of iron behavior during and after boron powder-dropping.

[1] F. Nespoli et al., Nucl. Mater. Energy 25 (2020) 100842.

[2] R. Lunsford et al., Nucl. Fusion 62 (2022) 086021.

[3] S. Masuzaki et al., Nucl. Mater. Energy 42 (2025) 101843.

[4] F. Nespoli et al., Nature Phys. 18 (2022) 350–356.

[5] F. Nespoli et al., Nucl. Fusion 63 (2023) 076001.

[6] M. Shoji et al., Nucl. Mater. Energy 25 (2020) 100853.

[7] T. Oishi et al., Plasma Sci. Technol. 23 (2021) 084002.



### Engineering Research & Development of Wall Conditioning Systems at HL-3

Chengzhi Cao, Yi Hu, Yanfeng Xie, Jun Zhou, Xiangmei Huang, HL-3 Team

Southwestern Institute of Physics, China.

The wall conditioning of tokamaks, particularly for ITER and future fusion reactors, is a crucial and indispensable process for regulating the state of the first wall, enabling plasma initiation, and managing fuel/impurity recycling. As plasma experiments advance, the conditions required for the wall become increasingly stringent. Consequently, ongoing innovation and advancement in wall conditioning technology are essential [1].

The HL-3 [2] research program is gearing up to initiate plasma experiments in achieving a more high plasma performance. Its systems are in the stages of further research and development to develop key technologies and delve into frontier fusion plasma physics. This report outlines the preparations for the wall conditioning (WC) systems, aimed at achieving the project objective.

The WC system comprises baking, glow discharge conditioning (GDC), and siliconization (SWC)/boronization (BWC) systems. The hot surface operation strategy has been meticulously designed by baking the main chamber and first wall at varying temperatures, and this integrated system ensures that the WC process is both efficient and effective. An upgraded GDC with a discharge current capability of up to 20 A ( $> 0.2 \text{ A/m}^2$ ) has been developed, allows for more uniform conditioning of the wall surfaces. To address fuel retention in the wall, the GDC operation mode ( $\text{H}_2/\text{D}_2$ ) combined with baking has been explored through isotopic changeover. Additionally, the newly implemented radio-frequency assisted GDC can be utilized to assess the fuelling removal efficiency in comparison to baking and/or traditional GDC. The integration of radio-frequency assisted GDC significantly expands the experimental toolkit, allowing researchers to assess and compare the fuel removal efficiency of various techniques. A plasma-enhanced chemical vapor deposition system, designed for SWC/BWC using  $\text{Si}_4\text{D}_6/\text{B}_2\text{H}_6$  ( $\text{B}_2\text{D}_6$ ), is currently under construction. This system is designed to condition the wall states, and it is beneficial to improve overall performance of the device. Additionally, a boron powder injection system has been developed, presenting an innovative method for the HL-3 BWC. This system has the potential to achieve more precise and controlled boron deposition, which may lead to improved wall conditioning and prolonged reactor operational lifetimes.

**Acknowledgements:** This work was supported by National Key R&D Program of China under Grant Nos. 2022YFE03020003, China National Nuclear Corporation basic research project (CNNC-JCYJ-202323), Sichuan province Natural Science Foundation and (2025ZNSFSC0383) and important Code & Standard research project of Sichuan province (ZYBZ2023-32).

**References:** [1] Chengzhi Cao, Xiangmei Huang, Yi Hu, et al., Nuclear Materials and Energy 42, (2025).

[2] W. Zhong, and HL-3 team, The Innovation 5,1 (2024).

### Influence of Deuterium Gas during Tungsten / Boron Film Deposition

Laurent Marot<sup>1</sup>, Matej Mayer<sup>2</sup>, Thomas Morgan<sup>3</sup>, Tomás Sousa<sup>1</sup>, Nicolò Lopopolo<sup>1</sup>, Ernst Meyer<sup>1</sup>

<sup>1</sup>Department of Physics, University of Basel, Switzerland; <sup>2</sup>Max-Planck-Institut für Plasmaphysik, Germany; <sup>3</sup>Dutch Institute for Fundamental Energy Research, Netherlands.

With the change of the ITER first wall material from beryllium to tungsten, the ITER Organization has developed a strategy for conditioning the tungsten wall for gettering impurities like

oxygen and water molecules, providing successful ignition of the deuterium plasma. Boronization using a glow discharge in diborane ( $B_2H_6$  or  $B_2D_6$ ) gas mixed with He is foreseen to coat the wall with a thin layer of boron, which acts as a getter.

The influence of deuterium during depositing boron or tungsten/boron film is an important question. Thin film layers of tungsten/boron were deposited by magnetron sputtering using argon and argon/deuterium mixed atmosphere. Chemical analysis was investigated using in vacuo X-ray photoelectron spectroscopy, the surface morphology was examined via scanning electron microscopy. The amount of deuterium in the film was analyzed using nuclear reaction analysis and thermal desorption spectroscopy.

Depending on the amount of boron in the film, the amount of deuterium varies, which also influences the desorption temperature. The idea is to link these results to the formation of tungsten boride characterized by X-ray photoelectron spectroscopy.

POA-7

### **Defect evolution in tungsten at high-temperature as a function of damage dose**

Andreja Šestan Zavašnik<sup>1</sup>, Janez Zavašnik<sup>1</sup>, Sabina Markelj<sup>1</sup>, Nejc Parkelj<sup>1</sup>, Miha Sajovic<sup>1</sup>, Srečo Škapin<sup>1</sup>, Thomas Schwarz-Selinger<sup>2</sup>

<sup>1</sup>Jožef Stefan Institute, Slovenia; <sup>2</sup>Max-Planck-Institut für Plasmaphysik, Germany.

Tungsten (W) is a key candidate material for the first wall and divertor components in future fusion reactors due to its high melting point, low sputtering yield, and favourable thermal properties. However, exposure to fusion-relevant neutron irradiation (14 MeV) leads to the formation of radiation-induced defects, which significantly impact material structural properties and can lead to an increased retention of hydrogen isotopes [1,2].

In our study, we used a W-ion irradiation of polycrystalline tungsten as a proxy for neutron-induced crystal structure damage, producing comparable crystal structure alterations but without material activation [3]. It is expected that the produced defect evolution will differ if damaging is conducted at room-temperature or at elevated temperatures. For this purpose, the polycrystalline reference samples were irradiated at 800 K with damage doses ranging from 0.02 dpa to 0.8 dpa. At this temperature, the vacancies are expected to become mobile and tend to cluster. The evolution of defects was systematically investigated using X-ray diffraction (XRD), Transmission Electron Microscopy (TEM), and deuterium retention analysis via  $^3\text{He}$  Nuclear Reaction Analysis (NRA). By combining several different analytical techniques, we were able to assess the structural damage on multiple length-scales, and correlate the structural damage and its interaction with the hydrogen isotopes.

At lower doses (0.02 dpa), dense distributions of small dislocation loops were dominant, while at higher doses (0.2 dpa), we observed a formation of nano-sized voids. A clear correlation between damage dose and deuterium retention was observed, with the increase in the D concentration in the samples damaged by higher damage dose.

[1] Tynan, G. R., R.P. Doerner, J. Barton, R. Chen, S. Cui, M. Simmonds, Y. Wang, J.S. Weaver, N. Mara, S. Pathak, Nucl. Mater. and Energy 12, 164–168 (2017).

[2] Y. Hatano, M. Shimada, T. Otsuka, Y. Oya, V.Kh. Alimov, M. Hara, J. Shi, M. Kobayashi, T. Oda, G. Cao, K. Okuno, T. Tanaka, K. Sugiyama, J. Roth, B. Tyburska-Püschel, J. Dörner, N. Yoshida, N. Futagami, H. Watanabe, M. Hatakeyama, H. Kurishita, M. Sokolov and Y. Katoh, Nucl. Fusion 53, 073006 (2013).

[3] Ogorodnikova O. V. and Gann V. J. Nucl. Mater. 460, 60–71, (2015)

POA-8

### **Status of the UCSD POSEIDON facility: An experiment for the study of simulated burning-plasma-material-interaction**

Matt Baldwin, Daisuke Nishijima, Marlene Patino, Brandon Schwendeman, Michael Simmonds, Anže Založnik, George Tynan

University of California San Diego, United States.

Energy producing D-T fusion systems require plasma-facing-materials (PFMs) capable of withstanding extreme plasma heat and particle loads, and also the damaging effects of neutrons. In laboratory PFM experiments, a target material is typically exposed to a dense plasma that simulates a fusion typical particle and heat flux. Likewise, in fusion material damage studies, at least some of the effects of neutrons in a material target surface region are studied with the use of high-energy accelerated ions that cause displacement damage in the cascades caused by knock-on atoms. Combining these two types of experiments to study materials response in a state more relevant to a burning plasma typically involves a stepwise procedure [1]. For instance, an example being, a damage step followed by a plasma exposure step. Unfortunately, this approach reduces the potential for examining the more realistic synergistic material response where both the plasma exposure and displacement damage occur together.

The Plasma On Simultaneous Energetic Incident Damage by iONs (POSEIDON) experiment at UCSD is a new facility for exploring the synergistic response of PFMs undergoing simultaneous high-flux plasma exposure and displacement damage in the near surface of PFMs. This new experiment couples the PISCES-RF helicon linear plasma system [2] and a 3 MV tandetron so as to focus, simultaneously, a high-flux plasma and high-energy damaging ions onto a PFM target, thus allowing material performance to be examined in an environment that emulates the effects of aging in a burning plasma scenario.

The presentation will provide an update on the operational status of POSEIDON and describe the parameter space, outline details on the onboard plasma and materials diagnostics, and present the first results of synergistic materials response in a PFM target undergoing simultaneous plasma exposure and displacement damage.

This work is supported by a US-DOE co-operative agreement, DE-SC0022528.

[1] T Schwarz-Selinger, Mater. Res. Express 10, 102002 (2023)

[2] M.J. Baldwin, D. Nishijima, M.I. Patino et al., Nucl. Mater. & Energy 36, 101477 (2023)

POA-9

### **Machine-learning force fields for hydrogen and vacancy complex in tungsten**

Yuki Noguchi<sup>1</sup>, Daiji Kato<sup>2</sup>

<sup>1</sup>Kyushu University, Japan; <sup>2</sup>National Institute for Fusion Science, Japan.

Tungsten (W) is used for plasma-facing components in nuclear fusion reactors, such as ITER and DEMO, due to its low tritium retention as well as high heat resistance and durability. However, experimental findings have shown that ambient deuterium (D) atoms in W can stabilize irradiation-induced defects resulting in an increase in D retention [1]. The formation of hydrogen-vacancy complexes in the irradiated W can provide clues to understanding the stabilization of irradiation-induced defects. In the present work, we developed a machine-learning force field (MLFF) for the hydrogen-vacancy complexes in W based on density func-

tional theory (DFT) calculations. In the present MLFF, structural data (total energy, forces, and the stress tensor) were obtained from the DFT calculations using VASP [2], and the Smooth Overlap of Atomic Positions (SOAP) descriptor [3] characterized the local atomic environments. Using Bayesian linear regression, unknown structural data are predicted with quantitative uncertainty. Then, an on-the-fly machine-learning approach [4] is used for sampling the learning data to improve the MLFF efficiently. With the present MLFF, we calculated the binding energy of H atoms to a monovacancy and compared it with previous calculations of DFT and model potentials [5,6]. For the vacancies trapping one to eleven H atoms, the difference between DFT values and the predicted values by the present MLFF was 0.47 eV at most, with the root mean squared error (RMSE) of 0.24 eV. The agreement is significantly better than those of the model potentials [6], allowing MLFF-based MD simulations to achieve accuracy close to that of DFT calculations.

[1] S. Markelj, T. Schwarz-Selinger, A. Založnik, et al., Nucl. Mater. Energy 12, 169–174 (2017)

[2] G. Kresse, and J. Furthmüller, Phys. Rev. B 54, 11169–11186 (1996)

[3] A. P. Bartók et al., Phys. Rev. B 87, 184115 (2013)

[4] R. Jinnouchi, F. Karsai, and G. Kresse, Phys. Rev. B 100, 014105 (2019)

[5] K. Ohsawa, T. Toyama, Y. Hatano, et al., J. Nucl. Mater. 527, 151825 (2019)

[6] L-F Wang et al., J. Phys.: Condens. Matter 29, 435401 (2017)

POA-10

### **A New Experimental System for Studying Defects and Deuterium Lattice Location in Tungsten Crystals by Ion Beam Methods**

Esther Punzón-Quijorna, Mitja Kelemen, Roberto Galende-Pérez, Primož Vavpetič, Primož Pelicon, Sabina Markelj

Jožef Stefan Institute, Slovenia.

We have recently acquired and installed a state-of-the-art 6-axis goniometer from Thermionics Laboratory Inc. (TLI) and National Electrostatic Corp (NEC) at the INSIBA endstation on 2 MV tandemron accelerator at Jožef Stefan Institute. This advanced system offers three translational and three rotational axes of movement. The angular resolution is 0.01 degrees, making it ideal for applications requiring detailed angular alignment, such as Rutherford Backscattering Spectrometry (RBS-C) and Nuclear Reaction Analysis (NRA-C) in channeling mode. RBS-C is a well-established method for studying lattice disorder and defect evolution induced by ion irradiation. Moreover, when combining RBS-C with NRA-C, we can gain insights into the positions of light atom species in the host material.

The goniometer features a versatile sample holder capable of continuous heating up to 1200°C and liquid nitrogen cooling for precise temperature control, alongside a sample bias up to 500 V. The system accommodates samples up to 4 cm in size and is integrated with a data acquisition system supporting up to five detectors for simultaneous spectra collection. Furthermore, an additional load-lock chamber with a magnetic arm ensures efficient sample handling without breaking the vacuum in the main chamber.

The goniometer has been successfully commissioned for channelling measurements. We performed RBS-C measurements on pristine W (111) single crystals and W (111) single crystals irradiated by 10.8 MeV W ions at different damage dose at 290 K reproducing previous measurements on these samples [1]. Simultaneous RBS-C and NRA-C was also performed to probe deuterium distributions in W-irradiated W (100) tungsten single crystals with defects decorated with D. There we have confirmed the observed different NRA-C signal shape depending on the

irradiation conditions during defect creation [2]. The set-up enables us to record RBS-C during heating a W-irradiated sample to study defect evolution during annealing. This cutting-edge setup, incorporated under the DeHydroC project, significantly enhances our capabilities in material science and fusion-related research.

This project was supported by EUROfusion and ARIS (Slovenian Research Agency).

[1] S. Markelj, et al., *Acta Materialia*, 263 (2024)

[2] S. Markelj, et al., *Nuclear Materials and Energy*, 38 (2024)

POA-11

### **Atomic-Scale Investigation of Re/Os Precipitation in Neutron-Irradiated Tungsten Using Atom Probe Tomography: Validation of FISPACT-II Nuclear Data**

Iuliia Ipatova<sup>1</sup>, Mark Gilbert<sup>1</sup>, Dmitry Terentyev<sup>2</sup>, Christina Hofer<sup>3</sup>, Ryo Shibahara<sup>4</sup>, Kazuhiro Kurano<sup>4</sup>, Kazutoshi Inoue<sup>4</sup>

<sup>1</sup>UK Atomic Energy Authority (UKAEA), United Kingdom; <sup>2</sup>Belgian Nuclear Research Center, Belgium; <sup>3</sup>University of Oxford, Department of Materials, United Kingdom; <sup>4</sup>Institute for Materials Research, Tohoku University, Japan.

Tungsten (W) is a material to be used in fusion reactors due to its high melting point and resistance to radiation damage. However, neutron irradiation [1] can induce the formation and evolution of rhenium (Re) and osmium (Os) precipitates within the tungsten matrix via through a sequence of neutron absorption reactions and beta- decays. It may significantly impact its microstructural stability and mechanical properties [2]. In this study, we employed Atom Probe Tomography (APT) to investigate the nucleation, growth, and interaction of Re and Os with radiation-induced defects in tungsten and its selected alloys neutron-irradiated in the Belgium material test reactor BR2 at SCK·CEN. These findings not only enhance our understanding of precipitation mechanisms in irradiated tungsten but also serve as a validation of the nuclear data predictions obtained from the FISPACT-II simulation code [3], contributing to improved modelling of fusion materials under extreme conditions.

APT analysis enables high-resolution, three-dimensional mapping of atomic distributions, allowing us to trace the formation of Re/Os clusters and examine their relationship with irradiation-induced defects such as voids and dislocations. Our observations reveal distinct nucleation sites for Re and Os precipitates, often in association with radiation-induced defects, which aligns with predictions made by FISPACT-II. We quantified the distribution, size, and composition of these clusters across several irradiation conditions (gradually increasing damage level and temperature), identifying parameters that drive their growth. This atomic-level insight is critical for validating FISPACT-II's predictive capability and understanding how Re/Os clusters evolve in the radiation-rich environments expected in fusion reactors.

The results demonstrate that Re/Os clustering is highly sensitive to neutron flux and temperature, with a tendency for precipitates to coalesce at higher irradiation doses, creating larger clusters that contribute to embrittlement. These findings underscore the influence of radiation-induced defects on tungsten's microstructural evolution under neutron bombardment, while also providing key experimental data to refine FISPACT-II's nuclear models. This study offers both validation and enhancement of nuclear data tools critical for predicting the performance of irradiated tungsten, supporting the development of more resilient tungsten-based materials for fusion applications.

## References

1. S.J. Zinkle, Advanced materials for fusion technology, Fusion Eng. Design, 74 (1–4) (2005), pp. 31–40
2. M.R. Gilbert , J.-C. Sublet , S.L. Dudarev , Spatial heterogeneity of tungsten transmutation in a fusion device, Nucl. Fusion 57 (4) (2017) 044002
3. J.-C. Sublet , J.W. Eastwood , J.G. Morgan , M.R. Gilbert , M. Fleming , W. Arter , FIS- PACT-II: an advanced simulation system for activation, transmutation and material modelling, Nucl. Data Sheets 139 (2017) 77–137.

POA-12

### **Ablation characteristics of fusion materials in preparation for local profiling of helium and hydrogen-isotopes with a novel laser ablation experiment**

Benedikt Buchner, Steffen Mittelmann, Udo von Toussaint

Max Planck Institute for Plasma Physics, Germany.

We present ablation studies of various metals performed with a novel Laser Ablation Mass Analysis (LAMA) experiment. The performed ablation studies on tungsten, EUROFER steel, aluminium and copper determining the respective ablation characteristics are necessary for the analysis of the Laser Induced Ablation Quadrupole Mass Spectrometry (LIA-QMS) experiments.

The LIA-QMS experiment uses an UV femtosecond pulsed laser with a pulse duration of 400 fs and a wavelength of 343 nm to determine the local distribution of hydrogen isotopes and helium with high spatial resolution in metallic substrates. This knowledge is critical for the design of plasma facing materials in future fusion devices. The ablation studies provide tabulated data correlating the laser fluence with the ablated depth and volume per pulse. Here, we determine minimum ablation rates of 14 nm and 9 nm at pulse energies of 444 nJ and 131 nJ for tungsten and EUROFER steel, respectively. These experiments extend the knowledge of ablation characteristics in the infrared spectrum [1,2] with results in the UV spectrum. We find ablation thresholds higher than those estimated by theoretical approaches [3], which is discussed in this contribution. These data provide a basis for LIA-QMS experiments on a selection of fusion relevant materials.

Based on these ablation studies, we developed a Bayesian deconvolution algorithm to obtain the depth profile of gaseous material from the measured QMS signals. We validate the algorithm by comparing the LIA-QMS results with the deuterium distribution measured by Nuclear Reaction Analysis (NRA). With this comparison, we demonstrate the ability of the LIA-QMS experiment to quantitatively study deuterium retention with similar depth resolution as current state-of-the-art methods such as NRA, but without the limitations of measurements at depths greater than a few micrometers.

We also present future optimization possibilities and limitations of the experiment due to the characteristics of the optical system used in the setup. In principle, the system can be used to determine quantitatively the local retention of any gaseous elements in metals of interest after studying the ablation characteristics of the respective material and calibrating the experiment for the respective gas. Future planned optimizations of the experiment for even better ablation characteristics and in-situ approximations of the ablated material will be presented.

[1] J. Byskov-Nielsen, et al., Applied Phys. A, 103(2), 2011;

[2] T. Genieys, et al., Advanced Optical Technologies, 9(3), 2020;

[3] E. G. Gamaly, et al., Physics of Plasmas, 9(3), 2002.

POA-13

### **Qualification activities of the first DTT divertor**

Selanna Roccella<sup>1</sup>, Davide Caprini<sup>1</sup>, Marco Cerocchi<sup>1</sup>, Francesco Crea<sup>1</sup>, Riccardo De Luca<sup>1</sup>, Francesco Giorgetti<sup>1</sup>, Pierdomenico Lorusso<sup>1</sup>, Annunziata Satriano<sup>1</sup>, Luigi Verdini<sup>1</sup>, Domanico Marzullo<sup>2</sup>, Gian Mario Polli<sup>3</sup>, Hélène Roche<sup>4</sup>, Nicolas Vignal<sup>4</sup>, Marianne Richou<sup>4</sup>, Henri Greuner<sup>5</sup>, Johann Riesch<sup>5</sup>, Bernd Boeswirth<sup>5</sup>, Katja Hunger<sup>5</sup>, Rudolf Neu<sup>5</sup>

<sup>1</sup>ENEA, Nuclear Department, Italy; <sup>2</sup>University of Trieste, Italy; <sup>3</sup>DTT S.C. a r.l., Frascati, Italy; <sup>4</sup>CEA, IRFM, France; <sup>5</sup>Max Planck Institute for Plasma Physics, Germany.

The DTT [1] divertor design required high heat flux (HHF) testing to validate some design choices: both HHF thermal fatigue and critical heat flux (CHF) test campaigns were conducted. Several small and medium scale mock-ups were produced and tested with different purposes. Fatigue tests were conducted to support the choice of a reduced armour thickness [2], which demonstrated that the monoblock with reduced thickness can withstand 1000 cycles at 20 MW/m<sup>2</sup> without any plastic deformation and without the onset of cracks when the toroidal width is 25 mm (maximum width for the vertical targets). Subsequently, a mock-up representative of the central target with 30 mm toroidal width was subjected to 1000 cycles at 16 MW/m<sup>2</sup> (which is the design load for this target) in the HHF test GLADIS facility at IPP in Garching. Results comparable to those of the previous campaign were found: no plastic deformation and no cracks on the surface. The CHF tests, conducted instead in the HADES e-beam facility in the CEA center in Cadarache, aimed at evaluating the need to equip the DTT divertor central horizontal target with a twisted tape. Surprisingly, the reduced loaded length (in the order of the expected plasma foot print) did not bring the hoped increases in CHF, highlighting the need to maintain the turbulator to ensure an adequate safety margin and excluding the possibility of a design simplification. During the CHF testing on 30 mm monoblocks, deep crack formation along the tube axis was observed following complete surface recrystallization. While operational loads remain significantly below CHF levels (with a minimum safety margin of 1.4), the gradual decrease of recrystallization temperature with prolonged high-temperature exposure [3] could cause the formation of deep cracks even at lower loads. This suggested further testing to verify the survival capability of the component with a monoblock of only 3 mm of thickness even when deep cracks are presented. A mockup representative of the horizontal targets was deliberately recrystallized and loaded until cracks formed in HADES. After that, the mockup was subjected to 1000 cycles at 16 MW/m<sup>2</sup>. No significant crack propagation or surface temperature variations were observed during this fatigue testing.

Finally, a small portion of the central horizontal target of the DTT divertor must be covered with flat W tiles instead of monoblocks. These flat-tiles are joined by solid state diffusion process to an OFE-Cu interlayer and subsequently joined to the CuCrZr cooling tube together with the monoblocks with the Hot Radial Pressing process. The process parameters were varied to allow the simultaneous joining of flat-tiles and monoblocks. To verify the resistance to thermal load of the developed flat-tile solution, small ad hoc mock-ups were produced and tested under thermal fatigue in the GLADIS facility.

[1] F. Romanelli et al., Nucl. Fusion 64, 111, (2024)

[2] S.Roccella et al., IEEE TRANSACTIONS ON PLASMA SCIENCE, 52, 9, 2024

[3] G. Pintsuk et al., Nuclear Materials and EnergyOpen AccessVolume 39June 2024

POA-14

### **Effect of bending and heat treatment on CuCrZr/316L interface for flat-type divertor target by explosive welding**

Siqing Feng<sup>1</sup>, Xuebing Peng<sup>2</sup>, Peng Liu<sup>2</sup>

<sup>1</sup>Anhui Vocational And Technical College, China; <sup>2</sup>Institute of Plasma Physics, Hefei Institutes of Physical Science, China.

The application of copper alloy in divertor faces great challenges. The explosive welded CuCrZr/316L composite plate can maintain good structural strength while ensuring efficient heat transfer, and is often used as a material for divertor target heat sink. In the development of continuous closed V-shaped structure of divertor target, which is beneficial to detachment, the composite plate can provide sufficient heat transfer effect when the bending radius of bonding interface is R60mm. However, it can cause leakage at the bonding interface of the bent area when subjected to high temperatures of 830 . This article describes the testing and analysis of the bonding interface of composite plates under different bending radii and high temperature treatments, which contain the tensile stress, microhardness, microstructure and elements diffusion, and finds the cause of leakage. The solid solution at 970 before bending can bring recrystallization of both CuCrZr and 316L, which can eliminate the work hardening caused by explosive welding. In the subsequent experiment of solution and R60mm radius bending, the bonding interface passed a helium pressure test of 4.5MPa.

POA-15

### **Putting the Sun in A Box – A Brief History of Plasma Facing Components**

Garreth Aspinall, Holly Staley-Wiggins, Paul Sherlock, Joe Bushell

Amentum, United Kingdom.

Amentums' fusion energy heritage goes back more than four decades. The highlights include supporting the Joint European Torus (JET) at UKAEA; serving as ITER's construction management-as-agent contractor as part of MOMENTUM, and coming right up to date with our work to support UKAEA across their range of programmes from Robotic Handling through to Design and Build projects and our support to the UKAEA STEP (Spherical Tokamak for Energy Production) programme. We will present an industry perspective on the development, design and manufacture of plasma facing components.

We have been involved in the design, development, and manufacture of PFCs from the mid-1990s. Our presentation will chart the evolution of PFC design from early development to full scale prototypes of ITER First Wall Panels (FWPs) and will include; Discussion of Early Beryllium tiled prototypes demonstrating the evolution of beryllium tile bonding methodology and the Thermal Fatigue Mock-Up used to demonstrate beryllium tile bonding on a water-cooled composite Stainless Steel – Copper heatsink. We will then move on to discussion of the Fusion for Energy (F4E) prototypes, the Semi-Scale Prototype a 1/6th section of a FWP, the Full Scale Prototype (FSP) which was the first panel manufactured to meet the design and quality assurance requirements of ITERs FWPs and the Advanced Design Mock-Up (ADMU) which was designed to reduce manufacturing costs of the ITER FWPs and improve manufacturability.

During the journey we will examine the evolution of PFC design before progressing to the development and testing of manufacturing techniques used for the successful production of these





POA-17

### **ITER NHF First Wall Panel thermomechanical plastic simulation of tungsten flat tiles**

Devansh Dhard<sup>1</sup>, Jose Miguel Pacheco Cansino<sup>1</sup>, Samuli Heikkinen<sup>1</sup>, Antonino Cardella<sup>2</sup>

<sup>1</sup>Fusion for Energy, Spain; <sup>2</sup>Technical University Munich, Germany.

ITER previously used Beryllium as the First Wall Panel (FWP) armour material. The switch to tungsten requires the full qualification of the armour bonding. While the qualification will need extensive experimental testing for acceptance, major factors i.e. tile size of castellated armour tiles, may be optimized by finite element simulations.

HIP diffusion bonding of the tungsten tiles to the CuCrZr-IG heatsink is expected to be carried out at 580 °C, which defines the residual stress-free state of the FWP. This leads to localized plastic deformation of the pure copper interlayer when cooled down to room temperature, due to differences on the thermal expansion of the bonded materials. Plastic deformation occurs again in a more repetitive manner during the High Heat Flux Test (HHFT) conditions, which resembles the FWP ITER operating conditions.

The simulation geometry is a representative cross section of a Normal Heat Flux (NHF) ITER FWP finger, which consist of a 12 mm thick tungsten tiles with variable footprint, joint to a 2 mm thick Oxygen Free Pure Copper compliance layer, in turn bonded to the CuCrZr heatsink and Stainless-Steel structure.

The ANSYS non-linear plastic thermomechanical FEA simulation utilizes temperature dependent material properties, ITER like cooling water parameters and HHFT thermal load conditions. An appropriate constitutive model of plastic theory is applied to the pure copper interlayer to calculate the level of strain obtained on each cycle, later to be used to predict its failure under low cycle fatigue. Past HHF Tests results using Beryllium armoured FWP prototypes allow further extrapolation to the feasibility of different tungsten tile footprint configurations.

Disclaimer: This publication reflects the views only of the author, and Fusion for Energy cannot be held responsible for any use which may be made of the information contained therein.

POA-18

### **Design and qualification of W based divertor components for Wendelstein 7-X**

Joris Fellingner<sup>1</sup>, Marianne Richou<sup>2</sup>, Gunnar Ehrke<sup>1</sup>, Falk Kunkel<sup>1</sup>, Gavriel Peyron<sup>2</sup>, Zhongwei Wang<sup>1</sup>, Jörg Tretter<sup>1</sup>, Katja Hunger<sup>1</sup>, Jeong-Ha You<sup>1</sup>, Rudolf Neu<sup>1</sup>, Marius Wirtz<sup>3</sup>, Anne Houben<sup>3</sup>, Daniel Dorow-Gerspach<sup>3</sup>, Ola Widlund<sup>4</sup>, Elena Tejado<sup>5</sup>, Boštjan Končar<sup>6</sup>, Matej Tekavčič<sup>6</sup>, Martin Draksel<sup>6</sup>

<sup>1</sup>Max Planck Institute for Plasma Physics, Germany; <sup>2</sup>CEA, IRFM, France; <sup>3</sup>Forschungszentrum Juelich GmbH, Germany; <sup>4</sup>RISE Research Institutes of Sweden, Sweden; <sup>5</sup>Universidad Politecnica de Madrid, Spain; <sup>6</sup>Jožef Stefan Institute, Slovenia.

Wendelstein 7-X, located at IPP in Greifswald, Germany, is the largest stellarator in the world with modular superconducting coils. It started plasma experiments with a watercooled plasma-facing wall including a CFC based divertor in 2022, allowing for long pulse operation.

As a next step in the future, plasma performance of a stellarator has to be demonstrated with carbon-free plasma facing materials to ensure low tritium retention. Therefore, a project was launched to develop a W based divertor. First task is to optimize the geometry of the plasma-facing surface of the divertor and baffles in order to prevent overloads, improve particle exhaust and maximize impurity retention in the divertor away from the core plasma. Second task in parallel is the structural design for a W based target module and the quali-

fication of suitable manufacturing technology, which is conducted in the framework of the EUROfusion funded WPDIV program.

This paper presents the current status of the structural design and qualification of the manufacturing technologies. The design assumes divertor modules of similar plasma facing shape, size and weight as for the current CFC divertor and the same cooling infrastructure. The design is based on hydraulic, thermal and mechanical analyses. A simplification of the manufacturing, inspection and installation steps and a maximization of the heat load capacity is pursued.

The main technology under qualification for high heat flux components is a CuCrZr heat sink made by additive manufacturing using laser powder bed fusion with a functionally graded plasma facing coating of W/Cu or WNiFe/Cu applied by cold gas spraying or low pressure plasma spraying. Alternatively, a mosaic of sandwich tiles out of W or WNiFe with a soft Cu interlayer is diffusion bonded onto the heat sink using a paste with nano-sized Cu particles at moderate pressure and temperature. The copper interlayer is applied onto the W based tiles by galvanization, casting or diffusion welding. Last step is a final machining of the plasma-exposed surface and the interfaces of the heat sink to the water supply lines and supports.

The paper shows current results of hydraulic and high heat flux tests, confirming the thermal and hydraulic simulations. Also, the challenges ahead are discussed to arrive at a fully qualified technological solution.

POA-19

### **Microscopic and macroscopic investigation of He bubbles formation on tungsten via in situ spectroscopic ellipsometry**

Federica Pappalardo<sup>1</sup>, Celine Martin<sup>1</sup>, Andrea Campos<sup>2</sup>, Gilles Cartry<sup>1</sup>, Thierry Angot<sup>1</sup>, Regis Bisson<sup>1</sup>, Marco Minissale<sup>1</sup>, Mounir Alfaazza<sup>3</sup>, Jonathan Mougnot<sup>4</sup>

<sup>1</sup>Aix-Marseille Univ, CNRS, PIIM, France; <sup>2</sup>Marseille Centrale, France; <sup>3</sup>Université d'Orléans, CEMHTI, France; <sup>4</sup>Université Sorbonne Paris Nord, CNRS, France.

In the experimental fusion reactor ITER, the divertor and first wall components will be made of tungsten (W) and will experience under operational regime both high heat fluxes and ion fluxes, mostly hydrogen isotopes and helium (He) ions. The interaction of such charged particles with W can induce material modifications [1-3], from microscopic lattice defects to mesoscopic damages such as near-surface (<50 nm) bubbles, already observed on W exposed to low energy (<100 eV) He ions at high temperatures (<1273 K) [4]. The formation of these near-surface structures can lead to a modification of the optical properties of W, for example by an increase of surface roughness.

In this work, we investigate the evolution of surface morphology and optical properties of W exposed to He plasma via in-situ spectroscopic ellipsometry. This technique uses a polychromatic source of polarized light (400-1000 nm) impinging on a sample and measures the change in its polarization upon reflection from the surface. The experimental setup is composed by a RF plasma chamber in which in situ spectroscopic ellipsometry measurements are realized during He plasma exposure of W samples. The He ion energy is around 80 eV, the He ion flux is  $2 \times 10^{19} \text{ m}^{-2}\text{s}^{-1}$  and after about 8 hours of plasma exposure the total fluence is  $5 \times 10^{23} \text{ m}^{-2}$ . We perform different plasma exposures varying multiple parameters (sample temperature, ion flux and initial W surface state), with a double purpose. First, we use ex-situ imaging techniques (SEM, AFM) to characterize microscopically the size and density of He bubbles as a function of temperature and grain orientation after the 8 hours of plasma exposure. Secondly, we couple these microscopy results with the in situ time resolved ellipsometry

data to reconstruct the temporal evolution of porosity and surface roughness during the 8 hours of plasma exposure, with an appropriate effective-medium layer model that takes into account the volume fraction of He bubbles (porosity) in W sub-surface. Finally, we validate our results using a model implemented in FEniCS code [5], which describes He bubbles growth and transport.

References:

- [1] A. Mahnard et al, Nucl. Fusion 57, 126012 (2017)
- [2] L. Gao et al., Nucl. Fusion 54, 122003 (2014)
- [3] D. Nishijima et al., Nucl. Fusion 45, 669–674 (2005)
- [4] R. Kolasinski et al., J. Appl. Phys. 131, 063303 (2022)
- [5] R. Delaporte–Mathurin et al., Sc. Reports 11:146681 (2021)

POA-20

### **Quantification of fusion materials using synthetic LIBS spectra and ANN enhanced by PSO optimized autoencoders for dimensionality reduction**

Sanath Shetty<sup>1</sup>, Matej Veis<sup>1</sup>, Paweł Gąsior<sup>2</sup>, Damian Sokulski<sup>2</sup>, Pavel Veis<sup>3</sup>

<sup>1</sup>Department of Experimental Physics, FMPI, Comenius Univ, Slovakia; <sup>2</sup>Institute of Plasma Physics and Laser Micro-fusion, Poland; <sup>3</sup>Comenius University, Faculty of Math, Physics and Informatics, Slovakia.

The development of fusion energy relies heavily on advanced materials capable of with-standing extreme conditions in plasma-facing (PF) components. Laser-induced breakdown spectroscopy (LIBS) has emerged as a powerful technique for PF material characterization, offering rapid, in situ elemental analysis [1].

With the increasing interest in the application of artificial intelligence in the horizon of spectroscopy, different algorithms have been tried to quantify the LIBS spectra. In this study, Autoencoders were utilized to reduce the dimensionality of LIBS spectra [2] while preserving critical spectral features. The autoencoders were optimized using particle swarm optimization (PSO) [3], to explore the parameter space to fine-tune the autoencoder architecture, enhancing its ability to represent spectral data in a lower-dimensional latent space. This dimensionality reduction not only improved computational efficiency but also facilitated the application of ANNs for elemental quantification. The performance of various ANN architectures, including fully connected neural networks and convolutional neural networks, was evaluated in terms of regression metrics. The synthetic LIBS spectra, with varying compositions of elements including W, Be, C, and B, along with contributions from atmosphere and impurities were obtained from the NIST LIBS database [4] to emulate realistic experimental conditions, including plasma temperature ranging from 0.6 to 1.8 eV.

This approach aligns with previous efforts [5] to leverage machine learning and LIBS for advancing fusion material research, aiming to achieve rapid, non-invasive, and reliable analysis of key elements in candidate materials. The integration of autoencoders with PSO introduces non-linearity into dimensionality reduction and thus represents a novel methodology for addressing the challenges associated with LIBS spectra, demonstrating the potential to significantly enhance the role of LIBS in fusion materials research.

Acknowledgments: This work has been carried out within the framework of the EUROfusion Consortium, funded by the European Union via the Euratom Research and Training Programme (Grant Agreement No 101052200 – EUROfusion). This work was also supported by

the SRDA (APVV-22-0548) and VEGA (1/0815/25, 2/0120/25).

- [1] G.S. Maurya, A. Marin-Roldan, P. Veis, et al, J. Nucl. Mat., 541, 152417 (2020).
- [2] E. Harefa and W. Zhou, Anal. Meth., 13, 41 (2021).
- [3] X. Xu and W. Ren, Appl Soft Comput, 116, 108321 (2022).
- [4] A. Kramida, Y. Ralchenko, et al., NIST Atomic Spectra Database, (2014).
- [5] P. Gqsior, M. Kastek, M. Ladygina et al. Phys Plasmas, 31, 5 (2024).

POA-22

### **Single-Size Model for Gas Bubble Evolution in Cluster Dynamics Framework**

Sophie Blondel<sup>1</sup>, Davis Freeman<sup>1</sup>, Samuel Haid<sup>1</sup>, Marc Milliot<sup>2</sup>, Brian Wirth<sup>1</sup>

<sup>1</sup>University of Tennessee, United States; <sup>2</sup>John Jay High School, United States.

Xolotl [1], a US Department of Energy open-source code, is a spatially dependent cluster dynamics model used to predict material defects evolution and behavior under extreme conditions such as in fusion energy system. The multi-scale approach provides the kinetic parameters needed for modeling plasma-material interactions. The model captures phenomena like defect implantation and gas bubble formation, bursting, surface evolution, defect diffusion and outgasing. Our main focus is helium irradiated tungsten and the code has been extended to account for hydrogen.

Standard cluster dynamics simulations track each cluster individually, requiring one equation per cluster, which becomes computationally prohibitive as larger clusters form, due to limitations in available memory. We developed a single size model for larger bubbles to address this challenge. It relies on consolidating all clusters above a specified size threshold into a single set of equations. This consolidation enables the model to efficiently compute the evolution of bubble concentration, as well as the average defect contents, while retaining the physics that occurs for small bubble sizes. It is tested against previous results obtained while benchmarking against molecular dynamics simulations and compared to experimental data from linear plasma irradiation [2] for pure He plasma. Lastly, the hydrogen extension of the single size model is used for predictions of typical burning plasma operation in ITER [3].

- [1] D. E. Bernholdt et al., Xolotl (available at: <https://github.com/ORNL-Fusion/xolotl>)
- [2] S. Blondel, D. E. Bernholdt, K. D. Hammond, et al., Nucl. Fusion 58, 12 (2018)
- [3] A. Lasa, S. Blondel, D. E. Bernholdt, et al., Nucl. Fusion 61, 11 (2021)

POA-23

### **Simulations of gap bridging and filling during transient PFC melt events**

Ladislav Vignitchouk, Svetlana Ratynskaia

KTH Royal Institute of Technology, Sweden.

Transient surface melting under high-energy loads is one of the main PFC damage channels that must be controlled in fusion devices with solid metal walls [1]. In addition to global morphology changes that can be caused by melt displacement and pile-up under plasma-induced forces, local deformations in the vicinity of gaps – such as castellations or inter-monoblock spaces – are of crucial importance owing to the possibility of liquid infiltration or bridging, which have been observed in multiple melting experiments [2-4]. These phenomena can modify the PFC response to electromagnetic loads, especially during disruptions, as bridges allow eddy currents to short through the gaps, potentially increasing the net force on

the vessel [1].

Here we report validation studies of multiphase Navier–Stokes simulations against published experimental data in two of the most representative scenarios for transient melt events: gap bridging upon ELM-induced tungsten leading-edge exposure in the divertor of ASDEX Upgrade [2,5], and disruption-induced castellation filling on main chamber beryllium JET PFCs [3]. In the first case, short-lived liquid pools created by ELM heat bursts were accelerated by thermionic currents towards an asymmetric step-like gap, which they managed to cross in these few instances where large enough melt thickness and velocity were achieved [2]. In the second case, melt was created uniformly on both sides of the gap and mobilized by halo currents during the current quench [3].

Numerical output is shown to reproduce post-mortem observables such as the total amount of melt displaced or infiltration depth, and to be consistent with previously established dimensionless stability criteria [6]. Moreover, the simulated evolution of the liquid’s deforming surface demonstrates the detailed mechanisms of bridge formation, highlighting in particular the importance of fluid bulging at the corner and the creation of overhangs, which facilitate subsequent melt transport. Lastly, the results of first predictive simulations of near-gap tungsten melting – analogous to the JET beryllium case described above – are presented to provide estimates of threshold heat and current load values relevant for ITER PFCs.

[1] M. Lehnen et al., J. Nucl. Mater. 463, 39 (2015)

[2] K. Krieger et al., Nucl. Fusion 58, 026024 (2018)

[3] I. Jezu et al., Nucl. Fusion 59, 086009 (2019)

[4] S. Ratynskaia et al., Nucl. Fusion 64, 036012 (2024)

[5] S. Ratynskaia et al., Nucl. Fusion 60, 104001 (2020)

[6] L. Vignitchouk et al., Nucl. Fusion 62, 036016 (2022)

POA-25

### **Studies of runaway electron impact on plasma facing surfaces in the DIII-D tokamak**

Dmitry Rudakov<sup>1</sup>, Eric Hollmann<sup>1</sup>, Claudio Marini<sup>1</sup>, Erick Martinez-Loran<sup>1</sup>, Matthew Beidler<sup>2</sup>, Jeffrey Herfindal<sup>2</sup>, Daisuke Shiraki<sup>2</sup>, Yueqiang Liu<sup>3</sup>, Igor Bykov<sup>3</sup>, Andrey Lvovskiy<sup>3</sup>, Charles Lasnier<sup>4</sup>, Jun Ren<sup>5</sup>, Svetlana Ratynskaia<sup>6</sup>, Panagiotis Toliás<sup>6</sup>, Richard Pitts<sup>7</sup>

<sup>1</sup>University of California San Diego, United States; <sup>2</sup>Oak Ridge National Laboratory, TN, United States; <sup>3</sup>General Atomics, San Diego, CA, United States; <sup>4</sup>Lawrence Livermore National Laboratory, Livermore, CA, United States; <sup>5</sup>University of Tennessee, Knoxville, United States; <sup>6</sup>KTH Royal Institute of Technology, Sweden; <sup>7</sup>ITER Organization, France.

Studies of post-disruption runaway electrons (RE) impact on plasma-facing surfaces were performed in the DIII-D tokamak using the Divertor Material Evaluation System (DiMES) with instrumented samples allowing unique measurements of the RE energy and pitch angles. Understanding the impact of REs on the first wall is critical for ITER and FPP, as it is needed for prediction of the effectiveness of disruption mitigation systems, determining safe performance limits, and for evaluations of machine safety [1]. Quantifying RE-induced wall damage is extremely challenging, and previous work has dominantly relied on post-mortem inspection. Graphite samples 5 cm in diameter were inserted into the lower divertor of DIII-D under well-diagnosed plasma conditions and struck with high current (600 kA) RE beams, allowing quantification of the RE wall impact at an unprecedented level.

The initial experiment featured a plain graphite sample with a semi-spherical dome of 3.3 cm

radius protruding over the divertor tile surface by 1 cm [2]. The sample had a built in thermocouple (TC) and was imaged by visible and IR cameras. Upon the RE beam impact, the top of the dome suffered an explosive destruction to a depth of  $\sim 1$  mm with an estimated volume loss of  $\sim 150$  cubic mm, and dust ejection was observed by the cameras. The surface temperature in the failure region was estimated to be  $\sim 3000$  C, consistent with rapid volumetric material failure and gas release due to sublimation. Modelling of the brittle failure of graphite using a novel workflow with KORC, Geant4 and COMSOL codes was able to reproduce the volume loss [3].

The following experiments used domed and flat samples instrumented with TCs, thermoluminescent dosimeters (TLD) to measure RE pitch angles, and shunts to measure current into the samples. RE energies of 2–4 MeV and pitch angles of  $\sin\sim 0.4$  were estimated from the TLD readings. Penetration depth of REs into the sample is found to be  $\sim 1$ –2 mm, as expected for the measured energies. Shot-to-shot variation in RE energy deposited into the samples is ranging between 1–10 kJ, indicating that the toroidal phase of the final loss instability is not locked, but highly variable. Current measurements into the samples show a narrow ( $100\ \mu\text{s}$ ) pulse of negative current during RE strike, followed by slower ( $200\ \mu\text{s}$ ) spike of positive current. The data therefore demonstrates that the final loss of REs to the wall is followed by a pulse of cold thermal ions to preserve ambipolarity.

This work was supported in part by the U.S. Department of Energy under DE-FC02-04ER54698, DE-FG02-07ER54917, DE-AC05-00OR2275, DE-AC52-07NA27344, DENA0003525, DE-SC0023378, and DE-FG02-95ER54309.

[1] B.N. Breizman et. al, Nucl. Fusion 59, 083001 (2024)

[2] E.M. Hollmann et. al, Plasma Phys. Control. Fusion, submitted

[3] S. Ratynskaia, et. al, Nucl. Fusion, accepted

POA-28

### **Erosion and Modification of Tungsten Surfaces Under Sequential Steady-State and High Heat Fluxes Transient Plasma Impacts**

Vadym Makhlai<sup>1</sup>, Igor Garkusha<sup>1</sup>, Yuliia Volkova<sup>1</sup>, Stanislav Herashchenko<sup>1</sup>, Yurii Petrov<sup>1</sup>, Dmytro Yelisyeyev<sup>1</sup>, Pavel Shevchuk<sup>1</sup>, Thomas Morgan<sup>2</sup>

<sup>1</sup>National Science Center 'Kharkiv Institute of Physics and Technology', Institute of Plasma Physics, Ukraine; <sup>2</sup>Dutch Institute for Fundamental Energy Research, Netherlands.

The extreme sequential thermal steady-state and transient energy deposition on the DEMO Plasma-Facing Components (PFCs) causes significant damage to the armor. Tungsten was chosen as the primary material for the PFCs of DEMO. The evaluation of tungsten grades requires thorough testing and qualification under extreme fusion-relevant conditions, including high heat and particle fluxes [1].

Samples of pure ITER-grade tungsten produced by PLANSEE [2] were used for the experiments. Steady-state pre-loading of samples was performed in the Upgraded Pilot-PSI (UPP) and Magnum-PSI facilities. Fluence ( $1025\ \text{m}^{-2}$ ;  $1026\ \text{m}^{-2}$ ;  $1027\ \text{m}^{-2}$ ) and temperature (400 K; 500 K; 600 K; 700 K) scans were performed during successive D – H – D plasma exposures within UPP. The same temperature scan was performed at a fluence of  $1027\ \text{m}^{-2}$  within Magnum-PSI. The energy of particles reached 40 eV under steady-state plasma loading [2]. High heat flux transient plasma impacts were carried out using the quasi-stationary plasma accelerator

QSPA Kh-50 [3, 4]. Surface heat loads exceeded the melting threshold (energy density up to 0.9 MJ/m<sup>2</sup>, pulse duration of 0.25 ms). The surface was initially at approximately room temperature before the plasma pulse. Surface analysis was conducted using an optical microscope and SEM. The development of surface morphology on the exposed targets, as well as cracking, is discussed.

Surface relief typical for physical sputtering was observed after steady-state plasma loading. Blisters were detected after exposure to a fluence of 1027 m<sup>-2</sup> at surface temperatures above  $T = 600$  K within Magnum-PSI. Pre-loaded samples were exposed within a small (up to 10) number of QSPA plasma pulses. Surface melting, the formation of re-solidified layers, and cracking of the sample surface were identified as the main features of the QSPA pulsed hydrogen plasma exposure with heat loads above the tungsten melting threshold. Networks of large (cell size up to 0.4 mm) and intergranular (cell size up to 40 mkm) cracks were registered. Crack widths reached up to 1 mkm. Pores resulting from the destruction of blisters were also observed. Surface modification and crack development led to an increase in the roughness of the exposed surfaces.

[1] J.H. You et al., Fusion Engineering and Design 174, 112988 (2022)

[2] J. K. Elenbaas, Master Thesis (2024)

[3] N. Mantel et al., Nucl. Fusion 62, 036017 (2022)

[4] V. A. Makhelai et al., Phys. Scripta 196, 124043 (2021)

POA-29

### **The influence of H plasma implantation on the low-cycle thermal fatigue cracking of plasma-facing tungsten in EU DEMO**

James Hargreaves<sup>1</sup>, Jeong-Ha You<sup>2</sup>, Francesca Maviglia<sup>3</sup>, Jordy Vernimmen<sup>1</sup>, John Scholten<sup>1</sup>, Thomas Morgan<sup>1</sup>

<sup>1</sup>Dutch Institute for Fundamental Energy Research, Netherlands; <sup>2</sup>Max Planck Institute for Plasma Physics, Germany;

<sup>3</sup>Eurofusion PMU, Germany.

Divertor re-attachment events in the EU DEMO tokamak will briefly expose its ITER-like tungsten (W) monoblock divertor to intense thermal loads of <70 MW m<sup>-2</sup>, posing a risk of surface melting, cracking and recrystallisation [1], [2]. Strikepoint sweeping is proposed as an emergency measure to protect against this damage. However, this will impose cyclic thermal loads on DEMO's divertor targets, which may, over time, induce low-cycle thermal fatigue (LCTF) cracking of plasma-facing W surfaces [3]. These surfaces will also be modified by plasma-material interactions during service, leading to blistering, fuzz, re-deposition and/or recrystallisation [4]. Hydrogen and neutron embrittlement, and high temperature creep effects may also arise [5]. This evolution of plasma-facing surface morphology, local microstructure and material properties may alter the nucleation and propagation behaviour of fatigue cracks, possibly reducing the divertor's fatigue life. Addressing the present lack of data on this potential synergy will be vital for accurate lifetime analysis of DEMO's tungsten divertor.

A novel Magnum-PSI experiment has investigated the effects of H plasma implantation on the LCTF cracking of W. DEMO-representative uniaxial strain ( $\epsilon$ ) ranges were determined by time-dependent thermo-mechanical finite element analysis of a DEMO monoblock, simulating strikepoint sweeping at 1 Hz over a 100 mm span. Polished W targets with and without a prior H plasma implantation phase ( $T_{surf} = 300$  °C, cumulative H fluence  $2.2 \times 10^{26}$  m<sup>-2</sup>) were subsequently exposed to 150, 300, 450 and 600 DEMO-representative thermal cycles of  $\epsilon =$



0.08–0.12% using a modulating H plasma. Differences in fatigue cracking behaviour between the two series were analysed via optical and scanning electron microscopy, with quantitative image analysis (segmentation & thresholding) undertaken using ImageJ.

W targets without prior H implantation were found to exhibit mm-scale fatigue cracks after less than 150 cycles, whereas the H-implanted targets survived for up to 450 cycles before the onset of cracking was observed. This suggests that the dislocations and surface damage induced by H implantation may delay fatigue crack nucleation. Supporting modelling and experimental results will be presented alongside preliminary studies on pre/ELM-cracked W targets, and plans for future work.

[1] F. Maviglia, et al, Fusion Eng. Des., 109–111, 1067–1071 (2016)

[2] J. H. You, et al, Fusion Eng. Des., 175, 13010 (2022)

[3] M. Li, et al, Fusion Eng. Des., 102, 50–58 (2016)

[4] T. W. Morgan et al. Phys. Scr., T171, 014065 (2020)

[5] Y. Li et al. Nucl. Fusion, 60–8, 086015 (2020)

POA-30

### **Tungsten based composites and heavy alloys exposed to ELM-y H-mode plasmas in the DIII-D tokamak**

Žana Popović<sup>1</sup>, Tyler Abrams<sup>1</sup>, Zachary Bergstrom<sup>1</sup>, Jonathan Coburn<sup>2</sup>, Florian Effenberg<sup>3</sup>, Tatsuya Hinoki<sup>4</sup>, Ryan Hood<sup>2</sup>, Carlos Monton<sup>1</sup>, Rudolf Neu<sup>5</sup>, Jun Ren<sup>6</sup>, Johann Riesch<sup>5</sup>, Dmitry Rudakov<sup>7</sup>, Ruben Santana<sup>1</sup>, Cedric Tsui<sup>2</sup>

<sup>1</sup>General Atomics, United States; <sup>2</sup>Sandia National Laboratories, United States; <sup>3</sup>Princeton Plasma Physics Laboratory, United States; <sup>4</sup>Kyoto University, Kyoto, Japan; <sup>5</sup>Max Planck Institute for Plasma Physics, Germany; <sup>6</sup>University of Tennessee, Knoxville, United States; <sup>7</sup>University of California San Diego, United States.

We report on a recent DIII-D experiment with tungsten heavy alloys (WHA), tungsten fiber silicon carbide fiber reinforced tungsten composite (WfSiCf/W), and functionally graded tungsten silicon carbide (FG-W/SiC) materials. As part of an international collaboration, these materials were exposed to H-mode plasmas in the lower divertor of the DIII-D tokamak using the Divertor Material Evaluation System (DiMES). The samples' integrity was preserved despite visible erosion, light edge melting of the protruding WHA samples, and minor delamination of a bi-layer W/SiC. Overall, no major damage or cracking was observed on any of the samples. Two DiMES probes ~5 cm in diameter housing 7 button samples of ~6 mm diameter, either flush with the surface or tilted 10° towards the incoming heat flux were subsequently exposed in the DIII-D divertor to H-mode plasmas with ~40 Hz ELMs and with a new programmed sweep of the plasma strike point over DiMES for optimal heat flux distribution across samples. This methodology enables a uniform heat flux deposition over the DiMES surface and a good comparison between different materials exposed in the same DiMES probe. The incident heat fluxes during and between ELMs were  $q_{(\perp, inter-ELM)} \approx 2 \text{ MW/m}^2$ ,  $q_{(\perp, intra-ELM)} \approx 6 \text{ MW/m}^2$  for the flush and  $q_{(\perp, inter-ELM)} \approx 15 \text{ MW/m}^2$ ,  $q_{(\perp, intra-ELM)} \approx 42 \text{ MW/m}^2$  for the angled samples. The surface morphology and elemental composition of the button samples of WHA (W-Ni-Fe and W-Ni-Cu), WfSiCf/W, and FG-W/SiC were pre-characterized using profilometry and SEM microscopy with EDS spectrometry. Post-mortem analyses with SEM/EDS found that angled samples of WHA had some surface damage without cracking but with minor edge melting, while the flush samples only showed signs of surface erosion. Local deposition of Ni, Fe, and Cu, distinguished by the typical “halo” deposition on the DiMES holder around the samples, was

also observed. Flush samples of WfSiCf/W and 3 gradients of annealed and non-annealed FG-W/SiC performed very well and demonstrated adequate resilience to the heat load of  $\sim 1.5\text{--}2.0\text{ MW/m}^2$ . Light surface erosion is visible in the post-exposure SEM images, with minimal fiber end melting of WfSiCf/W and minimal delamination of an annealed bi-layer of one of the FG-W/SiC samples. Erosion measurements from in-situ filtered visible imaging and spectroscopy confirming these findings are also discussed.

Acknowledgement: Work supported by US DOE under DE-FC02-04ER54698, DE-AC02-09CH11466, and DE-NA0003525.

POA-32

### **MatDB4Fusion: A new initiative to collect, merge, and leverage material properties data**

Philipp Lied<sup>1</sup>, Giacomo Aiello<sup>2</sup>, Zachary Bergstrom<sup>3</sup>, Arunodaya Bhattacharya<sup>4</sup>, Daniel Clark<sup>5</sup>, Thomas Davis<sup>6</sup>, Mark Gilbert<sup>7</sup>, Michael Gorley<sup>7</sup>, Cory Hamelin<sup>7</sup>, Jim Pickles<sup>8</sup>, Gerald Pintsuk<sup>9</sup>, Andrew Sowder<sup>10</sup>, Se-hila Gonzalez<sup>11</sup>

<sup>1</sup>FusionCatalyst, Germany; <sup>2</sup>EUROfusion, Germany; <sup>3</sup>General Atomics, United States; <sup>4</sup>University of Birmingham, United Kingdom; <sup>5</sup>Type One Energy Group, United States; <sup>6</sup>Oxford Sigma, United Kingdom; <sup>7</sup>UK Atomic Energy Authority (UKAEA), United Kingdom; <sup>8</sup>Tokamak Energy, United Kingdom; <sup>9</sup>Forschungszentrum Jülich GmbH, Germany; <sup>10</sup>Electric Power Research Institute (EPRI), United States; <sup>11</sup>Clean Air Task Force (CATF), United States.

A drastic acceleration of efforts is currently perceived in fusion energy research, driven by major breakthrough results in plasma physics and increasing investments with a growing number of private companies that seek partnership. However, there are severely limiting factors for the anticipated pace to realize fusion on the grid. One of the largest factors is the development of a set of basic materials suitable for various fusion operation conditions in harsh neutron irradiation spectra, qualified and validated in expensive irradiation campaigns. Entities from several nations went through this process for decades and accumulated data in large, but partial, databases of irradiated/non-irradiated material properties. However, these data are often not public or lack important background information in many cases and the necessary efforts to collect them are huge. Additionally, the rapid development of machine learning (ML) capabilities in recent years gives hope for reduced design uncertainties, qualification programme durations, and improved lifetime predictions, when properly applied to suitable datasets with sufficient quality and statistically-significant quantity.

Due to this urgent demand for data support, an international working group emerged in 2023, led by Clean Air Task Force (CATF). With the aim to create a unique and well-maintained global database for fusion material properties that could benefit the whole community (public and private organizations), the “Material Database for Fusion” (MatDB4Fusion) was born. It will collect all kinds of material properties data which are relevant for fusion device design in a flexible but structured manner with quality control, supported by many entities from different countries. While it should primarily host data for open access to benefit the scientific community the most, it may also serve as a secure area for restricted data under intellectual property rights from different stakeholders to allow for secure scientific exchange and/or analysis. Neutrality and internationality are considered as key-aspects, embodied by a steering committee and the cooperation with OECD-NEA as database host. MatDB4Fusion is aimed to act as single reference for all fusion device design approaches to access wealth of data that did not reach publication or attention, assess data gaps and reduce duplication of effort by improving focus of experimental campaigns, accelerate creation of codes and standards for qualification and

provide sufficient data for machine learning solutions. In addition to the purpose and scope of the database project, the talk will focus on its current development state and ways to participate or support our efforts.

POA-33

### **First wall simulated W-EUROFER mock-up characterization under HHF DEMO relevant conditions**

Javier de Prado<sup>1</sup>, Ignacio Izaguirre<sup>1</sup>, Daniel Dorow-Gerspach<sup>2</sup>, Emanuele Cacciotti<sup>3</sup>, Francesco Crea<sup>3</sup>, Maria Sánchez<sup>1</sup>, Riccardo De Luca<sup>3</sup>, Marius Wirtz<sup>2</sup>

<sup>1</sup>Universidad Rey Juan Carlos, Spain; <sup>2</sup>Forschungszentrum Jülich GmbH, Germany; <sup>3</sup>ENEA, Nuclear Department, Italy.

According to the latest designs of the DEMO First Wall (FW) component, a tungsten (W) layer will serve as the facing material, joined to EUROFER, which acts as the structural component and heat sink. While the characterization of both materials under relevant DEMO conditions has been extensively studied separately, few works have addressed the thermomechanical behavior of fully simulated FW components under high heat flux (HHF) conditions.

To address this challenge, after optimizing the W-EUROFER joint microstructure by modifying various brazing parameters and qualifying through small-scale HHF tests, simulated first wall mock-ups consisting of EUROFER cooling structures and W tiles were joined using brazing techniques with realistic intermediate materials. Ten W tiles were brazed to the EUROFER cooling structure using 50  $\mu$ m thick copper braze interlayers. Two mock-ups were subjected to 200 cycles of heat loads (20 s on/off) at each power level, ranging from 0.5 to 3 MW/m<sup>2</sup> in 0.5 MW/m<sup>2</sup> increments, ensuring steady-state equilibrium. Ultrasonic testing (UT) was conducted before and after HHF load application to assess joint quality and correlate potential failures and damage. Additionally, postmortem SEM analyses were performed to correlate joint microstructure with UT and HHF test results to determine the component's failure mechanisms.

Only one tile from batch 1 (tile 1.3) failed prematurely during the application of 2.0 MW/m<sup>2</sup>, which was attributed to pre-existing tungsten defects not related to the brazing process, as revealed by the as-brazed UT examination. The remaining four tiles from batch 1 (tiles 1.1, 1.2, 1.4, and 1.5) reached the final test step without thermal anomalies. However, at this level tiles 1.2, 1.4, and 1.5 failed during the last step, while tile 1.1 completed the test successfully.

In batch 2, tile 2.5 failed during the application of 1.0 MW/m<sup>2</sup>, also due to pre-existing tungsten defects detected by UT. Tiles 2.2, 2.3, and 2.4 withstood heat loads of 2 MW/m<sup>2</sup>, and tile 2.1 completed the entire test without overheating.

Postmortem analysis revealed that, despite some samples experiencing overheating events, most of those samples evidenced metallic continuity was in certain areas of the joint.

Although future efforts will focus on improving the joint's thermomechanical properties, the combined results of different European research units demonstrate the feasibility of this technology to conform to and withstand the relevant heat load conditions of the FW component.

POA-34

### **Heat Flux Test of the Small Thermal Shielding Mockups for the ITER Electron Cyclotron Heating Window Shielding Block**

Chen Yanyu<sup>1</sup>, Wang Pinghuai<sup>1</sup>, Chen Jiming<sup>1</sup>, Zhang Fu<sup>2</sup>, Wang Kun<sup>3</sup>, Li Qian<sup>1</sup>, Wei Zhengxing<sup>1</sup>

<sup>1</sup>Southwestern Institute of Physics, China; <sup>2</sup>International Thermonuclear Experimental Reactor, France; <sup>3</sup>ITER CNDA, China.

The Shielding Block at the electron cyclotron heating window requires the design of a special water-cooled 316LN device, SB11EH, to reduce thermal damage to the shielding block. This device is subjected to a heat flux of  $0.35 \text{ MW/m}^2$ , making it crucial to study the heat dissipation capability of the device and the thermal fatigue performance of the argon arc welded seams. Two small Mockups with runway shape were designed and fabricated, and steady-state and thermal fatigue tests were conducted on the EMS-400 SWIP in China. The heat flux densities for steady-state testing were  $0.35$  and  $0.5 \text{ MW/m}^2$ . For the thermal fatigue test, the heat flux density was  $0.5 \text{ MW/m}^2$ , with 6000 thermal cycles, 80 seconds of heating time, and 80 seconds of cooling time. In the thermal fatigue test, the surface temperature at the water outlet was slightly higher than at the inlet. The surface temperature at  $0.35 \text{ MW/m}^2$  was approximately  $260^\circ\text{C}$ , and at  $0.5 \text{ MW/m}^2$ , it was around  $335^\circ\text{C}$ , well below the heat-affected temperature of 316LN. During the thermal fatigue test, the surface temperature fluctuation of the Mockups was less than 15%, and no expansion or changes in surface temperature were observed at the artificial defect sites.

POA-36

### **A novel approach to studying divertor gap heat loads**

Miha Radež<sup>1</sup>, Jernej Kovačič<sup>2</sup>, Matic Brank<sup>2</sup>, Stefan Costea<sup>2</sup>, Leon Bogdanovič<sup>2</sup>, Tomaž Gyergyek<sup>3</sup>, Leon Kos<sup>2</sup>

<sup>1</sup>University of Ljubljana, Faculty of Mathematics and Physics, Slovenia; <sup>2</sup>University of Ljubljana, Faculty of Mechanical Engineering, Slovenia; <sup>3</sup>University of Ljubljana, Faculty of Electrical Engineering, Slovenia.

Heat loads to the divertor plasma-facing components (PFCs) are one of the main limiting factors in the operational space of future tokamaks. The current approach to divertor design is so-called "castellation" of the PFCs (monoblocks) to protect the leading edges of the components. However, it was recently proven that line-of-sight approach to the design of the divertor PFC castellation and consequent calculation of heat load distribution pattern is not sufficiently accurate for prediction of hot-spots on the material surface due to omission of cyclotron movement [1]. Alternatively, a ballistic approach as in [1] or a particle-in-cell (PIC) method as in [2] can be used to improve the accuracy, with the former neglecting the effects of the electric field and the latter having completely self-consistent electric field, but being computationally extremely demanding [3,4]. The electric field distorts the helical trajectories of the charged particles around the magnetic field lines, which in turn changes the heat flux footprint. In some cases space charge regions can occur due to different cross-field transport properties of electrons and ions.

We have constructed an approach that lies in between the two aforementioned, by making a semi-analytical approximation of the electric field on top of the prescribed magnetic field based on the loss cone of particles from the suggested velocity distribution function. After the fields are prescribed, we start injecting particles from the top of the simulation domain with different velocities in different phases of gyration from various positions. The particle path is integrated and intersection of the trajectory with the PFC is recorded as the location of

their deposition. From there, we can calculate the heat load pattern based on the deposition pattern of the test particles. The results are in good agreement with the PIC method [3,5]. This data can then be used to solve the heat equation for the PFC and deduce the their temperature profiles or be used in erosion calculations.

Acknowledgements: The authors acknowledge the financial support by the Slovenian Research and Innovation Agency (ARIS) through project NC-25005 and through research core funding P2-0405.

- [1] J. P. Gunn et al., Nucl. Fusion 57, 046025 (2017)
- [2] R. Dejarnac, Y. Corre, P. Vondraček, J. Gaspar, E. Gauthier, J. P. Gunn, M. Komm, J.-L. Gardarein, J. Horaček, M. Hron, J. Matejčík, R. A. Pitts, R. Panek, Nucl. Fusion 58, 066003 (2018)
- [3] F. Cichoki, P. Innocente, V. Sciortino, P. Minelli, F. Taccogna, Plasma Phys. Control. Fusion 66, 025015 (2024)
- [4] M. Komm, J. P. Gunn, R. Dejarnac, R. Pánek, R. A. Pitts, A. Podolnik, Nucl. Fusion 57, 126047 (2017)
- [5] M. Komm, R. Dejarnac, J. P. Gunn, A. Kirschner, A. Litnovsky, D. Matveev, Z. Pekarek, Plasma Phys. Control. Fusion 53, 115004 (2011)

POA-37

### **Helium bubbles at grain boundaries in low-energy helium plasma exposed tungsten: Atomic-scale characteristics and evolution kinetics**

Yu Li, Yi-Wen Zhu, Guangnan Luo, Haishan Zhou

Institute of Plasma Physics, Chinese Academy of Sciences, China.

The tungsten (W) plasma-facing material (PFM) and helium (He) plasma in fusion devices do not co-exist easily. He bubbles often form within W with an attending effect on surface morphology, mechanical behaviour, and transport of heat and hydrogen isotopes, etc. These properties are also sensitive to the grain boundary character, and the interactions between He bubbles and grain boundaries are therefore of importance. While atomistic calculations suggested some exotic behaviour of such interactions, experimental studies lagged behind. Here, we characterize He bubbles at the W grain boundaries by transmission electron microscopy (TEM). Polycrystalline tungsten specimens were first exposed to high-flux He plasmas in a linear plasma generator to create subsurface He bubbles. The site-specific lamellae were then lifted out by a focused ion beam to enable TEM analysis. Through high-resolution TEM, we found that the periodic arrangement of W atoms remained around the He bubble at a triple junction. In contrast, dislocated atoms were observed around He bubbles in the grain interior. More interestingly, we found evidence of grain boundary reconstruction due to the He bubbles. Furthermore, the bubble statistics as a function of the grain boundary misorientation angle, plasma exposure time, and target surface temperature were investigated and weak dependence was observed. All results can be explained by the strong trapping of He bubbles at the grain boundaries of W. In light of this, implications for the performance of W PFCs are discussed.

### **SALAMANDER: Advanced Multiphysics Simulation for Fusion Energy Systems**

Pierre-Clément Simon<sup>1</sup>, Casey Icenhour<sup>1</sup>, Guillaume Giudicelli<sup>1</sup>, Logan Harbour<sup>1</sup>, Lin Yang<sup>1</sup>, Derek Gaston<sup>1</sup>, Masashi Shimada<sup>1</sup>, Grayson Gall<sup>2</sup>, Amanda Lietz<sup>2</sup>, Mahmoud Eltawila<sup>3</sup>, April Novak<sup>3</sup>, Trevor Franklin<sup>4</sup>, Lane Carasik<sup>4</sup>, Helen Brooks<sup>5</sup>

<sup>1</sup>Idaho National Laboratory, United States; <sup>2</sup>NCSU, United States; <sup>3</sup>UIUC, United States; <sup>4</sup>VCU, United States; <sup>5</sup>UKAEA, United Kingdom.

The rapid deployment of fusion energy as a viable energy source requires advanced computational tools capturing the intricate multiphysics interactions in fusion systems. High-fidelity multiphysics computational tools are key to understanding and predicting the behavior of components under extreme conditions, such as plasma facing components (PFCs). PFCs endure severe thermal loads, repeated thermal shocks, and bombardment from plasma ions, neutral particles, and high-energy neutrons, posing significant challenges to their design and operational lifetime.

To address these challenges, the Fusion ENergy Integrated multiphys-X (FENIX) framework has been developed. Built on the robust Multiphysics Object-Oriented Simulation Environment (MOOSE) platform, FENIX leverages MOOSE's modular and open-source framework to integrate multiple high-fidelity simulation capabilities. These include heat transfer, solid mechanics, thermal hydraulics, neutronics through the Cardinal MOOSE-based application, and tritium transport analysis through the MOOSE-based version of the tritium migration analysis program, version 8 (TMAP8). Additionally, FENIX supports plasma edge modeling to support plasma-material interaction simulations. FENIX is designed to facilitate massively parallel multiphysics simulations, essential for large simulations required to accurately model fusion systems. The framework's development adheres to strict software quality assurance standards, ensuring reliability, traceability, and continuous improvements. The open-source nature of FENIX, complemented by extensive documentation and a continuous integration system, promotes collaborative development and workforce training.

In this presentation, we will demonstrate the capabilities of FENIX through a case study focused on the ITER-like divertor monoblocks. These components are critical for managing plasma impurities and high heat loads in fusion reactors. We will show preliminary results that showcase how FENIX models the complex multiphysics environment of PFCs. This enables us to capture multiphysics interactions around PFCs, ultimately accelerating their design and performance evaluation. As an integrated advanced modeling tools within a fully integrated framework, FENIX stands as a crucial asset to accelerate the deployment of fusion energy.

### **Primary and secondary metallic PFC damage induced by RE dissipation in FTU**

Marco De Angeli<sup>1</sup>, Panagiotis Tolias<sup>2</sup>, Svetlana Ratynskaia<sup>2</sup>, Dario Ripamonti<sup>3</sup>, Giorgio Maddaluno<sup>4</sup>, Giambattista Daminelli<sup>3</sup>, Elzbieta Fortuna-Zalesna<sup>5</sup>, Witold Zielinski<sup>5</sup>

<sup>1</sup>Institute for Plasma Science and Technology, CNR, Italy; <sup>2</sup>KTH Royal Institute of Technology, Sweden; <sup>3</sup>Institute of Condensed Matter Chemistry and Energy Technologies, CNR, Italy; <sup>4</sup>ENEA, C.R. Frascati, Italy; <sup>5</sup>Warsaw University of Technology, Poland.

ITER will begin with a temporary inertially cooled tungsten first wall allowing experience to be gained with runaway electron (RE) control and mitigation without risking damage to the final panels to be installed during DT operation [1]. For decades, it had been recognized that RE-PFC interaction leads to deep volumetric melting. However, only recently, it has been

realized that RE-PFC interaction can also lead to thermal shock driven material explosions [2,3] that could be accompanied by extensive wall cratering caused by the subsequent mechanical impact of the high velocity solid dust [4,5]. In the FTU tokamak, because of technical characteristics, uncontrolled highly energetic RE generation (15–35 MeV, 150–230kA) has been commonplace during operations [6], suggesting that FTU constitutes a good test bed for the study of RE-PFC interactions integrated over several experimental campaigns.

This work describes the primary localized RE-induced damage inflicted on the molybdenum-alloy poloidal limiter of FTU that could be summarized as (i) surface or deep melting; (ii) surface layer exfoliation of several millimeters; (iii) intergranular crack generation on the surface and in the bulk of tiles millimeters long; (iv) recrystallization and degradation of mechanical properties (hardness) of the bulk material.

This work also describes the secondary non-localized RE-induced damage inflicted on the molybdenum-alloy toroidal limiter of FTU by the impact of fast solid Mo dust, about  $70\mu\text{m}$  in size travelling with speeds up to 800 m/s, released by the PFC explosions that comprises (i) crater formation,  $100\mu\text{m}$  in diameter and  $10\mu\text{m}$  deep, (ii) bulk cracking; (iii) removal of the pre-existing co-deposited material.

In conclusion, this work shows that FTU could still safely operate despite the severe PFC damages caused by energetic RE-PFC interactions.

[1] R. A. Pitts et al., Nucl. Mater. Energy 42, 101854 (2025).

[2] M. De Angeli et al., Nucl. Fusion (Letter) 63, 014001 (2023).

[3] S. Ratynskaia et al., Nucl. Fusion (Letter), submitted.

[4] P. Tolas et al., Fus. Eng. Des. 195, 113938 (2023).

[5] M. De Angeli et al., Nucl. Mater. Energy 41, 101735 (2024).

[6] B. Esposito et al., Plasma Phys. Control. Fusion 59, 014044 (2017).

POA-41

### **Comparison between discrete and continuous energy formalisms used to model multi-level kinetic hydrogen trapping in PFM**

Sokay Chroeu, Jonathan Mougnot, Yann Charles, Monique Gaspérini

Université Sorbonne Paris Nord, CNRS, LSPM, France.

Simulation of hydrogen trapping by microstructural defects is a key factor to describe the underlying mechanisms of hydrogen transport in plasma-facing components. Atomistic simulations show that more than one hydrogen atom can be trapped around of a single material defect (as vacancy) and the detrapping energy depends on hydrogen filling [1]. Models of hydrogen transport at continuous scale were proposed based on the resolution of multiple discrete levels [2,3], i.e., solving as many equations as there are energy levels considering for each level a constant detrapping energy. For vacancy clusters, several dozen of hydrogen atoms can be trapped in a single defect. To avoid having too many equations to solve, Ebihara et al [4] have proposed a continuous formalism using a single equation for a trap based on the McNabb and Foster formalism [5] instead of a discrete system. In this case, detrapping energies are no longer constant but depends on the trap occupancy: higher is the occupancy, lower is the detrapping energy.

The aim of this study is to directly compare these discrete and continuous approaches, highlighting the need to correct the trapping kinetics in order to achieve a good agreement on the retention value between the two types of formalisms. First, the formalisms will be presented

and their disagreement will be underlined, both conceptually and through a hydrogen loading in iron and tungsten cases (showing the kinetics of charging and desorption with temperature in a 0D simulation). Recommendations for modifying the trapping kinetic constants are then given to enable matching between these formalisms. Finally, the various approaches implemented by finite element method will be used to reproduce a TDS spectrum of a tungsten sample and a transport simulation in a tungsten beam subjected to a thermal gradient. This work was supported by the ANR FEMHILIM project, grant ANR-22-CE08-0003 of the French National Research Agency (ANR).

- [1] J. Hou, X.-S. Kong, X. Wu, et al., *Nature Materials* 18 (8), 833–839 (2019)
- [2] K. Schmid, J. Bauer, T. Scharz-Selinger, et al, *Physica Scripta* T170, 014037 (2017)
- [3] E. A. Hodille, Y. Ferro, N. Fernandez, et al, *Physica Scripta* T167, 014011 (2016)
- [4] K.-i. Ebihara, Y. Sugiyama, R. Matsumoto, et al, *Metallurgical and Materials Transactions A* 52, 257–269 (2021)
- [5] A. McNabb and P. K. Foster, *Transactions of the Metallurgical Society of AIME* 227, 618–627 (1963)

POA-42

### **A code-comparison to establish a common-ground for component-level transport codes**

Gabriele Ferrero<sup>1</sup>, Etienne Hodille<sup>2</sup>, Raffaella Testoni<sup>1</sup>

<sup>1</sup>Politecnico di Torino, Dipartimento di Energia, Italy; <sup>2</sup>CEA, IRFM, France.

Tritium transport is a fundamental topic in the development of nuclear fusion reactors for sustainable and competitive energy production. Tritium breeding blankets and extraction systems must be as efficient as possible. Tritium handling systems are crucial to ensure fuel self-sufficiency, safe operations, and cost reduction. Component-level modeling supports design choices to build a more efficient system. In the last years, multiple component-level codes dedicated to simulating hydrogen isotope transport mechanisms, such as permeation across materials and trapping, have been developed, verified, and validated. This work presents a comparison between three codes, MHIMS, FESTIM, and mHIT, in different verification and validation benchmarks, and their application on the ITER tungsten monoblock. For the verification study, slab permeation is compared with analytical solutions. Then, to have a more comprehensive verification case, the method of manufactured solutions (MMS) is employed for the mHIT code, with both Sievert's law solubility and Henry's law solubility. Validation for the mHIT code is carried out through two thermo-desorption (TDS) experiments, with Tungsten [1] and EUROFER [2], following MHIMS [3] and FESTIM [4] example. Then, mHIT coupled with the heat transfer module is applied for the inventory evaluation of the ITER monoblock with 3 materials (W, Cu, CuCrZr), multiple traps, during a transient in 2 dimensions, and results are compared against previous FESTIM simulations [4]. Results show tritium buildup in the cold region of the monoblock, especially in the CuCrZr region, which is smaller in size than the W region and is far from the plasma implantation source. This application showcases the relevance of component-level modeling for more complex systems. Indeed, to analyze and design tritium components for a fusion power plant, such as a breeder blanket, a plethora of features are necessary, such as trapping, 3 dimensions, multimaterial interfaces, time dependent, chemical reactions and CFD coupling. The benchmarks showcased good agreement between the codes when applicable, and experimental results. Moreover, all the FESTIM and mHIT models are open-source and available at



[https://github.com/gabriele-ferrero/Titans\\_TT\\_codecomparison](https://github.com/gabriele-ferrero/Titans_TT_codecomparison), and can be employed as a learning resource for component-level modeling or a starting point to build new physics and extend the modeling capability of the softwares. This work demonstrates the coherence and the solid common ground between the codes, verifies some features which are already implemented, and can serve as a starting point for more complex transport features (e.g. chemical reactions, convection and turbulence coupling).

This work has been carried out within the framework of the TITANS project and has received funding from the European Commission 2022–2025 under grant agreement No 101059408.

- [1] O. V. Ogorodnikova, J. Roth, M. Mayer, Journal of Nuclear Materials 313–316 (2003)
- [2] F. Montupet-Leblond, E. Hodille, et al. Nuclear Fusion 62 (8) (2022)
- [3] E. A. Hodille, X. Bonnin et al. Journal of Nuclear Materials 467 (2015)
- [4] R. Delaporte-Mathurin, E. A. Hodille et al. Nuclear Materials and Energy 21 (2019) 100709.

POA-43

### **Diffusion of H atoms at the W/Cu interface: a kinetic model based on DFT data**

Yovany Silva-Solis<sup>1</sup>, Julien Denis<sup>2</sup>, Etienne Hodille<sup>2</sup>, Yves Ferro<sup>1</sup>

<sup>1</sup>Aix-Marseille University, CNRS, PIIM, France; <sup>2</sup>CEA, IRFM, France.

The study explored hydrogen (H) atom diffusion at the tungsten (bcc) - copper (hcp) W(001)/Cu(1120) interface [1,2] through a combination of DFT calculations, Arrhenius-type diffusion coefficient and Macroscopic Rate Equation (MRE) modeling. This investigation considered two diffusion paths across the interface, connected by a third path within the W/Cu interface plane. The potential energy profile of each path is established by electronic structure calculations based on DFT. The activation barriers within the copper network displayed significant variations among these paths due to the reconstruction of the Cu fcc bulk into a hcp structure in the vicinity of the interface. Additionally, diffusion properties are established in perfect tungsten and copper as a reference. They are compared to diffusivity across and parallel to the W/Cu interface. Notably, diffusion parallel to the interface is shown to be lower than that within the tungsten and copper bulks across the temperature range from 260K to 1000K. Subsequently, the hydrogen diffusion perpendicular to the interface plane was modeled and analyzed according to a kinetic model we built based on Macroscopic Rate Equations. The complex energy pattern of the diffusion path across the interface behaves like a two steps model. As a consequence, a reduced-two steps model is proposed to model the kinetic behavior of H transport across the W/Cu interface.

- [1] Y. Silva-Solis, J. Denis, E. A. Hodille, Y. Ferro, J. Phys: Condense Mater 36 (2024) 465001
- [2] Y. Silva-Solis, J. Denis, E. A. Hodille, Y. Ferro, Nuclear Materials and Energy Fusion, 37 (2023) 101516

POA-44

### **LIBS for in-situ characterisation of JET plasma facing components: autoencoder-based spectral data processing**

Paweł Gąsior<sup>1</sup>, Damian Sokulski<sup>1</sup>, Salvatore Almagia<sup>2</sup>, Juuso Karhunen<sup>3</sup>, Jari Likonen<sup>3</sup>, Shweta Soni<sup>4</sup>, Sahithya Atikukke<sup>4</sup>, Pavel Veis<sup>4</sup>, Sanath Shetty<sup>5</sup>, Matej Veis<sup>5</sup>, Jelena Butikova<sup>6</sup>, Sebastijan Brezinsek<sup>7</sup>, Rongxing Yi<sup>7</sup>, Ionuț Jecu<sup>8</sup>, Indrek Jõgi<sup>9</sup>, Jasper Ristkø<sup>9</sup>, Peeter Paris<sup>9</sup>, Corneliu Porosnicu<sup>10</sup>

<sup>1</sup>Institute of Plasma Physics and Laser Microfusion, Poland; <sup>2</sup>ENEA, Diagnostics and Metrology Laboratory, Italy;

<sup>3</sup>VTT Technical Research Centre of Finland Ltd, Finland; <sup>4</sup>Comenius University, Faculty of Math, Physics and Informatics, Slovakia; <sup>5</sup>Department of Experimental Physics, FMPI, Comenius Univ, Slovakia; <sup>6</sup>Institute of Solid State Physics, University of Latvia, Latvia; <sup>7</sup>Forschungszentrum Jülich GmbH, Germany; <sup>8</sup>UKAEA, Culham Campus, Abingdon, United Kingdom; <sup>9</sup>University of Tartu, Institute of Physics, Estonia; <sup>10</sup>INFLPR 409, Magurele, Romania.

Being a remote and typically contactless method, LIBS (Laser Induced Breakdown Spectroscopy) has emerged as a candidate for monitoring the fuel retention and chemical composition of the first wall and divertor in thermonuclear reactors. To verify its performance in reactor conditions, in-situ experiment with LIBS on remote arm has been performed on the Joint European Torus (JET) device, but prior to this, a preparatory investigation had been conducted at VTT. It employed calibrated samples as well as original targets from JET which had been characterized with the use of the set-up developed for LIBS @JET including 20 m fiber cable. The samples had been pre-characterised with various post-mortem methods as ion beam techniques, SIMS and optical profilometry. Besides the positive verification of the pre-experimental assumptions, the results also exposed potential issues as the signal fluctuations together with the presence of spectral artifacts may deteriorate reproducibility and increase uncertainties. The latter are accumulated in the estimation of plasma parameters and chemical composition.

A possible approach for reducing the influence of stochastic fluctuations is the application of machine learning model of autoencoder[1]. The algorithm applies artificial neural network to reduce data dimensionality by decreasing the number of neurons in subsequent latent layers. After the data passes the bottleneck, it is reconstructed by the layers with increasing neuron number and the output representation is compared with the original data to calculate the loss function. Following to this scheme, in generalization regime, the model is able to recover the deterministic part of the signal whereas the stochastic components are filtered out. Processed with this method, spectra acquired in the experiment may be used for training and testing the ML models for estimation of chemical composition, particularly characterization of fuel retention in Be codeposits.

[1] G.E. Hinton, R.R. Salakhutdinov, Science (80-. ). 313 (2006) 504–507.

POA-45

### **Deuterium retention in different tungsten-based alloys measured by LIBS, NRA and TDS**

Mauricio Gago<sup>1</sup>, Bernhard Unterberg<sup>1</sup>, Steffen Antusch<sup>2</sup>, Anne Houben<sup>1</sup>, Alexander Klein<sup>2</sup>, Arkadi Kreter<sup>1</sup>, Sören Möller<sup>1</sup>, Michael Rieth<sup>2</sup>, Gennady Sergienko<sup>1</sup>, Marius Wirtz<sup>1</sup>, Rongxing Yi<sup>1</sup>, Christian Linsmeier<sup>1</sup>

<sup>1</sup>Forschungszentrum Jülich GmbH, Germany; <sup>2</sup>Karlsruhe Institute of Technology, Germany.

Tungsten is the material of choice as plasma-facing material (PFM) for future fusion reactors such as ITER. DEMO will most probably use tungsten and tungsten-based materials for its first wall and divertor. One of the main factors in analysing whether a certain material can be used as PFM in a fusion reactor is its fuel retention. Tritium is extremely rare and expensive to produce, as well as radioactive. Due to economic and security concerns, the tritium inventory should remain as low as possible, and for ITER the limit is 700 g of tritium in the whole reactor. Likewise, any new material being developed should have an appropriate fuel retention behaviour according to the conditions in the reactor.

Several tungsten-based alloys were produced in KIT via powder injection moulding (PIM) and have been proven to have improved physical and mechanical properties when compared to tungsten, such as improved ductility, toughness, a lower ductile-to-brittle transition temperat-

ure (DBTT) and improved resistance to ELM-like thermal shocks. These alloys (W-1TiC, W-2Y<sub>2</sub>O<sub>3</sub>, W-3Re-1TiC, W-3Re-2Y<sub>2</sub>O<sub>3</sub>, W-1HfC and W-1La<sub>2</sub>O<sub>3</sub>-1TiC) have now been exposed to deuterium plasma in the linear plasma device PSI-2 and their deuterium retention behaviour, as a proxy for the tritium retention, was measured with different methods.

Their dynamic deuterium retention behaviour was, first, tested via in-situ laser-induced breakdown spectroscopy (LIBS). Nuclear reaction analysis (NRA) was then performed ex-situ to evaluate the deuterium retention at different depths and times after exposure. Thermal desorption spectroscopy (TDS) was later performed to determine the total static deuterium retention in the samples and to discern how big of an influence the alloying elements have on the retention behaviour and whether new retention mechanisms can be observed. All PIM tungsten alloys had a higher retention level than ITER-grade tungsten, with the samples containing Y<sub>2</sub>O<sub>3</sub> retaining approximately double as much deuterium.

POA-46

### **Oxidation of tungsten and its implications to tritium retention in decommissioning, maintenance and accident scenarios in future devices**

Eric Prestat<sup>1</sup>, Rongri Li<sup>2</sup>, Guillermo Alvarez-Diaz<sup>2</sup>, Imogen Haydon<sup>1</sup>, Livia Cupertino Malheiros<sup>2</sup>, Emilio Martinez-Paneda<sup>2</sup>, Mark Gilbert<sup>1</sup>

<sup>1</sup>UK Atomic Energy Authority (UKAEA), United Kingdom; <sup>2</sup>Imperial College London, United Kingdom.

Tungsten is one of the main plasma materials because of its excellent high thermal conductivity, low erosion rate, low fuel retention, and low neutron activation. However, tungsten oxidises readily with very low partial pressure of oxygen, and this can result in significant loss of first wall materials and dispersion of tungsten oxide in form of sublimated gas molecules or dust spalled off from the oxide scale. This can have a detrimental impact on the operation and the sustainability of the reactor. Recent modelling work has shown that one of the tungsten oxide phase (WO<sub>2</sub>) could act as a tritium barrier [1], which will impact the tritium retention of tungsten-based components. Therefore, it is important to understand the microstructure of the tungsten oxide scale (oxide phase formed and morphology). In this presentation, we will report on the results of tungsten oxidation experimental campaigns performed using a thermogravimetric analysis in a range of experimental conditions: temperature ranging between 450°C and 1200°C, varying relative humidity (0%, 30%, 60%) or various oxygen content (<5 ppm (pure nitrogen N<sub>4.8</sub>), 0.01%, 0.1%, 1% and 20%). The microstructure of the oxide scale has been characterised using Raman spectroscopy (in cross-section and wedge polished geometry), scanning electron microscopy and X-ray diffraction. For almost all experiment conditions other than low oxygen content, the oxide phase has been observed to be formed of three oxide layers: the first layer is a thin 30–50 nm thin WO<sub>2</sub> growing on metallic tungsten. The second layer is a 5–10 μm thick WO<sub>2.72</sub> oxide layer and finally, the rest of the oxide scale is formed of the WO<sub>3</sub> phase. The first layers (WO<sub>2</sub> and WO<sub>2.72</sub>) have similar thicknesses across most testing conditions (temperature, humidity, and oxygen content) and doesn't exhibit cracks and voids, while the WO<sub>3</sub> layer contains cracks and voids and has been observed to spall off during specimen handling. Interesting, at low oxygen content (<0.01%), only the WO<sub>2</sub> or WO<sub>2.72</sub> phase are formed (no WO<sub>3</sub> phase) and in pure N<sub>2</sub> (99.998%), solely WO<sub>2</sub> is formed. Current work is focusing on the impact of oxygen impurities in vacuum or inert gas to assess the potential impact of tungsten oxidation on plasma operation. Early results shows that the WO<sub>2</sub> phase is formed and measurement of hydrogen-isotope permeation through the oxide is in progress to assess its potential impact on tritium permeation and retention in first wall

component and confirm recent atomistic modelling results.

Acknowledgements: This work has been funded by STEP, a major technology and infrastructure programme led by UK Industrial Fusion Solutions Ltd (UKIFS), which aims to deliver the UK's prototype fusion powerplant and a path to the commercial viability of fusion. To obtain further information on the data and models underlying this paper please contact PublicationsManager@ukaea.uk.

[1] M. Christensen, et al. , Nucl. Mater. and Energy 38 101611 (2024)

POA-47

### **Comparison of D Retention for Advanced Plasma Facing Materials by D plasma exposure or D ion implantation**

Yasuhisa Oya<sup>1</sup>, Yuzuka Hoshino<sup>1</sup>, Shingo Okumura<sup>1</sup>, Ayumu Hayakawa<sup>1</sup>, Kenshiro Miura<sup>1</sup>, Fei Sun<sup>2</sup>, Suguru Masuzaki<sup>3</sup>, Makoto Oyaizu<sup>4</sup>, Robert Kolasinski<sup>5</sup>, Chase Taylor<sup>6</sup>, Teppei Otsuka<sup>7</sup>, Yuji Hatano<sup>8</sup>, Masashi Shimada<sup>6</sup>, Hao Yu<sup>8</sup>, Ryuta Kasada<sup>8</sup>, Akira Hasegawa<sup>8</sup>

<sup>1</sup>Shizuoka University, Japan; <sup>2</sup>Hefei University of Technology, China; <sup>3</sup>National Institute for Fusion Science, Japan; <sup>4</sup>National Institutes for Quantum Science and Technology, Japan; <sup>5</sup>Sandia National Laboratories, United States; <sup>6</sup>Idaho National Laboratory, United States; <sup>7</sup>Kindai University, Japan; <sup>8</sup>Tohoku University, Japan.

For the development of fusion plasma facing materials, tungsten (W) is thought to be one of the best candidates from the viewpoint of tritium (T) retention. However, findings from the Japan-US collaboration program PHENIX and FRONTIER showed that the irradiation damage enhances deuterium (D) retention, especially in the stable trapping sites introduced by neutron irradiation, which would enhance the potential hazard for fusion safety.

To overcome irradiation enhanced T retention and improve thermal and mechanical properties of W, alloying with minor elements like molybdenum (Mo), tantalum (Ta) has been proposed to enhance the recrystallization temperature and material strength. In addition, potassium (K) doping is another option to mitigate irradiation defects by forming K bubbles. In this study, the hydrogen isotope retention in W-Mo, W-Ta and K-doped W was extensively investigated, with a focus on correlating retention behavior with irradiation-induced defects.

Samples (6 mm diameter and 0.5 mm thickness) of W-1%Ta, W-3%Ta, W-5%Ta, W-5.2%Mo and 40ppm K-doped W were supplied by Tohoku University and A. L. M. T. Corp. Some of these materials were damaged by energetic 6 MeV Fe<sup>2+</sup> irradiation by TIARA facility in QST up to the damage level of 1 dpa at room temperature. Thereafter, the formation of irradiation damage was evaluated by Positron Annihilation Spectroscopy (PAS) using a <sup>22</sup>Na positron source. High flux D plasma exposure was performed at QST Rokkasho site or Shizuoka University with the ion fluence up to 7 x 10<sup>25</sup> D m<sup>-2</sup>. Thermal desorption spectroscopy was performed to evaluate D trapping energy and D retention.

It was found that the average positron lifetime for Fe<sup>2+</sup>-damaged W alloys increased as a function of irradiation damage level. However, the defect concentration associated with long positron lifetimes was lower in W-Ta and W-Mo, indicating the reduction of large irradiation defects by alloying with Ta and Mo. For the evaluation of D retention behavior, W-5.2%Mo exhibited quite lower D retention compared with pure W, and D desorption at temperatures below 700 K was substantially reduced. Even after introducing irradiation damage, D retention in W-5.2%Mo remained low, indicating that small D trapping sites by Fe<sup>2+</sup> irradiation was either not formed or recovered by addition of Mo. More detailed discussion in my presentation.

### **Evidence of helium trapping in the lower divertor targets of WEST after the 2018-2020 campaigns based on TOF ERDA and TEM analysis**

Iva Bogdanović Radović<sup>1</sup>, Zdravko Siketić<sup>1</sup>, Mathilde Diez<sup>2</sup>, Elodie Bernard<sup>2</sup>, Emmanuelle Tsitrone<sup>2</sup>, Antti Hakola<sup>3</sup>, Tomi Vuoriheimo<sup>4</sup>, Celine Martin<sup>5</sup>, Martiane Cabie<sup>6</sup>, Thomas Neisius<sup>6</sup>

<sup>1</sup>Ruder Bošković Institute, Croatia; <sup>2</sup>CEA, IRFM, France; <sup>3</sup>VTT Technical Research Centre of Finland Ltd, Finland; <sup>4</sup>Department of Physics, University of Helsinki, Finland; <sup>5</sup>Aix-Marseille Univ, CNRS, PIIM, France; <sup>6</sup>Aix-Marseille Univ, CNRS, CP2M, France.

In this work, we summarize the results of the Time-of-Flight Elastic Recoil Detection Analysis (TOF ERDA) measurements of different tiles (W-coated graphite tiles with and without markers and W-ITER-like PFUs) from the lower divertor of the WEST tokamak after the 2018 (C3), 2019 (C4) and 2020 (C5) campaigns. At the end of the C4 campaign of WEST, a special helium phase (He) was performed after the deuterium operation (D) [1]. The retention of the plasma fuel (He, D) and the near-surface composition (first 150–200 nm) of the co-deposited layers were determined. TOF ERDA is one of the few techniques that can measure the concentration and depth distribution of He in the first 150–200 nm of the sample, which is more than the expected depth for He retention.

W-coated graphite tiles from the Q4A sector, exposed during C1–C4 campaigns, located on the maximum outer strike points (OSP) and inner strike points (ISP) areas were selected for the measurement. The measurements were performed along the poloidal direction, from the high-field side (HFS) to the low-field side (LFS), to fully capture the complex elemental composition of the tiles after plasma field exposure. A significant He content was found in the impact point region (up to ~ 6 at.% at ISP and ~ 10 at.% at OSP) where presence of the nanobubbles was confirmed by TEM. However, He was also detected on larger depths (50–150) nm which can be assigned to He implantation. Third smaller peak of He (2 at.%) was found in the thick deposited layers toward the HFS mainly consisting of W, C, O, B and D [2].

For the ITER-like PFUs, 12 monoblocs (MBs) were selected for TOF-ERDA measurements from the lower divertor Q3B sector (PFU#13, exposed during C3 and C4 campaigns). Measurements were performed in both poloidal and toroidal directions on the same PFU. The highest concentrations of He were found in the HFS thick deposit area (2 at.%) and at the OSP (5 at.%). The He profiles on the monoblocks and the marker tiles were compared and discussed to determine similarities and differences.

[1] E. Tsitrone et al 2022 Nucl. Fusion 62 076028

[2] M. Balden et al. 2021 Phys. Scr. 96 124020

### **Investigating Tritium Retention in tungsten coated plasma facing components from the divertor region of the Joint European Torus (JET)**

Anete Stine Teimane<sup>1</sup>, Elina Pajuste<sup>1</sup>, Liga Avotina<sup>1</sup>, Matiss Sondars<sup>1</sup>, Jari Likonen<sup>2</sup>, Anna Widdowson<sup>3</sup>

<sup>1</sup>Institute of Chemical Physics, University of Latvia, Latvia; <sup>2</sup>VTT Technical Research Centre of Finland Ltd, Finland; <sup>3</sup>UKAEA, Culham Campus, United Kingdom.

The Joint European Torus (JET) has played a vital role in advancing nuclear fusion research and paving the way for future fusion power plants. Tritium retention is a critical aspect of plasma-facing wall component performance in fusion reactors as well as reactor safety due to radiological risks it may pose. It is also of importance in the case of tungsten and its

composites, which are the leading first wall and divertor candidate materials due to its high melting point and mechanical strength [1]. This study aims to investigate surface characteristics, tritium retention behaviour and effect of “baking” – currently considered thermal in-situ detritiation treatment – on tungsten composite plasma-facing wall components from JET and contribute to the understanding of tritium trapping within the bulk of the material.

Three ITER-like wall (ILW) experimental campaigns with deuterium-deuterium (D-D) plasma discharges at various operating conditions, including different plasma densities, temperatures, and exposure times have been conducted. In these campaigns tungsten coated carbon fibre composite (CFC) divertor tiles were exposed to D-D plasma. The plasma-facing surfaces of selected samples were characterized using scanning electron microscopy (SEM) in combination with energy-dispersive x-ray spectroscopy (EDX) and tritium retention was assessed using thermal desorption spectroscopy (TDS) and full combustion. “Baking” cycle was simulated by keeping the sample at 350 °C for 100h, followed by TDS and full combustion.

Results show tritium retention of 4–76 10<sup>12</sup> T atoms per plasma facing surface cm<sup>2</sup>. A deposition layer ranging from 2 to 40 µm in thickness was found to be present for all samples analysed in this study. An increase in tritium retention was observed by the increase in the thickness of the deposition layer. The deposition layer also negatively impacts the efficacy of tritium removal by “baking” at 350 °C. TDS analysis revealed 2–3 distinct desorption peaks. An increase of the desorption temperatures of about 70 °C can be noticed after performing a “baking” cycle.

[1] J. Linke, J. Du, T. W. Loewenhoff. Challenges for plasma-facing components in nuclear fusion, *Matter Radiat. Extremes* 4, 056201 (2019)

POA-53

### **Novel dynamic deuterium transport measurements using Upgraded Pilot-PSI**

Cas Robben<sup>1</sup>, Jort Kesteren<sup>1</sup>, Remco Timmer<sup>1</sup>, Wim Arnoldbik<sup>2</sup>, Maria Cunha<sup>1</sup>, Beata Tyburska-Pueschel<sup>1</sup>, Thomas Morgan<sup>1</sup>

<sup>1</sup>Dutch Institute for Fundamental Energy Research, Netherlands; <sup>2</sup>Detect99, Netherlands.

Upgraded Pilot-PSI (UPP) is a new linear plasma device recently commissioned at DIFFER. The uniqueness of UPP lies in the combination of ITER-relevant plasma loading and operando Ion Beam Analysis (IBA). This enables the live observation of dynamic processes such as deuterium (D) retention and transport, outgassing, isotope exchange, and preferential sputtering, at an accelerated pace.

The integration of operando IBA into a linear plasma device introduces challenges such as curved trajectories, ion beam-plasma interactions, and detector noise. Curved trajectories, originating from the interaction with the plasma confining magnetic field, introduces an energy shift in measured IBA spectra. Collisions with plasma species result in a spectrum tail. Additionally, different ionisation states in the ion beam are created, causing the creation of two ion beam spots. These issues lead to incorrect or uncertain composition and depth profile measurements. In order to deal with these issues, large enough samples are used to fit both ion beam spots, and pressures below 2 Pa were employed. These mitigation techniques enabled operando IBA measurements for the first time, and will be discussed here.

A polycrystalline W sample (8x8x0.3 mm<sup>3</sup>) was polished, annealed and cleaned before exposed to D plasma with an ion flux of 71023 m<sup>-2</sup> for 1800 s while maintaining a sample temperature of 500 K. Measured NRA depth profile evolution during the plasma exposure reveals that initially D is transported into the bulk layer. As the plasma fluence increases, the concentration rises

uniformly as a function of depth, indicating the occupation of trapping sites with varying energies. The D retention is proportional to the plasma fluence raised to the power of 0.3, deviating from the historical value of 0.5 [1].

[1] O.V. Ogorodnikova, J. Nucl. Mater 313, 469–477 (2003)

POA-55

### **Evaluation of the boronization effect on fuel retention in WEST long pulses**

Laura Laguardia<sup>1</sup>, Gabriele Gervasini<sup>1</sup>, Eleonore Geulin<sup>2</sup>, Alberto Gallo<sup>2</sup>, Regis Bisson<sup>3</sup>, Yann Corre<sup>2</sup>, Julien Denis<sup>2</sup>, Corinne Desgranges<sup>2</sup>, Annika Ekedahl<sup>2</sup>, Nicolas Fedorczak<sup>2</sup>, Jonathan Gaspar<sup>4</sup>, Alex Thomas Grosjean<sup>5</sup>, Etienne Hodille<sup>2</sup>, Antti Hakola<sup>6</sup>, Thierry Loarer<sup>2</sup>, Karl Krieger<sup>7</sup>, Pierre Manas<sup>2</sup>, Philippe Moreau<sup>2</sup>, Emmanuelle Tsitrone<sup>2</sup>, Stefane Vartarian<sup>2</sup>, Anna Widdowson<sup>8</sup>, Tom Wauters<sup>9</sup>

<sup>1</sup>Istituto per la Scienza e Tecnologia dei Plasmi, CNR, Milano, Italy; <sup>2</sup>CEA, IRFM, France; <sup>3</sup>CNRS, PIIM, France; <sup>4</sup>CNRS, IUSTI, France; <sup>5</sup>University of Tennessee Knoxville, United States; <sup>6</sup>VTI Technical Research Centre of Finland Ltd, Finland; <sup>7</sup>Max-Planck-Institut für Plasmaphysik, Germany; <sup>8</sup>UKAEA, Culham Campus, Abingdon, United Kingdom; <sup>9</sup>ITER Organization, France.

ITER will operate in a full metallic configuration (full W) and boronization mitigates risks associated with achieving  $Q = 10$ . With its fully –and actively– cooled W divertor, and boronization as one of the conditioning techniques, WEST is able to execute relevant experiments in view of ITER exploitation. The objective of this contribution is to use Residual Gas Analysis (RGA) to evaluate the boronization effect on the fuel retention during discharges, in steady state conditions, over an entire day of plasma operation.

WEST is equipped with neutral gas analysis diagnostic systems located at the midplane and at lower divertor pumping systems. Both systems are equipped with RGAs whilst an Optical Gas Analyzer (OGA) is also installed in the divertor system to determine the gas composition together with a gauge to measure total pressure. A cross correlation between RGA and OGA, provided by transforming the OGA H and D atomic ratios in hydrogen molecular ratios (H<sub>2</sub>, D<sub>2</sub>, HD), will be here provided. The effect of boronization on fuel retention is assessed by comparing analysis of neutral gas pumped during pre- and post- boronization sessions. Pre- and postboronization pulses were performed at the same plasma parameters, two weeks after a previous boronization and just before another boronization.

During the C9 experimental campaign, a special session was dedicated to calibrations during which hydrogen (H<sub>2</sub>) and deuterium (D<sub>2</sub>) were injected into the WEST chamber through a series of short pulses ( $\Delta t = 120$  ms) with increasing flow rates, making it possible, through proper data analysis, to estimate the sensitivities of the H<sub>2</sub> and D<sub>2</sub> for the RGA used in WEST. The RGA results of the data recorded during the whole day of plasma operations, cumulative 1000 s, show the exhaust's hydrogenic mixture, collected at the lower divertor, composed of D<sub>2</sub>, HD and H<sub>2</sub>. In the pre-boronization outgassing mixture, D<sub>2</sub> is the main species. During the first five post-boronization pulses, D<sub>2</sub> remains the dominant species in the outgassing mixture. After three subsequent long-pulses (72 s each), the species with the highest concentration becomes HD, followed by D<sub>2</sub> and H<sub>2</sub>. This behaviour is a consequence of boronization, particularly in this long pulse series, the temperature of the antenna protector limiter (LPA) and the inner bumper increases, leading to an additional H outgassing (since they represent a huge H reservoir), which exchanges isotopically with D on the fresh boron layer, causing the growth of the HD species.

POA-56

### **Hydrogen Retention in Plasma-Facing Components: Parameter Study**

Mikhail Lavrentiev<sup>1</sup>, Dinusha Jayasundara<sup>1</sup>, Tez Orr<sup>1</sup>, Celyn Sammons<sup>2</sup>

<sup>1</sup>United Kingdom Atomic Energy Authority (UKAEA), United Kingdom; <sup>2</sup>UKAEA and University of Manchester, United Kingdom.

We consider transient and steady state hydrogen content in several plasma-facing components (monoblock, first wall, limiter etc.) as a function of parameters that are either plasma-defined (incoming flux and plasma-facing temperature), or determined by construction (size, coolant-side temperature etc.). Penetration depth of incoming hydrogen ions is determined using molecular dynamics simulations [1]. Pre-existing and irradiation-induced traps are taken into account in the simulation. Using FESTIM software [2], we solve time-dependent hydrogen transport equations and determine time to reach steady state and the amount of mobile and trapped hydrogen. In order to estimate accuracy of the results obtained in commonly used one-dimensional simulations, they are compared with the results of two- and three-dimensional simulations. We identify the parameters that are most important for hydrogen retention and give estimates of the total retention in a fusion power plant.

[1] S. Towell, M. Lavrentiev, S. Lozano-Perez, IEEE Transactions on Plasma Science 52, 3662 (2024)

[2] R. Delaporte-Mathurin, J. Dark, G. Ferrero, et al., Int. J. Hydrogen Energy 63, 786 (2024)

POA-59

### **A calibration method for water signals during thermal desorption spectroscopy of deuterium from tungsten**

Thomas Schwarz-Selinger, Maximilian Brucker

Max Planck Institut for Plasma Physics, Germany.

Thermal desorption spectroscopy (TDS) is a widely used technique to characterise the interaction of hydrogen isotopes with fusion materials, not only in terms of total retention, but also to resolve de-trapping kinetics. However, very often only the release of the hydrogen molecules H<sub>2</sub>, HD and D<sub>2</sub> is considered. Heavier molecules, such as water, are typically ignored because of the difficulty in quantifying them.

In this contribution a methodology will be outlined that allows to calibrate water signals and hence absolutely quantify desorption of deuterium from tungsten in the form of heavy water. The methodology uses 5 to 100 nm thin tungsten oxide films electro-chemically grown on tungsten. The thickness of the resulting amorphous oxide is very well defined as it is determined only by the voltage applied in the anodic oxidation process and does not depend on the grain orientation (as it would be e.g. the case for thermal oxidation). Prior to oxidation, the recrystallized tungsten substrate is irradiated with 20 MeV tungsten to create defects within the first 2.3 μm from the surface. These defects are then decorated with deuterium by exposing the samples to low-energy deuterium (< 5 eV/D) from a low-temperature plasma. The absolute areal densities of oxygen and deuterium and their depth profiles are quantified with Nuclear Reaction Analysis (NRA) and Rutherford Backscattering Spectrometry using <sup>3</sup>He ions. During a slow TDS ramp of 3 K/min from room temperature up to 1000 K, desorption of 15 signals with mass to charge ratios between 1 and 44 amu/q are followed as a function of time. Above the initial plasma exposure temperature of 370 K the deuterium starts to desorb from the traps. At 900 K all D is released from the sample as confirmed by NRA.



The idea of using this pre-characterized sandwich structure of tungsten oxide on top of a known amount of trapped deuterium is the following: During TDS the deuterium is released from its traps and must migrate through the oxide where it converts partially to HDO and D<sub>2</sub>O or desorbs as HD or D<sub>2</sub>. Release of deuterium is hence expected only on mass channels 3, 4, 19 and 20 as HD, D<sub>2</sub>, HDO and D<sub>2</sub>O, respectively. The calibration procedure for HD and D<sub>2</sub> follows the description in [1]. The calibration of water is then reduced to closing the D balance when comparing the absolute amount of D released in total (from NRA) and the absolute amount of D released in form of HD and D<sub>2</sub> (from TDS).

With this calibration method it has been shown that for tungsten water desorption is dominant for many fundamental studies where deuterium retention values are in the range of 10<sup>20</sup> D/m<sup>2</sup> and its release can significantly alter spectrum interpretation [2]. As sample preparation proved to be highly reproducible, the method outlined can be applied to any TDS setup for in situ calibration of water signals.

[1] T. Schwarz-Selinger et. al, Nucl. Mater. Energy 17 228–234 (2018)

[2] K. Kremer et al., Nucl. Mater. Energy 30, 101137 (2022)

POA-60

### **Progress in laser-based surface analysis techniques for fusion applications – from laboratory experiments to reactor-class diagnostics**

Sebastijan Brezinsek

Forschungszentrum Jülich GmbH, Germany.

Laser-based surface analysis techniques have been developed and qualified in the last two decades for different nuclear fusion applications addressing plasma-wall interaction processes like erosion, deposition, fuel recycling, fuel retention, and fuel removal from plasma facing materials (PFM). These nuclear fusion applications cover laboratory analysis systems for ex-situ PFM studies exposed in tokamaks and stellarators, in-operando systems installed in linear-plasma devices and tokamaks permitting oxygen-free analysis of surfaces, and in situ analysis stations in controlled areas capable to deal with tritium as well as systems embedded on a remote handling arm addressing spatially resolved hydrogen isotope distribution and material composition without tile extraction.

The choice of the laser pulse duration (from ms to fs), laser wavelength (from UV to IR) and power density determines the dominant laser-material interaction process, namely, desorption or ablation. Desorption-based methods (LID) with typical pulse durations in the ms-range provide accurate access to volatile species like hydrogen isotopes and helium in the near surface. Detection is done by either gas composition analysis (LID-QMS) in vacuum systems or by spectroscopy (LIDS) in the presence of a background plasma. The challenge is the exact information about the heat affection zone and, in connection with hydrogen isotopes, diffusion. Ablation-based methods (LIA) with typical pulse durations in the ns-ps-fs-range provide information about the material composition including volatile species with depth resolution in the order of 100 nm depending on the investigated material. Detection is done by either gas composition analysis (LIA-QMS) in vacuum systems or by spectroscopy (LIBS). Lasers with ps-pulse duration have been identified as best compromise in sensitivity, ablation rate and heat diffusion and are the most promising candidate for future development. Quantification of the spectroscopic signals remains one of the challenges in LIBS in particular with tungsten. The research aims ultimately in (a) the development of a minimal invasive, in-operando

hydrogen isotope diagnostic for a reactor-class device like ITER to support the tritium control and safety case, and (b) the provision of a depth-resolved, high precision surface analysis station in a controlled area for physics studies on e.g. irradiated tungsten, the preferred reactor PFM, after plasma exposition. The progress in the research at the Forschungszentrum Jülich from initial laboratory experiments, pioneering experiments in TEXTOR, state-of-the-art experiments in JET and FREDIS, towards tritium monitor diagnostic designs for ITER, and an upgraded nuclear analysis station in the FZJ hot material lab will be presented. The scientific and technical readiness level for laser-based diagnostics regarding the needs for (a) and (b) will be critically assessed and paths for further optimisation presented.

Acknowledgements: The work is supported by the BMBF grant “SyrVBreTT”. This work has been partially carried out within the framework of the EUROfusion Consortium.

POA-61

### **Analysis of hydrogen transport and trapping in SS316L**

Floriane Montupet-Leblond<sup>1</sup>, Etienne Hodille<sup>1</sup>, Mickaël Payet<sup>1</sup>, Elodie Bernard<sup>1</sup>, Dominique Vrel<sup>2</sup>, Frédéric Miserque<sup>3</sup>, Christian Grisolia<sup>1</sup>

<sup>1</sup>CEA, IRFM, France; <sup>2</sup>LSPM, CNRS, France; <sup>3</sup>CEA, SCCME, France.

To design a tritium cycle with the right performances for a fusion reactor, the investigation of transport and trapping parameters of hydrogen in materials must be performed on all the materials that are involved in the tritium cycle of the plant. Stainless steel 316L (SS316L) is the nuance of steel that will be used in the tritium plant and for the fueling systems of ITER: a detailed understanding of its permeation and retention properties is therefore required.

To investigate these properties, Gas-Driven Permeation (GDP) experiments were performed with hydrogen on SS316L samples, yielding a diffusivity that hints at purely interstitial processes and a diffusion coefficient that is in line with literature results [1,2]. To confirm the purely interstitial nature of transport in this material, Thermal Desorption Spectrometry (TDS) experiments were performed on deuterium-loaded samples of SS316L. The resulting TDS spectra displayed a complex shape that seemed to bear the influence of several phenomena on top of bulk diffusion and trapping, in particular surface properties. Several additional experiments were performed to characterize the surface composition (X-Ray Photoelectron Spectroscopy, X-Ray Diffraction), to separate bulk diffusion and trapping from surface effects (TDS experiments performed on palladium-coated samples), and to assess the influence of the initial content of H<sub>2</sub> that stems from the industrial manufacturing process of SS316L.

Based on these experimental results, a TDS spectrum without any surface influence was obtained. Using the reaction-diffusion code MHIMS, which allows us to simulate 1D transport and trapping of hydrogen isotopes in materials, the validity of the interstitial diffusion hypothesis is discussed and a model for the transport and trapping of hydrogen in SS316L is proposed.

[1] SK Lee, S-H Yun, Han Gyu Joo, and Seung Jeong Noh. Deuterium transport and isotope effects in type 316L stainless steel at high temperatures for nuclear fusion and nuclear hydrogen technology applications. *Current Applied Physics*, 14(10):1385–1388, 2014.

[2] Tetsuo Tanabe, Yuji Yamanishi, Kenji Sawada, and Shosuke Imoto. Hydrogen transport in stainless steels. *Journal of Nuclear Materials*, 123(1–3):1568–1572, 1984.

POA-62

### **The Interplay of Ion Impact Angle and Energy on Mixed-Material Surface Concentrations in a DIII-D Tungsten Divertor**

Alec Cacheris<sup>1</sup>, Tyler Abrams<sup>2</sup>, Davis Easley<sup>3</sup>, Daisuke Shiraki<sup>3</sup>, Robert Wilcox<sup>3</sup>, Jeffrey Herfindal<sup>3</sup>, David Christian Donovan<sup>1</sup>

<sup>1</sup>University of Tennessee at Knoxville, United States; <sup>2</sup>General Atomics, United States; <sup>3</sup>Oak Ridge National Laboratory, United States.

During certain DIII-D tokamak plasma discharges, a shift of the average ion impact angle ( $\vartheta$ ) by several of degrees towards the divertor surface normal is predicted to increase the fractional carbon (C) coverage ( $\sigma_C$ ) of the tungsten (W) divertor by tens of percent. Preliminary RustBCA-GITR modeling results predict that recycling  $\vartheta$  may have varied by up to  $3^\circ$  during edge localized modes (ELMs) depending on the type of ion and plasma shot parameters [1]. We predict higher  $\sigma_C$  for plasma shots with higher C plasma impurity concentrations (%) and lower electron temperature ( $T_e$ ) at the divertor. At the outer strike point position during ELMs, the average divertor C % varied from 2.2 to 4% and average  $T_e$  varied from 29 to 57 eV between plasma shots [2]. In this experiment, we injected varying rates of D2 at the outboard midplane of DIII-D and assessed the impact on C % and W erosion in the Small Angle Slot V-Shaped W (SAS-VW) divertor. D $\alpha$  (656.19 nm), WI (400.9 nm), and CIII (465 nm) filterscopes and Langmuir probes were used to determine deuterium (D) and C fluxes on the divertor, along with gross W erosion. The Free Stream Recycling Model (FSRM) vastly overpredicts W erosion during ELMs when using the experiment plasma shot parameters and further overpredicts W erosion during ELMs for plasma shots with higher C %. To correct the FSRM predictions, we incorporate a near-surface mixed-material C/W layer by multiplying the FSRM predictions by the estimated fractional W divertor surface concentration [3]. C ion-W material interactions computed by binary collision code RustBCA obtain C/W model sputtering and reflection coefficients at various C and D ion impact energies ( $E_i$ ) and  $\vartheta$ . Variation in  $E_i$  and  $\vartheta$  are shown to have a large effect on the divertor C deposition and gross W erosion predictions. By coupling sputtered and reflected C and D distributions to GITR impurity transport codes, we provide novel estimations of the recycling C and D impact angle and consequent C coverage on a smooth W divertor surface. Ex-situ and computational surface roughness analysis of DIII-D SAS-VW tiles are currently underway to quantify the impact of surface roughness on  $\vartheta$  [4].

POA-63

### **Dust-Plasma Interaction Studies in the STOR-M Tokamak**

Nathan Nelson, LENAIC Cou  del, Chijin Xiao

University of Saskatchewan, Canada.

Interactions between the STOR-M plasma and injected tungsten (W) microparticles (dust) have been investigated [1]. STOR-M is a small tokamak with core plasma parameters similar to those in the edge of modern tokamaks, such as WEST and ASDEX-Upgrade. A pre-characterized dust plume is injected into STOR-M prior to the initiation of tokamak Ohmic Heating (OH) discharges and the delay time between dust injection and OH discharge controls the amount of in-vessel dust to be entrained in the tokamak plasma. Dust particles are heated in the plasma and become incandescent, allowing for their observation with two fast cameras.

It was found that dust injection may shorten, degrade, and even disrupt STOR-M discharges. By tuning the dust injection parameters, the effects of dust on plasma and plasma on dust

dynamics within plasma were studied [2]. We find that the Spitzer temperature and plasma duration decrease with the amount of in-vessel dust introduced. Neutral tungsten spectral line emission from the location near the dust dispenser scales with the amount of in-vessel dust at the OH discharge time. We also find that dust trajectories in STOR-M vary significantly with plasma parameters. When the center-of-mass of the dust plume is near the midplane, more ballistic trajectories are observed. However, when the center-of-mass of the dust plume is sufficiently above or below the midplane, trajectories exhibit significant toroidal acceleration in the direction of plasma flow measured with ion Doppler spectroscopy.

Post-mortem dust samples deposited on the bottom of the STOR-M vacuum vessel were collected and a bi-modal dust size distribution was determined. The first mode had the same mean size as the injected dust, while the second had 1/3 the mean size and a distribution peak that was larger for samples taken further downstream of the dust dispenser. These results indicate enhanced toroidal transport of small dust particles and/or the effects of dust ablation.

Tracking of dust particles using fast cameras and simultaneous measurement of the plasma flow velocity of the STOR-M plasma using Doppler Spectroscopy (C-VI impurity ions) revealed that an increased amount of in-vessel dust reduces the acceleration of plasma flow within the core. The statistical mean net force, measured from the dust trajectories, acting on dust particles was analyzed and compared the Barnes and Hutchinson/Khrapak models. It is found that the mean force is systematically larger than predicted by either model, though within an order of magnitude.

[1] Nelson, N., et al. Radiation Effects and Defects 177:1-2 (2022)

[2] Nelson, N., Davies, R., et al. Radiation Effects and Defects 178:11-12 (2023)

POA-64

### **Analysis and Modelling of the Relationship Between WI, WII, and WIII Emission Signals and Tungsten Net Erosion in the DIII-D Divertor**

Luca Cappelli<sup>1</sup>, Jerome Guterl<sup>2</sup>, Tyler Abrams<sup>2</sup>, Ulises Losada<sup>3</sup>, Žana Popović<sup>2</sup>, Zachary Bergstrom<sup>2</sup>

<sup>1</sup>ORAU, United States; <sup>2</sup>General Atomics, United States; <sup>3</sup>Auburn University, United States.

A new Local Particle Transport Monte Carlo code (LPTMC) based on previous works [1] has been developed to efficiently perform sensitivity studies on the key physics parameters affecting tungsten gross and net erosion in the DIII-D divertor, as well as future devices. The LPTMC simulations focus on W erosion caused by low-charged impurities (LCI), using doubly ionized carbon (C2+) as a proxy for DIII-D conditions, and high-charged impurities (HCI), with Cr10+ as a proxy for the dominant eroding species in Future Power Plants (FPP). A parameter scan was performed over electron temperatures ranging from 5 to 60 eV and densities between  $n_e = 10^{18}$  and  $10^{20} \text{ m}^{-3}$ . Results showed a significant finding for HCI-induced W sputtering: as zero order approximation there was a linear negative correlation between the log10 of the photon flux from neutral tungsten (WI emission) and the fraction of non-promptly re-deposited W ( $1 - f_{\text{prompt}}$ ). No such correlation was observed for LCI. This distinction arises because for HCI cases the sputtering yield scales with the square root of the electron temperature, resulting in a linear dependence of the eroded gross flux on electron temperature. In contrast, for LCI, the sputtering yield exhibits a more rapid and nonlinear variation with the electron temperature. This leads to a complex and non-unique relationship between net erosion and gross flux, making it more challenging to establish a clear correlation between WI emission and net

erosion. In both cases, the relationship could be better constrained and refined using data from other measurable W emission lines from higher ionization states such as WII and WIII. Understanding W net sources in tokamaks is crucial because W has a low acceptable concentration in the plasma core. Due to its high cooling efficiency W poses the risk of plasma destabilization and collapse [2]. Net sources, representing the actual amount of W entering the plasma, are smaller than gross fluxes due to prompt re-deposition. However, uncertainties in factors like far-scrape-off layer plasma and impurity transport, charge exchange (CX) bombardment, impurity concentrations, sheath physics, and atomic data introduce significant challenges in accurately assessing net W sources. Having a relationship to infer W net sources through spectroscopy would enable real-time monitoring of W sources, improve our understanding of impurity dynamics, and aid in designing future reactors.

Acknowledgements: Work supported by US DOE under DE-FC02-04ER54698 and DE-SC0015877

[1] L Cappelli, N Fedorczak, JP Gunn, et al., PPCF, 65 095001 (2023)

[2] V. Ostuni, J. Morales, J.-F. Artaud, et al., Nucl. Fusion, 62, 106034 (2022)

POA-65

### **Ex-situ LIBS study for the determination of boron content in WEST divertor tiles after the 2019 campaign**

Indrek Jõgi<sup>1</sup>, Peeter Paris<sup>1</sup>, Marta Malin Muru<sup>1</sup>, Elodie Bernard<sup>2</sup>, Mathilde Diez<sup>2</sup>, Emmanuelle Tsitrone<sup>2</sup>, Jari Likonon<sup>3</sup>, Antti Hakola<sup>3</sup>, Eduard Grigore<sup>4</sup>

<sup>1</sup>University of Tartu, Institute of Physics, Estonia; <sup>2</sup>CEA, IRFM, France; <sup>3</sup>VTT Technical Research Centre of Finland Ltd., Finland; <sup>4</sup>Acasa Institutul National pentru Fizica Laserilor, Plasmei si Radiatiei, Romania.

Laser Induced Breakdown Spectroscopy (LIBS) is a method developed for the remote composition analysis of layers deposited on the first walls and divertor components of fusion reactors [1,2]. The technique applies laser pulses to ablate a small amount of material, which forms a plasma plume and emits a spectrum characterizing the elements originating from the investigated material. The use of consequent laser pulses at the same spot allows to obtain elemental depth profiles with the resolution depending on the laser ablation rate. We have previously demonstrated the applicability of LIBS for the fuel retention analysis in the WEST divertor marker tiles removed after the 2018 (C3) campaign [3]. The present study focuses on the analysis and interpretation of the boron (B) content induced by boronisations in the surface layer of WEST divertor marker tiles removed after the 2019 experimental campaign (C4) and compare the evolution in respect to C3 campaign [4]. The six samples studied here were subjected to 16 boronisations and originated from different positions along the divertor s-coordinate including erosion and deposition regions.

The LIBS setup consisted of a Nd:YAG laser ( 8 ns pulse at 532 nm) and a Czerny-Turner type spectrometer coupled with an iCCD camera. The spectra were collected in the spectral window of 244 to 269 nm, which contained the elemental emission lines of W, Mo, C and B. The depth profiles showing the LIBS line intensities as the function of the applied laser pulse number at the same spot were generally consistent with the GDOES and SIMS depth profiles obtained from nearby tile positions [5]. The depth profiles corresponded to the expected deposition and erosion regions. The depth of B containing layer varied from tens of nanometers to several micrometers. The ablation rates of the deposit layers were 50-100 nm per laser shot,

comparable to the rates of bulk W and Mo layers. The study shows that the LIBS method is sufficiently sensitive and has adequate depth resolution to study the B composition in the deposit layers.

- [1] H.J. Meiden, S. Almaguer, J. Butikova et al., Nucl. Fusion 61, 125001 (2021)
- [2] D Zhao, S. Brezinsek, R. Yi et al., Phys. Scr 97, 024005 (2022)
- [3] I. Jögi, P. Paris, E. Bernard et al., J. Nucl. Eng 4, 96 (2023)
- [4] M. Diez, M. Balden, S. Brezinsek et al., Nucl. Mater. Energy 34, 101399 (2023)
- [5] A. Hakola et al., this conference

POA-66

### **Modeling of erosion/deposition patterns observed during WEST high-fluence campaign**

Alexis Huart<sup>1</sup>, Guido Ciraolo<sup>1</sup>, Yann Corre<sup>1</sup>, Nicolas Rivals<sup>1</sup>, Wojciech Gromelski<sup>2</sup>, Jamie Gunn<sup>1</sup>, Nicolas Fedorczak<sup>1</sup>, Mathilde Diez<sup>1</sup>, Jonathan Gerardin<sup>1</sup>, Alex Thomas Grosjean<sup>3</sup>, Christophe Guillemaut<sup>1</sup>, Juri Romazanov<sup>4</sup>

<sup>1</sup>CEA, IRFM, France; <sup>2</sup>IFPILM, Poland; <sup>3</sup>University of Tennessee Knoxville, United States; <sup>4</sup>Forschungszentrum Jülich GmbH, Germany.

A high fluence campaign with attached plasma conditions was conducted in WEST (spring 2023) to expose the ITER-grade actively-cooled divertor to ITER-relevant deuterium fluences. The same plasma discharge of 60s long was repeated hundreds of times, accumulating about 10,000 seconds of plasma with a maximum of  $6 \times 10^{26}$  part.m<sup>2</sup> of fluence measured by flush-mounted Langmuir probes on divertor [1]. During this campaign, deposited layers composed of tungsten with light impurities formed continuously, especially on the high-field side of the inner divertor leg. Erosion areas were also identified at both strike points where the heat and particle fluxes are high[1].

The goal of this work is to understand the patterns present on the divertor after the campaign and the influence of light impurities on the erosion and transport of tungsten, by modeling. Impurities of the plasma are tracked by visible spectroscopy, showing high content of nitrogen and boron all along the campaign, possibly due to the impact of plasma on the BN tiles of the inner bumper during current ramp-up. Residual oxygen and carbon are also present. A higher concentration of boron and nitrogen is observed on the inner side compared to the outer side. An analysis using visible spectroscopy (for WI 4009A radiance) and flush-mounted Langmuir probe measurements (to obtain ne and Te to derive local S/XB coefficient) estimates a tungsten gross erosion flux up to  $1 \times 10^{19}$  part.m<sup>2</sup>.s<sup>-1</sup>, leading to around 0.5  $\mu$ m of net erosion near the outer strike point for 10000 s of plasma, assuming 75% prompt redeposition rate[1], while post-mortem analysis suggests around 10  $\mu$ m of net erosion, in the same region.

To model those experimental observations, the first step is to simulate a plasma background with SOLEDGE3X-EIRENE, constrained by experimental measurements. Langmuir probe divertor profiles are matched by adjusting upstream density, power entering the SOL and transport coefficients. Plasma backgrounds are simulated without and with impurities (N, O) and used in ERO2.0 to simulate tungsten transport. ERO2.0 gives eroded and deposited tungsten flux on the wall and densities of tungsten inside the plasma. First result with 2% of oxygen concentration leads to 6  $\mu$ m of erosion at outer strike-points which is consistent with post mortem analysis in erosion dominated areas, but deposition dominated areas still cannot be explained.

[1] N. Fedorczak et al., Nuclear Materials and Energy, Vol. 41 (2024)

POA-67

### **Study on the influence of ELM and ELM-control methods on WD sputtering in EAST**

Qing Zhang, Fang Ding

Institute of Plasma Physics, HFIPS, Chinese Academy of Sciences, China.

Tungsten (W) tends to be selected as the preferred plasma-facing materials for future fusion reactors and the lifetime and service performance of W materials are limited by erosion processes. Physical sputtering caused by particle bombardment is believed to be the main erosion mechanism of W materials in fusion devices, however, a new W sputtering mechanism has been proposed in recent years, and its product is deuterated tungsten (WD) molecules [1,2]. Simultaneously studying the sputtering characteristics of W atoms and WD molecules is conducive to a more comprehensive understanding of the erosion of W materials.

Edge localized mode (ELM) is a type of instability in a tokamak. It appears in high constraint mode (H Mode) and large number of particles and heat are deposited on the first wall during ELM generation. The high particle and energy flux impinging to the divertor targets would not only bring large power loads, but also induce strong W sputtering, shortening the PFC lifetime. Previous studies have shown that Intra-ELM has a strong enhancement effect on the sputtering of tungsten atoms [3]. However, in this study, unlike tungsten atoms, for WD molecules, the radiation intensity of WD molecules in EAST divertor in Intra-ELM and Inter-ELM is not much different. According to previous studies, this may be related to the high target temperature caused by ELM. After a small amount of short pulses of neon gas are injected, the target temperature has dropped, significant ELM sputtering characteristics appeared in WD sputtering. The sputtering of tungsten for intra-ELM mainly comes from the sputtering of W atoms, and there is no obvious enhancement of WD radiation for intra-ELM. Low surface deuterium retention due to excessively high divertor temperature may be the reason. ELM control measures such as neon seeding will increase the sputtering of WD molecules by reducing the divertor temperature. The deeper reason is that the low divertor temperature has a high deuterium retention in the W surface layer.

[1] S. Brezinsek, Nuclear Materials and Energy 18 (2019) 50-55

[2] Q. Zhang, Nuclear Materials and Energy 33 (2022) 101265

[3] X. H. Chen, Nuclear Fusion 61 (2021) 046046

POA-68

### **Mixing and enrichment effects on low- and high-Z impurities from W carbides as PFM**

Tatyana Sizyuk<sup>1</sup>, Tyler Abrams<sup>2</sup>, Gregory Sinclair<sup>2</sup>, Ahmed Hassanein<sup>3</sup>

<sup>1</sup>Argonne National Laboratory, Lemont, United States; <sup>2</sup>General Atomics, San Diego, United States; <sup>3</sup>Purdue University, West Lafayette, United States.

Various W-based compounds are being considered as alternative plasma-facing materials (PFMs) for future fusion devices. Tungsten carbides are examples of such materials having microstructure under irradiation to be more stable than in pure W. Some of these materials have better mechanical properties and acceptable thermal conductivity; with overall performance dependent on C concentration. A layer of tungsten carbide can be used as an inset around the strike point to withstand high steady-state fluxes. This can help reduce plasma contamination and related issues compared to the high-Z material erosion during high energy transient

events. We studied plasma interactions with the surfaces of WC (and W<sub>2</sub>C) compounds and related effects of material erosion and changing properties/composition, potential plasma contamination, and D/T retention. Our preliminary analysis shows that while preferential C erosion and high W redeposition near the strike point prevents or significantly reduces C chemical erosion and T redistribution by co-deposition, relatively high C concentration outside the area of high particle fluxes can lead to enhanced T accumulation. We show that the surface enrichment in W near the strike point enhances D diffusion to the surface and desorption. These can significantly reduce D/T permeation to the bulk as compared to pure C and pristine WC surfaces. On the other hand, the significantly lower ion fluxes far from the strike point reduce C effect on D/T accumulation and redistribution.

These simulations predicted performance of evolved material at various irradiation conditions including DIII-D tokamak discharges and extrapolated results for fluxes in ITER-like devices. The impact of steady-state and ELMs plasma on the WC layer on the divertor surface were simulated to predict both W and C redistribution, surface erosion or buildup, and locations of the highest T accumulation due to co-deposition.

The upgraded ITMC-DYN package for atomistic modeling of under and above surface processes was used for these studies. The package integrates multispecies collisional interactions on the surface and within the sheath, particle motion due to Lorentz force, and diffusion with trapping and traps evolution effects. We implemented and compared various methods for the calculation of potential variation within the sheath. We implemented detailed simulations of near surface particle collisional interactions with the main plasma and with impurities accumulated. A concentration dependent diffusivity model of D in carbides was implemented and compared with experiments.

Work supported by the U.S. Department of Energy, Office of Science/Office of Fusion Energy Sciences, under Award Number(s) DE-AC02-06CH11357 and DE-FC02-04ER54698

POA-69

### **Thick deposited tungsten layer growth and characterization using Magnum-PSI**

Thomas Morgan<sup>1</sup>, Luc Bouwmeester<sup>2</sup>, Marcin Rasinski<sup>3</sup>, Erwin Zoethout<sup>1</sup>, Jort Kesteren<sup>1</sup>, Cas Robben<sup>1</sup>, Beata Tyburska-Pueschel<sup>1</sup>, Vairavel Mathayan<sup>1</sup>, Lambert van Breemen<sup>1</sup>, David Dellasega<sup>4</sup>, Matteo Passoni<sup>4</sup>, Luigi Bana<sup>4</sup>, Nora Lecis<sup>4</sup>

<sup>1</sup>Dutch Institute for Fundamental Energy Research, Netherlands; <sup>2</sup>Eindhoven University of Technology, Netherlands;

<sup>3</sup>Forschungszentrum Jülich GmbH, Germany; <sup>4</sup>Politecnico di Milano, Italy.

The recent decision by ITER to move from a Be to a W first wall has significant implications for material transport and deposition, and can be expected to lead to increased W layer growth rate in deposition regions. Recent studies in WEST and at Magnum-PSI have shown deposition of thick W layers from erosion and re-deposition processes can be formed which are poorly adhered to the original surface. In the case of WEST these have led to significant impact on the plasma performance, including stimulating plasma disruptions. Therefore it is important to better understand the formation and adhesion of these layers in a controlled fashion and under conditions close to those expected in ITER.

In this work a novel sputtering set-up was implemented in the Magnum-PSI linear plasma device. This enabled a W bar to be inserted into the plasma edge and biased to cause sputtering of the W in an Ar plasma ( $B=0.8$  T,  $\bar{n}=8 \times 10^{22}$  m<sup>-3</sup> s<sup>-1</sup>). This sputtered W was carried downstream by the plasma and deposited on an array of mixed W and Mo witness plates (WPs)



at <300 °C. The deposition rate and the initial surface roughness were varied to investigate their influence. Deposited layer thickness was later determined using weight gain of the WPs, FIB-SEM cross sections and RBS. This showed a strongly inhomogeneous deposition profile with layer thicknesses varying from 100's nm up to >10  $\mu$ m over a lateral region of around 3 cm diameter. IR camera images and SEM analysis shows flaking and delamination occurring from the highest deposition rate regions during the deposition process. These initiate at the layer-substrate interface, with the flaking region growing over time, indicating a layer thickness threshold for this process.

The layers are highly dense with small and columnar grain structure, similar to layer growth via magnetron sputtering. EDX analysis of the cross sections show that the layers are W with <10% Mo impurity. SEM images show that the partially delaminated layers show positive curvature, indicating the presence of residual tensile stress likely responsible for the delamination and flaking. Films deposited on rough samples were better adhered than polished ones. Further planned investigations include XRD, micro-indentation and scratch testing. The results help confirm that thick W layer growth in ITER may occur if W is entrained in the SOL and deposited, and could lead to poorly adhered layers which would present a risk of significant dust formation.

POA-70

### **Theoretical modelling of a non-hydrogenic plasma-wall interaction experiment in the GyM linear device**

Carlo Tuccari<sup>1</sup>, Gabriele Alberti<sup>1</sup>, Fabio Mombelli<sup>1</sup>, Matteo Passoni<sup>1</sup>, Andrea Uccello<sup>2</sup>, Anna Cremona<sup>2</sup>, Matteo Pedroni<sup>2</sup>, Juri Romazanov<sup>3</sup>

<sup>1</sup>Dipartimento di Energia, Politecnico di Milano, Milan, Italy; <sup>2</sup>Istituto per la Scienza e Tecnologia dei Plasmi, CNR, Milano, Italy; <sup>3</sup>Forschungszentrum Jülich GmbH, Germany.

Plasma-wall interaction (PWI) is a key topic to be addressed for the safe operation of nuclear fusion reactors. Non-hydrogenic species, like helium (He) produced by D-T fusion reactions or argon (Ar) injected in tokamaks to achieve detachment, need special attention. Their greater mass may enhance the erosion of plasma facing components (PFCs), moreover they are able to induce peculiar surface modifications on the material. Tungsten (W) is the primary candidate as divertor and first wall material in future devices, thanks to its low sputtering yields and high melting temperature. Linear plasma devices (LPDs) are crucial complementary testbeds to investigate PWI under ITER-relevant parameters not achievable in current tokamaks, such as particle fluxes and fluences. Furthermore, non-hydrogenic species can be useful to speed up the erosion process in LPDs experiments. In this framework, the modelling of these phenomena through numerical simulations and analytical models provides a powerful tool to support the interpretation of experiments, while strengthening the ability to extrapolate results to future devices.

This work provides such modelling, assessing machine-size erosion, migration and deposition, experienced throughout He and Ar PWI experiments in the GyM linear device [1], where W samples are exposed to the plasma. This is achieved by coupling a boundary plasma code with an erosion and impurity transport code, namely SOLPS-ITER and ERO2.0 [2,3].

Based on previous work [4,5], the results presented aim to progress towards an experimental validation of the ERO2.0 modelling. Preliminary simulations are performed to design an experiment capable of producing useful data for the validation. Therefore, the ideal position of diagnostics, like catchers to measure deposited layers and spectroscopy to detect

characteristic emission of impurities, is investigated, finding that the highest deposition can be measured in proximity of the sample-holder. The influence of plasma species, samples shape and samples material on the detectable signal is also evaluated. Finally, simulations are compared to experimental data to find an agreement and validate the modelling.

Acknowledgements: Part of this work is funded by Eni S.p.A.

- [1] A. Uccello, et al. *Front. Phys.* 11, 1108175 (2023)
- [2] X. Bonnin, et al, *Plasma Fusion Res.* 11, 1403102 (2016)
- [3] J. Romazanov, et al., *Phys. Scripta* 2017.T170, 014018 (2017)
- [4] F. Mombelli, et al., *Nucl. Fusion* 65, 026023 (2025)
- [5] G. Alberti, et al., *Nucl. Fusion* 63.2, 026020 (2023)

POA-71

### **Evaluation of erosion and deposition in JA DEMO divertor and the effects of tungsten impurities**

Makoto Oya<sup>1</sup>, Kazuo Hoshino<sup>2</sup>, Nobuyuki Asakura<sup>3</sup>, Yoshiteru Sakamoto<sup>3</sup>, Noriyasu Ohno<sup>4</sup>, Kazuaki Hanada<sup>1</sup>

<sup>1</sup>Kyushu University, Japan; <sup>2</sup>Keio University, Japan; <sup>3</sup>National Institutes for Quantum Science and Technology, Japan; <sup>4</sup>Nagoya University, Japan.

Sputtering erosion in plasma-facing wall (PFW) is an important issue regarding the lifetime and deposition layer. In a previous study [1], we evaluated the sputtering erosion by deuterium (D), helium (He) and argon (Ar) ions in JA DEMO divertor. By the sputtering erosion, W atoms are released from PFW and transport in plasma as an impurity. After the transport, some W impurities (atoms/ions) will irradiate to PFW and cause sputtering (self-sputtering). The sputtering by the W impurities have non-negligible effect on the erosion process due to their high sputtering yield. In addition to sputtering, reflection and deposition of W impurities will also occur on the PFW surface. In this study, we simulated the sputtering erosion, reflection and deposition of W impurities in JA DEMO divertor, in order to evaluate the distribution of erosion and deposition.

We performed a 3D Monte Carlo simulation on the W impurities irradiation. In this simulation, trajectories of W ions (charged up to 10) were traced from edge plasma to W-monoblock surface. (The edge plasma parameters were calculated by SONIC code.) After the W impurities irradiated to the surface, we calculate three surface processes; (1) sputtering, (2) reflection and (3) deposition. (1) In sputtering processes, the yield was calculated by semiempirical formula for physical sputtering, considering the incident energies and angles. (2) In reflection process, the coefficient was taken from available database, considering the energies and angles. (3) W impurities remaining on the surface (without the reflection) were considered to be deposited. In order to evaluate the poloidal distribution of erosion and deposition, we conducted this simulation in 31 positions (along poloidal direction) on outer target in JA DEMO divertor.

Simulation results indicated that sputtering and deposition rate depended on the poloidal positions. Deposition of W impurities was dominant near the strike point (plasma-detached region). However, sputtering was dominant away from strike point, when sputtering by other ions (D, He and Ar) were also considered. This was because sputtering rate by Ar and W impurities were high and deposition rate was low in the area. In addition, we will also calculate re-deposition of sputtered W atoms on W-monoblock surface.

[1] M. Oya et al., Nuclear Materials and Energy 41 (2024) 101793.

POA-72

### **Overview of Material Balance and Dust Production in JET Beryllium – Tungsten Wall from Post-Mortem Analysis Studies**

Anna Widdowson<sup>1</sup>, Charlie Ayres<sup>1</sup>, Joe Banks<sup>1</sup>, Aleksandra Baron-Wiechec<sup>2</sup>, Sebastijan Brezinsek<sup>3</sup>, Matthews Clancy<sup>1</sup>, Paul Coad<sup>1</sup>, Elzbieta Fortuna-Zalesna<sup>4</sup>, Kalle Heinola<sup>5</sup>, Matt Hook<sup>1</sup>, Ilona Karnowska-Peterski<sup>1</sup>, Ionuț Jecu<sup>1</sup>, Jari Likonen<sup>6</sup>, Marek Rubel<sup>7</sup>

<sup>1</sup>United Kingdom Atomic Energy Authority (UKAEA), United Kingdom; <sup>2</sup>Guangdong Technion – Israel Institute of Technology, China; <sup>3</sup>Forschungszentrum Jülich GmbH, Germany; <sup>4</sup>Warsaw University of Technology, Poland; <sup>5</sup>IAEA, Austria; <sup>6</sup>VTT Technical Research Centre of Finland Ltd, Espoo, Finland; <sup>7</sup>Uppsala University and KTH Royal Institute of Technology, Sweden.

Material balance and dust production in the JET Beryllium-Tungsten Wall (JET-Be-W) from the perspective of post-mortem analysis of plasma facing components and dust is discussed. Mass change data is summarised bringing newly presented results on net erosion in the main chamber and net deposition in the divertor showing the overall balance and implications for dust production.

Net deposition in the divertor is of the order 60 g after 19 hours of divertor plasma operations and the mass of dust collected is of the order 2 g, giving an upper dust conversion factor 2–4%. This value assumes that dust is a product of the disintegration of deposits. However, dust sources in JET are various, including flakes from damaged tungsten coatings on divertor tiles and beryllium droplets from melting by disruptions or runaway electrons and therefore in practice the conversion factor may be lower. There is both an order of magnitude reduction in the net erosion and deposition and in the dust conversion factor when comparing JET operations in carbon (C) with Be-W. This highlights again the importance of reducing chemical erosion processes and associated material migration to remote areas where deposits forming on cool surfaces result in flaking and dust formation.

Mass change data on Be limiter tiles show that net erosion is highest on the central section of the outer and inner mid-plane limiter tiles arising mainly from limiter plasma contact on start-up and ramp-down of plasmas. When considering net erosion and deposition across whole tiles and interpolating along all limiter beams the outer limiter remains the largest global erosion source, due in part to higher surface area, accounting for > 50 g net erosion per operating period compared with < 15 g at the inner limiter.

Other dust analysis results provide the first ever data on dust mobilisation beyond the main vacuum vessel to the active (tritium contaminated) exhaust line of a fusion device demonstrate the efficacy of the filtration system.

The global material balance will be discussed along with supporting plasma operations related data on beryllium spectroscopy and ion flux data. The amount of dust produced from erosion products and dust migration provide promising new data for dust management in future fusion devices.

POA-73

### **Elemental analysis of divertor marker tiles exposed during the 2018 (C3), 2019 (C4) and 2020 (C5) WEST campaigns**

Rodrigo Mateus<sup>1</sup>, Norberto Catarino<sup>1</sup>, Eduardo Alves<sup>1</sup>, Elodie Bernard<sup>2</sup>, Mathilde Diez<sup>2</sup>, Emmanuelle Tsitrone<sup>2</sup>, Jari Likonen<sup>3</sup>, Antti Hakola<sup>3</sup>

<sup>1</sup>IPFN, Instituto Superior Técnico, Universidade de Lisboa, Portugal; <sup>2</sup>CEA, IRFM, France; <sup>3</sup>VTT Technical Research Centre of Finland Ltd, Finland.

Marker tiles coated by tungsten (W) layers, with an additional thin molybdenum (Mo) interlayer, were installed at the lower divertor of WEST and retrieved for analysis after the end of the C3, C4 and C5 campaigns to investigate the erosion and deposition patterns over the entire phase 1 of the tokamak operation. Ion beam analysis (IBA) offers optimal analytical tools to probe these patterns [1]. In the present work, Rutherford Backscattering Spectroscopy (RBS) measurements were carried out to evaluate the local erosion or deposition behaviour, as the oxygen (O) contents, by following the depth profile of the W-based yield. Nuclear Reaction Analysis (NRA) led to the quantification of the co-deposited deuterium (2H), boron (B) and carbon (C) amounts. Chromium (Cr), iron (Fe) and copper (Cu) were identified as the main heavier co-deposited impurities and quantified by Proton Induced X-ray Emission (PIXE). Secondary Ion Mass Spectrometry (SIMS) was used for sensitive elemental depth profiling. Three sets of exposed samples retrieved from five toroidal positions along the radial coordinate of the divertor tiles, from the High Field Side (HFS) towards their Low Field Side (LFS) limits, were investigated. The evolution of the quantified elemental depth profiles and contents at the chosen locations was assessed after C3, C4 and C5. IBA results identified the main erosion and deposition patterns already observed in previous studies [1,2], which did not change over the entire tokamak operation. They point the presence of a smooth erosion plus thin deposition area nearby the HFS zone, followed by a strong deposition area adjacent to the Inner Strike line Position (ISP), erosion areas at the inner (ISP) and Outer Strike line Positions (OSP), and a thin deposition area nearby the LFS limit. The erosion patterns deeply evolved over time and the W layer above the Mo interlayer became completely removed after the C4 campaign, and significant co-deposits appear after C5 (OSP). There was not an evident evolution for the retained 2H, with maximum contents of the order of  $\sim 2 \times 10^{17}$  at/cm<sup>2</sup> [1] (C4 and C5). Similar trends were observed for the C co-deposition, with maximum contents varying from  $\sim 5 \times 10^{17}$  to  $\sim 3 \times 10^{18}$  at/cm<sup>2</sup>. A significant B co-deposition occurred during the C4 and C5 campaigns, with maximum contents of the order of  $\sim 2 \times 10^{19}$  at/cm<sup>2</sup> after C5 (HFS). Elemental depth profiles achieved by RBS-NRA and by SIMS deeply agree with each other.

[1] M. Balden et al, Phys. Scr. 96, 104020 (2021)

[2] M. Diez et al., Nucl. Mater. Energy 34, 101399 (2023)

POA-74

### **The influence of nitrogen seeding on beryllium erosion by hydrogen plasma**

Timo Dittmar<sup>1</sup>, Dmitry Borodin<sup>1</sup>, Sebastijan Brezinsek<sup>1</sup>, Ewa Pawelec<sup>2</sup>, Antti Hakola<sup>3</sup>, Karl Krieger<sup>4</sup>, Scott Silburn<sup>5</sup>, Emmanuelle Tsitrone<sup>6</sup>, Anna Widdowson<sup>5</sup>

<sup>1</sup>Forschungszentrum Jülich GmbH, Germany; <sup>2</sup>Institute of Physics, University of Opole, Poland; <sup>3</sup>VTT Technical Research Centre of Finland Ltd, Finland; <sup>4</sup>Max-Planck-Institut für Plasmaphysik, Germany; <sup>5</sup>UKAEA, Culham Campus, United Kingdom; <sup>6</sup>CEA, IRFM, France.

Prior to ITER's decisions to become an all-tungsten (W) machine, beryllium (Be) was fore-

seen as plasma facing material for the main chamber wall. The study of the chemical and physical interaction of Be with pure hydrogen or impurity seeded plasma was therefore of special importance to ensure safe and reliable operation of ITER: This is especially true for the usage of chemically reactive impurities such as nitrogen (N): Beryllium nitride does not decompose up to its melting temperature and Be as low Z material is strongly susceptible to physical sputtering by any impurity species. Therefore, in order to understand, model, and predict the interaction of nitrogen with the materials and conditions relevant for fusion devices, extensive experiments on laboratory (e.g. [1]) or tokamak scale (e.g. [2]) were performed. The first experiments in PISCES-B revealed that the introduction of nitrogen reduced the Be I and Be II molecular optical emission which was correlated with a reduced mass loss measurement. To transfer these findings experiments with consecutive, similar N seeded discharges were performed in JET. The quick repetition of these discharges allowed to raise the surface temperatures of the limiters and thereby study the temperature dependence of the N interaction. The analysis of optical emission spectroscopy data revealed a reduction of Be I, Be II line emission and molecular BeD band emission stronger than expected from the raise of the surface temperature, thus reduction of the near-surface fuel content, alone [3]. However, the effect of nitrogen seeding and temperature could not be clearly separated. In this contribution we will report on a set of experiments executed before the JET shutdown where a modified procedure of seeded and unseeded discharges allowed to separate these two and clearly show a diminishing effect of the nitrogen at limiter surface temperatures above 650 K restoring the erosion rate of unseeded plasma. Furthermore we will integrate the insights from this new research with the existing experimental data (ion beam, laboratory plasma, tokamaks) and modeling works to provide a comprehensive review of the current understanding of the involved processes and to summarize and conserve 15 years of research on the Be-N-D system. The transfer of knowledge from Beryllium to Boron will be assessed and expected similarities and difference discussed.

[1] T. Dittmar, et al., J. Nuc. Mat. 438 (2013) 988-991

[2] M. Oberkofler, et al., Fus. Eng. & Des. 89-99 (2015) 1371

[3] S. Brezinsek, et al., Nuc. Fus. 54 (2014) 103001

POA-75

### **Radio frequency plasma cleaning for Core Plasma Thomson Scattering diagnostic mirrors**

Youpeng Wang<sup>1</sup>, Artem Dmitriev<sup>1</sup>, Laurent Marot<sup>1</sup>, Paul Hired<sup>1</sup>, Tomás Sousa<sup>1</sup>, Maitane Amarika<sup>2</sup>, Gorka Beaskoetxea<sup>2</sup>, Aitor Marco<sup>2</sup>, Ulrich Walach<sup>3</sup>, Laura Sanchez<sup>3</sup>, Jordi Puig<sup>4</sup>, Ernst Meyer<sup>1</sup>

<sup>1</sup>University of Basel, Switzerland; <sup>2</sup>IDOM Consulting, Engineering, Architecture S.A.U., Spain; <sup>3</sup>Fusion for Energy (F4E), Spain; <sup>4</sup>ATG Europe, Spain.

Core Plasma Thomson Scattering (CPTS) is an optical diagnostic system that is foreseen to be located in Diagnostic Shielding Module #3 of Equatorial Port #10 for the electron temperature and density measurement in ITER. During the fusion plasma operation, the metallic mirrors integrated into the first mirror unit (FMU) are expected to be gradually contaminated due to plasma exposure, which leads to the severe degradation of their optical performance. Radio-frequency (RF) plasma cleaning is considered one of the most promising in-situ methods to restore these optical properties. To finally realize efficient contamination removal and to minimize the damage to mirror materials, it is of great necessity to understand the RF plasma parameters and test its cleaning capability for the current CPTS FMU design (without

pre-matcher) as a guidance to further improve the RF circuit design of CPTS FMU.

In this work, the RF plasma parameters, including mirror self-bias, ion flux and ion energy distribution function (IEDF), were first studied in a wide frequency range of 13.56MHz to 80MHz using retarded field energy analyzer (RFEA). Besides, the impact of DC grounding for the first mirror was also investigated by applying a notch filter, as the mirrors in CPTS FMU will be actively water-cooled [1] canceling the mirror DC bias. Additionally, based on the measured parameters, a series of cleaning experiments were conducted on mirror insets coated with an Al<sub>2</sub>O<sub>3</sub> layer to validate experimentally the removal of the contamination layer using RF low-temperature plasma exposure without a pre-matcher. To ensure proper cleaning, chemical composition and reflectivity of insets before and after cleaning were analyzed with X-ray photoelectron spectroscopy (XPS) and spectrophotometer. The cleaning result showed that ion energy is a decisive factor for a favorable cleaning and the detected redeposition of Fe sputtered from the adjacent housing indicated that FMU geometry requires further optimizations. Further, the evaluated standing wave ratio (SWR) using a directional coupler demonstrated the need for a pre-matcher for a better power coupling to the FMU. To provide a reference for the future pre-matcher design, the total impedance of FMU and ignited plasma was measured using a vector network analyzer (VNA) by direct and indirect methods at various frequencies.

The work leading to this publication has been funded by Fusion for Energy under the contract F4E-OMF-0847-01-01. This publication reflects the views of only the authors, and Fusion for Energy cannot be held responsible for any use which may be made with the information contained therein.

[1] M. Amarika, G. Beaskoetxea, G. Murga, et al., Fusion Eng. Des. 203 (2024) 114416

POA-76

### **Suppression of impurity release on the low field side tungsten limiter in EAST long-pulse discharges**

Fang Ding, Rui Ding, Haishan Zhou

Institute of Plasma Physics, HFIPS, Chinese Academy of Sciences, China.

The ITER new baseline considers the change of first wall material from beryllium (Be) to tungsten (W). This increases the risk related to increased core plasma radiation and thus has a direct impact on the achievement of the ITER high Q goal. The experiments in ASDEX Upgrade [1] and WEST [2] found that despite the gross W source from main chamber wall is much smaller than that from the divertor, its effect on the core W plasma density is sizeable, which can be mainly attributed to the effective contamination efficiency for low field side (LFS) produced W. Plasma start-up, RF heating, radiative impurities (Ne, Ar etc) and intrinsic impurities (O, C etc.) pose further issues associated with W sputtering on LFS-limiters. Wall passivation techniques (such as boronization and lithiation) have been implemented in present machines to minimize the influx of impurities. EAST, a superconducting tokamak devoted to long-pulse high-performance discharge, recently achieved a high-confinement mode discharge exceeding 1000 s, with a core electron temperature higher than 8.5 keV. The successful suppression of impurity influx from LFS-limiter, which is composed of ITER-like water-cooler W monoblock plasma-facing components (PFCs), plays a crucial role in the long-pulse discharges achieved in EAST. In this contribution, the principal elements inducing strong impurity sputtering on the

LFS-limiter are reviewed, and effective strategies for impurity suppression are discussed. In 2024, we developed a visible spectroscopic system for monitoring the impurity release from the LFS-limiter. We found that intense W sputtering occurs during the plasma start-up phase, the ICRF-heating phase, and the Ne impurity seeding phase. To minimize the impurity influx from the PFC surface, magnetic configuration, heating power, and wall conditioning were optimized to reduce the impurity source and ensure effective auxiliary heating coupling with the main plasma. We observed that the fresh lithium coating lasts  $\sim 50$  s with its effectiveness of impurity suppression in the long-pulse discharges, which depends on the incident particle flux and energy. Following the degradation of the surface coating, light impurities such as oxygen and carbon are released and W sputtering is enhanced, leading to plasma performance deterioration and even long-pulse discharge termination. Laser induced breakdown spectroscopy (LIBS) was employed to reveal the depth profile of impurities and the H/D ratio on the PFC surface, as well as the dependence of coating lifetime on incident particle flux. Eventually the real-time lithium coating based on a feedback model was implemented to continuously replenish the coating on the PFC surface so as to suppress the impurity release in long-pulse discharges, which could provide a reference for ITER.

[1] R. Dux, V. Bobkov, A. Herrmann, et al, J. Nucl. Mater 858, 390-391 (2009)

[2] J. Bucalossi, A. Ekedahl and the WEST Team, Nucl. Fusion 64, 112022 (2024)

POA-77

### **Erosion behavior of porous boron and boron-tungsten layers exposed to deuterium plasma in the GyM linear device**

Andrea Uccello<sup>1</sup>, Federico Gaspari<sup>2</sup>, Davide Orecchia<sup>2</sup>, Matteo Pedroni<sup>1</sup>, Irene Casiraghi<sup>1</sup>, Daria Ricci<sup>1</sup>, Natale Rispoli<sup>1</sup>, Jimmy Scionti<sup>1</sup>, David Dellasega<sup>2</sup>, Matteo Passoni<sup>2</sup>, Valeria Russo<sup>2</sup>, Fabio Subba<sup>3</sup>, Alessio Villa<sup>3</sup>, Alessandro Maffini<sup>2</sup>

<sup>1</sup>Istituto per la Scienza e Tecnologia dei Plasmi, CNR, Italy; <sup>2</sup>Politecnico di Milano, Italy; <sup>3</sup>NEMO Group, Dipartimento di Energia, Politecnico di Torino, Italy.

As part of ITER re-baselining efforts started in 2023, it is planned to change the first wall material from beryllium to tungsten (W). The loss of beryllium's capability to getter low-Z impurities like oxygen (O), may necessitate a substitute. Based on current tokamak experience, boronization seems a viable solution. Adding boron (B) to ITER's plasma-facing materials may have strong implications for the migration process, particularly regarding the properties of deposited layers. A thorough understanding of their behavior during plasma exposure is crucial for properly controlling plasma-wall interaction when ITER becomes operational.

This work investigates micrometer-thick B and B-W porous layers exposed to plasma under ITER first wall-relevant conditions. Nanoparticle-aggregate B and B-W films, with thicknesses of 1-2  $\mu\text{m}$ , were deposited on silicon using femtosecond pulsed-laser deposition [1]. B coatings with 5%-50% of bulk density and B-W coatings with W concentration <35at.% were produced, with O content <10at.%. Deuterium plasma exposures were conducted in the GyM linear device with ion flux of  $4 \times 10^{20} \text{ m}^{-2} \cdot \text{s}^{-1}$ , applying a negative bias voltage to the samples for ion energy tuning. Layer erosion, morphology evolution, and W enrichment were investigated over an ion energy range of  $E=40-225 \text{ eV}$  and fluences of  $\sim 7.25 \times 10^{23}-3.0 \times 10^{24} \text{ m}^{-2}$ .

The effective sputtering yield of B layers from mass loss data for  $E>70 \text{ eV}$  aligns with SDTrimSP values within 20%, but it is up to five times higher at  $E=40 \text{ eV}$ , which may be related to ion-assisted chemical erosion at the sample exposure temperature of 650 K [2]. The morphology

of all B and B-W films changed from nanoparticle aggregates to a needle-like structure aligned with the magnetic field (80 mT), as shown by SEM and AFM. The onset and properties of the needles (diameter and spacing) were influenced by ion energy, fluence, layer density, and W concentration. W enrichment in B-W films, resulting from preferential B sputtering, is evident from Raman spectra analysis and EDX data, showing an increase in W at.% of up to 30%.

Acknowledgements: The authors acknowledge the financial support of the European Union Next Generation EU and Italian Ministry of University and Research as part of the PRIN 2022 program, project “Nanomaterials for Fusion: experimental and modeling of nanostructured materials and plasma-material interactions for inertial & magnetic confinement fusion” (Project ID: 2022N5JBHT, CUP: D53D23002840006).

[1] D. Orecchia, et al., *Small Struct.* 5, 2300560 (2024)

[2] A. Annen, and W. Jacob, *Appl. Phys. Lett.* 71, 1326 (1997)

POA-78

### **Tungsten-diamond composite for plasma-facing materials**

Shaokai Tang<sup>1</sup>, Thomas Morgan<sup>2</sup>, Nicu Scarisoreanu<sup>3</sup>, Beata Tyburska-Pueschel<sup>2</sup>, Jort Kesteren<sup>2</sup>, Maria Cunha<sup>2</sup>, Paul Mummery<sup>1</sup>, Aneeqa Khan<sup>1</sup>

<sup>1</sup>The University of Manchester, United Kingdom; <sup>2</sup>Dutch Institute for Fundamental Energy Research, Netherlands;

<sup>3</sup>National Institute for Laser, Plasma and Radiation Physics, Romania.

Conventionally, tungsten has been identified as the best plasma-facing material (PFM) candidate for nuclear fusion applications. However, a recent study has ranked Diamond (1st) and Tungsten (3rd) as top candidates for PFMs following screening using comparisons of thermal properties, sputtering, and hydrogen isotope inventory [1]. Both materials have high melting points, while the diamond's thermal conductivity is unparalleled ( $\sim 2200 \text{ W/(m}\cdot\text{K)}$  at 293 K). The high atomic number means tungsten ( $Z=74$ ) has a higher physical sputtering threshold energy, 10 times more than diamond ( $Z=6$ ) [1]. Carbon-based materials are also susceptible to chemical erosion by hydrogen isotopes, producing co-deposition. On the other hand, diamond has a much lower hydrogen isotope diffusion coefficient than tungsten, which can limit the penetration of hydrogen isotopes into bulk materials [2,3]. Existing studies on tungsten have identified oxidation, recrystallisation, embrittlement, and radiation-induced degradation as problems. Tungsten cannot resolve fusion material challenges alone.

There is a need to fill the research gaps in other promising PFMs, especially diamond materials. This work studies the plasma-material interaction (PMI) of deuterium plasma with CVD diamond and tungsten-coated CVD diamond. Relatively thick tungsten layers ( $\sim 1.5 \text{ }\mu\text{m}$ ) are coated on the diamond substrates for the first time, using pulsed laser deposition. These aim to combine the best properties of two materials, sputtering resistance from W and excellent thermal and mechanical properties from diamond. Experiments in the Magnum-PSI linear plasma device exposed both materials to low-energy (35 eV), high-flux ( $>1.4 \times 10^{23} \text{ m}^{-2} \text{ s}^{-1}$ ) deuterium plasma with fluences from  $3.6 \times 10^{24}$  to  $1 \times 10^{26} \text{ m}^{-2}$ . Both materials show good resistance and stability to relatively low fluence of deuterium, no erosion or delamination were found. After high fluence deuterium exposure, a novel porous surface topography on CVD diamond and wavy delaminations (stress relief pattern) on W/Diamond composites are observed. However, these are not found on samples that were exposed to helium plasma, indicating these features are deuterium-related. The detection of C-H bands with optical



spectroscopy during the deuterium exposure also suggests the diamond surface is etched by deuterium. Nanoindentation experiments on W coating disclose its ductility and good bonding strength. The deuterium concentration at the bonding interface to delamination is determined by the ion beam facility at DIFFER. X-ray diffraction (XRD) measures the W coating's compressive stress, creating the wavy pattern during delaminations. Strain and bonding strength calculated from the dimensions of the wavy pattern agrees with XRD and nanoindentation results. Delamination initiation occurs at the sample edges due to the fact the PLD coating is thinner at the sample edges so deuterium diffuses to the bonding interface faster. Calculations are made on heat and deuterium diffusion in the composite, suggesting the bonding interlayer is a barrier of both.

[1] A. Fedrigucci, et al., PRX Energy, 3(4), 043002 (2024)

[2] D.J. Cherniak, et al., Geochim. Cosmochim. Acta, 232, 206–224 (2018)

[3] T. Tanabe, Phys. Scr., T159, 014044 (2014)

POA-79

### **Advancements in the design of a W-based coating as protective barrier for liquid Sn-based divertor**

Davide Vavassori<sup>1</sup>, Luigi Bana<sup>1</sup>, Marco Bugatti<sup>1</sup>, Matteo Iafrati<sup>2</sup>, Matteo Passoni<sup>1</sup>, David Dellasega<sup>1</sup>

<sup>1</sup>Politecnico di Milano, Italy; <sup>2</sup>ENEA, Frascati, Italy.

Plasma Facing Components (PFCs) based on liquid metals (LMs) represent an interesting option for the realization of future fusion reactors such as DEMO [1]. Focusing on the divertor region, PFCs with LMs would allow improved capabilities compared to conventional solid high-Z metal PFC in terms of heat removal, sensitivity to neutron damage or impurity control. Moreover, they would be characterized by self-healing behaviour. Currently, the most mature LM-based divertor designs consider the use of low melting point metals such as lithium (Li) or tin (Sn) which, however, promote severe corrosion on materials conventionally employed in fusion devices (e.g., copper (Cu)). This represents a challenge to mitigate for the development of these PFC designs, such as the liquid Sn-based divertor proposed by ENEA [2].

Surface coating technology emerges as possible solution to overcome the previously described issue. Among physical vapor deposition (PVD) methods, sputtering techniques can be appealing in the context of surface protection since they allow to obtain high quality coatings also considering large area substrates of industrial relevance [3]. In this respect, polished Cu substrates coated with tungsten (W) based films deposited by High Power Impulse Magnetron Sputtering (HiPIMS) demonstrated an enhanced corrosion resistance during experiments in contact with liquid Sn [4]. Specifically, engineered coatings presenting an amorphous-like layer composed by tungsten and aluminium (W-Al) exhibited superior performances, evidencing how the coating characteristics (e.g., morphology and microstructure) controlled by HiPIMS process parameters majorly determined their final effectiveness as corrosion barriers.

Here we present progress related to the design of such W-based corrosion barrier, developed in a two-fold direction. Firstly, considering the W-Al coating as case-study, we performed corrosion experiments aimed to assess the role of coating thickness and substrate roughness, since they are relevant aspects to consider toward practical applications. Post-mortem analysis revealed that the coating protective behaviour benefited from the higher thickness in case of polished substrates. On the other hand, an excessive substrate roughness facilitated penetration of LM, regardless of the thickness of the protective coating. Secondly, exploiting

different magnetron sputtering approaches, we investigated the growth of alternative W-based coatings, with particular focus on morphology and microstructure evolution induced by deposition parameters variation.

- [1] J.S. Hu, et al., Nucl. Mat. En. 41, 101776 (2024)
- [2] S. Roccella, et al., J. Fus. En. 39, 462–468 (2020)
- [3] J. T. Gudmundsson, Plasma Sour. Sci. Tech. 29, 11 (2020)
- [4] D. Vavassori, et al., Surf. Coat. Tech. 494, 131449 (2024)

POA-81

### **Inverse finite element based methodology applied to ITER grade tungsten: a model for mini-flat tensile specimens**

Francisco Miranda<sup>1</sup>, Aleksandr Zinovev<sup>2</sup>, David Bermudez Parra<sup>3</sup>, Alexander Bakaev<sup>2</sup>, Dmitry Terentyev<sup>4</sup>, Kim Verbeken<sup>5</sup>, Thomas Pardoen<sup>6</sup>

<sup>1</sup>Université Catholique de Louvain, Louvain-la-Neuve. Belgian Nuclear Research Centre SCKCEN, Mol., Belgium; <sup>2</sup>Belgian Nuclear Research Centre SCKCEN, Mol., Belgium; <sup>3</sup>Belgian Nuclear Research Centre SCKCEN, Belgium and Universidad Politécnica de Madrid, Spain; <sup>4</sup>Belgian Nuclear Research Centre SCKCEN, Mol. Ghent University, Department of Materials, Textiles and Chemical Engineering, Ghent, Belgium; <sup>5</sup>Ghent University, Department of Materials, Textiles and Chemical Engineering, Ghent, Belgium; <sup>6</sup>Université Catholique de Louvain, Louvain-la-Neuve. WEL Research Institute, Wavre, Belgium.

Finite element simulations are the conventional method for performing structural analysis on systems and components. For these calculations to be effective, it is crucial to provide accurate input information to the solver, such as strength and ductility properties, often obtained from uniaxial tensile testing. For designing of components where tungsten plays a structural role, such as in the divertor of fusion devices, it may be necessary to provide true stress-strain deformation behavior and mechanical properties beyond the onset of necking, which is difficult relying on the standard approach. An alternative is to obtain these properties as output from finite element analysis.

In the nuclear industry, it is of particular interest to derive mechanical properties using minimal material volume. This requirement arises from constraints such as the limited irradiation volume available, irradiation-induced activation of specimens, the high cost of irradiation campaigns, and the need to minimize the generation of radioactive waste. Application of small specimen test techniques (SSTT) is becoming a standard approach for testing of nuclear-relevant materials. Therefore, the finite element model developed in the present work, was provided with tensile test results obtained on subminiaturized flat specimens.

The tensile tests were conducted on ITER-specification tungsten provided by AT&M (China) and ALMT (Japan): materials that will be used for ITER's divertor components. These materials were subjected to hot rolling thermomechanical treatment during manufacturing to improve the strength and ductility. The tensile experiments were conducted at temperatures relevant to the operational conditions of ITER, ranging from the ductile-brittle transition temperature (DBTT) to the recrystallization temperature (RXT), at which the microstructure and mechanical properties change significantly.

The objective of this work is to develop a finite element model that reproduces the ductile behaviour of tungsten beyond the onset of necking under fusion relevant temperature with the help of inverse finite element analysis. Using experimental engineering stress-strain curves as input, the analysis returns true stress-strain curves as output which can be used in structural

analysis of components. Finally, scanning electron microscopy is employed to analyse the effect of different testing conditions on the fracture surface and microstructure of both studied tungsten grades.

POA-82

### **Effect of baseplate preheating on the crack formation of W-W<sub>2</sub>C during Laser Powder Bed Fusion**

Aljaž Iveković<sup>1</sup>, Črtomir Donik<sup>2</sup>, Irena Paulin<sup>2</sup>, Petra Jenuš<sup>1</sup>

<sup>1</sup>Jožef Stefan Institute, Slovenia; <sup>2</sup>Institute of Metals and Technology, Slovenia.

Laser Powder Bed Fusion (L-PBF) is an additive manufacturing technique that creates three-dimensional objects by selectively melting layers of metallic powder. By using a high-energy density laser, it's possible to achieve complex geometries, even with refractory metals like tungsten. However, L-PBF of tungsten presents significant challenges due to its inherent properties, such as a high melting point, high melt viscosity and surface tension, excellent thermal conductivity and a high ductile-to-brittle transition temperature. As a result, the L-PBF process for tungsten often leads to cracked or porous parts (lack-of-fusion porosity).

A combined approach of preheating to temperatures above the DBTT (>400 °C) with an active oxygen-getter alloying strategy was suggested as a pathway to eliminate cracks in L-PBF W parts completely [1]. Baseplate preheating reduces the thermal gradient during processing, thus minimizing the residual stresses accumulated in the material. The addition of carbon and in-situ formation of W-W<sub>2</sub>C composite material has shown potential as an armour material of the diverter [2]. Additionally, it was successfully applied to suppress crack formation during L-PBF of Mo [3].

In this work, we investigate the effect of baseplate preheating on temperatures above the DBTT (up to 1000 °C) during L-PBF of W with the addition of 4 at.% of C. During solidification carbon reacts with W to form small carbide precipitates located at the grain boundaries and within the grains. As a result of constitutional undercooling, significant grain refinement of the microstructure is observed with the transition from planar (typical for pure W) to cellular solidification. Baseplate preheating to 600 °C and 1000 °C resulted in an increase in densification with nearly full density obtained at 1000 °C. Although microcracks were not completely eliminated, the crack length and crack density were significantly reduced.

**Acknowledgements:** This work has been carried out within the framework of the EUROfusion Consortium, funded by the European Union via the Euratom Research and Training Programme (Grant Agreement No 101052200 — EUROfusion). Financial support from the FWO-ARIS Weave project 'Functionally Graded Materials with Interpenetrating Phases made of Immiscible Alloys' under Grant No G093822N (FWO) and N2-0324 (ARIS) is acknowledged.

[1] B. Vranken et al. Additive Manufacturing 46 102158 (2021)

[2] S. Novak, et al. Mater. Sci. and Engin.: A, 772, 138666 (2020),

[3] L. Kaserer, et al. Int. J. Refract. Met. Hard Mater. 84 105000 (2019)

POA-83

### **Predicting irradiation hardening and microstructural evolution in ion-irradiated Eurofer97: a nanoindentation study supported by CPFEM and TEM**

Tymofii Khvan, Katarzyna Mulewska, Łukasz Kurpaska, Witold Chromiński, Michał Stróżyk

National Centre for Nuclear Research, Poland.

Reduced activation ferritic/martensitic (RAFM) steels are the main candidates for the construction of structural components in future fusion and Gen IV nuclear reactors. To ensure safe and stable reactor employment, RAFM-based materials require efficient methods for their characterization under harsh operational conditions. Constantly enduring neutron irradiation, their mechanical properties degrade and may cause a failure of the component. However, neutron irradiation for research purposes is an expensive and long process, so it becomes a major limiting factor to steadily investigate its effect and deliver new research data. Hence, a safer, more paced, and cheaper solution of ion irradiation as a tool for surrogating the neutron damage is becoming more and more popular. As ions are characterized by their penetrating ability, the introduced damage is non-uniformly distributed and densely accumulated on the sub-surface. To correctly estimate their impact, nanoindentation technique is widely applied. The presented study demonstrates a semi-empirical approach to effectively interconnect the ion and neutron radiation-induced hardening in RAFM steels, introduced in a range of irradiation conditions. The applied set of tools, based on nanoindentation and tensile tests, as well as their simulations using crystal plasticity finite element method, allows us to extract the irradiation effect on the material law, and accurately reproduce the experimental data. Ultimately, the analysis performed on an ion-irradiated specimen can provide the macroscale (neutron irradiated) yield stress values in a range of dpa doses, which accurately correlate with the literature. The complementary investigations of the microstructural evolution done by focused ion milling and transmission electron microscopy are compared with their computational analogue to confirm the predictive capability of the method. Globally, the presented research is aimed at the establishment and validation of the computationally experimental procedure to precisely deduce the temperature-dependent irradiation hardening in metallic materials for nuclear applications.

POA-84

### **Brazability study of W2C-reinforced tungsten alloy to EUROFER for first wall application in DEMO fusion reactor**

Ignacio Izaguirre<sup>1</sup>, Javier de Prado<sup>1</sup>, Maria Sánchez<sup>1</sup>, Aljaž Iveković<sup>2</sup>, Petra Jenuš<sup>2</sup>, Alejandro Ureña<sup>1</sup>

<sup>1</sup>Universidad Rey Juan Carlos, Spain; <sup>2</sup>Jožef Stefan Institute, Slovenia.

Current efforts in developing new tungsten materials for plasma-facing components aim to overcome the intrinsic thermomechanical limitations of pure tungsten. The ductile-to-brittle transition temperature (DBTT) around 400°C, along with recrystallization and grain growth above 1200°C, could compromise the component's operational life and challenge the application of pure tungsten within the DEMO fusion reactor's operational window.

To address these issues, current strategies for stabilizing tungsten are focused on particle reinforcement. This involves incorporating oxide (e.g., Y<sub>2</sub>O<sub>3</sub>) or carbide particles into the tungsten matrix, which has been shown to improve mechanical properties to some extent. This study examines the joinability of a W2C-reinforced tungsten alloy, synthesized through carbide precursor reaction during sintering, to ferritic-martensitic steel (EUROFER97) for the DEMO reactor's first wall. Brazing technology was selected, using a 50 μm thick copper filler interlayer.

The study includes wetting analyses to evaluate particle reinforcement effects in the tungsten matrix and explores various brazing parameters (temperatures of 1110°C and 1135°C, and dwell times of 3 and 10 minutes) to optimize the braze microstructure. The resultant brazed joints were characterized microstructurally (SEM) and mechanically (HV and shear tests) to assess quality.

W2C-reinforced tungsten material demonstrated its viability for brazing, showing good wettability characteristics with the filler material (<60° contact angle). The application of the brazing cycle did not result in microstructural and hardness modifications in the bulk material. However, the EUROFER base material exhibited a hardening process up to 440 HV compared to the 220 HV measured in the as-received condition.

The examination of the braze microstructure revealed the formation of a diffusion layer at the W-braze interface, 1–2 μm thick. Above this phase and below the copper braze, the formation of an Fe-rich phase was detected. Additionally, the incorporation of copper into EUROFER, following grain boundary paths, was observed. The modification of the brazing parameters led to the formation of thicker diffusion and Fe-rich phases as the parameters became more energetic. In the case of the Fe-rich phase, the increase in brazing temperature resulted in the formation of a continuous layer instead of isolated phases.

The mechanical characterization of the brazed joints reported shear strengths of  $280 \pm 30$  MPa and  $216 \pm 60$  MPa for brazing conditions at 1110°C and 1135°C, respectively. Finally, the modification of the EUROFER hardness previously exposed indicates the necessity of assessing a tempering treatment after the brazing cycle.

POA-85

### **Comparative study of mechanical properties of W-Cu composites with Diamond TPMS geometries**

Diana Knyzhnykova<sup>1</sup>, Petra Jenuš<sup>1</sup>, Saša Novak<sup>1</sup>, Irena Paulin<sup>2</sup>, Borut Žužek<sup>2</sup>, Nejc Novak<sup>3</sup>, Robert Lürbke<sup>4</sup>, Alexander Von Mueller<sup>4</sup>, Rudolf Neu<sup>4</sup>, Aljaž Iveković<sup>1</sup>

<sup>1</sup>Jožef Stefan Institute, Slovenia; <sup>2</sup>Institute of Metals and Technology, Slovenia; <sup>3</sup>University of Maribor, Faculty of Mechanical Engineering, Slovenia; <sup>4</sup>Max Planck Institute for Plasma Physics, Germany.

Tungsten-copper composites are a promising material for the divertor in fusion reactors as a heat-transfer material due to copper's ability to transfer heat efficiently and tungsten's ability to withstand extreme temperature loads. The current design of the divertor, consisting of W monoblocks connected to a copper alloy (CuCrZr) cooling tubes, causes significant thermal stress at the interface. The use of W-Cu composites can significantly reduce these stresses and improve component durability. Such composites can be realized by fabricating W frameworks by laser powder bed fusion (LPBF), followed by infiltration with molten Cu. Utilizing triple-periodic minimum surface (TPMS) Diamond structure as the basic unit cell of the W framework geometry, results in a highly interconnected network of material with a high surface-to-volume ratio, thereby promoting more efficient heat flux throughout the structure. TPMS structures are divided into walled and skeletal types. Walled structures are distinguished by a uniform TPMS thickness (wall) throughout the geometry, where the porosity of the structures can be altered by modifying the wall thickness. On the other hand, skeletal structures are designed by altering the volume of the solid material between TPMS surfaces. Comparing these two types will allow us to evaluate their effect on mechanical properties, which will facilitate the development of composites with specified use.

Cube shaped W samples with a side size of 1.5 cm were designed with a Diamond TPMS struc-

ture with porosity ranging from 10% to 90% for both architectures: walled and skeletal. Finite element modeling was used to identify areas of structural vulnerability and to determine which of the two architectural configurations exhibited more significant stress accumulation. The analysis revealed that at high porosity values the skeletal type structure exhibits higher stress concentrations, which renders it more susceptible to fracture in comparison to the walled type structure. The simulation results revealed a similar trend for the structures of both architectures with a porosity range of 10% to 40%.

Following manufacturing of W-Cu composites, using LPBF and infiltration by Cu, the samples were characterized in terms of density, microstructure and compressive strength. After printing, the walled structure had a higher W content than the designed value, which consequently affected the compression testing of W-Cu composites. The walled structure showed more brittle behavior than the skeletal structure. Specifically, the skeletal structure with a porosity range of 80% to 40% maintained elastic behavior, whereas the walled structure exhibited brittle failure at a porosity of 40%. The findings will contribute to optimizing the design for manufacturing W-Cu composites with enhanced properties.

POA-86

### **Temperature-dependent grain boundary permeation in tungsten investigated by hydrogenography**

Fahrudin Delic, Armin Manhard, Udo von Toussaint  
Max Planck Institute for Plasma Physics, Germany.

For estimating hydrogen transport and retention in materials for nuclear fusion, the materials are usually treated as spatially homogeneous, or at least as a stack of homogeneous material blocks. However, in practice metals are usually not monocrystalline, but contain a certain amount of grain boundaries. These can have different properties from the grain bulk. Several previous experimental studies have shown a tendency towards amplified diffusion for smaller grain sizes in Ni (e.g., [1]), while simulations of, e.g., W and Ni have shown divergent results, depending on the exact structure of the investigated boundary (e.g. [2, 3]).

We therefore studied the temperature-dependent permeation of deuterium through grain boundaries in tungsten using a newly developed hydrogenography technique [4], which employs patterned films to laterally resolve hydrogen permeation flux density on the back side of the permeation samples. The indicator dots change colour if they absorb hydrogen that has permeated through the sample. Going beyond the proof-of-principle [4], we developed a tungsten oxide layer as a hydrogen indicator that works reliably at higher temperatures than the previously used yttrium thin films. We furthermore established a methodology for quantifying the results, which relies on point-to-point comparison of pristine and exposed samples.

Plasma-driven permeation using a constant deuterium fluence from a low-temperature plasma source was performed on 50  $\mu$ m thick recrystallized tungsten samples at various exposure temperatures between 300 K and 660 K. The results clearly show that up to 600 K, permeating hydrogen isotopes emerge from the back surfaces of the samples almost exclusively at grain boundaries, which highlights the importance of these microstructural features for H isotope transport. With increasing temperature, a larger fraction of grain boundaries becomes favourable for hydrogen transport, up until temperatures of around 600 K. At 660 K, additionally a halo of enhanced hydrogen flux density emerges around several permeating grain boundaries. This suggests that hydrogen isotopes that were captured

by grain boundaries start to desorb back into the grain bulk. We interpret this as the first indication of the transition from the preferential transport of hydrogen along grain boundaries towards predominant bulk permeation.

- [1] A.M. Brass, A. Chanfreau, Acta Mater. 44, 3823–3831 (1996)
- [2] U. von Toussaint, et al., Phys. Scr. T145, 014036 (2011)
- [3] D. Di Stefano, M. Mrovec, C. Elsässer, Acta Mater. 98, 306–312 (2015)
- [4] A. Manhard, U. von Toussaint, P. Sand, M. Stienecker, Nucl. Mater. Energy 36, 101498 (2023)

POA-87

### **An experimental assessment of interatomic potentials for fusion-relevant ion-solid combinations**

Philipp M. Wolf, Eduardo Pitthan, Daniel Primetzhofer  
Uppsala University, Sweden.

Accurate interatomic potentials are essential for the precise prediction of interactions between fusion plasmas and first-wall materials. For slow ions, these interactions are complicated by dynamic processes and solid-state effects, making ab-initio predictions highly complex. Additionally, experimental reference data remains scarce due to significant experimental challenges involved.

Here, we present experimental data for the interatomic potential at low velocities in fusion-relevant ion-solid combinations, specifically He and D on W and Fe. The magnitude of the interatomic potential is determined based on angular scans of single crystal W and Fe samples using Time-of-Flight Low-Energy Ion Scattering (ToF-LEIS) [1], a non-destructive surface analysis method. By adjusting a correction factor applied to the screening length in the Thomas-Fermi-Molière (TFM) model in Molecular Dynamics (MD) simulations, we fit the widths of shadow cones, present as minima in the experimental angular scans, thereby extracting the interatomic potential for these atom combinations.

Furthermore, we compare the interatomic potentials derived in this study with commonly used models, including the uncorrected TFM potential, the Ziegler-Biersack-Littmark (ZBL) model, as well as previously published DFT predictions and experimental reference data. Our results indicate a lower interatomic potential for all studied combinations, particularly those involving He, than predicted by the TFM and ZBL models, while we observe a good agreement for the He-W and He-Fe cases with DFT predictions.

The presented experimental assessment of interatomic potentials will be helpful in the improved prediction of sputter yields and atomic displacements during irradiations. Combined with experimental measurements of the sputter yield the here presented accurate interatomic potentials will further allow the calculation of more precise displacement energies.

- [1] D. Primetzhofer, S. N. Markin, M. Draxler, et al., Surf. Sci. 602, 2921 (2008)

POA-88

### **Helium irradiation induced the crystallographic orientation change of tungsten via grain rotation**

Cuncai Fan  
Zhejiang University, China.

Tungsten (W) has been perceived as one of the most promising plasma facing materials

(PFMs) for future fusion reactors. In the past decade, its behaviour under irradiation and helium (He) plasma interaction has been extensively studied. However, some key knowledge gaps still exist, such as the influence of crystallographic orientation on the surface and subsurface evolutions.

We found that the implantation of 30 keV He<sup>+</sup> at room temperature can slightly reduce the grain size of a polycrystalline W sample [1], and it can also induce the formation of new surface grains in the single-crystalline W 100 and W 110 samples [2]. Interestingly, the single-crystalline W 111 sample can remain its initial orientation after He implantation. According to our electron backscatter diffraction (EBSD) analyses and transmission electron microscopy (TEM) observations, the radiation-induced grains are all <111>-oriented, and they are formed through the grain rotation of matrix around its in-plane <110> axis, presumably driven by the energy difference between the channelling and non-channelling crystallographic orientations [3]. Moreover, we found that the He-implanted W samples experience different behaviours in terms of the He thermal desorption spectroscopy (TDS), which might be caused by the He implantation induced the crystallographic orientation change of W.

[1] Cuncai Fan and Xunxiang Hu. "Recovery and recrystallization of warm-rolled tungsten during helium thermal desorption spectroscopy annealing." *Journal of Nuclear Materials* 569 (2022): 153914.

[2] Cuncai Fan, Congyi Li, Chad M. Parish, Yutai Katoh, and Xunxiang Hu. "Helium effects on the surface and subsurface evolutions in single-crystalline tungsten." *Acta Materialia* 203 (2021): 116420.

[3] Cuncai Fan, Yutai Katoh, and Xunxiang Hu. "Impact of helium irradiation on the crystallographic orientation change in single-crystalline tungsten." *Nuclear Fusion* 61, no. 7 (2021): 076011.

POA-89

### **Influence of the addition of Fe on the CrTaVW medium entropy alloy for Nuclear Fusion applications**

Ricardo Martins<sup>1</sup>, Vasco Valadares<sup>1</sup>, Bernardo Monteiro<sup>1</sup>, António P.Gonçalves<sup>2</sup>, José B.Correia<sup>3</sup>, Andrei Galatanu<sup>4</sup>, Elena Tejado<sup>5</sup>, José Y.Pastor<sup>5</sup>, Marta Dias<sup>1</sup>

<sup>1</sup>Instituto de Plasmas e Fusão Nuclear (IPFN), Universidade de Lisboa, Portugal; <sup>2</sup>C2TN, Instituto Superior Técnico, Universidade de Lisboa, Portugal; <sup>3</sup>Laboratório Nacional de Energia e Geologia (LNEG), Portugal; <sup>4</sup>National Institute of Materials Physics, Romania; <sup>5</sup>Universidad Politecnica de Madrid, Spain.

Nuclear fusion holds great potential as a clean energy source, however, constructing its facilities can be quite challenging. One of the key hurdles is the development of materials capable of withstanding the extreme environments encountered in fusion reactors. Within ITER divertors monoblocs, tungsten displays high Ductile-to-Brittle Transition temperature while the heat sink CuCrZr alloys require for optimum service temperatures lower than W facing components. Additionally, the thermal expansion coefficient of the W is smaller than that of CuCrZr, which can cause stresses at the interfaces. Consequently, an intermediate layer is required to ensure effective thermal transport while maintaining operational temperatures within acceptable limits.

The study presented here shows the results on microstructural and thermal characterization of the equiatomic CrTaVW medium entropy alloy and CrFeTaVW high entropy alloy, to be applied as a thermal barrier. Both alloys were prepared by spark plasma sintering, and analyzed



using differential thermal analysis, X-ray diffraction, and scanning electron microscopy. A differential thermal analysis of the HEA shows that up to 1500 °C, the structure is stable and doesn't suffer solid state transformations. Thermodynamic calculations predict a preeminent body-centered cubic-type structure formation that is confirmed by X-ray diffraction of the milled powder and has a presence of WC and Cr<sub>0.5</sub>Fe<sub>0.5</sub> phases. With the intention of globalizing the microstructure's phases, the consolidated CrFeTaVW alloy was annealed at 1100 °C and 1300 °C for 8 days. After annealing, the microstructure evidences four distinct phases: W-rich; Fe and Ta-rich; Cr and V-rich; Ta and V-rich. In the X-ray diffraction of the annealed samples, the presence of Fe<sub>2</sub>Ta and Cr<sub>0.5</sub>V<sub>0.5</sub> phases are also visible. Thermal diffusivity properties show that the addition of iron reduces the thermal diffusivity by 2 mm<sup>2</sup>/s with the increase in temperature. Therefore, due to its multiple phase and stable microstructure, the CrFeTaVW high entropy alloy, has a great potential for high-temperature applications in nuclear fusion.

Acknowledgements: IPFN activities were supported by FCT – Fundação para a Ciência e Tecnologia, I.P. (UIDB/50010/2020, <https://doi.org/10.54499/UIDB/50010/2020>; project UIDP/50010/2020, <https://doi.org/10.54499/UIDP/50010/2020>; project LA/P/0061/2020, <https://doi.org/10.54499/LA/P/0061/2020>). This work has been carried out within the framework of the EUROfusion Consortium, funded by EU via Euratom Research and Training Programme (Grant Agreement No 101052200 – EUROfusion).

POA-90

### **Structural and mechanical characterization of functionally graded W/EUROFER coatings for fusion applications**

Siyu Zhang, Ashwini Kumar Mishra, Jarir Aktaa  
Karlsruhe Institute of Technology (KIT), Germany.

The First Wall is a critical component for the realization of DEMO, as it must transfer incoming heat in the MW/m<sup>2</sup> range into electricity while withstanding extreme thermal and mechanical stresses. W coating with functionally graded W/EUROFER interlayer is planned to be a protective over structural steel the First Wall. W/EUROFER grade material addresses challenges like delamination and high thermal stresses caused by coefficients of thermal expansion. W/EUROFER coatings were deposited over a steel substrate using low-pressure plasma spray. Five interlayers between steel and top W coating with varying volume fractions of W from 25% to 75 % were deposited. Structural and mechanical characterization of these interlayers was performed in this work. Individual interlayers were extracted and the scanning electron microscopic, EDX and XRD were performed. SEM images were analyzed to study the microstructure of the coating and porosity analysis. EDX was performed to determine the actual volume fraction of W and EUROFER in each interlayer and XRD data analyzed to determine the phases in the coating. Furthermore, micro-indentations were performed on these coatings to determine the mechanical properties of the individual interlayer and compare with micro-tensile test results. These results will help to predict the behavior of FGM coatings fusion-relevant conditions, which will improve the coating design.

**Assessing the Viability of Tungsten/Silicon Carbide Plasma Facing Components**

Zachary Bergstrom, Ruben Santana, Žana Popović, Carlos Monton, Tyler Abrams

General Atomics, United States.

General Atomics has been pursuing the development of novel functionally graded tungsten-silicon carbide (W/SiC) plasma-facing components suitable for future fusion pilot plant designs, such as the GAMBL concept [1]. Previously, W-SiC bi-layer samples exhibited higher erosion rates and significant delamination during plasma exposure. To increase adhesion and mitigate these issues, functionally graded W/SiC alloys were fabricated with two distinct gradient thicknesses. Additionally, some of the samples were annealed at 1000 °C for 1 hour to evaluate the impact of thermal treatment. A total of five samples were fabricated and subjected to H-mode plasma exposure in the lower divertor of DIII-D using the divertor material evaluation system [2]. Pre- and post-exposure analyses were conducted using scanning electron microscopy (SEM) and energy dispersive spectroscopy (EDS) to assess surface roughness and elemental composition. The results demonstrated that functionally graded W/SiC samples outperformed W-SiC bi-layers, with no delamination and minimal surface modification. Samples that were annealed prior to plasma exposure exhibited increased surface roughening compared to non-annealed samples; however, none of the substrate material was found on the surface, indicating that the W coating remained robust in the functional graded samples. X-ray diffraction (XRD) was performed on samples before and after annealing to characterize structural changes across various functional gradients and substrates. The samples were found to contain significant proportions of tungsten, silicon, silicon carbide, and tungsten disilicide. Simulated XRD spectra of W/SiC phases, derived from density functional theory, were compared with experimental data to identify peaks corresponding to less well-defined phases. These findings indicate that W/SiC functionally graded alloys represent a promising material for first-wall technology in fusion reactors, offering high thermal conductivity, excellent erosion resistance, and minimal impurity sourcing. This study supports the potential application of W/SiC components as durable and robust plasma-facing materials in fusion energy systems.

Acknowledgements: Funding supported by General Atomics internal research and development.

[1] Tillack, M. S., et al. "GAMBL—A dual-cooled fusion blanket using SiC-based structures." *Fusion Engineering and Design* 180 (2022): 113155.

[2] Rudakov, D. L., et al. "Net versus gross erosion of silicon carbide in DIII-D divertor." *Physica Scripta* 2020.T171 (2020): 014064.

## Study of degradation of tungsten-based materials for fusion reactors by thermal load testing

Ester Duchková<sup>1</sup>, Ondřej Čížek<sup>2</sup>, Michal Hájíček<sup>2</sup>, Petr Havlík<sup>3</sup>, Jiří Matějčíček<sup>4</sup>, Mark Murtazin<sup>1</sup>, Matěj Peterka<sup>4</sup>, Roman Petráš<sup>1</sup>, Ladislav Vála<sup>1</sup>, Jiří Zýka<sup>2</sup>

<sup>1</sup>Research Centre Řež, Czech Republic; <sup>2</sup>UJP PRAHA a.s., Prague, Czech Republic; <sup>3</sup>Faculty of Mechanical Engineering, Brno University of Technology, Czech Republic; <sup>4</sup>Institute of Plasma Physics of the Czech Academy of Sciences, Czech Republic.

During operation of fusion facilities plasma facing components (PFCs) are subjected to high thermal loads. The ability of these components to withstand severe operational conditions is limited by the material. Given that, the use of materials with specific performance such as high melting temperature, high sputtering resistance, high thermal conductivity and low neutron activation is required for PFCs. Therefore, tungsten and tungsten-based materials are prime candidates for this application.

Exposure of the material to thermal loads results in mechanical stresses and various forms of surface degradation and microstructural changes in the material volume. To assess the viability of the tungsten and tungsten-based materials as PFC candidates, the W and W-Cu samples were subjected to thermal loading simulating heat load pulses expected in fusion facilities during plasma instabilities.

Thermal loading experiments were performed using an electron beam welding device, a Pro-Beam K26 equipped with EBG 60-150. During testing the W and W-Cu samples were subjected to short pulses ( $\sim 1$  s) of thermal loads of 10, 15, 20, 30 and 40 MW/m<sup>2</sup>. Temperature inside the samples was measured using thermocouples while temperature on their surface was determined by means of a pyrometer. In parallel, a thermal model was developed in ANSYS Fluent software allowing simulation of the temperature profile at different depths of the sample and its evolution during the tests. The experimental data were compared with the thermal model and showed very good agreement.

Surface degradation of tungsten after the testing with different thermal loads has been studied by means of a scanning electron microscope. In general, a dense net of intergranular cracks was observed on the surface of tungsten and tungsten-copper composite samples in the loaded area for all the loading conditions. Inspection of a cross-section revealed well-developed cracks propagating in an intergranular manner only when exposed to the highest thermal loads (30-40 MW/m<sup>2</sup>). Tungsten subjected to cyclic thermal loading exhibited surface roughening in a form of thermal grooving and slip bands. Microstructural changes in terms of recrystallization of the material were observed only in the bulk material of tungsten-copper composite.

## Hydrogen retention in tungsten at ELM-relevant energies

Sophie Towell<sup>1</sup>, Mikhail Lavrentiev<sup>2</sup>

<sup>1</sup>University of Oxford, United Kingdom; <sup>2</sup>United Kingdom Atomic Energy Authority (UKAEA), United Kingdom.

The interaction between plasma-facing materials and hydrogen isotopes remains a critical challenge for fusion reactor design, particularly regarding fuel retention and material degradation. This study employs molecular dynamics simulations using LAMMPS [1] to investigate the sequential effects of deuterium bombardment on tungsten surfaces at different impact energies. We examine how the ordering of different impact energies: 100 eV representing typ-

ical plasma exposure, and 5 keV representing ELM-like events, influences hydrogen retention mechanisms and material response.

Simulations were performed using classical molecular dynamics with validated interatomic potentials for the W-D system [2]. Tungsten surfaces were subjected to sequential deuterium bombardment at 773 K. The impact energy sequences investigated were: (1) initial exposure at 100 eV followed by 5 keV impacts, and (2) initial exposure at 5 keV followed by 100 eV impacts. Analysis focused on deuterium retention profiles, defect formation, and surface morphology evolution.

Results demonstrate that the ordering of impact energies significantly affects both the spatial distribution and total quantity of retained deuterium. Initial high-energy (5 keV) impacts create numerous trap sites that influence subsequent low-energy retention behaviour. Conversely, initial low-energy exposure results in near-surface deuterium accumulation that modifies the material response to subsequent high-energy impacts. These findings are compared with experimental results from both undamaged and pre-damaged tungsten samples.

This work provides new insights into the role of sequential plasma exposure conditions on hydrogen retention mechanisms in fusion-relevant materials, with implications for plasma-facing component lifetime predictions and fuel retention management strategies.

[1] A.P Thompson et al., *Comp. Phys. Comm* 271, 10817 (2022).

[2] L.-F. Wang, X. Shu, G.-H. Lu, and F. Gao, *J. Phys.: Cond. Mat.* 29, 435401 (2017).

POA-96

### **In-situ Measurement of Helium-Induced Surface Modification in Tungsten using Advanced Characterization Techniques**

Robert Kolasinski, Feng-Jen Chang, Jonathan Coburn, Antonio Cruz

Sandia National Laboratories, United States.

This study applies a combination of diagnostic techniques to investigate how the structure and composition of advanced tungsten (W) materials are altered by plasma exposure. We used in-situ spectroscopic ellipsometry to monitor the evolution of nanoscale surface morphology changes. In addition, we applied a recently developed in-situ low-energy ion beam analysis technique to gain insights into changes in surface composition. Finally, high-resolution thermal desorption spectroscopy (TDS) was used to quantify helium (He) trapped in the near-surface region. To create suitable plasma exposure conditions, we used a linear plasma device capable of producing an RF discharge. This configuration enabled us to achieve conditions conducive to observing the nucleation of near-surface helium bubble networks and the initial formation of tungsten nanostructures. Typical plasma parameters were:  $E_{ion} = 75$  eV;  $ion = 7.6 \times 10^{20} \text{ m}^{-2} \text{ s}^{-1}$ ,  $ion = 1.5 \times 10^{25} \text{ m}^{-2} \text{ s}^{-1}$ .

Building on our previous work [1], we initially applied these techniques to polycrystalline, coarse-grained tungsten specimens exposed at temperatures ranging from 500 to 1000 °C. We correlated the in-situ spectroscopic ellipsometry results with post-mortem high-resolution helium ion microscopy and focused ion beam profiling. Under the specified plasma conditions, we measured the He-induced nanostructure layer growth rate in real time for ion energies up to 250 eV, up to “fuzz” layer thicknesses > 900 nm. The tungsten specimens were then heated in a vacuum chamber equipped with a high-resolution mass spectrometer (Extrel Max50). Using electron beam heating it was possible to anneal the samples up to 1800 °C to desorb the implanted He. We found that, for an incident fluence of  $6 \times 10^{24} \text{ He m}^{-2}$ , the retained He varied

between  $1.8 \times 10^{20} - 6.0 \times 10^{21}$  He  $\text{m}^{-2}$  (corresponding to a retained fraction ranging between  $10^{-4} - 10^{-5}$ ).

The characterization techniques described above are now being applied to more complex commercially developed alloys (including W doped with K and Re), as well as ultra-high temperature ceramics. These materials have inherently more complex composition, which can be altered by surface-to-bulk transport caused by He bubble growth. To assess these effects, we will rely on a recently-developed in-situ low-energy ion beam analysis technique, which can provide insight into changes in surface composition. Preliminary results from testing these materials will be presented.

Sandia National Laboratories is a multi-mission laboratory managed and operated by National Technology & Engineering Solutions of Sandia, LLC (NTESS), a wholly owned subsidiary of Honeywell International Inc., for the U.S. Department of Energy's National Nuclear Security Administration (DOE/NNSA) under contract DE-NA0003525.

[1] R. D. Kolasinski, C. -S. Wong, A. Engel, J. A. Whaley, F. I. Allen, and D. A. Buchenauer, J. Appl. Phys. 131 (2022) 063303.

POA-97

### **Effect of deuterium on defect evolution in tungsten**

Fredric Granberg<sup>1</sup>, Victor Lindblad<sup>1</sup>, Jintong Wu<sup>1</sup>, Daniel Mason<sup>2</sup>

<sup>1</sup>Department of Physics, University of Helsinki, Finland; <sup>2</sup>UK Atomic Energy Authority, United Kingdom.

Tungsten is the chosen material for the plasma facing components in fusion reactors. The wall material will not only be bombarded by energetic particles, but light ions will be able to diffuse into the material. Several experimental studies have shown that having deuterium present during irradiation will significantly affect the deuterium retention of the material [1], compared to a sample at the same dose without deuterium. This indicates that there are more vacancy-type defects present to accommodate them. A sample first irradiated and then subjected to deuterium showed around  $1.6 \times$  deuterium retention, which was explained by every vacancy in the sample being filled with around 5 deuterium atoms, which is the stable value predicted [2]. However, the greater defect accumulation when deuterium is present cannot be explained by this.

To understand the synergetic effect of deuterium and irradiation, high-dose irradiation simulations were carried out on different setups. Samples with deuterium present were compared to samples without deuterium at doses on the sub-dpa scale. We observed, as experimentally, that having deuterium present will increase the amount of retained defects, and therefore more overall deuterium retention [3]. Once the trend was confirmed, the factors leading to this were analysed. We found that several factors played a role in this discrepancy. We found that a greater number of defects are stable, if the vacancies are filled with deuterium compared to empty vacancies. Another factor was the recombination of Frenkel pairs is hindered by deuterium being present in the vacancies. The effect of larger defect structures, such as voids filled with deuterium or unfilled, were investigated, and their effect on defect production was studied.

[1] S. Markelj, T. Schwarz-Selinger, M. Pecovnik et al. Nucl. Fusion 59 (8) (2019) 086050

[2] D. R. Mason, F. Granberg, M. Boleining, et al. Phys. Rev. Mater. 5 (2021) 095403

[3] V. Lindblad, D. R. Mason, F. Granberg, J. Nucl. Mater. 603 (2025) 155422

POA-98

### **High-dose long-time defect evolution in tungsten studied by atomistically informed Object Kinetic Monte Carlo simulations**

Jintong Wu<sup>1</sup>, Juan-Pablo Balbuena<sup>2</sup>, Zhiwei Hu<sup>3</sup>, Ville Jantunen<sup>1</sup>, Marie-France Barthe<sup>3</sup>, Maria Jose Caturla<sup>4</sup>, Fredric Granberg<sup>1</sup>

<sup>1</sup>University of Helsinki, Finland; <sup>2</sup>Universidad de Alcala, Spain; <sup>3</sup>University of Orleans, France; <sup>4</sup>Universidad de Alicante, Spain.

Tungsten is one of the plasma-facing materials in proposed nuclear fusion reactors, due to its high melting point and high thermal conductivity. Irradiation of tungsten has been studied for decades, both computationally and experimentally. From the computational perspective, Molecular dynamics simulations can precisely give us the atomic-scale view, which is widely used to study the mechanisms behind defect production and evolution during prolonged irradiation.

Recent research has examined the feasibility of using cascade simulations [1] and integrating an accelerated method [2] to achieve high doses. While these accelerated techniques offer a more efficient means of reaching higher dose levels, they remain largely constrained to nanosecond timescales, leading to dose rates much higher than those observed experimentally. Furthermore, energetic cascades can significantly alter defect morphology, highlighting the need to account for overlap effects—an aspect often neglected in many large-scale simulation approaches. To address these challenges, our methodology combines molecular dynamics simulations with larger-scale models, specifically Object Kinetic Monte Carlo simulations. This hybrid approach aims to preserve atomic-level accuracy while achieving experimental dose rates. By comparing our results with conventional high-dose molecular dynamics simulations and experimental studies, we gain a more precise understanding of high-dose irradiation at realistic dose rates. Our developed workflow might solve the problems with existing workflows, where atomistic reactions affect the outcome at timescales far beyond the reach of the atomistic model itself.

[1] F. Granberg, J. Byggmästar, K. Nordlund, Journal of Nuclear Materials 556 (2021) 153158

[2] F. Granberg, D. R. Mason, J. Byggmästar. Computational Materials Science 217 (2023) 111902.

POA-99

### **ITER EU First Wall Panel CuCrZr cooling rate study**

Margherita Sardo<sup>1</sup>, Samuli Heikkinen<sup>2</sup>, Jose Miguel Pacheco Cansino<sup>2</sup>, Marta Freitas<sup>3</sup>, Nuno A. Marques<sup>3</sup>, Sergio A. Reis<sup>3</sup>, Monica Mendes Reis<sup>3</sup>

<sup>1</sup>ATG Europe, Italy; <sup>2</sup>Fusion for Energy, Spain; <sup>3</sup>Instituto de Soldadura e Qualidade (ISQ), Portugal.

ITER EU First Wall Panels (FWPs) contain CuCrZr-IG (ITER grade) as heat sink material, which is subject to thermo-mechanical loads during operation. The precipitation-hardening CuCrZr-IG alloy requires a solution annealing heat treatment with rapid cooling followed by ageing treatment to achieve the desired mechanical properties. In the past, a minimum cooling rate of 60°C/min after solution annealing was demonstrated to ensure the proper precipitation hardening. Due to the large FWPs size and dimension accuracy, gas cooling was chosen to avoid the large deformations and oxidation that quenching in water or oil would cause. The effectiveness of the treatment depends mostly on the part's mass, type of

gas used and furnace characteristics. A cooling rate of 60°C/min was proven difficult to be achieved using nitrogen because of FWP mass (around 1.5 tons), while the use of other gases (e.g. helium) is not economically viable for a large-scale FWP series manufacturing.

The cooling rate study is performed on samples of CuCrZr-IG to simulate the conditions the material will experience when incorporated into a full-scale panel. After solution annealing, different cooling rates (20°C/min, 30°C/min, 40°C/min, 50°C/min, 60°C/min) was tested to study mechanical and physical properties of CuCrZr-IG alloy, to see whether the slower cooling rate could be applied on full scale FWPs. The experimental results have shown that cooling rates, lower than 60°C/min, do not have a substantial detrimental effect on material strength, when all heat cycles that correspond to FWP manufacturing route are applied. Material subject to slower cooling rates have shown compliance with HIP manufacturing process requirements, in most cases.

The test results include yield strength, ultimate strength, elongation, grain size and hardness. Although there are no specific requirements regarding the hardness of the material, this property may serve as a future resource to predict other material properties without the need for destructive testing on full-scale FWPs.

CuCrZr-IG from two suppliers was tested. The effect of different cooling rates proven to be similar on the two supplier's materials, even though one supplier shows values consistently above the other, in absolute terms.

Disclaimer: The work leading to this publication has been funded by Fusion for Energy under contracts F4E-OMF-1019 and F4E-OMF-1082. This publication reflects the views only of the author, and Fusion for Energy cannot be held responsible for any use which may be made of the information contained therein.

## Poster session PO-B (Thursday)

22 May, 16:45 - 18:45

POB-1

### Plasma performance and qualification of optical plasma diagnostics at the JULE-PSI linear plasma generator

Michael Reinhart, Rahul Rayaprolu, Dirk Nicolai, Marc Sackers, Gennady Sergienko, Arkadi Kreter, Sebastian Brezinsek, Bernhard Unterberg, Christian Linsmeier

Forschungszentrum Jülich GmbH, Germany.

The new linear plasma generator JULE-PSI at Forschungszentrum Jülich [1] aims to conduct Plasma-Wall-Interaction Experiments with neutron-irradiated, activated materials and Tritium-containing plasma-facing materials. Prior to JULE-PSI being transferred to the Hot-Cell-Environment, where such samples can be handled, a systems & plasma commissioning phase outside the Hot Cell is ongoing.

The main goals of the commissioning phase are: 1) Testing of all relevant machine components, 2) Implementation of plasma diagnostic systems and 3) Optimization of the plasma scenarios and performance.

In this work, we present the following plasma diagnostic systems implemented and qualified at JULE-PSI: A Single-tip Langmuir probe, an optical emission spectrometer (OES, wavelength range 300–890 nm) and a 2D Hyperspectral Camera [2]. With these diagnostics, all important plasma parameters like electron temperature, electron density, ion flux density, plasma potential and plasma composition (impurities) can be measured, with the Langmuir probe and the Hyperspectral Camera also providing spatially resolved measurements to investigate radius and shape of the plasma column.

Results for different magnetic fieldline configurations in the arc discharge plasma source, as well as for different plasma species (Argon, Neon, Helium and Hydrogen) are presented. The results are compared between the different diagnostic methods and also to the other linear plasma generator at Forschungszentrum Jülich, PSI-2. We show that the plasma performance is very sensitive to the magnetic fieldline configuration. With optimised fieldline configuration, plasma density (up to  $10^{19} \text{ m}^{-3}$ ), electron temperature (up to 10 eV) and ion flux (up to  $10^{22} \text{ m}^{-2}\text{s}^{-1}$ ) exceed the values reached at PSI-2 for similar discharge powers, proving that JULE-PSI produces plasma efficiently. The radius and shape of the plasma column is also influenced by the magnetic field; the aim for JULE-PSI is to produce a plasma column of ~5 cm diameter with a flat-top plasma profile.

A special focus is on the reliability of the spectroscopic measurements compared to the Langmuir Probe measurements. Substituting the Langmuir probe as a standard diagnostic with passive diagnostics (OES or hyperspectral camera) is preferred for the future operation in a hot-cell environment. However, reaching the same accuracy of the Langmuir probe with a simple optical emission spectrometer proved to be difficult, and eventually more advanced diagnostics such as the 2D Hyperspectral camera are required for substituting the Langmuir probe measurements.

[1] B. Unterberg et al., Fusion Eng. Des. 86 (2011)

[2] C. Li et al., Rev. Sci. Instrum. 94, 083501 (2023)



POB-2

### **The DIII-D Full Wall Change-Out Project: High-Level Options and Key Research Considerations**

Tyler Abrams<sup>1</sup>, Florian Effenberg<sup>2</sup>, Andrea Garofalo<sup>1</sup>, Suk-Ho Hong<sup>1</sup>, Adam McLean<sup>3</sup>, Christopher Murphy<sup>1</sup>, Craig Petty<sup>1</sup>, Karl Schultz<sup>1</sup>, Morgan Shafer<sup>4</sup>, Gregory Sinclair<sup>1</sup>, Theresa Wilks<sup>5</sup>

<sup>1</sup>General Atomics, United States; <sup>2</sup>Princeton Plasma Physics Laboratory, Princeton, United States; <sup>3</sup>Lawrence Livermore National Laboratory, United States; <sup>4</sup>Oak Ridge National Laboratory, United States; <sup>5</sup>Massachusetts Institute of Technology, United States.

The DIII-D program is embarking on a project to replace all of its graphite plasma-facing component (PFC) surfaces with tungsten to address the key plasma-material interaction and core-edge integration challenges for fusion energy. The challenge lies in maintaining key DIII-D strengths: probing dissipative exhaust regimes, integrating reactor-relevant edge and pedestals, and developing and qualifying new core scenarios with PFCs made of a material that is widely accepted as reactor-relevant. Key challenges and proposed solutions for the transition of DIII-D to an all-W wall, which are being developed with extensive U.S. and international community consultation, will be discussed.

With an all-metal wall, fundamental changes to DIII-D start-up and conditioning procedures will occur. Plasma configurations and manipulation techniques are also being re-developed for the low carbon environment. Many diagnostic systems require substantial modification to continue to deliver essential program measurements, as well as new capabilities associated with the wall change mission. Retaining DIII-D's unique ability to reverse the toroidal magnetic field direction versus a "fish-scaling" approach to avoid leading edge metal melting is being analysed. DIII-D engineering teams are exploring a range of means to achieve decarbonisation as quickly as feasible. A staged implementation is proposed where the surfaces that experience higher heat flux are made of W, and the lower heat flux (including recessed) surfaces are made of W-coatings other metals, such as TZM, to accelerate the timeline. In later years the remaining parts of the wall will be changed to W, eventually including more innovative divertor elements (e.g., negative triangularity) and/or advanced tungsten alloys.

As fusion devices transition from carbon to metal walls, DIII-D is well-positioned to lead by supporting scenario development and wall integration. With its flexibility and advanced diagnostics, DIII-D will play a crucial role in integrating new materials, advancing ITER's mission, and addressing key research gaps essential for the development of U.S. fusion power plants (FPPs). Through international collaboration with long-pulse devices, DIII-D will utilize its unique capabilities to develop viable low-collisionality scenarios for ITER and FPPs.

Work supported by US DOE under DE-FC02-04ER54698, DE-AC02-09CH11466, DE-AC05-00OR22725, DE-AC52-07NA27344, and DE-SC0014264.

POB-4

### **SOLPS-ITER modelling of a deuterium plasma discharge in the GyM linear plasma device**

Alessio Villa<sup>1</sup>, Andrea Uccello<sup>2</sup>, Fabio Subba<sup>1</sup>, Matteo Passoni<sup>3</sup>, Irene Casiraghi<sup>2</sup>, Giuseppe Francesco Nallo<sup>1</sup>, Fabio Mombelli<sup>3</sup>, Alessandro Maffini<sup>3</sup>

<sup>1</sup>NEMO Group, Dipartimento di Energia, Politecnico di Torino, Italy; <sup>2</sup>Istituto per la Scienza e Tecnologia dei Plasmi, CNR, Italy; <sup>3</sup>Dipartimento di Energia, Politecnico di Milano, Italy.

Controlling plasma-wall interactions (PWIs) is a key challenge in the field of nuclear fusion, as it directly impacts the efficiency, safety, and operational reliability of future reactors. Linear

Plasma Devices, such as GyM, play a crucial role in studying PWIs by replicating charge-exchange neutral fluences characteristic of ITER's main chamber. Projectile energy is tuned via electrical target biasing [1].

The SOLPS-ITER code is employed to reproduce experimental trends of electron density and temperature observed in GyM. Originally developed for simulating the Scrape-Off Layer in toroidal devices, the code has been successfully applied to non-hydrogenic plasmas in GyM, including argon and helium [2]. The work on SOLPS-ITER provides experimental code validation in a regime with limited existing literature. Also, it helps to reveal physical mechanisms whose details are not completely apparent from measurements, and to potentially predict scenarios beyond experimental reach.

This study focuses on a deuterium plasma produced in GyM with a peak electron density of  $4.2 \times 10^{16} \text{ m}^{-3}$ , a peak electron temperature of 8.8 eV and a molecular deuterium pressure of  $5.7 \times 10^{-4}$  mbar. A sensitivity scan is conducted over pumping efficiency, cross-field anomalous transport coefficients and absorbed electron power. In the simulations, the absorption probability of neutral particles at the pumping surfaces ranges from 0.0070 to 0.0085, while cross-field anomalous transport coefficients vary between 0.25 and  $1.5 \text{ m}^2 \text{ s}^{-1}$ . The absorbed power is maintained between 300 and 600 W. The power deposition profile is discussed in terms of its radial and axial distribution. A comparison with GyM experimental trends demonstrates agreement with the measured density profiles well within 20%.

The output of this work will provide a plasma background which can represent the basis for further development of an integration with the ERO2.0 code, enabling the study of the impact on plasma-facing material properties.

Acknowledgements: the authors acknowledge the financial support of the European Union Next Generation EU and Italian Ministry of University and Research as part of the PRIN 2022 program, project “Nanomaterials for Fusion: experimental and modeling of nanostructured materials and plasma-material interactions for inertial & magnetic confinement fusion” (Project ID: 2022N5JBHT, CUP: D53D23002840006).

[1] A. Uccello, et al., *Front. Phys.* 11, 1108175 (2023).

[2] F. Mombelli, et al., *Nucl. Fusion* 65, 026023 (2024).

POB-5

### **Plasma modelling with SOLPS-ITER to support the design of the new high-density BiGyM linear plasma device**

Irene Casiraghi<sup>1</sup>, Jimmy Scionti<sup>1</sup>, William Bin<sup>1</sup>, Stefano Cipelli<sup>2</sup>, Daria Ricci<sup>1</sup>, Marcelo Baquero-Ruiz<sup>3</sup>, Ivo Furno<sup>3</sup>, Lyes Kadi<sup>3</sup>, Philippe Guittienne<sup>3</sup>, Christine Stollberg<sup>3</sup>, Renat Karimov<sup>3</sup>, Elena Tonello<sup>3</sup>, Andrea Uccello<sup>1</sup>

<sup>1</sup>Istituto per la Scienza e Tecnologia dei Plasmi, CNR, Milano, Italy; <sup>2</sup>CRF – Università degli Studi di Padova, Padova, Italy; <sup>3</sup>Swiss Plasma Center (SPC) – EPFL, Lausanne, Switzerland.

Plasma-material interactions are a critical challenge for future nuclear fusion reactors and are extensively studied in linear plasma devices (LPDs) such as GyM. This device operates within a plasma density range of  $10^{15}$ – $10^{17} \text{ m}^{-3}$ , electron temperatures below 15 eV, and ion fluxes up to  $10^{21} \text{ m}^{-2} \text{ s}^{-1}$ , making it suitable for investigating plasma-wall interactions in tokamak main chambers, excluding the divertor. To address plasma conditions relevant to divertors, characterised by densities of  $\sim 10^{19} \text{ m}^{-3}$  and ion fluxes approaching  $10^{23} \text{ m}^{-2} \text{ s}^{-1}$ , GyM is presently

being upgraded to BiGyM. BiGyM will feature helicon-wave-sustained plasmas generated by two 10 kW birdcage antennas operating at 13.56 MHz, like those of the RAID LPD [1], enabling high plasma densities. Additionally, BiGyM will be equipped with a LIBS diagnostic and a new axial sample exposure.

This contribution presents BiGyM and highlights ongoing design efforts, focusing on plasma modelling performed using the SOLPS-ITER code.

BiGyM modelling was informed by parametric studies of a RAID plasma, examining the impact of absorbed power, power density distribution profile, particle absorption at pumping surfaces, particle diffusion, and energy transport coefficients. RAID simulations were validated with experimental data collected by a pressure gauge sensor, a Thomson scattering system, a double Langmuir probe.

BiGyM simulations predict plasma conditions and explore their dependence upon input power and gas pressure. In particular, for a BiGyM helium plasma with representative operating conditions ( $B=20\text{mT}$ ,  $p_{\text{neutral}}=0.8\text{Pa}$ ,  $P_{\text{injected}}=3\text{kW}$ ), electron density and temperature along the axis were estimated at  $(1.5-2.0)\times 10^{19}\text{m}^{-3}$  and 4–5 eV, respectively. Various magnetic configurations and gas injection locations were also investigated. At a fixed absorbed power density, changes in plasma density and temperature remain within 15% across different magnetic configurations.

These findings provide crucial insights for BiGyM layout, vessel structure, and magnetic configuration, ensuring it achieves divertor-relevant plasma parameters.

#### Acknowledgments

This work has been carried out within the framework of Italian National Recovery and Resilience Plan (NRRP), funded by the European Union - NextGenerationEU (Mission 4, Component 2, Investment 3.1 - Area ESFRI Energy - Call for tender No. 3264 of 28-12-2021 of Italian University and Research Ministry (MUR), Project ID IR0000007, MUR Concession Decree No. 243 del 04/08/2022, CUP B53C22003070006, "NEFERTARI").

This work was partly funded by the Swiss National Science Foundation, Grant 200020-204983.

#### References

- [1] A.Uccello et al, Front. Phys. 11, 1108175 (2023)
- [2] I.Furno et al, EPJ Web Conf. 157, 03014 (2017)

POB-6

#### **Impact of nitrogen seeding on edge plasma transport on CFETR X-divertor with EMC3-EIRENE modelling**

Tian Xie<sup>1</sup>, Yujian Wang<sup>1</sup>, Hang Li<sup>2</sup>, Wei Zhang<sup>3</sup>, Dezhen Wang<sup>4</sup>

<sup>1</sup>Northeast Agricultural University, China; <sup>2</sup>College of Physics and Optoelectronic Engineering, Shenzhen University, China; <sup>3</sup> Institute of Plasma Physics, Chinese Academy of Sciences, China; <sup>4</sup>School of Physics, Dalian University of Technology, China.

The impact of nitrogen seeding on edge plasma transport on Chinese Fusion Engineering Testing Reactor (CFETR) X-divertor configuration has been investigated by three-dimensional (3D) Monte Carlo transport code EMC3-EIRENE[1-2]. The EMC3-EIRENE code has the ability of 3D magnetic configuration reconstruction, which enables us to estimate the effect of different nitrogen injection positions on 3D edge plasma transport behaviors[3-4]. The electron density and temperature profiles show a toroidally asymmetric distribution with upstream nitrogen

seeding, which is attributed to the non-uniform profile of nitrogen ions density and power dissipation in corresponding poloidal locations. While for downstream nitrogen seeding, the most nitrogen ions located in private flux region lead to a relatively symmetric distribution in toroidal direction. The deposition behavior of nitrogen impurity ions on 3D divertor plates of CFETR has been investigated to evaluate nitrogen seeding effect on the deposited profile of electron density and temperature. It is found that the upstream nitrogen seeding results in several lobe structures of deposition pattern for electron density and temperature on divertor targets, whereas a perturbed deposition profile is achieved for downstream nitrogen seeding.

Acknowledgements:

This work was supported by National Natural Science Foundation of China under Grant No. 12235002, 11805134, 12175273, National magnetic confinement fusion energy development research project under grant No. 2022YFE03190200 and Young Talents Project of Northeast Agricultural University No. 54970112.

[1] Feng Y. et al Contrib. Plasma Phys. 44 57–69 (2004)

[2] Reiter D. et al Fusion Sci. Technol. 47 172 (2005)

[3] Xie T. et al Nucl. Fusion 58 106017 (2018)

[4] Xie T. et al Plasma Phys. Control. Fusion 61 115006 (2019)

POB-7

### **LH Power and core line integrated density impact on impurity sources and W prompt re-deposition for various plasma shapes in WEST**

Alex Thomas Grosjean<sup>1</sup>, David Christian Donovan<sup>1</sup>, Pascal Devynck<sup>2</sup>, Nicolas Fedorczak<sup>2</sup>, Louis Fevre<sup>3</sup>, Jonathan Gerardin<sup>2</sup>, Jamie Gunn<sup>2</sup>, Christophe Guillemaut<sup>2</sup>, Benoit Guillermin<sup>2</sup>, Curtis A. Johnson<sup>4</sup>, Christopher C. Klepper<sup>4</sup>, Sean Robert Kosslow<sup>1</sup>, Brian Putra<sup>1</sup>, Nicolas Rivals<sup>2</sup>, Ezekial A. Unterberg<sup>4</sup>

<sup>1</sup>University of Tennessee Knoxville, United States; <sup>2</sup>CEA, IRFM, France; <sup>3</sup>Institut Jean Lamour IJL, Université de Lorraine, France; <sup>4</sup>Oak Ridge National Laboratory, United States.

WEST's unique characteristics with nearly all tungsten (W) PFCs offer an ideal platform to study plasma operations and plasma scenario development for long-pulsed, actively cooled, fully W-PFC tokamaks. W erosion/redeposition of the PFCs and the resulting pollution of the plasma will be a major challenge for next step devices, such as ITER and SPARC. In WEST, when the plasma is in a lower single null (LSN) configuration, the upper divertor is assumed to be a low impurity source relative to the lower divertor and limiters. However, the upper divertor is more poorly screened, which may result in a non-negligible source of core pollution. To investigate upper divertor impurity contribution to core pollution, a dedicated plasma shape change experiment was performed (420kA) during which the primary separatrix was driven away from the upper divertor (5/35/110/165mm) with a constant secondary X-point position in the same shot. These shapes were performed from ohmic-only discharges to 4MW of injected LH power for a range of core line integrated densities (+/-10% from reference) in order to characterize their impact on impurity sourcing and radiated power. A comprehensive array of diagnostic measurements were taken at/near the upper and lower divertor targets to measure  $n_e$ ,  $T_e$ , and impurity fractions near the target (BII, CII, NII, OII, and WI), obtained with the integrated multidiagnostic available at WEST [1]. The newly installed McPherson enabled W gross erosion (WI) and net erosion (WII) measurements. Experimental results from these shapes show significant differences in the impurity sources at the upper divertor (-90%), lower divertor inner

(+250%) and outer (+10–15%) targets for light impurities and W. The total radiated power also decreased from step to step (~5–10%). This increase in impurity sourcing from the inner lower divertor could be explained as open magnetic field lines coming from the boundary plasma stagnation point that intercepted the upper divertor prior to shifting the separatrix is now intercepting the inner divertor. The line integrated density scan performed does not seem to impact significantly impurity sources for the various shape tested. The power scan shows an increase of the impurity sources but do not seem to vary significantly their ratio from one shape to another. The decreased upper divertor contribution to core pollution is mainly compensated by the increase of lower inner divertor. This may suggest a core pollution to wall sources equilibrium in WEST which is hard to modify despite strong plasma shape changes.

Acknowledgements: This work is supported by the U.S. DOE under Grant Number DE-SC0020414.

[1] A. Grosjean et al., “Development of an Integrated Multidiagnostic to Assess the High-Z Impurity Fluxes in the Metallic Environment of WEST Using IMAS,” IEEE Transactions on Plasma Science, pp. 1–6, 2022, doi: 10.1109/TPS.2022.3187619.

POB-9

### **Deuterated ammonia formation, emission and dissociation in a nitrogen-seeded, Ohmic JET low-recycling plasma**

Roni Mäenpää<sup>1</sup>, Mathias Groth<sup>1</sup>, Henri Kumpulainen<sup>2</sup>, Andrew Meigs<sup>3</sup>, Ewa Pawelec<sup>4</sup>, Detlev Reiter<sup>5</sup>, Juri Romazanov<sup>2</sup>, Anthony Shaw<sup>3</sup>, Sebastijan Brezinsek<sup>2</sup>

<sup>1</sup>Aalto University, Finland; <sup>2</sup>Forschungszentrum Jülich GmbH, Germany; <sup>3</sup>UKAEA, United Kingdom; <sup>4</sup>Institute of Physics, University of Opole, Poland; <sup>5</sup>Institute for Laser and Plasma Physics, Heinrich-Heine-University, Germany.

A new deuterated ammonia (ND<sub>3</sub>) formation, emission and dissociation model implemented using the ERO2.0 Monte Carlo-code predicts a peak line-integrated ND band emission intensity 50% higher than measured by the vertically-viewing divertor spectrometer in nitrogen-seeded, low-recycling, Ohmically heated Joint European Torus (JET) plasmas [1]. By assuming a greater kinetic energy release (KER) of 10 eV instead of 1 eV upon the dissociation of ND<sub>3</sub> and its radicals, the model instead predicts a peak line-integrated ND band emission intensity 25% lower than measured. Together these predictions support the assumption of thermal re-release of incident nitrogen atoms and ions from the divertor targets as nitrogen molecules (N<sub>2</sub>) and ND<sub>3</sub> in equal fractions.

Band emission from the ND radical has previously been measured in nitrogen-seeded divertor plasmas in the JET and ASDEX Upgrade tokamaks [2, 3]. However, a comparison between measurements and a numerical model has been lacking. The model in this work makes use of the AMMONX database [4] for electron impact dissociation and ionization rates of ammonia molecules, and recent computational estimates of the electron impact excitation rates of the ND radical [5]. The fraction of incident nitrogen released as N<sub>2</sub> and ND<sub>3</sub> in the model is set to be independent of the surface temperature and material composition, and is consistent with the maximum rates of ammonia production observed in measurements of tokamak divertor plasmas [6] as well as with measurements performed in small-scale devices with high surface fluxes of reactive hydrogen and nitrogen species [7].

For JET Contributors, see the author list of “Overview of T and D-T results in JET with ITER-like wall” by CF Maggi et al. to be published in Nuclear Fusion Special Issue: Overview and Summary Papers from the 29th Fusion Energy Conference (London, UK, 16–21 October 2023)

- [1] M. Oberkofler et al. J. Nucl. Mater. 438 (2013) S258–S261
- [2] E. Pawelec et al. J. Phys.: Conf. Ser. 959 (2018) 012009
- [3] A. Drenik et al. Nucl. Fusion 59 (2019) 046010
- [4] S. Touchard et al. Nucl. Mater. Energy 18 (2019) 12–17
- [5] R. Snoeckx et al. Plasma Sources Sci. Technol. 32 (2023) 115020
- [6] T. Reichbauer et al. Fusion Eng. Des. 149 (2019) 111325
- [7] J. H. van Helden et al. J. Appl. Phys. 101 (2007) 043305

POB-10

### **Advantages of highly radiating plasma in negative triangularity for a stable plasma material interface**

Livia Casali<sup>1</sup>, David Eldon<sup>2</sup>, Tomas Odstroil<sup>2</sup>, Ray Mattes<sup>1</sup>, Austin Welsh<sup>1</sup>

<sup>1</sup>University of Tennessee, Knoxville, United States; <sup>2</sup>General Atomics, United States.

Highly radiating plasmas in strongly shaped negative triangularity (NT) have been demonstrated for the first time through the use of reactor-relevant seeding gases, i.e., neon, argon, and krypton, as extrinsic impurities featuring simultaneously high performance, divertor heat flux reduction and intrinsically no ELMs in the DIII-D tokamak [1]. We demonstrate that integration of NT configuration with high radiation can lead to confinement improvement with stabilization effects originating from collisionality,  $E \times B$  shear and profiles changes due to impurity radiation cooling. Simultaneously, a reduction of the divertor heat flux with increasing radiation has been demonstrated for all radiators and is well captured by SOLPS-ITER modeling with multi-impurities (D+C+Ar/Ne/Kr). Seeding with Kr and Ar lead to a reduction of the parallel heat flux at the divertor entrance compared to N and Ne effectively alleviating the power exhaust by reducing PSOL, which is one of the main advantages of working in NT configuration. Higher impurity compression for Ar and Kr is found compared to N and Ne. The high-Z impurities provide volumetric dissipation at lower concentrations at the separatrix up to ~90% in agreement with experimental estimates for fuel dilution. Thus, the same divertor conditions can be obtained with a reduced impurity concentration at the separatrix, which is important for core-edge integration. Matched discharges where only the B<sub>t</sub> direction was changed exhibit highly asymmetric emission well reproduced by SOLPS-ITER modeling which highlights the impact of drifts on impurity distribution, radiation and ionization pattern. Core-edge integrated simulations with the new developed SICAS code (SOLPS-ITER Coupled to ASTRA-STRAHL) [2] provides self-consistent background plasma and impurity transport from the divertor to the core with good agreements with experimental data. These results support that there is a path to highly radiating, high performance NT plasma with low PSOL which all enable a stable plasma material interface.

- [1] L. Casali et al 2025 Plasma Phys. Control. Fusion 67 025007, [2] A. Welsh et al 2025 Nucl. Fusion 65 044002

POB-11

### **Thermal modelling of ITER castellated fingers with phase change using control volume finite element method**

Matic Brank, Gregor Simic, Jernej Kovacic, Stefan Costea, Leon Bogdanovič, Miha Radež, Leon Kos

University of Ljubljana, Faculty of Mechanical Engineering, Slovenia.

The ITER first wall panels are built of castellated tungsten fingers with an advanced cooling system called hypervapotron. This design enables the first wall to withstand high heat loads arriving from the plasma while maintaining structural integrity with fast heat removal from the plasma-facing components (PFCs). This work presents a numerical study of thermal behaviour of castellated fingers that are subjugated to high heat loads. In our workflow first the spatially distributed heat loads to specific PFCs are assessed using the field-line tracing (FLT) techniques for a specific plasma configuration with an in-house FLT code named L2G [1]. The calculated heat fluxes are used as boundary conditions in the second step of the workflow, where a thermal model incorporates them together with the temperature dependent material properties to simulate a realistic plasma-wall interaction scenario. The heat equation for the PFC is then solved using control volume finite element method, developed in Python and optimized using Cython the result being the distribution of the temperature inside the PFCs. Additionally, OpenMP is used to utilize parallelisation for assembling the matrices and solving the system of equations. Phase change phenomena is explicitly considered here for potential melting of the PFC material under these extreme heat loads.

Results demonstrate the method's capability to predict temperature distributions across the castellated geometry for a realistic plasma scenarios. This model gives insight into temperature distribution on castellated fingers and gives more realistic insight into thermal loading of the ITER first wall. The model helps in understanding of where dangerous hot spots might form and how well the components can withstand plasma operation, which is crucial in the design of safe operational spaces for the reactor. This information is also valuable for improving the designing of future PFCs. The results presented here can be further used for thermomechanical studies to assess material deformation under high thermal loads or for synthetic diagnostic where radiation from the first wall can highly affect the interpretation of noise on diagnostic systems such as IR cameras, bolometers, etc.

[1] Gregor Simic, "Enhancements and applications of the SMITER magnetic field line tracing and heat load mapping code package," SOFE Conference, Oxford, UK, 2023.

[2] V. R. Voller, Basic Control Volume Finite Element Methods for Fluids and Solids. World Scientific Publishing Co., Pte. Ltd. 5 Tohccxxvc, 2009.

POB-12

### **In-vessel and depth-resolved hydrogen isotope composition analysis in JET by LIBS operated on a remote handling arm**

Rongxing Yi<sup>1</sup>, Rahul Rayaprolu<sup>1</sup>, Jari Likonen<sup>2</sup>, Salvatore Almagia<sup>3</sup>, Ionuț Jecu<sup>4</sup>, Gennady Sergienko<sup>1</sup>, Anna Widdowson<sup>4</sup>, Sahithya Atikukke<sup>5</sup>, Timo Dittmar<sup>1</sup>, Juuso Karhunen<sup>2</sup>, Pawel Gasior<sup>6</sup>, Marc Sackers<sup>1</sup>, Shweta Soni<sup>5</sup>, Erik Wüst<sup>1</sup>, Jelena Butikova<sup>7</sup>, Wojciech Gromelski<sup>6</sup>, Antti Hakola<sup>2</sup>, Indrek Jögi<sup>8</sup>, Peeter Paris<sup>8</sup>, Jasper Ristkok<sup>8</sup>, Pavel Veis<sup>5</sup>, Sebastijan Brezinsek<sup>1</sup>, The UKAEA RACE Team<sup>4</sup>

<sup>1</sup>Forschungszentrum Jülich GmbH, Germany; <sup>2</sup>VTT Technical Research Centre of Finland Ltd, Finland; <sup>3</sup>ENEA, Diagnostics and Metrology Laboratory, Italy; <sup>4</sup>UKAEA, Culham Campus, United Kingdom; <sup>5</sup>Comenius University, Faculty of Math, Physics and Informatics, Slovakia; <sup>6</sup>Institute of Plasma Physics and Laser Microfusion, Poland; <sup>7</sup>Institute of Solid State Physics, University of Latvia, Latvia; <sup>8</sup>University of Tartu, Institute of Physics, Estonia.

As the world's most successful Tokamak, JET achieved a groundbreaking milestone in nuclear fusion during its final deuterium-tritium experimental campaign (DTE-3) in 2023 by setting a new world energy record[1]. However, one critical safety aspect, the fuel retention distribution within the vessel walls after DTE-3, remains an unresolved challenge. To investigate

the fuel retention, a laser-induced breakdown spectroscopy (LIBS) system has been deployed. Compactly integrated into a laptop-sized box, the setup is mounted on a remote handling arm inside the JET vessel. Spectral data collected through this system is transmitted via a 20m long optical fiber and subsequently split among multiple spectrometers for analysis. This paper mainly focuses on the results from a Littrow spectrometer with large etendue and high spectral resolution ( $F/\#$  3.75,  $f=750\text{mm}$ ), which is used to record spectra of Hydrogen ( $\text{H}\alpha$ ) and its isotopes.

For the LIBS setup, the 800ps (10mJ) laser achieves a spatial and depth resolution of 130 $\mu\text{m}$  and 180nm on tungsten (1000 pulses), respectively. Meanwhile, the peaks of H isotopes present in the spectral window of 654–658nm can remain detectable for more than 18 $\mu\text{s}$  with this laser under Ar atmosphere at standard atmospheric pressure. Spectra obtained after different delay times show clearly that H and D can be separated after 8  $\mu\text{s}$ . However, D and T cannot yet be distinguished by visible inspection, therefore spectral fitting is the only viable method to extract T signal due to its lower concentration ratio and high full width at half maximum (FWHM).

During the LIBS measurement campaign, with the help of the remote handling arm, over 800 positions were analyzed in the W divertor, providing both spatial distribution and depth profiles of retained H isotopes after the complex post-DT clean-up phase in H and baking in JET, which is crucial for improving the safety and wall material design of future fusion reactors. Note, the tile will also be analyzed post-mortem with more advanced LIBS techniques such as DP-LIBS in tritium-compatible laboratory arrangements in FZJ in order to increase the LIBS LoD for Tritium further.

[1] <https://euro-fusion.org/eurofusion-news/dte3record/>

POB-13

### **Current Status of High Heat Flux Testing at the HELCZA facility**

Ladislav Vála, Richard Jílek, Tomáš Kubásek, Lukáš Toupal

Research Centre Řež (CVR), Czech Republic.

HELCZA is a High Heat Flux (HHF) test facility equipped with an electron beam gun of 800 kW power which is dedicated for testing large, full-scale mock-ups and plasma facing components (PFC) for fusion reactors. Recently the HELCZA facility finished an extensive test campaign of beryllium Full-Scale Prototypes (FSP) of the ITER First Wall and Alternative Design Mock-Ups (ADMU). Over a period of more than two years, this campaign rigorously evaluated the performance of the HELCZA facility in conducting fatigue testing under HHF conditions, with heat fluxes reaching up to 3 MW/m<sup>2</sup> on beryllium components. The successful outcome of this campaign demonstrates facility suitability for such demanding testing scenarios.

Due to ITER's transition from Beryllium to Tungsten First Wall (FW), the facility encounters new challenges. To enable the HHF testing of tungsten plasma facing components like the Inner Vertical Target (IVT) of the ITER divertor, while avoiding health and safety concerns associated with Beryllium, the comprehensive decontamination of the entire facility, all the auxiliary equipment and the HELCZA site was performed in 2024. As a next step, the efforts at the HELCZA facility are now focused on the qualifications and then subsequent HHF testing campaigns of large tungsten components such as IVT test assemblies.

Disclaimer: The work leading to this publication has been funded by Fusion for Energy



under contracts F4E-OPE-319-01 & 02 & 03. This publication reflects the views only of the authors, and Fusion for Energy cannot be held responsible for any use which may be made of the information contained therein.

POB-16

### **Different tungsten structure divertor performance on EAST**

Damao Yao

Institute of Plasma Physics, Hefei Institutes of Physical Science, Chinese Academy of Science, China.

ITER like monoblock structure tungsten divertor was developed and installed in EAST in 2014. Up to now the divertor operated ten years and different issue occurred in different campaign plasma operation. For examples: tungsten melt, cooling pipe leakage, joint leak and so on. To avoid tungsten melt divertor plate alignment was optimized, and joint structure was optimized to improve pipe to end-box welding properties. Monoblock capacity to remove heat load is limited and heat flux distribute not uniform or alignment is not so good will cause hot spot and tungsten melt. Another important problem is after years operation what about the interface of tungsten to copper and copper to CuCrZr pipe cannot be detected. UT detect was done for out of common monoblock unit showed defect occurred on the interface of W-Cu and Cu-CuCrZr.

To improve heat load remove capacity flat type tungsten divertor plate was developed. Mock-up test in electron beam facility showed even heat flux up to 20MW/m<sup>2</sup> temperature on tungsten surface still under 1000 centigrade degree. Flat type divertor plate was installed in EAST in 2020 and found heat flux on divertor plate is not uniform some tungsten slices on plate edge were crack, melt or break off. Plate was shaped to improve this issue. The performance of divertor plate also related with high energy particles deposit allocation and thickness of tungsten slices. Both physics and engineering are exploring to improve the performance.

POB-17

### **Interfacial mechanical properties of multilayer structures for high heat flux components of divertor**

Qianqian Lin, Lei Cao, Damao Yao

Institute of Plasma Physics, Hefei Institutes of Physical Science, Chinese Academy of Sciences, China.

The high heat flux components of the divertor are typically designed with multi-layer metal composite structures, where the mechanical properties of the interface are critical to the success or failure of the design. To obtain the data of interfacial mechanical properties, the special test specimens and fixtures were designed for mechanical property tests of two interfaces in W-Cu-CuCrZr-316 L four-layer materials. The uniaxial tensile testing (UTT) and shear tests were performed to obtain the tensile and shear strength of the interface and its toughness at room temperature. The problems of difficult clamping in the interface tensile test and deviation of shear surface in the interface shear test were solved by the novel structural design of specimens and fixtures. The Cu-CuCrZr interface of the specimens were fabricated by two different processes: vacuum brazing and hot isostatic pressing (HIP), and the effects of these two methods on the mechanical properties of the interfaces were compared. The strength and fracture characteristics of W-Cu interface, Cu-CuCrZr interface and Cu layer were analyzed and compared by fracture morphology and fracture topography. The results show that the vacuum brazing seemed to be superior to the HIP.

Acknowledgements: This work was supported by Comprehensive Research Facility for Fusion Technology Program of China under Contract No. 2018-000052-73-01-001228.

- [1] Philipps V. J. Nucl. Mater, 2011, 415(1): S2-S9
- [2] Mou N, Han L, Yao D, et al., Fusion Eng. Des., 2021, 169: 112670
- [3] Martin E, Camus G, Schlosser J, et al. J. Nucl. Mater. 2009, 386: 747-750
- [4] Yao D M, Luo G N, Zhou Z B, et al. Physica Scripta, 2015, 2016(T167): 014003
- [5] Lei L I, Le H A N, Pengfei Z I, et al. Plasma Sci. Technol., 2021, 23(9): 095601

POB-18

### **Structure design and brazing technologies for HFS first wall on the NBI shine-through area of the EAST device**

Xianke Yang<sup>1</sup>, Damao Yao<sup>2</sup>, Lei Yin<sup>2</sup>

<sup>1</sup>University of Science and Technology of China, China; <sup>2</sup>Institute of Plasma Physics, Hefei Institutes of Physical Science, Chinese Academy of Science, China.

To avoid high Z impurity sputtering due to plasma interaction and neutral beam injector (NBI) radiation, graphite is adopted as the plasma facing material (PFM) of the high field side (HFS) first wall on the NBI shine-through area (NBISTA). In the experimental advanced superconducting tokamak (EAST), graphite tiles are bolted to the CuCrZr heat sinks by screw on the NBISTA, but cracks, fractures and ablations were observed on the graphite tiles after experimental campaigns because of insufficient heat removal capability. Thus, a new structure design which adopting modular pattern panels with active cooling was proposed for the HFS first wall on the NBISTA. In the new design, graphite tiles were brazed to the CuCrZr heat sink, and the oxygen-free copper (OFC) sheet was adopted between graphite tiles and CuCrZr heat sinks as stress-buffer layer. Steady heat transfer analysis of those panels was carried out and results show that the heat removal capacity satisfied the required maximum heat load at 4.5 MW m<sup>-2</sup>. Meanwhile, AgCuTi foil filler and CuSnTi foil filler were used in the brazing technologies and one-step brazing was developed to achieve the bonding of graphite/OFC/CuCrZr. The optimum brazing process temperature curve was determined by scanning electron microscopy (SEM), energy dispersive spectrometry (EDS) and shear strength experiment. In addition, the mock-ups manufactured utilizing above brazing technologies endured cyclic high heat loads in the high heat flux (HHF) tests, which indicated that the graphite/OFC/CuCrZr bonding processed by one-step brazing had good heat removal capability.

Acknowledgements: This work was supported by MCF Energy R&D Program (2018YFE0312300), Comprehensive Research Facility for Fusion Technology Program of China under Contract No.2018-000052-73-01-001228 and the Science Foundation of the Institute of Plasma Physics, Chinese Academy of Sciences (Grant No.DSJJ-18-03).

- [1] Yao D, Bao L, Li J, et al., Plasma Science and Technology 10, 367(2008).
- [2] Zhao X, Wang Y, Hu C, et al., Journal of Fusion Energy 34,925(2015).
- [3] Mou N, Han L, Yao D, et al., Fusion Engineering and Design 169,112670(2021)
- [4] Li L, Han L, Zi P, et al., Plasma Science and Technology 23,095601(2021).

### **Qualification activities of thermally sprayed W-coated small-scale steel mock-ups of the DTT first wall modules**

Maurizio Furno Palumbo<sup>1</sup>, Gabriele De Sano<sup>2</sup>, Riccardo De Luca<sup>3</sup>, Matteo Iafrati<sup>3</sup>, Paolo Innocente<sup>4</sup>, Laura Laguardia<sup>5</sup>, Damiano Paoletti<sup>2</sup>, Gian Mario Polli<sup>2</sup>, Bruno Riccardi<sup>2</sup>, Selanna Roccella<sup>3</sup>, Rudolf Neu<sup>6</sup>, Bradute-Eugen Ghidersa<sup>7</sup>

<sup>1</sup>ENEA, Department of Fusion and Technology for Nuclear Safety and Security, Italy; <sup>2</sup>DTT S.c.a.r.l., Italy; <sup>3</sup>ENEA, Nuclear Department, Frascati, Italy; <sup>4</sup>CNR, Padova, Italy; <sup>5</sup>Istituto per la Scienza e Tecnologia dei Plasmi, CNR, Milano, Italy; <sup>6</sup>Max Planck Institute for Plasma Physics, Germany; <sup>7</sup>Karlsruhe Institute of Technology (KIT), Germany.

The current design of the First Wall (FW) of the Divertor Tokamak Test (DTT) facility [1] is mainly featured by actively cooled steel-based plasma-facing components (PFCs), provided of a tungsten (W) coating at both the Outboard Side (OFW) and the Inboard Side (IFW) of DTT. At the OFW the heat-sink design is based on steel plates with internal cooling channels, while at the IFW coaxial steel pipes are foreseen.

In order to qualify the design of the OFW-PFCs against thermal fatigue, small-scale mock-ups were manufactured by means of additive manufacturing technology, namely selective laser melting, and a W-coating was deposited on their plasma-facing surface. Since the requirements considered for the W-coating are dictated by the plasma-wall interaction due to the charge-exchange neutrals (CX), which are preferentially originating close to locations with external gas puffing, the OFW was chosen as reference for the coating qualification, requiring higher coating thicknesses. Plasma spraying (PS) is selected as deposition method.

This work presents i) the rationale of the selection and the optimization of the coating process – Air PS provided with Inert-Gas flowing – operated by tuning the relevant process parameters (i.e. spray efficiency, atmosphere control); ii) the results of the characterization of preliminary samples, according to a qualification scheme, mainly based on the porosity, purity, bonding and desorption tests; iii) the results of W deposition on the OFW small-scale mock-ups (~ 80x100 mm<sup>2</sup>) by using the optimized process parameters, and iv) the qualification of coatings with respect to the thermal fatigue by means of testing at the HELOKA facility where 5000 cycles at 0.5 MW/m<sup>2</sup> (with inlet water conditions relevant for DTT: 60 °C, 4 MPa and mass flow up to 3 kg/s) were performed.

Finally, ultrasonic tests carried out on the small-scale mock-ups with the aim to qualify both the design and manufacturing route are presented.

[1] F. Romanelli, et al. “Divertor Tokamak Test Facility project status of design and implementation”, Nuc. Fus. 64(11), 112015 (2024)

### **Engineering Overview of the Upgrade KSTAR Divertor System**

Sungjin Kwon<sup>1</sup>, Soo-Hyeon Park<sup>1</sup>, Yong Bok Chang<sup>1</sup>, Nak Hyong Song<sup>1</sup>, Hong-Tack Kim<sup>1</sup>, Sang Woo Kwag<sup>1</sup>, Hyung Ho Lee<sup>1</sup>, Jong Man Lee<sup>2</sup>, Hwnag Rae Cho<sup>2</sup>, Do Yoon Kim<sup>2</sup>, Soocheol Shin<sup>3</sup>, Henri Greuner<sup>4</sup>, Bernd Boeswirth<sup>4</sup>

<sup>1</sup>Korea Institute of Fusion Energy, Korea, Republic of; <sup>2</sup>Vitzrotech Co. Ltd., Korea, Republic of; <sup>3</sup>Tae Sung S&E Inc., Korea, Republic of; <sup>4</sup>Max Planck Institute for Plasma Physics, Germany.

The Korea Superconducting Tokamak Advanced Research (KSTAR) facility plans to enhance its heating system by upgrading the external heating power to 24 MW to sustain high-performance plasma operation for extended durations. The previous KSTAR divertor, which utilized carbon tiles without active cooling, was unable to withstand the increasing heat

power. Consequently, research for upgrading the KSTAR divertor system began in 2019. The upgraded KSTAR divertor system adopts a water-cooled tungsten monoblock concept, similar to the type used in ITER. Tungsten is the most robust and promising plasma-facing material in high heat flux plasma environments. Additionally, the combination of a CuCrZr heat sink and pressurized water coolant effectively dissipates the heat applied to the divertor. The upgraded divertor system features a single-null configuration and consists of 64 cassette divertor modules arranged at the bottom of the vacuum vessel. Each divertor module comprises an inner target, a central target, an outer target, and a cassette body, with support structures connecting the components.

In previous studies, CFD analyses were performed to validate the thermal stability of the entire divertor module. The results confirmed that the design could operate within the thermal allowable range at a heat flux of  $10 \text{ MW/m}^2$  [1]. To further assess the structural integrity under thermal loads and additional loads such as electromagnetic forces, dead weight, and seismic loads, the upgraded KSTAR divertor was evaluated for plastic collapse, ratcheting, fatigue, and buckling in accordance with ASME code standards. These analyses supported that the divertor is reliable from both thermal and mechanical perspectives. Furthermore, a 1,000-cycle high heat flux test was carried out under  $20 \text{ MW/m}^2$ , confirming that the design and quality of the KSTAR divertor target were sufficient to withstand thermal loads, despite the occurrence of tungsten recrystallization.

Based on the results of these engineering analyses and tests, the KSTAR divertor system was fabricated. The most critical manufacturing process involved joining two dissimilar metals: casting was used to bond tungsten to the Cu interlayer, while the Hot Isostatic Pressing (HIP) process was applied to join the Cu and the CuCrZr tube. Following the optimization of the manufacturing process and rigorous quality assurance procedures, the KSTAR divertor modules were sequentially fabricated and successfully installed in October 2023. Since installation, the divertor has completed two operational campaigns without any major issues and remains in reliable operation.

[1] S. Kwon et al., Fusion Science and Technology 77 699–709 (2021).

POB-24

### **Experimental and numerical study on ratcheting effects of CuCrZr as heat sink in divertor monoblock**

Peng Liu

Institute of Plasma Physics, Hefei Institutes of Physical Science, China.

CuCrZr has been chosen as the heat sink material for the divertor and blanket in the fusion machine, which will be subjected to alternating heat loads during operation. The CuCrZr material will undergo progressive cyclic deformation, resulting in ratcheting failure. It is essential to conduct experimental research on the ratcheting performance of the CuCrZr alloy under working conditions to provide test data and references for fatigue prediction. It is proved that the ratchet effect has a significant influence on the fatigue life of the CuCrZr material. Based on the uniaxial ratcheting tests at 300, the study examined the impact of stress amplitude and mean stress on ratcheting. Several models were used to correct the stress amplitude, the results show that Walker model and Goodman model are in good agreement with the experimental results, when substituted into Basquin equation for the ratchet fatigue prediction of CuCrZr alloy. A constitutive model was established based on the test results to describe the ratcheting

behavior of CuCrZr alloy at 300°C. The finite element simulation using the model was conducted for a ITER-like monoblock to evaluate the ratchet damage and fatigue of the CuCrZr heat sink tube.

POB-25

### **Manufacturing and high heat flux testing of advanced target mock-ups for the EU-DEMO Divertor target**

Pierdomenico Lorusso<sup>1</sup>, Selanna Roccella<sup>1</sup>, Mariano Di Bartolomeo<sup>1</sup>, Emanuele Cacciotti<sup>1</sup>, Marco Cerocchi<sup>1</sup>, Riccardo De Luca<sup>1</sup>, Luigi Verdini<sup>1</sup>, Katja Hunger<sup>2</sup>, Patrick Junghanns<sup>2</sup>, Alexander Von Mueller<sup>2</sup>, Henri Greuner<sup>2</sup>, Johann Riesch<sup>2</sup>, Jeong-Ha You<sup>2</sup>

<sup>1</sup>ENEA, Nuclear Department, Frascati, Italy; <sup>2</sup>Max Planck Institute for Plasma Physics, Germany.

Among the R&D tasks undertaken for the technological development of plasma facing components, a research activity has been undertaken in EUROfusion to pursue the consolidation and verification of the current target concepts envisioned for DEMO, i.e., the ITER-like baseline concept and the back-up concept with tungsten-fiber reinforced copper (Wf-Cu) pipes.

Focus has been addressed on the back-up solution (Wf-Cu pipes) finding alternative technological solutions for monoblock-pipe joining in order to reduce the use of materials having high activation and/or degradation under neutron irradiation. Among the brazing alloys tested for the monoblock/Wf-Cu pipe joint, the Gemco commercial alloy has been selected as the most suitable, thanks to its good joining capability and low content of Nickel, which suffers high neutron activation. However, the use of Wf-Cu pipes instead of standard CuCrZr ones makes difficult the joining, maybe because of the low coefficient of thermal expansion of the pipe due to the relevant content of W that makes difficult recover the gap between the surfaces to be joined (necessary for the assembly) during the brazing process. In order to exclude the eventual influence of the joining process parameters, a preliminary experimental sensitivity analysis has been carried out by realizing joining tests between W monoblocks and Wf-Cu pipes using Gemco, changing in each test one parameter at a time (i.e., Cu interlayer, monoblock-pipe free gap, thermal cycle, positions of the items in the furnace). Then, small mock-ups with four W monoblocks having different Cu interlayer thickness have been manufactured.

The present paper describes the manufacturing activities which led to the fabrication of small mock-ups. In particular, fabrication, testing at High Heat Flux (HHF) conditions and analyses of the ENEA-IPP-28 small mock-up are presented. Non-destructive examinations by ultrasonic testing have been performed pre- and post-HHF tests to assess the structural integrity of the mock-up and the reliability of the joining. Furthermore, microscopic examinations at different magnifications have been carried out to highlight microstructural modifications, recrystallization, and potential defect propagation due to thermal cycling.

POB-26

### **Tungsten Coating Options for Plasma-Facing Surfaces of an inertially cooled ITER First Wall**

Takeshi Hirai, Lei Chen, Franck Dechelette, Frederic Escourbiac, Ryan Hunt

ITER Organization, France.

One of the major changes in the new ITER baseline is inclusion of the tungsten (W) armour on the First Wall (FW) instead of beryllium [1]. A second important aspect of the new baseline is the introduction of a two-step assembly program in the ITER research plan for technical risk

mitigation. The first assembly includes installation of an inertially cooled temporary FW with W armour. This is later followed by the second assembly which installs an actively cooled W armour FW for fusion power operation. Tungsten coatings ( $\geq 20$  micro m) on stainless steel are an attractive option for less loaded areas of the temporary FW.

Various W coating production processes were assessed based on a literature study. Plasma spray and physical vapor deposition W coating processes were selected for sample production for tests. The test program includes characterization of W coatings (e.g. microstructural examination, outgas, bonding strength tests) and High heat flux (HHF) tests. The HHF test will assess thermal fatigue performance under long ( $>1$  s) and short ( $<2$  ms) pulse loadings.

This contribution reports the planned development and qualification of tungsten coatings for use at ITER.

Disclaimer: The views and opinions expressed herein do not necessarily reflect those of the ITER Organization.

[1] P. Barabaschi, et al., ITER Progresses into New Baseline, submitted to SOFT 2024.

POB-28

### **A Blanket Component Test Facility at General Atomics to Advance Fusion Technologies**

Giacomo Dose, Brian Grierson, Paul Beharrell, Kenneth Khumthong, Bruce Lombardo, Panto Mijatovic, Nikolai Norausky, Mark Tillack, David Weisberg

General Atomics, United States.

In this work, we present the preconceptual design of a non-nuclear, high field Blanket Component Test Facility (BCTF). The mission of BCTF is to test components at engineering-relevant scales and in prototypic thermal, hydraulic, and magnetic environments. Blanket components play a critical role inside a fusion reactor core since they are required to breed the tritium needed to reach fuel self-sufficiency. To achieve this goal, the blankets must incorporate a breeding material, generally containing lithium, which operates at high temperatures. However, current blanket technologies present a low readiness level ( $\sim 2-3$ ) since they have not yet been tested and qualified at reactor-relevant operating conditions. This technological gap is due, in part, to the lack of test stands for blanket components available to the fusion community. BCTF requirements have been developed with community input and include (i) magnetic field up to 8.5 T, representative of the field that tokamaks would experience at the inner midplane, (ii) large experimental volume of 0.75 m<sup>3</sup> (0.5x1x1.5 m<sup>3</sup>), (iii) liquid metal breeder loops at relevant temperatures (300–700 °C), (iv) surface ( $\sim$  MW/m<sup>2</sup>) and simulated volumetric heating ( $\sim$  MW/m<sup>3</sup>), and (v) auxiliary coolant and heat rejection loops (e.g. 8 MPa helium). This allows for the reproduction of the relevant non-nuclear environment to qualify meter-scale blanket components and to identify the failure modes due to slow electromagnetic transients, thermal fatigue, creep, and corrosion/erosion due to the liquid metals (e.g., Li, PbLi). Moreover, the facility allows operation at high Hartmann and Reynolds number ( $1e4 - 1e5$ ), which provides an appropriate platform to experimentally benchmark and validate the models simulating mass and heat transport in MHD forced convection flow. The preliminary process flow diagram of the facility as well as the piping and instrumentation diagram will be shown, with the aim of assessing the feasibility of the concept and identifying the critical aspects of the design. The total cost and duration of the BCTF is minimized by incorporating infrastructure and capability developed during fabrication of the ITER central solenoid (CS), including excess Nb<sub>3</sub>Sn CS

conductor and a supercritical helium cryoplant.

Acknowledgements: Work supported by General Atomics corporate funding.

POB-29

### **Linear Stability of Liquid Metal Free-Surface Flows on Inclined and Cylindrical Substrates: Effects of Transverse Magnetic Fields**

Simone Mingozzi<sup>1</sup>, Eric Favre<sup>2</sup>, Ricardo Puente<sup>2</sup>, Thomas Morgan<sup>3</sup>, Alessandro Tassone<sup>4</sup>

<sup>1</sup>Renaissance Fusion and Technical University of Eindhoven, France; <sup>2</sup>Renaissance Fusion, France; <sup>3</sup>Dutch Institute for Fundamental Energy Research, Netherlands; <sup>4</sup>Sapienza University of Rome, Italy.

Liquid Metals (LMs) are pursued for Plasma-Facing Components (PFCs) by public and private nuclear fusion programs. For instance, Renaissance Fusion coated the interior of a cylindrical chamber with a thick LM layer at room temperature, flowing at speeds of order 1 m/s. The company is now developing improved experiments at fusion-relevant temperatures and with fusion-relevant, Lithium-based liquids. The stability of such fast, curved, free-surface LM flows in an external magnetic field is relatively understudied at the present. The present study contributes to filling that gap.

Specifically, we conduct a linear stability analysis accounting for both capillary and Magneto-Hydro-Dynamic (MHD) effects under the inductionless approximation. The analysis assumes base flow configurations with a single non-zero component of the velocity field. Case studies are defined by a geometrical configuration, the key dimensionless numbers (i.e., Reynolds, Froude, Weber, Hartmann, Stuart numbers) and the corresponding steady-state unperturbed base flow solutions. The perturbation equations are then formulated retaining their primitive format stemming from the linearisation of the Navier-Stokes and MHD equations. The resulting differential eigenvalue problem is ultimately solved using the finite elements software COMSOL Multiphysics®. The eigenspectrum and eigenfunctions are analyzed to identify potential instabilities in the assessed configurations.

The computational setup is validated against existing literature, covering both non-MHD and MHD cases. Two MHD LM flow configurations subjected to a flow-transverse uniform magnetic field are then examined: (i) a free-surface LM layer flowing onto an inclined plate and (ii) a thick, suspended, free-surface LM layer flowing over the inside of a cylindrical substrate.

The study aims at the onset of instabilities and focuses on the influence of a transverse magnetic field, providing insights for future LM wall investigations and designs.

POB-30

### **EMC3-EIRENE simulations of boron transport in wall conditioning experiments on EAST upgraded divertor**

Yan Qin<sup>1</sup>, Tian Xie<sup>1</sup>, Guizhong Zuo<sup>2</sup>, Wei Zhang<sup>2</sup>, Jiansheng Hu<sup>2</sup>, Yühe Feng<sup>3</sup>

<sup>1</sup>Northeast Agricultural University, China; <sup>2</sup>Institute of Plasma Physics, Chinese Academy of Sciences, China; <sup>3</sup>Max-Planck-Institut für Plasmaphysik, Germany.

Three-dimensional (3D) coupled plasma fluid and kinetic neutral edge transport Monte Carlo code EMC3-EIRENE has been used to study boron (B) transport in EAST H-mode experiments with B powder injected at top J port for real-time wall conditioning. A good agreement between experimental measurements and simulation results has been obtained for the electron density and temperature profile with the help of the parameters scanning of particle and energy cross-field transport coefficients. The transport characteristic of B(1~3)+ ions shows an

asymmetry distribution along toroidal direction while a symmetry distribution is gained for B(4-5)+ ions. The calculated profile of B(1~3)+ ions mostly locate at the upper private region, which is attributed to the dominated friction force. While the B(4-5)+ ions penetrate into the closed magnetic surface due to the leading thermal force, which exhibits a uniform density distribution at closed magnetic surface. The comparative study indicates that B(1~3)+ ions have a more obvious impurity screening effect, in comparison with B(4-5)+ ions. The impact of B powder injection on the divertor flux deposition has been investigated by the EMC3-EIRENE code. The simulated profile of heat flux and particle flux deposited on lower divertor plates shows a moderate reduction compared with no B powder injection scenario.

POB-31

### **Initial physics assessment of liquid lithium divertor for the DIII-D tokamak**

Gregory Sinclair, Tyler Abrams, Giacomo Dose  
General Atomics, San Diego, United States.

Outfitting a portion of the lower divertor of the DIII-D tokamak with liquid lithium (Li) surfaces is predicted to yield moderate decreases in target plasma temperatures without significant dilution or plasma cooling inside the separatrix. Simulations of stationary DIII-D plasma discharges diverting to lithium divertor targets were performed using the plasma solver package SOLPS-ITER coupled to a lithium sputtering/evaporation model [1]. For an incident heat flux of  $5 \text{ MW m}^{-2}$ , the Li surface reaches an equilibrium temperature  $\sim 850 \text{ C}$ , as estimated using a time-dependent, multi-phase thermal model. Due to significant adatom erosion and evaporation at high surface temperatures, moderate changes in the incident plasma temperature have no effect on the total erosion rate. Impurity radiation increases near the cool edge (compared to using C) but decreases further upstream. Varying the incident heat flux (via changes to injected power) and the Li divertor coverage indicate viable operating windows to produce plasmas that minimize surface erosion and fuel dilution. Li may be used as an alternative plasma-facing wall solution in future devices due to its low recycling and plasma contamination potential. As a second phase of the project to upgrade the DIII-D plasma-facing wall to tungsten [2], periodic replacements of the lower divertor are envisioned to close gaps in power exhaust and advanced materials. The physics basis for a liquid Li divertor in DIII-D is thus being developed to inform prospects for future engineering, installation, and operation activities. Additional physics effects, such as the recycling rate on Li surfaces and the impact of erosion on heat flux mitigation will also be examined.

Acknowledgements: Work supported by General Atomics corporate funding.

[1] T. Abrams et al., Nucl. Fusion 56, 016022 (2015)

[2] T. Abrams et al., this conference.

POB-32

### **SOLPS-ITER Predictions for Upstream Impurity Concentration Dependence on Deuterium Recycling in the Spherical Tokamak Advanced Reactor (STAR)**

Eric Emdee, Thomas Brown, Robert Goldston, Andrei Khodak, Rajesh Maingi, Jonathan Menard  
Princeton Plasma Physics Laboratory, United States.

Creating acceptable divertor heat fluxes while maintaining low upstream plasma dilution is a critical step for designing a viable fusion reactor. Flowing liquid metal divertors provide an



attractive pathway to lowering the PFC temperature for a given heat flux [1]. However, liquid lithium is also well known to reduce deuterium recycling when the lithium surface temperature is below some critical value, typically taken to be 420°C [2]. In this presentation, we quantify the effect of recycling reductions on the upstream impurity leakage with a flowing liquid lithium target. SOLPS-ITER, a couple fluid-kinetic plasma edge code, is used to predict impurity concentration at the Last Closed Flux Surface (LCFS) in the Spherical Tokamak Advanced Reactor (STAR), an FPP design with SOL power of 135MW. An analytical model for the target temperature of a Capillary Porous Surface with Fast flowing liquid lithium (CPSF) [3], coupled with SOLPS-ITER, has been developed previously for predictive modeling of NSTX-U [4]. This target temperature coupling provides self-consistent, radially varying lithium emission from the target, assuming lithium flows radially across the plasma impinging surface. Results show that the average lithium concentration at the last closed flux surface can be made to be below 0.03, given the correct combination of deuterium gas puffing and neon injection, at flow speeds of 1 m/s for a variety of uniform deuterium target recycling coefficients. Zeff values of less than 2.5 were simultaneously achieved, indicating an acceptable reactor operation space is possible [5]. Due to the strong temperature variations as lithium flows radially across the target in this design, radial variation of deuterium recycling is expected. In addition to the temperature calculation with uniform recycling coefficient, a simultaneous calculation with radially varying deuterium recycling coefficient is presented. The deuterium recycling coefficient model assumes Langmuir flux of deuterium from the walls based on LiD decomposition studies [6], and takes into account SOLPS calculated deuterium flux into the target.

[1] P. Rindt, T.W. Morgan, G.G. van Eden, et al. Nucl. Fusion 59 056003 (2019)

[2] M. Morbey et al. PSI-26 Presentation (2024)

[3] A. Khodak and R.M. Maingi Phys. Plasmas 29 072505 (2022)

[4] E.D. Emdee, R.J. Goldston, A. Khodak, et al. Nucl. Fusion 64 086047 (2024)

[5] C.E. Kessel, D.B. Batchelor, P.T. Bonoli, et al. Fus. Eng. and Design 135 356–369 (2018)

[6] E. Veleckis J. Nucl. Mater 79 20–27 (1979)

POB-33

### **Impact of boron injection location on divertor heat flux in EAST wall conditioning experiments with EMC3-EIRENE modelling**

Baizeng Li<sup>1</sup>, Tian Xie<sup>1</sup>, Guizhong Zuo<sup>2</sup>, Wei Zhang<sup>2</sup>, Jiansheng Hu<sup>2</sup>, Yühe Feng<sup>3</sup>, Dezhen Wang<sup>4</sup>

<sup>1</sup>Northeast Agricultural University, China; <sup>2</sup> Institute of Plasma Physics, Chinese Academy of Sciences, China; <sup>3</sup>Max-Planck-Institut für Plasmaphysik, Germany; <sup>4</sup>School of Physics, Dalian University of Technology, China.

The heat flux deposition on divertor plates in EAST H-mode plasma experiments with boron powder injection for real-time wall conditioning has been investigated by three-dimensional (3D) Edge Monte Carlo transport code EMC3-EIRENE. The simulated profiles of electron density and temperature are consistent with experimental measurements by edge reciprocating Langmuir probe installed on EAST with the help of the scanning study of anomalous particle and energy transport coefficients. In order to acquire mitigation of plasma-material interactions, boron powder injected at different poloidal locations has been investigated to evaluate its influence on heat flux deposition on divertor plates. It is found that boron powder injected at inner and outer strike points gives rise to a toroidally asymmetric profile of heat flux deposition on the in- and out-board divertor targets, respectively. The 3D effects of the boron radiation on the heat flux distribution have been performed by using field line tracing technique, which indicates that boron impurity injected at the lower strike points can radiate more power and

result in a lower heat flux distribution compared with boron impurity injected at upstream.

POB-38

### **Thermal shock resistance of a tungsten-diamond composite under extreme transient heat loads**

Christophe Guillemaut<sup>1</sup>, Marianne Richou<sup>1</sup>, Mathilde Diez<sup>1</sup>, Steven Lisgo<sup>2</sup>, Martiane Cabie<sup>3</sup>, Alan Durif<sup>1</sup>, Laurent Gallais<sup>4</sup>, Jean-Laurent Gardarein<sup>5</sup>, Jonathan Gaspar<sup>6</sup>, Benoit Guillermin<sup>1</sup>, Jamie Gunn<sup>1</sup>, Celine Martin<sup>5</sup>, Marco Minissale<sup>5</sup>, Gregory de Temmerman<sup>7</sup>

<sup>1</sup>CEA, IRFM, France; <sup>2</sup>Independent Researcher, Canada; <sup>3</sup>Aix-Marseille Univ, CNRS, CP2M, France; <sup>4</sup>Aix-Marseille University, CNRS, Centrale Marseille, Institut Fresnel, France; <sup>5</sup>Aix-Marseille University, CNRS, PIIM, France; <sup>6</sup>CNRS, IUSTI, France; <sup>7</sup>Zenon Research, France.

High heat flux components damage under repetitive thermal shocks is a concern for long-term operations of magnetic confinement fusion devices. Typically, armor materials for these components involve refractory high Z metals like tungsten (W). Despite W high melting point and very good tolerance for erosion, its poor thermal properties (thermal conductivity of  $\sim 100 \text{ W.m}^{-1}\text{K}^{-1}$  at  $20^\circ\text{C}$  for W) make it prone to very high thermomechanical stresses during thermal shocks leading to recrystallization, cracking and melting.

On the other hand, the very high thermal conductivity of Chemical Vapor Deposition (CVD) diamond ( $\sim 2000 \text{ W.m}^{-1}\text{K}^{-1}$  at  $20^\circ\text{C}$ ) allows outstanding performances under thermal shocks [1] but its erosion properties are comparable to graphite [2]. In this context, tungsten-diamond test samples made of a  $\sim 1 \text{ mm}$  thick CVD diamond substrate for a uniform and fast distribution of heat with a  $\sim 10 \text{ m W}$  coating for protection against erosion were manufactured.

The objective at this stage was to verify the viability of the metal-diamond interface under fusion relevant thermal shocks. In order to find an optimal design, various options were considered: mono and poly-crystal CVD diamond substrates, different thickness of CVD diamond substrates, pure W coatings and a molybdenum interlayer between the W coating and the diamond substrate. Different levels of thermal shocks were also performed with a laser [3,4] on these samples:

- up to 10000 cycles of 1 ms at  $0.6\text{--}3 \text{ GW.m}^{-2}$  to simulate fast transients like edge-localized modes, disruptions and runaway electrons,
- up to 20 cycles of 1 s at  $100 \text{ MW.m}^{-2}$  to simulate the reattachment of the divertor plasma.

Microscopic inspection as well as focused ion beam analysis performed on the post-mortem samples showed pristine W coatings and W-diamond interfaces for all samples tested under slow transients at  $100 \text{ MW.m}^{-2}$  and for the samples tested under fast transients up to  $1.7\text{--}2 \text{ GW.m}^{-2}$  included. For comparison, test bulk W samples of the same dimensions cut from ITER-grade W monoblocks [5] showed cracked and melted surfaces at the lowest thermal loads and extending with the power density.

A modelling effort of these experiments was also carried out with COMSOL to help understand the behavior of the samples under thermal shocks.

[1] G. de Temmerman et al., Nucl. Fusion 51 (2011) 052001

[2] G. de Temmerman et al., Phys. Scr. T138 (2009) 014013

[3] M. Minissale et al., Rev. Sci. Instrum. 91 (2020) 035102

[4] T. Vidal et al., J. Nuc. Mater. 530 (2020) 151944

[5] T. Hirai et al., Journal of Nuclear Materials 463 (2015) 1248–1251

POB-39

### **Innovative STEAM Heat Shield for Ultra-High Heat Flux in Tokamak Divertors**

Jan Horacek<sup>1</sup>, Vaclav Sedmidubsky<sup>2</sup>, Anna Horacek<sup>2</sup>, Jan Prevratil<sup>1</sup>, Maria Reji<sup>1</sup>, Tomas Plechacek<sup>2</sup>, Marek Janata<sup>1</sup>, Zdenek Kutilek<sup>1</sup>, Lukas Sedlacek<sup>1</sup>, Michal Bousek<sup>1</sup>, Tomas Romsy<sup>3</sup>, Pavel Zacha<sup>3</sup>, Zdenek Vesely<sup>4</sup>, Matej Hruska<sup>4</sup>, Jan Hruby<sup>5</sup>, Matěj Peterka<sup>1</sup>, Slavomir Entler<sup>1</sup>

<sup>1</sup>Institute of Plasma Physics, Czech Academy of Sciences, Czech Republic; <sup>2</sup>Faculty of Nuclear Sciences, Czech Technical University, Czech Republic; <sup>3</sup>Faculty of Mechanical Engineering, Czech Technical University, Czech Republic; <sup>4</sup> New Technologies Research Centre, University of West Bohemia, Czech Republic; <sup>5</sup>Institute of Thermomechanics, Czech Academy of Sciences, Czech Republic.

This study presents an innovative STEAM heat shield designed for tokamak divertors, however, might be useful also in microwave gyrotrons, microelectronics, rocket combustion chambers, military etc. Our innovative heat shield, utilizing a lamellated copper plate and water boiling (without pressure rise), was tested under an air plasmatron jet, validated by heat transfer simulations and the heat flux quantified by several independent thermovision and calorimetry methods. Experimental results demonstrated the system's ability to withstand ultra-high steady-state heat flux. After minor melting quantifying the critical heat flux limit, the shield absorbed 36 kW with 43 MW/m<sup>2</sup> for an additional 22 minutes without further damage and no observed time limit. This seems to be a world record among known steady-state heat shield technologies. This may relieve the long-standing thermonuclear fusion devices challenge that plasma load in tokamak divertors must be suppressed below 20 MW/m<sup>2</sup>. Significant improvement of STEAM is possible via further geometry optimization, increasing the water speed and pressure (so far only 1/4 litres per second at few bars inlet).

POB-40

### **Thermal analysis of the W/Cu flat-type component as the lower divertor target in EAST**

Junling Chen, Dahuan Zhu, Chunyu He, Binfu Gao, Wenxue Fu, Rui Ding

Institute of Plasma Physics, Chinese Academy of Sciences, China.

Tungsten-copper flat-type component is one of the candidates for plasma-facing components for the future fusion devices, owing to its flexible heat sink design and thus possible high heat load exhaust capacity, making it a focus of significant research interest. Since 2021, a self-designed and manufactured high performance W/Cu flat-type component have been installed and tested on the outer horizontal target of the lower divertor in EAST. However, many damages in form of melting, cracking and exfoliation were found after cyclic plasma discharges. To evaluate the thermal performance of W/Cu flat-type components with different chamfers, especially the maximum parallel heat flux they can withstand, Fluent is employed to calculate the temperature distribution, which can provide scientific guidance for plasma operations.

Such simulation considered the actual experimental conditions including in-situ heat flux distribution, where installation misalignment was controlled within 0.6 mm, the heat flux incident angle was limited to no more than 5°, and when the absolute value of the toroidal magnetic field exceeded 2 T, the incident angle was kept below 3.7°. For W/Cu flat-type components with chamfer angles of 3.76° and 5.19°, the parallel heat flux required to melt OFC is always lower than that for W, indicating that OFC may be melted first. However, for the component with 2.4° chamfer, OFC also melts first when the heat flux incident angle exceeds 2.5°, while W melts first when the incident angle is below 2.5°. Additionally, a linear relationship between the maximum temperatures of W and OFC was founded, and this linear function varies with the in-

cident angle, which provide a basis for monitoring the temperature of OFC in EAST's flat-type components.

Such simulation and analysis offer key data for the plasma operation of EAST, and provide unique reference for application of W/Cu flat-type components in other devices.

POB-43

### **Thermal fatigue study of different advanced tungsten materials at a wide Gaussian power density distribution at the OLMAT high heat flux facility**

Daniel Alegre<sup>1</sup>, Pablo Fernández-Mayo<sup>1</sup>, David Tafalla<sup>1</sup>, Alfonso De Castro<sup>1</sup>, Jesus G. Manchon<sup>1</sup>, Sophie Shick<sup>1</sup>, Carmen Garcia Rosales<sup>2</sup>, Elisa Sal<sup>2</sup>, Marius Wirtz<sup>3</sup>, Jan Coenen<sup>3</sup>, Yiran Mao<sup>3</sup>, Eider Oyarzabal<sup>1</sup>, The OLMAT Team<sup>1</sup>

<sup>1</sup>Laboratorio Nacional de Fusion, CIEMAT, Spain; <sup>2</sup>Ceit Technology Center (Centro de Estudios e Investigaciones Técnicas), Spain; <sup>3</sup>Forschungszentrum Jülich GmbH, Germany.

The expected lifetime of plasma-facing materials is one of the main reasons for the difficulties in achieving an economically viable nuclear fusion reactor, in both the divertor and main wall areas. New and different advanced armor concepts are being studied for both areas, as their steady state and transients heat loads are very different [1].

The OLMAT High Heat Flux (HHF) facility, described in [2], has already demonstrated its capabilities for thermal fatigue testing of different advanced tungsten materials under conditions close to those in a future reactor [3]. In this work, the wide NBI beam (20 cm) has been taken advantage of to simultaneously expose 30 tungsten samples of different types to a Gaussian power density distribution between 1 and 14 MW/m<sup>2</sup> (the expected steady state heat loads in EU-DEMO [1]): 10 PM-Wf/W [4]; 11 ITER-like W; 7 WCrYZr self-passivating alloy [5]; and 2 porous tungsten samples produced by additive manufacturing by the company AENIUM (whose quality needs to be improved). A total of 2000 pulses of 100 ms duration were applied at a mean temperature of 200–300 °C. This is about half the expected number of pulses in the EU-DEMO divertor armor.

All ITER-like W and WCrYZr samples showed surface intergranular cracks increasing in number and length with power density, even at values as low as 1 MW/m<sup>2</sup>. These results are in contrast to other HHF devices where no damage was observed below a certain threshold (approximately <7 MW/m<sup>2</sup>). This enhanced cracking is thought to be related to the H embrittlement caused by the high energy of the H particles in the OLMAT beam: 10–30 keV, in the order of the expected particle energy of ELMs in the EU-DEMO, even mitigated (as mainly the particle flux is reduced). The PM-Wf/W has showed cracks only in the W fibers themselves, which is not expected to affect its macroscopic properties. The implications of the findings of this work for the EU-DEMO operation are discussed, as they may indicate significant damage even by mitigated ELMs in some parts of the main wall (expected to last many years).

[1] F.Maviglia et al. Nucl. Mat. Ener. 26, 100897 (2021)

[2] D.Alegre et al. J. Fus. Energy. 39, 411 (2020)

[3] D. Alegre et al. Nucl. Mat. Ener. 38, 201615 (2024)

[4] Y.Mao et al. Mat. Sci. Eng. A. 817, 141361 (2021)

[5] E. Sal et al., Nucl. Mat. Ener. 24, 100770 (2020)

POB-44

### **Optical Spectroscopy as a diagnostic tool at the high heat flux test facility GLADIS**

Hans Maier<sup>1</sup>, Henri Greuner<sup>1</sup>, Johann Riesch<sup>1</sup>, Bernd Boeswirth<sup>1</sup>, Rudolf Neu<sup>1</sup>, Adam Kuang<sup>2</sup>, Jason Trelewicz<sup>3</sup>

<sup>1</sup>Max Planck Institute for Plasma Physics, Germany; <sup>2</sup>Commonwealth Fusion Systems, MA, United States; <sup>3</sup>Stony Brook University, NY, United States.

The interaction of a plasma-facing material with an energetic hydrogen beam can lead to electronic excitation of atoms ejected from the target. After excitation, each chemical element emits a unique set of spectral lines.

GLADIS [1] is a high heat flux test facility equipped with two 1 MW hydrogen ion sources, which can each provide a Gaussian beam with central power densities of 5 – 45 MW/m<sup>2</sup> and a FWHM of 150 mm.

The facility was recently equipped with a spectrometer with a spectral range of about 270 nm – 800 nm and a 4096 pixel CMOS detector. Light is coupled into the spectrometer by using an optical fibre. Therefore, the collector optics can be placed at any available window on the vacuum vessel.

At GLADIS optical spectroscopy can be employed for various different purposes, for which also different lines of sight are used:

The tested object can be placed in the line of sight of the collector optics. In this geometry light emitted from the surface of the tested object is guided into the spectrometer together with line radiation from excited atoms emitted from the surface of the tested object and light emitted by hydrogen. This has the disadvantage that at high surface temperatures the spectrum may be dominated by the Planck radiation emitted from the hot test object.

This effect can be eliminated by placing the line of sight of the collector optics tangential to the irradiated surface of the test object. In this geometry the collection of perturbing Planck radiation can be nearly fully avoided and only emission from excited atoms originating from the test object surface is collected (besides radiation from hydrogen). In both geometries, samples of tungsten (heavy) alloys, e.g. W-Ni-Fe or W-Ti-Cr have been analysed. The time-resolved measurements recorded during GLADIS pulses show that the intensity of the collected line radiation scales rather well with the vapour pressures of alloying metals.

In addition, optical spectroscopy can also be used to gather information about the GLADIS hydrogen beam itself: If a geometry is employed, which avoids the collection of light from the target, one can very well observe the Balmer series together with its Doppler-shifted components stemming from accelerated hydrogen.

Examples on those different applications will be shown.

[1] H. Greuner et al., J. Nucl. Mater. 367–370 (2007) 1444

POB-45

### **Development of inhomogeneous high heat flux loading pattern for mimicking loading conditions of plasma-facing materials in tokamaks**

Daniel Dorow-Gerspach<sup>1</sup>, Renaud Dejarnac<sup>2</sup>, Gerald Pintsuk<sup>1</sup>, Marius Wirtz<sup>1</sup>, Christian Linsmeier<sup>1</sup>

<sup>1</sup>Forschungszentrum Jülich GmbH, Germany; <sup>2</sup>Institute of Plasma Physics of the Czech Academy of Sciences, Czech Republic.

High heat loads with peak heat fluxes of 10 MW/m<sup>2</sup> to 20 MW/m<sup>2</sup> are expected in the divertor regions of future fusion reactors like ITER and DEMO but also smaller tokamaks like COMPASS-

U. The armour material will be mainly tungsten, but e.g., the manufacturing method, thickness, microstructure including particles or alloying elements are still open questions. High heat flux tests on these plasma-facing materials, small samples or whole components, are usually done by applying as homogeneous loads as possible on them and investigate their influence, with or without cycling, on the evolving temperatures and structures. However, the peak heat load in a tokamak fusion device is concentrated in a narrow region around the strike line which thickness is much smaller than the sizes of most of the W-tile designs.

Within the framework of the EUROfusion WPPWIE project, the flexibility of the electron beam facility JUDITH 2 was used to develop beam patterns to mimic the complex and narrow energy flux density distributions (so called Eich's profiles [1]) expected in COMPASS-U tokamak [2]. The specified heat load maxima have been 35 MW/m<sup>2</sup> for 3 sec. and 70 MW/m<sup>2</sup> for 0.5 s with an Eich's profile, and for comparison a homogeneous load of 20 MW/m<sup>2</sup> for 3 s.

A pattern creator was developed with which the point distances in two dimensions can be adjusted independently. For instance, the distance increases linearly in one direction and quadratic in the other one. Number of points and repetitions and thus the total time of one pulse can be defined as well as the size of the loaded area. By covering a small part of the W sample with a cooled Cu-beam dump, a sharp drop in the energy deposition can be realized. These developed loading patterns were then successfully applied (10 pulses each) on three, inertially cooled, 120 x 75 x 30 mm<sup>3</sup> W-blocks of different manufacturers. The temperature distribution is compared with the simulated one, showing the intended loading characteristic. This study shows exemplarily the capability to apply precise and deliberately inhomogeneous high heat fluxes of varying pulse times.

[1] T. Eich, et al., Scaling of the tokamak near scrape-off layer H-mode power width and implication for ITER, Nucl. Fusion 53 (2013) 093031

[2] P. Vondracek, et al., Preliminary design of the COMPASS Upgrade tokamak, Fusion Eng. Des. 169 (2021) 112490

POB-46

### **Mechanical and Microstructural Characterization of Structural Materials for Nuclear Applications with Inverse Finite Element Analysis**

David Bermudez Parra<sup>1</sup>, Dmitry Terentyev<sup>2</sup>, David Garoz<sup>3</sup>

<sup>1</sup>Belgian Nuclear Research Centre SCKCEN, Belgium, and Universidad Politécnica de Madrid, Spain; <sup>2</sup>Belgian Nuclear Research Centre SCKCEN, and Ghent University, Belgium; <sup>3</sup>Escuela Técnica Superior de Ingenieros Industriales, UPM, Spain.

Development and characterization of structural materials for future fusion reactors represents a critical focus area in advancing fusion research. This work presents a study of tensile mechanical properties supported with microstructural analysis of the fracture surface. Tensile testing, performed according to the guidelines of the ASTM E8/E8M standard, provides data on Ultimate Tensile Strength, Yield Strength, and ductility. Several important structural materials for fusion applications are considered, namely: high-Cr ferritic martensitic steel EURO-FER97, copper-chromium-zirconium according to ITER specification, nickel-based super alloy Inconel600, austenitic stainless steel 316LN, titanium grade 2 and titanium-stabilized austenitic stainless steel 15-15Ti.

Fractographic analysis of tested specimens is performed to identify characteristic features of failure mechanisms such as ductile dimple rupture due to micro-void formation and coalescence. A microstructural evaluation is conducted using scanning electron microscopy

(SEM) to complement the mechanical results. Energy-dispersive X-ray spectroscopy (EDX) is employed for a more detailed compositional analysis, while electron backscatter diffraction (EBSD) provides insights into grain size, orientation, and texture evolution during deformation. These analyses link microstructural features, such as phase distribution, inclusions, and grain boundary characteristics, with the observed mechanical properties and failure modes.

As a final step, the obtained experimental information is applied in combination with inverse finite element analysis (IFEA) to deduct the true stress – true strain constitutive laws for each material, as well as to determine the parameters of the damage model (using Gurson-Tvergaard-Needleman formalism) to correctly capture the mechanical failure. To process the experimental data and get the best FEM fit we used the procedures developed earlier in Ref. [1,2] for EUROFER97 steel and tungsten. The IFEA results are compared with experimental engineering stress-strain curves and reduction of area at fracture demonstrating the accuracy of the obtained constitutive laws.

POB-47

### **Investigating heat flux behavior and power dissipation in the Shape and Volume Rise divertor of DIII-D**

Jun Ren<sup>1</sup>, Robert Wilcox<sup>2</sup>, Huiqian Wang<sup>3</sup>, Ryan Hood<sup>4</sup>, Cedric Tsui<sup>4</sup>, Morgan Shafer<sup>2</sup>, Suk-Ho Hong<sup>3</sup>, David Christian Donovan<sup>1</sup>

<sup>1</sup>University of Tennessee, Knoxville, United States; <sup>2</sup>Oak Ridge National Laboratory, United States; <sup>3</sup>General Atomics, United States; <sup>4</sup>Sandia National Laboratories, Livermore, United States.

The newly implemented Shape and Volume Rise (SVR) divertor, designed with increased plasma volume and upper triangularity, significantly enhances edge pressure and pedestal performance in DIII-D. In the upper single-null configuration, a significant in-out divertor asymmetry in power deposition was observed. Most of the power was directed toward the outer leg, resulting in a peak heat flux in the SVR divertor that was approximately twice as high as that at the inner divertor location. At 60% Greenwald density, measurements in the SVR divertor revealed a wide and flat heat flux profile extending from the outer strike point (OSP) to the far scrape-off layer (SOL) at normalized poloidal flux,  $\Psi_i 1.04$ . With nitrogen impurity gas puffing, the perpendicular heat flux near the OSP decreased by 80%, dropping from approximately 3.5 MW/m<sup>2</sup> to less than 0.7 MW/m<sup>2</sup>. However, the heat flux in the far SOL remained high, indicating particle detachment at the OSP while maintaining an attached divertor condition in the SOL. In contrast, with neon impurity gas puffing, the heat flux at both the OSP and far SOL was reduced to levels below 1 MW/m<sup>2</sup>. The resulting heat flux profile was flat and exhibited minimal decay, even in the far SOL.

These observations were enabled by an array of Surface Eroding Thermocouples (SETCs) deployed in the SVR divertor. The small divertor volume, combined with the short leg length of the normal SVR configuration, necessitates reliable heat flux measurements to investigate heat flux dynamics and power dissipation under various operational scenarios. These finds suggest that the SVR divertor provides effective local dissipation at the ceiling target. This conclusion aligns with measurements from recessed SETCs, which indicate that radiative power at the ceiling target contributes over 60% of surface heating during detachment. However, the SVR divertor lacks sufficient capability to spread dissipation into the far SOL or achieve full detachment along the divertor. This limitation may stem from inadequate baffling effects outside the ceiling divertor region and requires further investigation to identify the

optimal divertor solution for the SVR configuration.

Work supported by the Department of Energy under Award Number(s) DE-FC02-04ER54698, DE-SC0023378, DE-AC05-00OR22725 and DE-NA0003525.

POB-48

### **Performance of recrystallized and molten Tungsten surfaces under fusion relevant loads**

Marius Wirtz, Mauricio Gago, Gerald Pintsuk, Bernhard Unterberg

Forschungszentrum Jülich GmbH, Germany.

One of the most crucial points in the field of fusion research for ITER, DEMO and future fusion reactors is the choice and the design of plasma facing materials (PFMs) and components. The chosen materials have to withstand severe environmental conditions in terms of steady state (up to 20 MW/m<sup>2</sup>) and transient heat loads (up to 1 GW/m<sup>2</sup> and above). Beside these thermal loads, PFMs are also exposed to high particle fluxes such as hydrogen, helium and neutrons, which will deteriorate the material properties and therefore have a significant impact on the thermal shock response and other material properties.

This work focuses on the damage response of tungsten under very high power loads such as plasma disruptions and vertical displacement events. The formation of recrystallized and molten layers on the PFMs surface will have a strong influence on the material properties and subsequently on the damage behavior under further steady state and transient loads.

Tungsten produced by Plansee meeting the ITER material specifications was exposed to thermal transients with power densities above the melting threshold in the linear plasma device PSI-2 to generate layers of molten material with a depth of  $\sim 200$  nm on the loaded surface. Subsequently, these pre-damaged samples were exposed to ELM-like thermal shock events using a high energy laser and additionally to the pure thermal exposure the pre-damaged tungsten samples were exposed to H/He background plasma as well as subsequent and simultaneous transient thermal events.

All induced surface modifications such as melting, crack formation and roughening due to plastic deformation were analyzed by scanning electron microscopy, light microscopy, laser profilometry and metallographic means. The characterization of the damage behavior and the comparison of the already available threshold values of as-received and recrystallized material with the new data on re-solidified material will add information to the database for the impact of melt layer formation on damage formation and erosion of the PFM and subsequently the lifetime of PFMs after such intensive heat load events.

The results show already that the damage evolution of molten and solidified surface is much faster than on as-received samples. This embarks the risk of a shorter lifetime and severe surface damage during operation of a fusion reactor.

POB-49

### **Design challenges for the COMPASS Upgrade closed tungsten divertor**

Mikulas Durovec<sup>1</sup>, Renaud Dejarnac<sup>1</sup>, Petr Vondracek<sup>1</sup>, Philippe Chappuis<sup>2</sup>, David Sestak<sup>1</sup>

<sup>1</sup>Institute of Plasma Physics of the Czech Academy of Sciences, Czech Republic; <sup>2</sup>CHAPS Engineering, France.

COMPASS Upgrade (COMPASS-U) is a new full metal tokamak with tungsten (W) plasma facing components under construction at the Institute of Plasma Physics in Prague, Czech Republic[1,2]. Whilst most of the first wall components have a final design, the bottom closed W divertor is entering the preliminary design phase. The expected large constraints such as high



electro-magnetic loads, high energy flux density at targets ( $<100 \text{ MW/m}^2$ ), large thermal expansion combined with its relatively small size ( $R = 0.9 \text{ m}$ ,  $a = 0.27 \text{ m}$ ), tight tolerances and a lack of space make it challenging to design. This contribution describes the main objectives and associated challenges in designing the COMPASS-U closed W divertor.

The main goals include the final design of the divertor itself but also halo current straps, thermal anchors for passive cooling, and shaped tungsten tiles to hide leading edges and allow apertures for dedicated diagnostics. The closed tungsten divertor for COMPASS-U is based on a cassettes concept forming a stiff ring with its own challenges. Complex analyses associated with the reduced space and the high level of performance are required, as well as resolving engineering challenges such as manufacturing and machining of the different components (W tiles and Inconel cassettes), misalignment management and tolerance control, material selection to withstand both high temperatures and high electromagnetic loads, but also to ensure thermal compatibility with tungsten tiles. Such a divertor will support the COMPASS-U mission to provide critical insights into plasma-wall interaction and power exhaust, strengthening the foundation for future fusion devices and contributing to the realization of the EUROfusion roadmap.

POB-50

### **High Heat Flux Testing of Erosion Markers: Electrical Resistivity and Alumina Diffusion in Tungsten via Four-Point Probe**

Amelia Deleau<sup>1</sup>, Caroline Hernandez<sup>1</sup>, Anastasios Skarlatos<sup>2</sup>, Zarel Valdez-Nava<sup>3</sup>, David Malec<sup>3</sup>

<sup>1</sup>CEA, IRFM, France; <sup>2</sup>Cea Saclay laboratoire DIGITEO, France; <sup>3</sup>Université Toulouse Paul Sabatier, France.

The WEST (Tungsten-W Environment in Steady-state Tokamak) divertor is exposed to intense fluxes of heat and particles [1], making it one of the most heavily stressed components in the system. The heat and particle fluxes yield extreme temperatures, hence the need of tungsten. These conditions induce erosion on the tungsten components, necessitating meticulous monitoring to ensure the integrity and longevity of the divertor's components and to maintain the performance and safety of the tokamak during operation [2]. In that way, erosion markers have been designed to correlate their thickness to their electrical resistance. The markers that were fabricated via Physical Vapor Deposition (PVD), are composed of a bulk tungsten substrate with a thin alumina interlayer (0.2–5  $\mu\text{m}$ ) and a top tungsten layer (5–30  $\mu\text{m}$ ) [3]. In view of integrating such erosion markers in WEST, their behaviour under cyclic high heat fluxes have been assessed in the electron beam facility HADES [4]. The effects of temperature and transient thermal loads, such as Edge Localized Modes (ELMs) [5] have been considered. Testing was conducted at three target temperatures: 1000°C, 1500°C, and 1800°C. After cycling, physical characterisations have been performed (Scanning Electron Microscopy (SEM) and Energy-Dispersive X-ray Spectroscopy (EDX)) and the thickness of the W layer has been determined by measuring the electrical resistivity of the top layer using the four-point probe method.

There was no delamination of the top tungsten layer of the erosion markers after a thermal cycling of 1000°C (100 cycles of 2-second exposures), whereas coating delamination was observed for samples temperatures exceeding a single excursion to 1300°C.

While the measured thickness of the W layer did not vary after thermal cycling, significant variations of the electrical resistivity were observed. These variations have been attributed to the interdiffusion of W and alumina layers within the markers, which has been confirmed by the SEM observation and EDX analysis.

These findings highlight the thermal stability limits of tungsten/alumina interlayers. They also demonstrate their mechanical integrity under simulated transient power loads typical of tokamak environments. This study provides a first set of data for the design of electrical resistance-based erosion markers and highlights the importance of interlayer selection and thermal resistance in harsh plasma-facing applications.

[1] J. Bucalossi et al., Nucl. Fusion 64, 112022 (2024).

[2] N. W. Eidietis, 2021 VOLUME 77, 738 (2021).

[3] M. Firdaouss et al., Fusion Eng. Des. 124, 207 (2017).

[4] Fusion Eng. Des. 192, 113769 (2023).

[5] J. Nucl. Mater. 241–243, 182 (1997).

POB-51

### **Modelling of RE induced damage of BN tiles of WEST inner limiter**

Tommaso Rizzi<sup>1</sup>, Svetlana Ratynskaia<sup>1</sup>, Panagiotis Tolas<sup>1</sup>, Yann Corre<sup>2</sup>, Mathilde Diez<sup>2</sup>, Mehdi Firdaouss<sup>2</sup>, Jonathan Gerardin<sup>2</sup>, Raphael Mitteau<sup>2</sup>, Cédric Reux<sup>2</sup>

<sup>1</sup>KTH Royal Institute of Technology, Sweden; <sup>2</sup>CEA, IRFM, France.

Modelling of the runaway electron (RE) damage induced during the 2023–2024 experimental campaigns on the boron-nitride (BN) tiles mounted on the inner bumpers of the WEST tokamak has been attempted based on the available empirical input and experimental constraints. Post-mortem analysis of the tiles revealed significant surface deformation, with the most severely damaged regions exhibiting material loss with a depth of up to 1 mm. The erosion is observed to be symmetric with respect to the tile main axis. The excavated volume is interpreted as the result of cumulative damage on each tile taking place in about ten discharges with RE impact on the inner bumpers clearly established by visible and IR videos. Magnetic equilibrium reconstruction indicates a grazing magnetic field incidence of about  $0.3^\circ$  relative to the tile flat top. A zero pitch angle is assumed for the incident REs, due to the lack of more refined information concerning the RE momentum distribution. Furthermore, the post-mortem detection of activated W radioisotopes [1] suggests the presence of high-energy electrons (greater than 10 MeV) in the RE beam, in agreement with IR Wide Angle measurements in WEST. Thus, the initial kinetic energies are scanned within the range of 10 to 30 MeV.

A newly developed work-flow for the modelling of RE-induced brittle failure [2], recently validated against a controlled DIII-D experiment on a protruding graphite dome [3], is employed here with the aforementioned RE-incidence specifications. Monte Carlo simulations of RE transport into BN are performed with Geant4, providing maps of the volumetric heat source, which constitutes input to linear thermoelastic response FEM simulations carried out with COMSOL Multi-physics. Temperature-dependent material properties are incorporated into the thermomechanical model, which also accounts for the strong anisotropy in the coefficient of thermal expansion. Local failure is predicted according to the Rankine criterion, typically used for brittle materials, which compares the principal stresses with the ultimate strength (tensile or compressive). For a single discharge, the first code-chain simulations with 10 MeV and 20 MeV RE initial kinetic energy revealed a symmetric region of failure in a layer of thickness around  $50\text{ }\mu\text{m}$  and  $70\text{ }\mu\text{m}$ , respectively, which is consistent with the experimental evidence.

[1] M. Houry et al., Invited talk, 50th EPS Plasma Physics Conference, Spain, July 2024.

[2] S. Ratynskaia, P. Talias, T. Rizzi et al., Nuclear Fusion (in print).

[3] E. Hollmann, C. Marini, D. Rudakov et al., Plasma Phys. Control. Fusion (submitted).

POB-52

### **JT-60SA Divertor: Combining Advanced Simulation and Additive Manufacturing to propose an Enhanced Design for a Tungsten Actively Cooled Divertor**

Diogo Dias Aleixo<sup>1</sup>, Mehdi Firdaouss<sup>1</sup>, Thierry Baffie<sup>2</sup>, Pierre-Eric Frayssines<sup>2</sup>, Hervé Gleyzes<sup>2</sup>, Pierre Lechevalier<sup>1</sup>, Alizée Thomas<sup>2</sup>, Valerio Tomarchio<sup>3</sup>, Marianne Richou<sup>1</sup>

<sup>1</sup>CEA, IRFM, France; <sup>2</sup>Université Grenoble Alpes, France; <sup>3</sup>F4E, Germany.

The JT-60SA divertor upgrade requires developing high-performance actively cooled plasma-facing components capable of withstanding 10 MW/m<sup>2</sup> in steady-state (< 100s), up to 15 MW/m<sup>2</sup> during 5 s and 20 MW/m<sup>2</sup> during 2 s (water cooled at 7 m/s, 20 bar, 40°C).

Hypervapotron is designed with fins perpendicular to water flow direction within a rectangular cooling channel. This design aims to local vaporization and further condensation of water to transport very efficiently the heat from the top surface to the coolant. In fusion area, hypervapotron heat sinks are usually machined and welded from forged CuCrZr parts. While effective, they present limitations in terms of integration due to manufacturing constraints. Additive Manufacturing (AM), specifically Laser Powder Bed Fusion (LPBF), enables optimized geometries while minimizing assembly defects, thanks to its precision and ability to create complex designs.

Thermo-hydraulic simulations using Ansys Fluent were employed to analyze performance of defined fin geometries (pressure drop, maximum wall temperature). In addition to the forged hypervapotron design (reference design), two promising designs [1,2] were assessed: a chevron-fin configuration, and a diagonal-fin configuration. The chevron and diagonal designs exhibited superior thermal performance, reducing wall temperatures by up to 20°C compared to the reference, but resulted in an increased pressure drop by a factor 2.

In order to test the performances under high heat flux, three 260 mm-long mock-ups with each fin design (reference, diagonal, chevron) were produced via LPBF with geometries adapted to additive manufacturing constraints. In particular, the internal channels were redesigned with triangular shape to be self-supporting, avoiding pressure drop issues identified in CFD analysis. As Hot Isostatic Process (HIP) is expected for joining CuCrZr to W tiles and 316L structure, an innovative manufacturing route using HIP as thermal treatment is tested and mechanically assessed. Comparison of HIP treatments on LPBF and forged CuCrZr samples revealed distinct microstructural behaviors. At 1040°C, LPBF CuCrZr exhibited complete recrystallization, while forged CuCrZr showed abnormal grain growth. Vickers hardness for LPBF material is lower than forged CuCrZr and decreases with HIP temperature contrary to expectations. Further experiments made with different cooling rates revealed that the LPBF CuCrZr is less sensitive to cooling rates compared to forged material. Microscopic investigations at nano scale are necessary to understand these results before tuning the LPBF and/or the HIP parameters.

[1] Lim, J. H., & Park, M. (2022). Fusion Science and Technology, 78(5), 395–413.

[2] Kaewchoothong, N. et al. (2017). Theoretical and Applied Mechanics Letters, 7(6), 344–350.

POB-53

### **Melting threshold at toroidal gaps of ITER divertor monoblocks under repetitive ELM transients**

Konstantinos Paschalidis<sup>1</sup>, Svetlana Ratynskaia<sup>1</sup>, Panagiotis Tolias<sup>1</sup>, Richard Pitts<sup>2</sup>

<sup>1</sup>KTH Royal Institute of Technology, Sweden; <sup>2</sup>ITER Organization, France.

Melting of toroidal gap (TG) edges on the ITER divertor tungsten monoblocks (MB) under edge localized mode (ELM) impact is predicted to occur at much lower energy densities than for the top surface [1]. It is a particular concern given that TG edges cannot be protected at the outer divertor target by MB shaping [2] and is expected to be possible already in the first deuterium H-mode plasmas that will be attempted on ITER during the Start of Research Operations (SRO) phase in the newly re-baselined Research Plan [3]. This study addresses the critical thresholds for TG edge melting under repetitive ELM impact during SRO H-mode experiments at half nominal toroidal field ( $B_T = 2.65$  T) and plasma current ( $I_p = 7.5$  MA).

MEMENTO has been employed for the heat transfer simulations. It is a finite difference code for modelling macroscopic melt damage of plasma-facing components in fusion environments [4]. The implemented physics model consists of the thermoelectric magnetohydrodynamic equations coupled with heat conduction including phase transitions, reduced by the shallow water and magnetostatic approximations for uniform material composition [5]. In the present work, only the heat conduction module is used, since melt motion at the TG edges violates the shallow water approximation.

The loading thresholds for TG melting due to a single ELM impacting an MB preheated by a steady inter-ELM flux have been investigated in [2] using several simplifications to allow scoping studies. Here, the cumulative effects of repetitive Type I ELM loading are investigated, using 3D simulations adopting temperature-dependent  $W$  thermophysical properties based on state-of-the-art recommendations [6].

Comparison between the results of the scoping studies in [2] and the 3D MEMENTO simulations, reveals that the melting thresholds in [2] were underestimated by 25%, improving the prospects for avoidance of TG edge melting if ELMs are unmitigated in SRO H-modes. The impact of ELM mitigation was also studied, highlighting the importance of ELM frequency and providing guidance for the minimum mitigation levels required to avoid TG edge melting in early ITER H-modes.

[1] R. A. Pitts et al., Nucl. Mater. Energy 20 (2019) 100696

[2] J. P. Gunn et al., Nucl. Fusion 59 (2019) 126043

[3] R. A. Pitts et al., Nucl. Mater. Energy 42 (2024) 101854

[4] K. Paschalidis et al., Fus. Eng. Des. 206 (2024) 114603

[5] S. Ratynskaia et al., Phys. Scr. 96 (2021) 124009

[6] P. Tolias, Nucl. Mater. Energy 13 (2017) 42-57

POB-54

### **ps Laser Induced Breakdown Spectroscopy and Mass Spectrometry - Deuterium depth resolution, removal fraction and uncertainties**

Sören Möller<sup>1</sup>, Christoph Kawan<sup>1</sup>, Arkadi Kreter<sup>1</sup>, Gennady Sergienko<sup>1</sup>, Marcin Rasinski<sup>1</sup>, Erik Wüst<sup>1</sup>, Sebastian Brezinsek<sup>1</sup>, Eduard Grigore<sup>2</sup>

<sup>1</sup>Forschungszentrum Jülich GmbH, Germany; <sup>2</sup>Acasa Institutul National pentru Fizica Laserilor, Plasmei si Radiatiei, Romania.

Laser Induced Breakdown Spectroscopy (LIBS) is used as an in-situ surface analysis technique in nuclear fusion research. LIBS is used in many current fusion experiments and foreseen for future fusion experiments and reactors for the analysis of sputtering and tritium retention. LIBS uses high power laser pulses to remove material from the sample surface. The laser energy produces a plasma, which enables a compositional analysis of the removed material through spectroscopy and released gas through mass-spectrometry. A depth analysis can be conducted through consecutive laser pulses, each ablating a thickness of the order of 10 nm. Therefore, improving accuracy and resolution of LIBS is an ongoing research topic.

For the quantification of LIBS, MeV ion-beam analysis (IBA) is a common tool. The comparison of pre and post IBA of the LIBS analysis area reveals the amount of ablated material, which is then used for calibration of the LIBS signal. In this work, we extend this IBA approach by a 900 point IBA tomography of a 5x5 mm<sup>2</sup> area around five ps-laser craters of 1 mm and 0.2 mm nominal diameter and 5 m depth. A 10x10 mm<sup>2</sup> Mo sample with a 5 m D loaded W layer is used. IBA uses a 150 m 3 MeV 3He nuclear reaction analysis to analyse the D retention and release. Electron microscopy and profilometry of the area provide additional data.

The results show a release of up to 99.1 % of the D in the laser crater centre. In to the nominal 1 mm diameter laser crater, 71.4 % of the D is removed. The lateral D profiles connect this to the edge effects, in agreement with profilometry results. The laser crater is not rectangular, but trapezoid/sigmoid shaped. The difference in removed material between the ideal rectangular and the real sigmoid shape agrees to the remaining D.

Additionally, we observed remaining D at the crater centre, although the D containing layer is completely removed by the laser. Interestingly, this D is found at a depth of 2-4 m below the crater floor, while no D is found in 0-2 m depth. The heat deposited by the laser enabled D diffusion into the bulk, but also outgassed the D from the heat affected first 2 m. Therefore, we conclude a 2 m desorption halo exists around the crater, enabling calculating the desorption related D depth resolution and the accuracy limit of LIBS.

POB-55

## **Deuterium Uptake and Isotope Exchange in Tungsten Displacement-damaged at High Temperature**

Laurin Hess, Thomas Schwarz-Selinger

Max Planck Institute for Plasma Physics, Germany.

Retention of hydrogen fuel in tungsten is an active area of research, as it is an integral part of modeling the tritium inventory and licencing of future fusion reactors. It has been shown that hydrogen isotope retention significantly increases due to displacement damage, as produced by 14 MeV fusion neutrons. Most research on this has focused on point defects such as vacancies. However, at temperatures that will be present at the first wall and the divertor, single vacancies become mobile and can form clusters. These clusters can grow to nm-sized voids, as was found for fission neutron-irradiated tungsten [1]. Hydrogen isotope retention in and release from such voids are expected to be different compared to point effects because molecular hydrogen is theorized to appear [2,3]. While many experiments studied the behavior of hydrogen in point defects, very little research has been done to examine the behavior of hydrogen in these voids.

To improve the understanding of nm-sized voids, the uptake and isotope exchange of hydrogen in tungsten displacement-damaged at elevated temperatures was studied. This was done by self-damaging tungsten single crystals by irradiation with 20 MeV tungsten ions at 1370

K. Created defects were decorated with different fluences up to  $3 \times 10^{25}$  D/m<sup>2</sup> of 5 eV deuterium from a low-temperature plasma at an exposure temperature of 370 K. The retention of deuterium was measured via <sup>3</sup>He Nuclear Reaction Analysis as a function of D fluence. To study isotope exchange, deuterium loaded samples have been exposed to different fluences up to  $7.5 \times 10^{25}$  H/m<sup>2</sup> of 5 eV protium, with the remaining deuterium measured.

Results show that retention proceeds from the surface with maximum D concentrations of 1.4 at%. In contrast to tungsten damaged at room temperature, fully decorated samples do not show a step-like depth profile but rather a peak at  $\approx 0.2$   $\mu$ m and an approximately linear decrease of deuterium concentration into depth. Deuterium close to the surface exchanges at speeds associated with point defects, however some deuterium close to the damage peak appears to exchange significantly slower. As voids would be largest close to the damage peak, we speculate that the isotope exchange in voids is much slower than in point defects, or even non-existent. Thermal desorption spectroscopy is presently underway to determine the binding energy of the residual deuterium to give indication of their trap types.

[1] M. Klimenkov et al., Jour. Nucl. Mat. 572 (2022) 154018

[2] J. Hou et al., Nat. Mat. 18 (2019) 833-839

[3] M. Zibrov, K. Schmid, Nucl. Mat. Eng. 30 (2022) 101121

POB-56

### **Deuterium Retention in Boron-Based Codeposits**

James Davis, Hikaru Tanaka, Steven Theriault, Eric Nicholson  
University of Toronto, Canada.

The move toward an all-tungsten first wall in ITER has led to an increased interest in the use of boron surface layers to protect the tungsten from erosion and the plasma from the subsequent contamination. In turn, the erosion of boron will lead to the creation of codeposited layers. While boronization has been in use for decades, there is little information on the structure and deuterium content of high boron-content codeposits.

We have previously looked at the hydrogen content of midplane codeposits from DIII-D with a boron content  $\sim 50\%$  [1], where the hydrogen content was found to be very similar to pure carbon codeposits. More recently, we have been using sputter-deposition to investigate the properties of C/Si codeposits [2]. This method allows us to create codeposits under well-controlled conditions, enabling us to investigate the structural details of the deposits as a function of the deposition conditions, such as temperature.

As it will be necessary to periodically remove any codeposits, either for tritium recovery, or for operational considerations (eg., flaking, power loading, etc.), knowing the likely chemical structure of the deposits may be of practical importance. In the current work, we have prepared high boron content codeposits using B<sub>4</sub>C as a sputter source. The D content of the deposits has been measured by TDS, indicating a D content similar to that found in C/Si and pure C sputter-deposited codeposits [2]. XPS will be used to investigate the elemental content and chemical bonding structure in the deposits. Future work will look at codeposits formed using pure boron as the sputter source.

[1] J.W. Davis, P.B. Wright, R. Macaulay-Newcombe, et al., "Chemical erosion of boronized films from DIII-D tiles," Journal of Nuclear Materials, 290-293 (2001) 66-70.

[2] A.W. Cruse and J.W. Davis, "Deuterium Reclamation from C-Si Codeposits Using Thermo-oxidation", Nuclear Materials and Energy 38 (2024) 101629

POB-59

### **Hydrogen isotope interaction in laboratory boron layers**

Eduard Warkentin, Anne Houben, Marcin Rasinski, Hans Rudolf Koslowski, Timo Dittmar, Arkadi Kreter, Bernhard Unterberg, Christian Linsmeier

Forschungszentrum Jülich GmbH, Germany.

Fuel permeation and retention in fusion reactor wall materials are important issues for plasma operation and safety reasons in ITER. The loss of the hydrogen isotope tritium, which will be used as fuel, has to be estimated and prevented.

Due to the change of the ITER first wall material from Be to W, oxygen and other impurities in the vessel are not sufficiently gettered by a W wall. A thin boron layer which is applied during the regular wall conditioning phase can solve the problem and a more efficient plasma operation can be obtained. The applied B layer will be eroded during plasma operation on parts of the first wall with plasma impact. In addition there will be parts of the wall where B will be not eroded, but re-deposited and accumulated. The hydrogen isotope retention and permeation in these layers are important for the tritium inventory.

In order to investigate hydrogen retention and permeation of boron coatings, pure and mixed boron layers (approx. 100 nm) with varying content of D were fabricated oxygen-free by magnetron sputter deposition on W, Si and steel substrates.

Surface morphology, layer homogeneity and thickness were examined via scanning electron microscopy, focused ion beam and energy dispersive X-ray spectroscopy. The composition of the samples, especially the oxygen content, were analysed in more detail through X-ray photoelectron spectroscopy and Fourier transform infrared spectroscopy.

After characterization, the deuterium permeation flux of the boron coated samples was measured and the layer permeabilities were obtained.

Boron coated samples were exposed with different hydrogen isotope plasmas and ions. Afterwards, the hydrogen isotope retention was investigated by nuclear reaction analysis and thermal desorption spectroscopy.

POB-60

### **Fuel imbalance and accumulation of protium in a fusion power reactor**

Yuri Igitchkanov, Thomas Giegerich

Karlsruhe Institute of Technology, Germany.

The fusion power plant operation with a fuel cycle including a direct internal recycling [1] aims to increase the fuel burnup fraction and to reduce the tritium inventory. However, the formation of protium and tritium in the reactor chamber is concomitant to DT fusion reactions and the release of tritium from the first wall can lead both to an accumulation of protium followed by the fuel dilution and deuterium/tritium imbalance in the reactor chamber followed by the power dip.

In this work, we estimate the accumulation of protium in the reactor chamber due to fuel recirculation, when the exhaust gas mixture returns after purification back to the reactor chamber, depending on the separation fraction of metal foil pumps [2] and the duration of the pulse. It is found that the acceptable concentration of protium is limited by requirements of a self-sustained reaction to occur.

It is shown that in order to achieve maximum burn, in the case of fuel imbalance, when tritium forms by both DD reactions in the plasma and (n,p) reactions in the first wall, a lower tritium concentration will be required from an external source to the reactor chamber.

As far as the permissible concentrations of light and heavy impurities released from the material structure of the reactor chamber are concerned, they are limited either by excessive power radiation losses or by plasma pressure increase above the ballooning limit. The limitations of the relevant impurities expected in the DEMO reactor plasma are assessed.

[1] Ch. Day, T. Giegerich., “The Direct Internal Recycling concept to simplify the fuel cycle of a fusion power plant”, *Fusion Engineering and Design* 88 (2013) 616–620.

[2] B.Peters, S.Hanke, C.Day, *FED* 136 (2018) 1467–1471

POB-61

### **Dynamics of Deuterium Retention in Tungsten and Deposited Boron Thin Films During Plasma Exposure Using In-Operando Nuclear Reaction Analysis in DIONISOS**

Joey Demiane<sup>1</sup>, Camila Lopez Perez<sup>2</sup>, Kevin Woller<sup>1</sup>

<sup>1</sup>MIT – PSFC, United States; <sup>2</sup>Ken and Mary Alice Lindquist Department of Nuclear Engineering, Pennsylvania State University, United States.

Experiments on the dependence of the dynamics of deuterium (D) retention on particle fluence and surface temperature in hot-rolled polished polycrystalline tungsten (W) are being conducted under steady-state D plasma exposure in DIONISOS using in-operando Nuclear Reaction Analysis (NRA) with a <sup>3</sup>He ion beam as baseline experiments for lithium-wetted or Boron coated tungsten. DIONISOS is an RF helicon plasma device equipped with the capability to simultaneously perform ion beam analysis (IBA) and plasma exposures.

A commercial tokamak will operate in short or long plasma pulses, requiring the vacuum vessel to be pumped down between pulses. The outgassing of dynamically retained fuel from the walls significantly affects the time needed to pump down to the required base pressure and start a new pulse, thus limiting the reactor’s operating time. Additionally, the loss of fusion fuel, especially tritium (T), to the walls is undesirable, presenting further challenges in achieving T fuel self-sufficiency. A major obstacle in studying dynamic retention is the rapid release of fuel from the material after plasma termination, making it undetectable ex-situ.

Two sets of steady-state D plasma exposures with constant flux (approx  $10^{21} \text{ m}^{-2} \text{ s}^{-1}$ ) will be conducted on DIONISOS reproducing the same conditions on the first wall of a tokamak (particle flux and temperature) and the fluence of one or few pulses depending on the scenario. The first set will focus on temperature dependence (200C, 500C, and 750C), while the second set will investigate fluence dependence ( $10^{24}$ ,  $10^{25}$ , and  $10^{26} \text{ m}^{-2}$ ). The study aims to deduce, using in-operando NRA, the relationship between the dynamics of D retention and both particle fluence and surface temperature, while maintaining constant particle impact energy (50eV).

POB-62

### **The effect of surface-near helium on deuterium retention in EUROFER**

Sabina Markelj<sup>1</sup>, Thomas Schwarz-Selinger<sup>2</sup>, Janez Zavašnik<sup>1</sup>, Andreja Šestan Zavašnik<sup>1</sup>

<sup>1</sup>Jožef Stefan Institute, Slovenia; <sup>2</sup>Max-Planck-Institut für Plasmaphysik, Germany.

It was shown experimentally for tungsten, that He retained close to the surface influences the transport and retention of hydrogen isotopes (HI). Namely, recent experiments studying the interaction of HIs and He, using He seeded D plasmas, showed that the addition of He leads to reduced blistering accompanied by a reduced D retention [1]. Recently, we have performed a systematic series of D exposures for tungsten where He was pre-implanted



near the surface. Deuterium and helium depth profiling showed increased D retention at the depth where He was implanted. Nevertheless, retention in the bulk was reduced five times as compared to a He-free reference sample [2]. In this contribution, the same methodology was applied to EUROFER97 to clarify the effect of surface-near helium on deuterium transport into and retention in the bulk.

To quantify the influence on D uptake at the surface, He was implanted into EUROFER97 samples close to the surface with 1 keV ions with different fluences and at different temperatures. 20 MeV W irradiation was performed before or after the He implantation to create defects within the first 3  $\mu\text{m}$ . Samples were then exposed to a low flux, low energy (100 eV/D) D ion beam at 370 K. One He-free W-irradiated EUROFER97 reference sample was also exposed to low energy D ions for comparison. The defects created by W ions trap penetrating D and make it hence possible to quantify D transport into the layer below the He layer using  $^3\text{He}$  nuclear reaction analysis (NRA). Measured D depth profiles show reduced uptake of D in the He-irradiated samples with major D retention near the surface where He is expected to be implanted. The reduction of D uptake is reduced by a factor of two compared to He-free sample. Surface analysis of the possible He bubbles are ongoing for the sample with the largest He fluence of  $5.5 \times 10^{21} \text{ He/m}^2$ . Results will be discussed and compared to tungsten.

[1] M. Baldwin et al. Nucl. Fusion, vol. 51, p. 103021, 2011 and Nucl. Fusion vol. 57, p. 076031, 2017

[2] Markelj et al. in preparation

POB-63

### **A critical overview of ion beam methods for the determination of H isotopes in reactor materials: depth profiling and micro-beam analysis aspects**

Marek Rubeļ<sup>1</sup>, Laura Dittrich<sup>1</sup>, Sunwoo Moon<sup>1</sup>, Per Petersson<sup>1</sup>, Eduardo Pitthan<sup>2</sup>, Daniel Primetzhofer<sup>2</sup>, Anna Widdowson<sup>3</sup>

<sup>1</sup>KTH Royal Institute of Technology, Sweden; <sup>2</sup>Uppsala University, Sweden; <sup>3</sup>UKAEA, Culham Campus, Abingdon, United Kingdom.

The assessment of fuel inventory is both an absolute need for a viable reactor operation, and a true challenge from the analytical point of view. Over thirty methods and/or technical approaches have been proposed for in-situ and ex-situ measurements of D, T and omnipresent H. The aim is to determine the total amounts, their lateral and depth distribution, and elemental surroundings. Herein, the focus is on ion beam methods, while other means are discussed in [1].

$^3\text{He}$ -based nuclear reaction analysis (NRA) is commonly used for depth profiling of D up to a depth of around 20  $\mu\text{m}$  in light targets, whose other components (e.g. Be, B, C, N, O) are simultaneously determined. Micro-beam NRA gives high-resolution data on the areal distribution of D, Be and C on the W surface located in the gap between the tungsten lamellae of the divertor module from JET. With heavy ion elastic recoil detection analysis (HI-ERDA) quantities and depth profiles of all species from H to U can be obtained up to a depth not exceeding 400–800 nm, as documented for H and D, and several elements on Be limiters from JET [2].

T can be studied both by NRA and HI-ERDA. The detection limits (in trace analysis) for both methods are  $\sim 5 \times 10^{14} \text{ atoms cm}^{-2}$ , thus for T corresponding to  $0.9 \text{ MBq cm}^{-2}$ . Studying samples of such activity already poses safety problems. Secondly, the data for materials after the first D-T campaign (DTE1) in JET in 1997, and also those recently obtained on laboratory-prepared

tritiated W [3,4] have shown that the  $T(3\text{He,d})4\text{He}$  NRA,  $Q = 14.3$  MeV, requires samples of activity exceeding 100 MBq. Also the reactions  $T(12\text{C},\gamma)11\text{B}$  and  $T(12\text{C,p})14\text{C}$  require hot samples [5], while the  $T(\text{D},n)$  process produces high energy neutrons. All these facts may seriously limit IBA of materials after full D-T campaigns. A set of similar research issues occurs also in studies of tritium breeding compounds such as lithium salts, beryllides, intermetallic and ceramic materials.

Advantages and limitations regarding applicability, sensitivity, selectivity, quantification, spatial and depth resolution will be presented and relevant examples will be given. There is no single technique providing all needed information in one run. The experience gathered over the years points to the need for combining several analytical methods/approaches to obtain a comprehensive characterization of isotopes in reactor materials.

[1] Y. Torikai et al., This conference.

[2] L. Dittrich et al., Fusion Engin. Design 192, 113620 (2023)

[3] S. Markelj et al., Nucl. Mater. Energy 28,101057 (2021)

[4] S. Markelj et al., Nucl. Mater. Energy 38, 101586 (2024)

[5] I. Bykov et al., Nucl. Instrum. Meth. B273, 250 (2012)

POB-64

### **Application of the ERO2.0 Code to Plasma-Material Interaction Studies in GyM and BiGyM Devices**

Francesco Cani, Irene Casiraghi, Anna Cremona, Daria Ricci, Laura Laguardia, Andrea Uccello

Istituto per la Scienza e Tecnologia dei Plasmi, CNR, Milano, Italy.

Plasma-wall interaction plays a critical role in determining the overall performance and longevity of tokamaks. The integrity of plasma-facing components, particularly in high-performance machines like ITER and future fusion reactors, is a key challenge. Specifically, plasma-material interactions (PMI) can result in erosion, impurity generation, and degradation of material surfaces, all of which can negatively impact plasma confinement, impurity control, and the thermal efficiency of fusion reactors. Linear plasma devices, such as GyM [1] and its upgraded version BiGyM (expected to be operational by late 2025), are essential testbeds for investigating PMI in a controlled and cost-effective manner, enabling the achievement of ITER-relevant fluences. In this context, modeling tools play a crucial role in providing an accurate interpretation of the experimental data.

This work focuses on the application of the erosion and impurity transport Monte-Carlo code ERO2.0 to GyM for interpretative purposes and to BiGyM for predictive analysis. In particular, ERO2.0 has been used in support of argon plasma experiments devoted to the determination of the spectroscopic parameter  $S/XB$  of tungsten (W) for an accurate estimation of the geometrical loss factor [2]. Simulation outcomes have been compared to net erosion data from W mass loss measurements and emission line intensities from spectroscopy data. The emphasis of the ERO2.0 modelling activity on BiGyM is on the deposition of wall and sample-holder materials on the surfaces of exposed samples during PMI experiments. GyM and BiGyM background plasmas were produced using SOLPS-ITER edge code and provided to ERO2.0, taking advantage of the coupling between the two codes, as demonstrated in previous works [3].

[1] A. Uccello, et al., Front. Phys. 11, 1108175 (2023)

[2] A. Cremona, et al., Nucl. Mater. Energy 17, 253 (2018)

[3] F. Mombelli, et al., Nucl. Fusion 65, 026023 (2025)

POB-66

### **Modelling of boron dust with the MIGRAINE code**

Lorenzo Boccaccia, Panagiotis Tolias, Svetlana Ratynskaia, Ladislav Vignitchouk

KTH Royal Institute of Technology, Sweden.

Boronization is mandatory for the all-tungsten ITER reactor, as it is expected to expand the operational space and allow easier start-up [1]. On the other hand, ions and charge-exchange neutrals will effectively sputter light boron atoms. The eroded boron will be ionized and transported to preferential accumulation sites where unstable boron layers could lead to the generation of dust via delamination. Apart from being a safety issue, boron dust could potentially remobilize prematurely and inhibit plasma breakdown [2]. Despite the extensive experience with tungsten and beryllium dust, it is difficult to make projections for boron dust because of the competing effects. Their relative strength depends on material constants associated with various microphysical processes whose values are very uncertain [3]. Moreover, as far as ion- and electron-surface interactions are concerned, boron has not been investigated as much as tungsten and beryllium. Therefore, the understanding of the transport and survivability of boron dust in ITER requires systematic modelling effort with dedicated dust transport codes.

Here we report on updates of the MIGRAINE code to handle boron dust and droplets. MIGRAINE solves the coupled momentum, enthalpy, charge and mass evolution equations for given plasma profiles. MIGRAINE boasts the most complete description of microphysical processes [4] together with the most reactor-relevant electron and ion collection models in magnetized plasmas [5]. These elements are essential for the accurate of heat balance, which defines the dust surface temperature, which in turn dictates the vaporization rate and thus impurity production [2,3]. State-of-the-art semi-empirical descriptions based on reliable experiments as well as on Monte Carlo or on Molecular Dynamics simulations are utilized to characterize the source terms for boron, namely: secondary electron emission, electron backscattering, ion-induced electron emission, thermionic emission, thermal radiation, ion backscattering, and physical sputtering. Moreover, various temperature-dependent thermophysical and mechanical properties, that are important for heat transfer and dust-wall impacts, are specified. Preliminary results for boron dust ablation rates in plasma background with typical edge parameters are presented.

[1] R A Pitts, A Loarte, T Wauters et al., Nucl. Mater. Energy 42, 101854 (2025).

[2] S Ratynskaia, A Bortolon, S I Krashennnikov, Rev. Mod. Plasma Phys. 6, 20 (2022).

[3] S Ratynskaia, L Vignitchouk, P Tolias, Plasma Phys. Control. Fusion 64, 044004 (2022).

[4] L Vignitchouk, P Tolias, S Ratynskaia, Plasma Phys. Control. Fusion 56, 095005 (2014).

[5] L Vignitchouk, S Ratynskaia, P Tolias, Plasma Phys. Control. Fusion 59, 104002 (2017).

POB-67

### **Examination of plasma-induced surface morphology using spectroscopic ellipsometry**

Daisuke Nishijima<sup>1</sup>, Mitsutaka Miyamoto<sup>2</sup>, Matt Baldwin<sup>1</sup>, George Tynan<sup>1</sup>

<sup>1</sup>University of California San Diego, United States; <sup>2</sup>Shimane University, Japan.

Plasma bombardment onto a material can lead to surface morphology changes, which

can then affect material properties. For instance, tungsten (W) fuzz can reduce the thermal diffusivity, sputtering yield, and secondary electron emission, and also increase the probability of occurrence of arcing. Thus, in-situ surface monitoring during plasma discharge is desired to better understand and control plasma-material interactions.

We have examined the capability of spectroscopic ellipsometry (SE) in an ex-situ setting in preparation for in-situ SE surface analysis in the PISCES-RF linear plasma device. In short, SE analysis yields two parameters, Psi and Delta, as a function of wavelength, in a range of 400 – 1000 nm in our system (J.A. Woollam: iSE), which characterize the change in polarization state of the probe light beam caused by reflection from the sample. Therefore, Psi and Delta are influenced by structures mainly on the surface for absorbing materials (metals).

Here, two types of surface structures, W fuzz and chromium (Cr) cones, were investigated. W and Cr samples were exposed to He plasma in the PISCES-A linear plasma device. By varying the He<sup>+</sup> ion fluence, W samples with different W fuzz layer thicknesses ( $t_{fuzz} = 0 - 1500$  nm) and Cr samples with different heights of Cr cones ( $t_{cone} = 0 - 410$  nm) were prepared. Ex-situ measurements confirmed that (Psi, Delta) plots of W fuzz agree well with Ref. [1], where in-situ, as well as ex-situ, SE measurements of W fuzz ( $t_{fuzz} = 0 - 900$  nm) were performed. Moreover, it is found that  $t_{fuzz}$  can be evaluated from a change in Delta with the fuzz growth. In comparison with W fuzz, where Delta monotonically decreases with increasing  $t_{fuzz}$ , (Psi, Delta) plots of Cr cones behave differently; Delta first decreases and then increases with increasing  $t_{cone}$ . This indicates that SE analysis can distinguish fuzz and cones. Preliminary results of in-situ SE analysis during plasma exposure in PISCES-RF will also be presented in the conference.

Acknowledgements: This work is supported by the U.S. Department of Energy Cooperative Agreement No. DE-SC0022528, JSPS KAKENHI Grant No. 22KK0038 and No. 23K25854, and the US-Japan Cooperation in Fusion Research and Development.

[1] R.D. Kolasinski et al., J. Appl. Phys. 131, 063303 (2022)

POB-68

## **Sputtering of Tungsten Surfaces by Different Ion Types: A Molecular Dynamics Simulation Approach**

Faith Kporha, Fredric Granberg  
University of Helsinki, Finland.

Plasma-facing components (PFC), made of tungsten, are eroded by sputtering caused by energetic ions. Some ions, such as argon and neon, are utilized for radiative cooling [1] and sputtering of the wall material can also lead to W self-sputtering [2]. The sputtering of PFCs can negatively affect the optimal functioning of tokamaks, impacting both lifespan and efficient generation of energy. Therefore, understanding the sputtering process is essential for the design of future tokamaks. Molecular dynamics (MD) simulations serve as a powerful tool for investigating the underlying mechanisms of sputtering, as they provide an atomistic view of the process, by simulating individual atoms and their interactions. The results which can be obtained play a significant role in parameterizing larger-scale models that predict various parameters, including the lifespan.

We conducted MD simulations of pristine W surfaces, examining the effects of Ar, Ne, and W ions with varying energies and incident angles across different surface orientations. In addition

to analyzing sputtering and reflection yields, we analyzed the angular distributions of sputtered species. Our findings revealed that lighter ions (Ar, Ne) exhibited reduced sputtering at larger incoming angles, while sputtering was enhanced by the heavier W ions. Reflection yields also varied significantly, with lighter ions producing high yields and W ions demonstrating angle-dependent behavior. The angular distributions of sputtered W atoms highlighted the influence of both surface orientation and ion energy. At lower energies, distinct peaks were observed for each ion type, while at higher energies, similar symmetric distributions emerged for all ion types. Additionally, we differentiated between reflected and sputtered W, which is often not the case in experiments. Beyond 45 degrees the reflection dominated, which is significant as it suggests that higher incident angles could reduce the net W erosion with a trade-off being increased reflection that could lead to impurity redistribution. We also investigated the impact of implanted deuterium in W. We discovered that D directly affected the sputtering yield of W. Furthermore, we observed that some implanted D could be recovered, as it, too, is subject to sputtering.

POB-70

### **Comparison of methods for erosion/redeposition measurements of plasma-facing components in fusion devices**

Caroline Hernandez, Amelia Deleau, Mathilde Diez, Etienne Delmas, Mehdi Firdaouss, Marianne Richou  
CEA, IRFM, France.

During the operation of a fusion reactor, Plasma Facing Components (PFCs) are subject to erosion caused by plasma interactions, which can affect their integrity and the overall performance of the reactor. Accurate measurement of tungsten erosion is therefore crucial to evaluate the lifetime of the PFCs and guarantee optimal operation of the reactor.

In a majority of tokamaks, multilayer coatings deposited on PFCs are used as erosion markers. After tokamak operation, PFCs with erosion markers are removed from the tokamak and post mortem analysis (using Ion beam analysis, electronic microscopy) allows high resolution measurement of the erosion.

However, this method requires the removal of components from the machine, specifically difficult for actively cooled components, making it unsuitable for routine monitoring.

In projection of tokamak operations, where dismantling actively cooled components is challenging, we aim to develop a non-destructive technique usable directly within the tokamak to enable monitoring of PFC erosion. In WEST, the erosion rate has been determined using ion beam analyses and scanning electron microscopy techniques around 0,1nm/s [1].

In this work, we propose to review non-destructive techniques that may be applied for the assessment of the erosion rate in a tokamak.

The reviewed techniques include : X-ray fluorescence, optical microscopy, confocal microscopy, laser-induced breakdown spectroscopy (LIBS), four probes methods, eddy current testing, three-dimensional measuring machine (CMM), and laser-based ultrasonic measurements. Some of these methods may not be used under vacuum but could serve as potential steps in the development and refinement of the required measurement techniques.

Some measurements were performed in laboratory under common atmosphere on WEST actively cooled divertor targets. As an example, confocal microscopy stands out as a particularly promising technique, as it enables non-contact scanning of large surfaces with sensitivities ranging from 0.15 to 1  $\mu$ m. Similarly, LIBS offers a sensitivity of approximately 1  $\mu$ m, making it highly suitable for precise erosion monitoring. Most of the techniques examined require the

use of erosion markers, such as multilayer coatings, or reference marks to enable accurate measurements.

In this study, the sensitivity and applicability (erosion marker implantation, resolution) of each technique are evaluated, providing insights into their applicability for their possible use in Tokamak.

[1] M. Balden et al 2021 Phys. Scr. 96 124020

[2] A. Hakola et al 2021 Nucl. Fusion 61 116006

POB-71

## **Tungsten erosion and injection investigations in the stellarator Wendelstein 7-X during OP2.2**

Chandra Prakash Dhard<sup>1</sup>, Sebastijan Brezinsek<sup>2</sup>, René Bussiahn<sup>1</sup>, Birger Buttenschön<sup>1</sup>, Dario Cipciar<sup>1</sup>, David Ennis<sup>3</sup>, Joris Fellinger<sup>1</sup>, Erik Flom<sup>4</sup>, Tomasz Fornal<sup>5</sup>, Yu Gao<sup>1</sup>, Isabel Garcia-Cortés<sup>6</sup>, Dorothea Gradic<sup>1</sup>, Tomas Gonda<sup>3</sup>, Carsten Killer<sup>1</sup>, Alexander Knieps<sup>2</sup>, Petra Kornejew<sup>1</sup>, David Kriete<sup>3</sup>, Maciej Krychowiak<sup>1</sup>, Oleksandr Marchuk<sup>2</sup>, Andreas Langenberg<sup>1</sup>, Kieran Joseph McCarthy<sup>6</sup>, Daniel Medina-Roque<sup>6</sup>, Dirk Naujoks<sup>1</sup>, Novimir Pablant<sup>7</sup>, Arun Pandey<sup>1</sup>, Mohammad Faisal Siddiki<sup>8</sup>, Lukasz Syrocki<sup>5</sup>, Naoki Tamura<sup>1</sup>, Sebastian Thiede<sup>1</sup>, Thomas Wegner<sup>1</sup>, The W7-X Team<sup>1</sup>

<sup>1</sup>Max Planck Institute for Plasma Physics, Germany; <sup>2</sup>Forschungszentrum Jülich GmbH, Germany; <sup>3</sup>Auburn University, AL, United States; <sup>4</sup>Thea Energy, Kearny, United States; <sup>5</sup>Institute of Plasma Physics and Laser Microfusion, Poland; <sup>6</sup>Laboratorio Nacional de Fusión, CIEMAT, Spain; <sup>7</sup>Princeton Plasma Physics Laboratory, United States; <sup>8</sup>University of Wisconsin-Madison, United States.

Tungsten has emerged as a favourable material for the plasma-facing components (PFCs) in the nuclear fusion devices. It has been incorporated in several tokamaks, however, in the stellarator, with 3D geometry, its suitability as PFCs, in terms of erosion, redeposition, ionization, transportation and accumulation of the impurity particles in the plasma core, is yet to be demonstrated. In the Wendelstein 7-X (W7-X), tungsten PFCs are being introduced stepwise by increasing the surface area over the last few plasma campaigns [1]. During the recent OP2.2 campaign, the tungsten PFCs surface areas of about 2 m<sup>2</sup> (out of 47 m<sup>2</sup>) in the heat shield and about 0.8 m<sup>2</sup> (out of 33 m<sup>2</sup>) in the baffle, were provided.

During OP2.2, dedicated experiments for the tungsten sputtering were conducted, by using dedicated island control coils to drive higher heat/particle fluxes onto the tungsten baffle areas and simultaneously introducing the impurity gas N<sub>2</sub>/Ne/Ar seeding. In addition, tungsten samples were also exposed to the plasma island via the multi-purpose manipulator by varying the exposure position and duration. Tungsten injection was carried out using the tracer-encapsulated solid pellets (TESPEL) and Laser blow-off (LBO). The plasma discharge conditions were varied in two different magnetic configurations, i.e., standard and high mirror. Observations were made at the edge with UV spectroscopy, Langmuir probes and thermal He-beam diagnostic, and in the plasma core with high-resolution X-ray imaging spectroscopy (HR-XIS), high-efficiency XUV overview spectrometer (HEXOS) and pulse height analysis (PHA). Tungsten W I and W II line signals were detected by the UV edge spectrometers having a line of sight on the baffle tiles. Tungsten signals from the erosion, TESPEL/LBO injection and intrinsic background were observed by the multiple core spectroscopies showing variations in the intensities by varying the island geometry and impurity seeding. The Langmuir probe measurements at the divertor have shown divertor plasma temperatures of about 10 eV and asymmetry in the edge density for the upper and lower island divertors. A detailed analysis will be presented at the conference.

[1] D. Naujoks et al, Nuclear Material Energy 37 (2023) 101514.

POB-73

### **Progress on ELM and inter-ELM tungsten erosion & re-deposition measurements in the DIII-D tokamak using ultraviolet spectroscopy**

Ulises Losada<sup>1</sup>, David Ennis<sup>1</sup>, Stuart Loch<sup>1</sup>, Dane van Tol<sup>1</sup>, Tyler Abrams<sup>2</sup>, Adam McLean<sup>3</sup>, Gilson Ronchi<sup>4</sup>, Dmitry Rudakov<sup>5</sup>, William Wampler<sup>6</sup>, David Kriete<sup>1</sup>

<sup>1</sup>Auburn University, AL, United States; <sup>2</sup>General Atomics, United States; <sup>3</sup>Lawrence Livermore National Laboratory, United States; <sup>4</sup>Oak Ridge National Laboratories, TN, United States; <sup>5</sup>University of California San Diego, United States; <sup>6</sup>Sandia National Laboratories, NM, United States.

Ultraviolet (UV) spectroscopic measurements of tungsten (W) gross-erosion and re-deposition obtained in the DIII-D tokamak demonstrate ~10 times larger erosion rates during Edge Localized Modes (ELMs) than in inter-ELM phases. A 5 cm diameter W-coated Divertor Materials Evaluation System (DiMES) sample was exposed to low frequency ELMs (~20 Hz) in the DIII-D tokamak. W gross erosion rates during ELMs are obtained from W I emission lines combined with S/XB coefficients derived from previous L-mode experiments [4], and agree with previous results [1,2]. A W I spectral line at 255.13 nm has been identified for W gross-erosion measurements due to its high intensity and because it is driven directly from the ground state and is consequently not affected by metastable levels. The 255.13 nm line is measured by high-resolution ultraviolet spectroscopy during both L- and H-mode experiments using W samples in DiMES, located in the DIII-D lower divertor. Simultaneously, W I and W II emission lines were detected at 265.65 and 265.80 nm, respectively, allowing for re-deposition measurements.

Neutral tungsten (W I) emission at 400.88 nm, measured by fast visible spectroscopy, has been previously utilized for in-situ spectroscopic measurements of W gross-erosion during ELMs [1, 2]. However, the dependence of W I emission at 400.88 nm on metastable state electron populations could influence erosion measurements [3]. Alternatively, measuring several W I emission lines across the UV wavelength range (200 – 400 nm) can enhance gross-erosion measurements. In addition, the simultaneous observations of neutral W and emission from higher charge states allows for spectroscopic estimates of W re-deposition rates. The evolution of S/XB ratios for W I and W II emission lines during ELMs is discussed. Electron temperature measurements extracted from W emission line ratios during inter- and intra-ELM phases are benchmarked against Langmuir probes and presented. UV measurements of ELM and inter-ELM tungsten gross erosion are compared with results from visible spectroscopy. W re-deposition fractions of ~75% were determined from a singly ionized emission line (265.80 nm) with no appreciable variation between ELM and inter-ELM phases.

Supported by the US Department of Energy under awards DE-SC0015877, DE-FG02-00ER54610 and DE-FC02-04R54698.

[1] A. Huber et al. (2020) NME 25, 100859

[2] T. Abrams et al. (2017) NF 57, 056034

[3] C. Johnson et al. (2020), PPCF 62, 125017

[4] U. Losada et al. PSI 2023

POB-74

### **Insulator thickness dependence on RF sheath-induced sputtering**

Gayatri Dhamale<sup>1</sup>, Marlene Patino<sup>2</sup>, James Myra<sup>3</sup>, Matt Baldwin<sup>2</sup>, George Tynan<sup>2</sup>, Juergen Rapp<sup>1</sup>

<sup>1</sup>Oak Ridge National Laboratory, United States; <sup>2</sup>University of California San Diego, United States; <sup>3</sup>Lodestar Research Corporation, United States.

Radio frequency (RF) sheath-induced helicon window erosion in linear plasma devices has become a concern, as the impurities originating from the window may be transported toward the downstream target, affecting plasma-material interactions [1]. To address this impurity generation issue, the use of RF-transparent high-Z material coatings on the plasma-facing helicon window surface has been proposed due to their lower sputtering yields [2]. To measure the sputtering yields, these coatings were RF biased and exposed to the PISCES-A experimental conditions. In RF sheath-induced sputtering, the sputtering yield results from the spread in the ion energies, making it higher compared to equivalent DC sheath-induced sputtering. Our hypothesis is that the average ion energy in the former case corresponds to the applied RF bias voltage (zero-to-peak) at the insulator surface [3], and that it decreases with an increase in the insulator thickness [4]. To test this hypothesis, an electrically floating thin Mo-sheet (~0.5 mm) was placed in front of a HfO<sub>2</sub>-coated Si<sub>3</sub>N<sub>4</sub> target, which then exposed to He-plasma and RF biased to 70 VRF (zero-to-peak) in the PISCES-A linear plasma device. The sputtering yields of Mo were measured for the two different insulating target thicknesses, 1.58 mm and 6.35 mm, in separate plasma discharges. The measured sputtering yields of Mo by He for thin and thick insulating targets were compared with the theoretical sputtering yield curve of Mo by He [5]. We observed that the average ion energy was close to the applied RF bias voltage (zero-to-peak). We concluded that increasing the insulator thickness may not significantly reduce RF sheath-induced sputtering, as the average ion energies remain close to the RF bias voltage for both the insulator thicknesses.

Acknowledgments:

This work is supported by the DOE Office of Science, Office of Fusion Energy Science, under contract number DE-AC-5-00OR22725.

References:

- [1] G. Dhamale, M. J. Baldwin, M. S. Islam, et al., Plasma Phys. Control. Fusion 66 095015 (2024)
- [2] J. Rapp, M. J. Baldwin, C. J. Beers et al., IEEE Trans. Plasma Sci. 52, 9, 3885–3891 (2024)
- [3] M. I. Patino, R. P. Doerner, G. R. Tynan, Nucl. Mater. Energy 23, 100753 (2020)
- [4] J. R. Myra, D. A. D'Ippolito, J. A. Rice et al., J. Nucl. Mater. 249, 190–198 (1997)
- [5] R. Behrisch, W. Eckstein, Topics Appl. Phys. 110 33–187 (2007)

POB-75

### **Effects of surface roughness on sputter yield of Mo under laboratory and tokamak conditions**

Mitja Kelemen<sup>1</sup>, Sabina Markelj<sup>1</sup>, Karl Krieger<sup>2</sup>, Thomas Schwarz-Selinger<sup>2</sup>, Espedito Vassallo<sup>3</sup>, David Dellasega<sup>4</sup>, Matteo Passoni<sup>4</sup>, Antti Hakola<sup>5</sup>, Martin Balden<sup>2</sup>, Andreas Mutzke<sup>2</sup>, Primož Pelicon<sup>1</sup>, Rok Zaplotnik<sup>1</sup>, The ASDEX UPGRADE Team<sup>6</sup>, The EUROfusion Tokamak Exploitation Team<sup>7</sup>

<sup>1</sup>Jožef Stefan Institute, Slovenia; <sup>2</sup>Max Planck Institute for Plasma Physics, Germany; <sup>3</sup>Istituto per la Scienza e Tecnologia dei Plasmi, CNR, Italy; <sup>4</sup>Politecnico di Milano, Italy; <sup>5</sup>VTT Technical Research Centre of Finland Ltd, Espoo, Finland; <sup>6</sup>see author list of H. Zohm et al, 2024 Nucl. Fusion 64 112001, Germany; <sup>7</sup>see author list of E. Joffrin et al 2024 Nucl. Fusion 64 112019, Germany.



The issue of erosion of plasma-facing components in thermonuclear fusion has been extensively studied in recent years. Previous research has focused on the effects of incidence angle on sputter yields for smooth surfaces [1] and has been extended to model surfaces with well-defined periodic surface roughness of approximately 25 nm [2]. However, to accurately predict the erosion of reactor plasma exposed components, their surface morphology must be studied in real fusion experiments. In this work, the experimental study was divided into three parts. For all cases, thin films of Mo (~120 nm) were deposited via pulsed laser deposition onto graphite substrates with varying surface roughness, ranging from 5 nm to 2–3  $\mu\text{m}$ . The first experiment involved laboratory studies with SDTrimSP-3D simulations; the second and third involved exposing samples to deuterium discharges in ASDEX Upgrade (AUG) in L-mode and H-mode, respectively. The thickness of Mo layers was measured before and after the experiments with RBS using a 4He ion beam. Surface roughness was characterised by AFM for intermediate values or by CLSM for high values.

In the laboratory, we irradiated samples with 1 keV/D ions from an electron cyclotron resonance ion gun. Samples were exposed to different angles of incidence ( $0^\circ$  to  $70^\circ$ ) and D ion fluences in the range of  $10^{23}$  D/m<sup>2</sup>. These experiments served for validation of the calculated sputter yields using Monte Carlo code SDTrimSP-3D [3], for which we obtained good agreement [4].

The same types of samples were exposed to D plasma in AUG. Using the AUG-DIM-II divertor manipulator, the samples were mounted near the outer strike point with a particle incident angle of approximately  $60^\circ$  in both plasma scenarios.

The results obtained in AUG show decreased erosion on samples with higher surface roughness in both plasma scenarios, which is in good agreement with data collected in the laboratory.

[1] R. Behrisch, W. Eckstein (Eds.): Sputtering by Particle Bombardment, Topics Appl. Physics 110, 33–187 (2007)

[2] R. Arredondo et al. Nuclear Materials and Energy 18 (2019) 72

[3] U. von Toussaint, A. Mutzke, and A. Manhard. Sputtering of rough surfaces: a 3D simulation study. Phys. Scr., 2017(T170):014056, 2017

[4] M. Kelemen et al. Journal of Nuclear Materials 555 (2021) 153135

POB-76

### **Plasma-chemical mechanism of surface destruction of the diagnostic system components inside EAST vacuum vessel**

Lidia Lobanova, Shouxin Wang, Hui Lian, Xiaoqian Cui, Jihui Chen, Rong Yan, Ling Zhang, Viktor Afanas'ev, Haiqing Liu

Institute of Plasma Physics, Chinese Academy of Sciences, China.

Experience with mirrors on the EAST tokamak shows catastrophic degradation of their surfaces as a result of each experimental campaign. A study was conducted on the first mirrors made of polycrystalline molybdenum, used for the POINT system in the EAST tokamak. The results of XPS analysis indicate that the content of redeposited elements from structural materials (B, Zn, Fe, Cu) is less than 1%. However, the entire surface of the mirrors is covered with molybdenum oxides, with MoO<sub>3</sub> being predominant. Experiments demonstrated effective removal of MoO<sub>3</sub> due to heating the mirrors. The volatility of MoO<sub>3</sub> is associated with the extremely low vapor pressure of MoO<sub>3</sub>. Removal of MoO<sub>3</sub> also occurs due to the exposure to deuterium plasma.

The cyclical nature of tokamak operation (technical breaks following plasma discharge

phases) and a significant amount of water (5%) in the residual gases are notable features. During technical breaks, a water film several tens of nm thick forms on the surface, which promotes effective oxidation.

Optical diagnostics of the surface of the mirrors revealed the appearance of characteristic lines along the intercrystalline spaces and round craters on the initially mirror-like surface, which are the consequence of radiation defect formation due to exposure to deuterium plasma. Channels arising from defect formation became centers for the oxidation of Mo.

When removing a layer of 3  $\mu\text{m}$  from the surface, polishing and etching with reagents revealed a structure with significantly larger grain sizes than on the mirror surface. The reduction in grain size is associated with deuterium implantation, leading to changes in the material's technological characteristics and embrittlement.

The issue of additional plasma-chemistry processes causing degradation of the mirror surfaces due to lithium coating is discussed. The presence of water and Li leads to the formation of LiOH, which interacts with MoO<sub>3</sub> to produce easily soluble stable molybdates and polymolybdates of lithium that cover the surface. It should be emphasized that these chemical processes do not obey Arrhenius' law, as they are accompanied by plasma exposure.

Questions regarding plasma-chemical degradation of the surfaces of transition metals (Mo, W) are relevant but poorly studied. A number of experimental facts, related, for example, to the sharply different degrees of oxidation of Mo subjected to D and He implantation, remain mere empirical results. The aim of this work is to draw attention to these issues.

Acknowledgements: This work was supported by the National MCF Energy R&D Program of China (Grant No. 2019YFE0304003 and Grant No. 2022YFE03080002).

POB-77

## **ERO2.0 modelling of divertor marker erosion in ASDEX Upgrade L-mode**

Samuli Saari<sup>1</sup>, Antti Hakola<sup>1</sup>, Juuso Karhunen<sup>1</sup>, Martin Balden<sup>2</sup>, Christoph Baumann<sup>2</sup>, Aaro Järvinen<sup>1</sup>, Karl Krieger<sup>2</sup>, Henri Kumpulainen<sup>2</sup>, Jari Likonen<sup>1</sup>, Juri Romazanov<sup>2</sup>

<sup>1</sup>VTT Technical Research Centre of Finland, Finland; <sup>2</sup>Forschungszentrum Jülich GmbH, Germany.

Erosion of small marker surfaces in an experiment [1, 2] conducted at ASDEX Upgrade was reproduced by ERO 2.0 [3] simulations in close agreement with post-mortem measurements. In the experiment 5 × 5 mm<sup>2</sup> and 1 × 1 mm<sup>2</sup> Au marker spots were exposed to a series of high-temperature L-mode plasmas in the low-field side strike point region to serve as proxies for measuring net and gross erosion of W, respectively. An ERO2.0 simulation setup was created for the experiment, using background plasma corresponding to the Langmuir probe data during the experiment, surface definitions matching the experimental geometry and newly generated energy- and angle-dependent sputtering data for Au produced with the SDTrimSP code [4].

The simulated net erosion of the Au markers agreed closely with the measured values with remaining deviations at the strike point most likely due to experimental uncertainties of the strike point conditions and position. This radical improvement from the earlier ERO modelling of the experiment [2] is primarily attributed to the new angular dependency of the sputtering data for Au, yielding 2–4 times stronger gross erosion in comparison to the previously used yield estimates given by the Bohdanský formula with no angular dependency. The erosion of the Au markers was induced mainly by the light B, C and N impurities defined as fixed concentrations in the background plasma.

The Au markers were found to undergo up to 15—20 times stronger net erosion in comparison to a uniform W surface. This was attributed to 3—4 times stronger gross erosion of Au in comparison to W and deposition of the eroded Au mostly outside of the markers. Consequently, the simulations suggest strongly compromised capability of the experimentally studied Au markers acting as proxies for W in erosion studies due to the significantly higher gross erosion yield of Au and the insufficient size of the 5 x 5 mm<sup>2</sup> markers for successful representation of net erosion.

- [1] A. Hakola et al., Nuclear Fusion 61 (2021) 116006
- [2] A. Hakola et al., Nuclear Materials and Energy 25 (2020) 100863
- [3] J. Romazanov et al., Physica Scripta T170 (2017) 014018
- [4] A. Mutzke et al., SDTrimSP Version 6.00, IPP Report 2019-02

POB-78

### **First Coupling of SOLEDGE3X-QLKNN10D: Integrated W Modelling Accounting for Neoclassical Effects**

Naren Varadarajan, Guido Ciraolo, Hugo Bufferand, Pierre Manas, Luca Cappelli, Nicolas Rivals, Patrick Tamain, Srikanth Sureshkumar, Ludovica de Gianni, Virginia Quadri, Nicolas Fedorczak  
CEA, IRFM, France.

Machines such as WEST, and ITER have opted to utilise Tungsten – for the first wall in the form of W coating or bulk W, and in the form of W monoblocks for their divertors. Moreover, in WEST the radiated fraction is estimated to be 50%, independent of the input power. Given this, accurate modelling of W from its erosion and subsequent redeposition at PFCs, to its transport in the edge and the core taking into account feedback on the power crossing the separatrix, is crucial. Building on previous work [1], the SOLEDGE-3X multi-fluid code was used to perform integrated modelling of W from the first wall to the core. To accurately model turbulent core transport of the main ion and electrons, a coupling was made with QLKNN-10D [2] – a neural network trained on the QuaLiKiz code. Additionally, neoclassical transport of W in the core due to collisions with the main ion must be accounted for, and hence the algorithm used in FACIT [3] was introduced into SOLEDGE-3X to do the same. For the erosion of W at the PFCs, the Eckstein-Preuss formula was used, as well as an analytical formula for prompt-redeposition. Using these tools, comparisons of W modelling were made between SOLEDGE-3X and ERO 2.0., with good agreement of the gross sputtered fluxes and sites of W accumulation in the edge. This comparison paves the way for future experimental comparison with the aim of recovering the radiated fraction in WEST.

#### REFERENCES:

- N. Varadarajan et al., JNM (2024). <https://doi.org/10.1016/j.nme.2024.101818>
- K. L. van de Plassche, Phys. Plasmas (2020). <https://doi.org/10.1063/1.5134126>
- P. Maget et al, PPCF 62, 105001 (2020); D. Fajardo et al, PPCF 64, 055017 (2022)

POB-79

### **Evolution of elemental depth profiles on co-deposited layers at the divertor region of the WEST tokamak during its Phase 1 operations**

Antti Hakola<sup>1</sup>, Jari Likonen<sup>1</sup>, Tomi Vuoriheimo<sup>2</sup>, Eduard Grigore<sup>3</sup>, Indrek Jõgi<sup>4</sup>, Peeter Paris<sup>4</sup>, Elodie Bernard<sup>5</sup>, Mathilde Diez<sup>5</sup>, Emmanuelle Tsitrone<sup>5</sup>

<sup>1</sup>VTT Technical Research Centre of Finland Ltd, Finland; <sup>2</sup>Department of Physics, University of Helsinki, Finland;  
<sup>3</sup>Acasa Institutul National pentru Fizica Laserilor, Plasmei si Radiatiei, Romania; <sup>4</sup>University of Tartu, Institute of Physics,

In fusion reactors, co-deposited layers, potentially rich in tritium, can be formed on plasma-facing components (PFCs) during plasma operations. To cast light on the formation mechanisms and structure of such deposits, we have investigated elemental depth profiles on divertor PFCs, removed from the WEST tokamak after three individual campaigns (labelled as C3, C4, and C5). Special wall tiles, consisting of tungsten (W) and molybdenum (Mo) marker layers (thickness 1–2 micrometers) and produced for erosion and deposition studies during the Phase 1 operations of WEST [1] were analyzed using Secondary Ion Mass Spectrometry (SIMS) and Glow Discharge Optical Emission Spectroscopy (GDOES). All the tiles originated from distinct toroidal locations of the WEST divertor, corresponding to the maxima of the magnetic ripple on the low-field (outer) and high-field (inner) side. The obtained results were compared to the data available from Laser Induced Breakdown Spectroscopy (LIBS) measurements [2,3]. The focus was set on determining detailed depth profiles for the plasma fuel (predominantly deuterium (D)) and typical impurities (boron (B), carbon (C), oxygen (O), and elements from steel) after each campaign and correlating them with the erosion and deposition patterns of the marker materials W and Mo. Both SIMS and GDOES indicate the thickest deposits having formed towards the end of Phase 1 while their composition does not show radical differences between C3, C4, and C5. Besides noticeable re-deposition of W and Mo, the layers mainly consist of B, C, and O. The thickest deposits (up to several micrometers) have been measured on the high-field side, next to the strike point, exhibiting relatively homogeneous profiles for the different elements – except for D which is more superficially (~1 micrometer) accumulated on the layers. In addition, thinner deposits (<0.5 micrometers) occur further (a few cm) into the scrape-off layer both on the inner and outer sides of the divertor. In these regions, a more complicated, dynamic picture can be observed between erosion and deposition: small but progressive erosion of the markers from C3 to C5 accompanied with comparable deposits forming on the top during each campaign.

[1] J. Bucalossi et al., Nucl. Fusion 62 (2022) 042007

[2] I. Jögi et al., J. Nucl. Eng 4, 96 (2023)

[3] I. Jögi et al., this conference

POB-80

### **Impact of helium plasma implantation on tungsten softening approaching detached plasma conditions at the divertor region**

Anthony Flament<sup>1</sup>, Maxime Lemetais<sup>2</sup>, Alan Durif<sup>1</sup>, Federica Pappalardo<sup>3</sup>, Marco Minissale<sup>3</sup>, Laurent Gallais<sup>3</sup>, Guillaume Kermouche<sup>2</sup>, Marianne Richou<sup>1</sup>

<sup>1</sup>CEA, IRFM, France; <sup>2</sup>Mines Saint-Etienne, CNRS UMR 5307 LGF, France; <sup>3</sup>Aix-Marseille Université, CNRS, PIIM, France.

Tokamak aims at confining magnetically deuterium-tritium plasma. Due to imperfect magnetic confinement the plasma facing components (PFCs), must endure intense thermal loads (10–20 MW/m<sup>2</sup>), ions fluxes and neutrons bombardment notably at the divertor region. Tungsten is commonly employed as plasma facing material due to its high melting point and low hydrogen isotope chemical affinity; however, under repeated 20 MW/m<sup>2</sup> thermal heat flux, tungsten damage generated. Damage includes cracking but also softening (recrystallization / recovery) which promotes the accumulation of plastic strain. Tungsten softening is known to decrease the material crack resistance and hardness. Depending on the tungsten monoblock

design, softening may play a role on macro-crack initiation and propagation limiting thus the PFC lifetime under tokamak operational conditions. Up to date, softening kinetics were investigated for pure tungsten under annealing. Nevertheless, plasma-wall interaction, in particular helium implantation, seems to play a role on softening kinetics between 900 and 1900 K [1] but its exact impact remains unclear. This study aims at assessing the effect of helium plasma implantation on hot-rolled tungsten recrystallization kinetics approaching detached plasma conditions at divertor region [2]. Sixteen hot-rolled, highly cross-rolled tungsten samples ( $5 \times 4 \times 3$  mm<sup>3</sup>), were subjected to different laser annealing treatments (1783 K for 200s and 1000s, 1643 K for 3000s) and subsequently implanted with helium plasma (here, ion incident energy was around 19.5 eV and a fluence of  $1.8 \times 10^{24}$  He.m<sup>-2</sup>, as comparison ITER ion incident energy). The samples were analyzed performing Electron Backscatter Diffraction (EBSD) analysis and Vickers hardness measurements. Vickers tests have been done varying the loaded charge (1 kg, 200 g, 100 g) to assess the potential influence of helium at different depth (from 3 to 9  $\mu$ m). Results indicate that hardness tests results do not highlight significant helium effects at the explored loading scales. This trend is confirmed whatever the helium irradiation and annealing performed. Complementary EBSD analysis reveal also such irradiation mimicking detached plasma conditions does not significantly impact tungsten sample softening.

[1] Thompson, M.A.T. et al, JNM 559 (2022) 153448.

[2] Tsitrone, E et al, Nucl Fus 62, no7 (2022) 076028

POB-81

## **Thermophysical and thermomechanical properties of Tungsten-based (W-Ti-Ta-Cr-V) High-Entropy Alloys**

Zori Harutyunyan

Imperial College London, United Kingdom.

Due to its fusion-favourable properties, such as high melting point, good thermal properties, and low tritium retention, tungsten has been successfully applied as a PFM in large research reactors such as JET (UK), ASDEX Upgrade (Germany), WEST (France), and has also been identified as the baseline PFM for ITER. In future commercial fusion plants like DEMO, the fluxes of heat and particles to the PFM are predicted to be even higher than in ITER. Moreover, the pulse duration time of plasma burning will be significantly longer. Under such operating conditions, W degrades excessively and is not suitable for use in future fusion power plants. High entropy alloys (HEAs) provide a transformative opportunity to design materials that are more tolerant to extreme conditions. In particular, W-Ti-Ta-Cr-V HEAs have been identified as displaying a good combination of thermal stability and resistance to helium plasma and neutron irradiation. However, there is currently limited information on their thermophysical and thermomechanical properties. This work presents a systematic investigation of the properties of the W50-(Ti-Ta-Cr-V)50 composition from room temperature to  $\sim 1500$  °C. The alloys are manufactured using powder metallurgy techniques, including ball milling and spark plasma sintering (SPS). The parameters for sintering were optimised to tailor the grain size and porosity. A comprehensive study of the thermomechanical properties is presented. The 4-point bend method was used to determine the ductile-to-brittle transition temperature, which is compared to data on pure tungsten that was sintered and tested in identical conditions. Lastly, the thermophysical parameters are reported. Specifically, the laser-flash method, dilatometry, and differential scanning calorimetry data are combined to determine thermal conductivity. Some initial results of

their behaviour under fusion relevant plasma conditions will be presented, including irradiation with heavy tungsten ions at the Dalton Cumbria Facility in the UK.

POB-82

### **Impact of Phase Decomposition on Performance of SMART Tungsten-Based Alloys for a First Wall of DEMO**

Duc Nguyen-Manh<sup>1</sup>, Eric Prestat<sup>1</sup>, Mark Gilbert<sup>1</sup>, Damian Sobieraj<sup>2</sup>, Jan Wrobel<sup>2</sup>, Jie Chen<sup>3</sup>, Andrey Litnovsky<sup>3</sup>

<sup>1</sup>United Kingdom Atomic Energy Authority (UKAEA), United Kingdom; <sup>2</sup>Warsaw University of Technology, Poland;

<sup>3</sup>Forschungszentrum Julich GmbH, Germany.

Tungsten alloys have been selected as a potential first wall material for DEMO and other near-term fusion reactors. Tungsten is a good candidate due to its high melting point, low sputtering by plasma particles, relatively short-term activation, low tritium retention, and high thermal conductivity. However, pure tungsten behaves poorly in loss-of-coolant accident environments, where contact with the surrounding atmosphere causes rapid oxidation releasing radioactive tungsten dust into the air or form hazardous gaseous tungsten volatile oxides. To tackle this, Self-passivating Metallic Alloys with Reduced Thermo-oxidation (SMART) have been suggested that incorporate additions of Cr, Y, and Zr that, will preferentially form protective scales of their own oxides on the surface, inhibiting the tungsten oxide formation [1].

Alloying of these elements into tungsten, however, is not straightforward as our recent integrated modelling and experimental investigations have suggested that the as-manufactured single-phase solid solution microstructures can be thermodynamically unstable with a tendency to decompose at elevated temperature. Using first-principles approach combining Density Functional Theory (DFT), cluster expansion technique with Monte-Carlo simulations [2], it has been found that alloying only 0.6Y (in wt%) has reduced the spinodal phase decomposition in W-Cr binary by 400°C while co-alloying Y and Zr has increased the segregation trend between W and Cr in their quaternary alloys [3]. Our fundamental findings are strongly supported by the experimental studies of self-passivating W-11.4Cr-0.6Y alloys annealed at 1000°C for varying duration to induce phase decomposition [4]. The microstructure evolution process under annealing and oxidation by in-situ environmental Scanning/Transmission Electron Microscope also reveals the observation of W/Cr phase segregation in a good agreement with modelling predictions. The mechanical properties and the oxidation performance of the phase decomposed SMART-W alloys were investigated and compared to the as-sintered material. Our results and further multiscale materials modelling using machine-learning approach present promising prospects of the phase-decomposed microstructure in the scaling up toward the industrial production of self-passivating alloys for first wall applications.

**Acknowledgements:** This work has been carried out within the framework of the EURO-fusion Consortium, funded by the European Union via the Euratom Research and Training Programme (Grant Agreement No 101052200). DNM, EP and MG acknowledge funding from the RCUK Energy Programme Grant No. EP/W006839/1.

[1] A. Litnovsky, et al., *Metals*, 11, 1255 (2021).

[2] D. Nguyen-Manh, et al., *Phys. Rev. Materials*, 5, 065401 (2021).

[3] D. Sobieraj, et al., *Metals*, 11, 743 (2021); *J. Alloys Metall. Syst.*, 2, 100011 (2023).

[4] J. Chen, et al., *Nucl. Mater. Energy*, 41, 101762 (2024).

POB-83

### **First attempts for industrialization of tungsten fiber-reinforced tungsten composites**

Yiran Mao<sup>1</sup>, Ute Wilkinson<sup>2</sup>, Jan Coenen<sup>1</sup>, Daniel Wilkinson<sup>2</sup>, Johann Riesch<sup>3</sup>, Christian Linsmeier<sup>1</sup>

<sup>1</sup>Forschungszentrum Jülich GmbH, Germany; <sup>2</sup>Dr. Fritsch Sondermaschinen GmbH, Germany; <sup>3</sup>Max Planck Institute for Plasma Physics, Germany.

The development of plasma-facing materials (PFMs) for future fusion reactors requires advanced mechanical and thermal properties to withstand the extreme challenges of high heat flux, plasma exposure, and neutron irradiation. This is especially true for the divertor region, where surfaces are exposed to intense thermal and particle fluxes. Tungsten is one of the most suitable materials for the use as a PFM in the divertor region due to its favorable properties such as low erosion rate, high sputtering threshold, excellent thermal conductivity, and high melting point. However, considering the high thermal loading/thermal stress combining plasma exposure and neutron irradiation/embrittlement, one of the major concerns for tungsten as PFMs is its intrinsic brittleness. To avoid cracking and components failure, toughening tungsten has been widely investigated, among which tungsten fiber-reinforced tungsten composites (Wf/W) are developed using an extrinsic toughening mechanism, which could provide damage resilience against neutron embrittlement.

Recently, a type of aligned long fiber Wf/W (L-Wf/W) based on a powder metallurgical fabrication process was developed, demonstrating advanced fracture toughness while retaining other application-relevant properties. One critical factor for this damage resilience is the existence of a dedicated interface between W fiber and W matrix. In addition, the relatively easy production process suggests the feasibility and basis of industrialization.

This work reports on the initial progress in industrializing L-Wf/W, with a focus on adapting the lab sintering process to an industrial sintering process and optimizing process parameters. To improve the sinterability of tungsten and achieve higher density, various tungsten powders were explored, including commercial W powders, bimodal mixtures of different particle sizes, and granulated W powders. At the dedicated interface, the thickness of yttria coating on the fibers was also optimized to ensure effective separation between the fibers and the matrix. Series of samples were produced with different dimension up to 100mm x 100mm x 4mm. After optimization, samples with high density and desired pseudo ductility were prepared. A major challenge in this work involved balancing the densification of the tungsten matrix with controlling fiber recrystallization and mitigating damage to the yttria interface.

POB-84

### **Recent Advances in Tungsten Fiber-Reinforced Composites for Fusion Reactor Applications**

Jan Coenen<sup>1</sup>, Yiran Mao<sup>1</sup>, Alexander Lau<sup>1</sup>, Rui Shu<sup>1</sup>, Juan Du<sup>2</sup>, Johann Riesch<sup>3</sup>, Christian Linsmeier<sup>1</sup>

<sup>1</sup>Forschungszentrum Jülich GmbH, Germany; <sup>2</sup>Southwestern Institute of Physics, Chengdu, China; <sup>3</sup>Max Planck Institute for Plasma Physics, Germany.

Tungsten fiber-reinforced tungsten composites (Wf/W) offer a promising solution to mitigate the intrinsic brittleness of tungsten (W), a leading candidate for plasma-facing components in fusion reactors. These advancements build upon the concept of extrinsic toughening mechanisms, achieving pseudo-ductility through material design realized using advanced fabrication techniques.

This contribution provides an overview of the recent achievements on manufacturing, with a focus on highlighting techniques that show promise for component development and further

material optimization.

With the aim of producing Wf/W based on 2D or 3D continuous fiber pre-forms the materials have been manufactured using powder metallurgy (PM) as well as Chemical Vapour Deposition and Infiltration (CVD/CVI). Sizes of up to 100x100mm square PM Wf/W and 180 x85 mm CVD Wf/W have been achieved. Compared to conventional W the composites show significant improvements in fracture toughness exhibiting multiple toughening mechanisms, including fiber bridging, crack deflection, and fiber plastic deformation, with energy dissipation dominated by the latter.

One of the recent breakthroughs in manufacturing has been achieved using CVI with a three-dimensional temperature gradient, enabling the efficient processing of textile packages in a single step. This method addresses the scalability, cost, and design limitations of traditional Spark Plasma Sintering (SPS) and conventional CVD methods. Furthermore, the CVI approach allows the integration of additional elements, such as copper, to enhance the joining to cooling structures.

The samples produced exhibit fracture energies one to two orders of magnitude greater than those of current baseline tungsten materials. Near full-density composites (>90%) have been successfully fabricated. High-temperature tensile tests (up to 1000°C) and in-situ crack propagation observations confirm enhanced toughness and improved crack resistance.

As part of these novel production techniques also three-dimensional tungsten fiber reinforcement were fabricated.

Performance under simulated fusion reactor conditions has demonstrated similar sputtering resistance and comparable deuterium retention as compared to baseline tungsten.

These recent advancements highlight significant progress in the field of Wf/W composites.

POB-85

### **Evaluation of hydrogen isotopes desorption dynamics for tungsten rhenium alloy**

Yuzuka Hoshino<sup>1</sup>, Robert Kolasinski<sup>2</sup>, Yasuhisa Oya<sup>1</sup>

<sup>1</sup>Shizuoka University, Japan; <sup>2</sup>Sandia National Laboratories, United States.

Tungsten (W) is a promising candidate for plasma facing materials (PMFs) in fusion reactors due to its higher melting point and lower sputtering yield. W will be exposed to high fluxes of deuterium (D) and tritium (T), as well as helium (He) ash. In addition, 14 MeV neutrons produced by D+T fusion reactions will be irradiate the W PMFs, leading to the transmutation to rhenium (Re) in W matrix. For steady-state operation in a fusion reactor, it is crucial to understand the dynamics of hydrogen isotopes, including desorption, dissolution, trapping/de-trapping and permeation in W-Re alloys. However, knowledge of these dynamics in W-Re is currently limited.

In this study, we aim to investigate the dynamics of hydrogen isotopes through plasma exposure experiments focusing on the desorption behaviour. We used 6 mm diameter W-10%Re alloy disks with 0.5 mm thickness. The specimens were installed in the plasma driven permeation (PDP) device at Shizuoka University, where we studied its permeation behaviour over a temperature range of 723 K and 823 K. A 13.56 MHz RF power supply with a maximum output of 3 kW was used to generate a 550 W plasma discharge with a neutral pressure of 1.0 Pa. We then calculated the plasma flux from the current-voltage (I-V) characteristics measured by a double Langmuir probe, yielding an ion flux of  $1.0 \times 10^{21} \text{ m}^{-2} \text{ s}^{-1}$ . The permeating H<sub>2</sub>, HD, and D<sub>2</sub> fluxes were measured using a mass spectrometer calibrated with a deuterium standard leak. Thermal desorption spectroscopy (TDS) was performed to evaluate the retention behaviour from room



temperature up to 1173 K with the heating rate of 0.5 K s<sup>-1</sup>.

We evaluated the D desorption behaviour for both undamaged W and W-10%Re following a plasma fluence of  $1.0 \times 10^{25}$  D m<sup>-2</sup>. The major D desorption temperatures were found to be in the same temperature range for both materials, though with the W-10%Re exhibiting higher retention than W. The addition of Re appears to enhance the solute D concentration rather than creating new trapping sites. In this presentation, we will discuss diffusion and release of hydrogen isotopes from these materials based on the results of the permeation and TDS experiment discussed above.

POB-88

### **Evidence for sputtering of D and O adsorbed on W(110) by a D<sub>2</sub><sup>+</sup> ion beam**

Latournerie Matthieu, Thierry Angot, Eric Salomon, Marco Minissale, Regis Bisson

Aix-Marseille Université, CNRS, PIIM, France.

The divertor and first wall of ITER will be made of tungsten (W) thus a detailed understanding of their interaction with fusion fuel is needed. In particular, characterizing the release kinetics of hydrogen isotopes from W materials is important to model fuel recycling [1], which could be influenced by impurities such as oxygen (O) [2]. Recently, an Auger Electron Spectrometer (AES) has been added to the Temperature Programmed Desorption (TPD)-ion implantation apparatus AMU-PSI to quantify thin films of O in the sub-monolayer (sub-ML) regime, and determine their influence on deuterium (D) release kinetics from W. In this contribution, we present, first, how D ion implantation affects D release kinetics at various D coverage suggesting self-sputtering and, second, how D ion implantation sputters sub-ML O on W.

Starting with a clean W(110) sample, we realize various D exposures either by thermal neutral D<sub>2</sub> exposure (surface loading) or by 500 eV D<sub>2</sub><sup>+</sup> ion (bulk loading). Surface loading with a D coverage of 0.25 ML gives a desorption temperature of 540 K. Increasing the D surface coverage to 1.00 ML, decreases the desorption temperature down to 455 K. These results agree with Whitten and Gomer [3]. Bulk loading with D<sub>2</sub><sup>+</sup> ion implantation in the  $10^{19-20}$  D<sup>+</sup>.m<sup>-2</sup> range gives desorption temperature that are systematically lower than surface loading. One could interpret it as an increased of the surface coverage with D atoms due to diffusion from the bulk to the surface. However, modifications in the line shape of the TPD peak suggests that self-sputtering of D adsorbed at the surface by D ions occurs simultaneously with bulk loading. Then, we deposited 0.5 ML of O at the surface of W(110) and exposed it to the D<sub>2</sub><sup>+</sup> ion beam to evaluate the corresponding poorly-known sputtering yield. To this purpose, we use AES to quantify the evolution of O coverage with increasing D ions fluence. We show that for D ions at 250 eV/D and at normal incidence, the sputtering yield for O adsorbed on W is  $4 \times 10^{-3}$ . This sputtering yield is smaller than the one for a massive C target, consistent with the higher mass of O. Finally, using a Low-Energy Electron Diffractometer, we measure a loss of periodicity of the initial O surface lattice, supporting the observation of D-ion-induced depletion of O observed by AES.

[1] Smirnov et al., Physics of Plasmas 27 (2020) 032503

[2] Dunand et al., Nuclear Fusion 62 (2022) 054002

[3] Whitten and Gomer, Surface Science (1998) 409

### Applications of a newly developed tungsten-boron potential

Nima Fakhrai Mofrad, Antoine Clement, Andrea Sand

Aalto University, Finland.

In fusion reactors, the choice of suitable plasma-facing materials (PFMs) is essential to ensure safety and economic efficiency [1]. Nevertheless, the choice of PFMs in fusion reactors is continually advancing due to the high complexity of plasma-wall interactions (PWIs) and, in particular, erosion. For example, beryllium was highlighted as a promising PFM due to its low atomic number and affinity for oxygen, aiding in maintaining plasma purity and reducing energy losses [2]. Currently, tungsten (W) is considered the optimal plasma-facing material, due to lower erosion rates, tritium retention, and dust production [3].

However, tungsten walls would need to be conditioned through boronization, which is a process that deposits a thin layer of boron (B) on the tungsten surface. Although boronization has shown success with carbon walls [4], not much is known regarding the chemical and physical properties of the deposited boron layer. In particular, the rate of erosion of the boronized surface is not known [5]. To address this question, our research aims to study erosion within the W-B system using molecular dynamics (MD) simulations. To facilitate these studies, we have developed a Tersoff-type interatomic potential [6] for the W-B system. The potential was fitted on properties obtained from density functional theory (DFT) calculations, including cohesive energies and lattice parameters for various configurations of each element, characteristics of a number of alloys, and various molecular structures.

The potential demonstrates good performance in measuring the general bulk properties of each element and their alloys. Furthermore, it provides good predictions for both sputtering and reflection yields from the surface, thus highlighting its proficiency in studying erosion.

[1] Ward, D. J., and Dudarev, S. L., *Materials Today*, 11, 46 (2008).

[2] G. Federici, *Phys. Scr.*, 1 (2006).

[3] R.A. Pitts et al., *Nuclear Materials and Energy*, 101854 (2025).

[4] J. Winter, *Plasma Phys. Control. Fusion*, 38, 1503 (1996).

[5] K. Schmid and T. Wauters, *Nuclear Materials and Energy*, 101789 (2024).

[6] J. Tersoff, *Phys. Rev. B* 37, 6991 (1988).

### Development of W<sub>2</sub>C-reinforced W for a plasma-facing armour material

Petra Jenuš<sup>1</sup>, Sabina Markelj<sup>1</sup>, Anže Abram<sup>1</sup>, Andreja Šestan Zavašnik<sup>1</sup>, Aleksander Učakar<sup>1</sup>, Andrei Galatanu<sup>2</sup>, Magdalena Galatanu<sup>2</sup>, Elena Tejado<sup>3</sup>, José Y. Pastor<sup>3</sup>, Marius Wirtz<sup>4</sup>, Gerald Pintsuk<sup>4</sup>, Aljaž Iveković<sup>1</sup>

<sup>1</sup>Jožef Stefan Institute, Slovenia; <sup>2</sup>National Institute of Materials Physics, Romania; <sup>3</sup>Departamento de Ciencia de Materiales-CIME, ETSI Caminos, Canales y Puertos, Universidad Politécnica de Madrid, Spain; <sup>4</sup>Forschungszentrum Jülich GmbH, Germany.

Tungsten is considered as the material of choice for the divertor application of fusion power plants due to its intrinsic thermo-physical properties. However, one main drawback is the recrystallization induced reduction of its mechanical properties at elevated temperatures. Therefore, the aim of the conducted research was to improve the material properties to be able to resist especially the high thermal loads imposed on the divertor during operation. We will show that the particle reinforcement of fusion-relevant tungsten through the incorpor-

ation of tungsten sub-carbide W<sub>2</sub>C particles at the grain boundaries is demonstrated to be an effective way of eliminating the oxygen present in the starting powder without subjecting it to the hydrogen atmosphere at elevated temperatures [1]. At the same time the densification is being promoted, composite's microstructure is being strengthened and flexural strength at room and high temperatures is increased when compared to the pure tungsten [2]. While higher concentration of W<sub>2</sub>C particles lead to the refined grain sizes and higher hardness, low concentration (2-3 wt%) of W<sub>2</sub>C particles dispersed in isotropic W matrix displayed the DBTT between 200 and 400 °C, which is lower or comparable to the isotropic and IGP [3] tungsten. Additionally, the prolonged thermal treatment (ageing) at temperatures above 1250 °C with retention times from 1 to 7 days confirmed that the presence of W<sub>2</sub>C particles at W grain boundaries prevents the abnormal growth of W grains. The examination of D retention revealed that the composite in which W was reinforced by 4 wt% of W<sub>2</sub>C, and it was  $(78.7 \pm 2.9) \cdot 10^{19}$  D/m<sup>2</sup> and  $(148.4 \pm 1.5) \cdot 10^{19}$  D/m<sup>2</sup> for a D exposure temperature of 370 K and 523 K, respectively [4].

High thermal stability coupled with good mechanical properties, comparable or even better thermal shock behaviour than W, reasonable thermal transport properties ( $> 100$  W/mK @ 1000°C) make the W-W<sub>2</sub>C composites a very interesting and competitive material for the DEMO divertor application. /

#### REFERENCES:

- [1] A. Šestan et al., "Tungsten carbide as a deoxidation agent for plasma-facing tungsten-based materials," J. Nucl. Mater., vol. 524, pp. 135–140, Oct. 2019.
- [2] S. Novak et al., "Beneficial effects of a WC addition in FAST-densified tungsten," Mater. Sci. Eng. A, vol. 772, no. September 2019, p. 138666, Jan. 2020.
- [3] C. Yin, D. Terentyev, T. Pardoen, R. Petrov, and Z. Tong, "Ductile to brittle transition in ITER specification tungsten assessed by combined fracture toughness and bending tests analysis," Mater. Sci. Eng. A, vol. 750, no. February, pp. 20–30, 2019.
- [4] P. Jenuš et al., "Deuterium retention in tungsten, tungsten carbide and tungsten-ditungsten carbide composites," J. Nucl. Mater., vol. 581, no. April, pp. 0–6, 2023.

POB-91

#### **Manufacturing of Potassium-doped Tungsten ITER-type monoblock PFC mock-up for the high heat flux test**

Eunnam Bang<sup>1</sup>, Hyoungh Chan Kim<sup>1</sup>, Jeongseok Kim<sup>2</sup>, Heung Nam Han<sup>2</sup>

<sup>1</sup>Korea Insititute of Fusion Energy (KFE), Korea, Republic of; <sup>2</sup>Seoul National University (SNU), Korea, Republic of.

Tungsten is an essential plasma-facing material for realizing fusion. Currently, pure tungsten is primarily used for manufacturing components for divertors, However, for the next fusion reactor beyond ITER, high-performance tungsten alloys that exceed the capabilities of pure tungsten need to be developed. In this persepective, we have fabricated potassium(K)-doped tungsten(W) and manufactured an ITER-type monoblock mockup capable of high heat flux testing.

For the manufacturing of the K-doped W monoblock mock-up, commercial W powder with 0.0033 wt% K content was used to fabricate sintered specimens. The powder underwent hydrogen reduction at 1200 °C for 2 hours to reduce its oxygen content, followed by spark plasma sintering(SPS) at 1700 °C under vacuum with varying pressures. The sintering pressure was initially set to 20 MPa, then increased to 80 MPa at 1000 °C, and maintained until the end

of the process. The relative density of the specimens was  $99.76 \pm 0.01\%$ , and the average grain size was  $3.20 \pm 1.26$ . The Vickers Hardness ranged from 470 to 480, from the center to the edge of the specimens. The K-doped W exhibited a similar dislocation density compared to heat-treated ( $1450^\circ\text{C}$ ) pure tungsten from commercial products; however, the ductile-to-brittle transition temperature (DBTT) occurred at a temperature range approximately  $100^\circ\text{C}$  lower due to enhanced plasticity by the potassium doping [1].

The W monoblock was joined to a Cu interlayer using gas pressure casting method, and then the W/Cu and CuCrZr heat sink were bonded through a hot radial pressing (HRP) process in hot isostatic pressing (HIP) equipment [2]. The K-doped W necessitated different processing conditions for machining and casting compared to commercial pure W. Additionally, different bonding temperature and pressure were required between K-doped W/Cu casting monoblock and the CuCrZr heat sink during the HRP process. While the ordinary HRP process was conducted at  $580^\circ\text{C}$  and 60 MPa, the K-doped W required higher processing conditions with  $650^\circ\text{C}$  and 70 MPa. Analysis will be necessary to determine how the material properties such as high hardness affect machinability and HIP conditions. The manufactured mock-up will be tested under high heat flux to compare its performance with that of pure tungsten [3].

[1] G.M. Min, et al., J. of Material Sci. and Tec., 223, 264–274 (2025)

[2] E.N. Bang, et al., Fusion Eng. and Des. 176, 113021 (2022)

[3] H.C. Kim, et al. Fusion Eng. and Des. 193, 113800 (2023)

POB-92

### **Growth of deuterium supersaturated surface layer with increasing ion flux and fluence in plasma-exposed tungsten**

Anže Založnik<sup>1</sup>, Witold Chromiński<sup>2</sup>, Łukasz Ciupiński<sup>2</sup>, Thomas Schwarz-Selinger<sup>3</sup>, Daisuke Nishijima<sup>1</sup>, Marlene Patino<sup>1</sup>, Michael Simmonds<sup>1</sup>, Matt Baldwin<sup>1</sup>, George Tynan<sup>1</sup>

<sup>1</sup>University of California San Diego, United States; <sup>2</sup>Faculty of Materials Science and Engineering, Warsaw University of Technology, Poland; <sup>3</sup>Max-Planck-Institut für Plasmaphysik, Germany.

Deuterium (D) supersaturated surface layer (DSSL) in tungsten (W) is a roughly 10 nm thin layer caused by low-energy D plasma exposure. Due to its extremely high D content (10 or more at. %), it can play a significant role in fusion fuel recycling and retention.

After its experimental verification [1], additional experimental and theoretical studies have been conducted in recent years to study its formation and properties. The study by Nishijima et al. [2] showed that DSSL exists at ion incident energies much lower than initially expected, down to around 45 eV. Their additional work [3] also showed evidence of DSSL thickness dependence on D ion flux and fluence.

This work seeks to expand the range of D ion fluxes and fluences to study the growth of DSSL as a function of these two parameters. W samples were exposed to D plasma in the PISCES-RF linear plasma device to various fluxes and fluences at a constant sample temperature of 400 K and ion energy of 60 eV. The D ion fluxes spanned over an order of magnitude, being  $7\text{E}20$ ,  $4\text{E}21$ , and  $3.8\text{E}22$  D/m<sup>2</sup>s. The fluence ranged from  $3\text{E}24$  to  $9\text{E}24$  D/m<sup>2</sup> in the case of the lowest D flux, and from  $7\text{E}24$  to  $3.4\text{E}25$  D/m<sup>2</sup> for the rest. After the exposure, the samples were analyzed by nuclear reaction analysis (NRA), scanning transmission electron microscopy (STEM), and thermal desorption spectroscopy (TDS).

The DSSL thickness was measured by analyzing the STEM high-angle annular dark-field (HAADF) images. A strong correlation of the DSSL thickness with D ion flux and fluence was

found. A layer thickness of  $\sim 10.5$  nm was observed in the case of the highest exposure flux and fluence ( $3.8E22$  and  $3.4E25$  D/m<sup>2</sup>), whereas the layer was only  $\sim 4$  nm thick in the case of the lowest value of the two parameters ( $7E20$  and  $3E24$  D/m<sup>2</sup>). The DSSL thickness was found to monotonically increase with both. The STEM-HAADF images of the layers appear blurred, indicating a possible alteration of crystallinity and/or an extremely high concentration of induced defects.

This work is supported by the U.S. Department of Energy Cooperative Agreement No. DE-SC0022528.

[1] L. Gao, W. Jacob, U. von Toussaint, et al., Nucl. Fusion 57, 016026 (2017)

[2] D. Nishijima, M. Tokitani, D. Nagata, et al., Nucl. Fusion 63, 126003 (2023)

[3] D. Nishijima, M. Tokitani, D. Nagata, et al., Nucl. Fusion 64, 068002 (2024)

POB-93

### **Defect production in tungsten under sub-threshold energy irradiation: Role of hydrogen and surface effects**

Hao-Xuan Huang, Yuhao Li, Hongbo Zhou, Guang-Hong Lu

Beihang University, China.

Tungsten (W) is considered as the most promising candidate for plasma-facing materials (PFMs) and will be irradiated by low-energy hydrogen isotopes (HIs, e.g., deuterium and tritium) in future fusion devices. This triggered enormous research effort on the interaction of HIs with W, especially considering the radioactivity and self-sufficiency of fusion fuel tritium. Despite the low solubility of HIs in W, their concentration can reach up to  $\sim 10$  at.% in the surface region after low-energy plasma irradiation, which is generally attributed to the irradiation-induced vacancies that accommodate additional HIs atoms. It is important to note that, however, the kinetic energy of incident HIs transferred to W is far below the energy threshold to create a Frenkel pair, and the underlying mechanism of defect production under sub-threshold energy irradiation is still unclear.

Here, we explicitly elucidated the critical role of H and surface on the defect production in W at sub-threshold energy using the molecular dynamic simulations. The average threshold displacement energy (TDE) in bulk W only slightly decreases with the increasing of H concentration, because of the inhibiting effect of H segregation on the recombination of temporary Frenkel pairs. More importantly, the H effects are significantly magnified in the surface region. On the one hand, the maximum kinetic energy transferred from 400 eV H to W can reach up to  $\sim 21$  eV due to the double-hit process, which is two times higher than that predicted by the conventional elastic collision model. On the other hand, the direction of momentum transferred to W is completely random, including both upward and downward from the surface. Accordingly, the lowest TDE ( $\sim 15$ – $21$  eV at sub-surface layers with the depth of 6.7–11.1 Å) is lower than the maximum kinetic energy transferred to W. This suggests that the low-energy H irradiation generates the Frenkel pairs directly in the surface region. Our findings explicitly clarified the kinetic process and underlying mechanism of defect production at sub-threshold energy, and provide an important reference for understanding the performance of W-PFMs under low-energy HIs irradiation.

### **Synergy of helium ion irradiation and thermal annealing in tungsten: a combined effort of experiment and simulation**

Jiaguan Peng<sup>1</sup>, Long Cheng<sup>1</sup>, Hongxian Xie<sup>2</sup>, Xiuli Zhu<sup>3</sup>, Xiancai Meng<sup>4</sup>, Yuhao Li<sup>1</sup>, Linyun Liang<sup>1</sup>, Sijie Hao<sup>1</sup>, Zheng Wang<sup>1</sup>, Yue Yuan<sup>1</sup>, Hongbo Zhou<sup>1</sup>, Guang-Hong Lu<sup>1</sup>

<sup>1</sup>Beihang University, China; <sup>2</sup>Hebei University of Technology, China; <sup>3</sup>North China Electric Power University, China; <sup>4</sup>Institute of Plasma Physics, Chinese Academy of Sciences, China.

Helium could be introduced in tungsten by various ways in tokamaks such as helium plasma exposure, helium ion irradiation, and the product of tritium decay or transmutation. The synergy of helium and temperature is of great importance when evaluating material degradation, considering the wide operation window of materials. In this work, by utilizing helium ion irradiation and thermal annealing in tungsten, the macroscopic change of recrystallization and microscopic changes of tungsten microstructure and helium bubble are investigated. And the underlying mechanism governing the microscopic changes are further evaluated using molecular dynamics and phase field modelling.

Helium ion irradiation in rolled tungsten utilized a novel ion source delivering 40 keV helium ion at a high flux of  $1 \times 10^{20} \text{ m}^{-2} \text{ s}^{-1}$ . The helium irradiation fluence ranges from  $5 \times 10^{21} \text{ m}^{-2}$  to  $1 \times 10^{23} \text{ m}^{-2}$  at a sample temperature of  $\sim 673 \text{ K}$ . By annealing helium-irradiated tungsten up to  $2000 \text{ K}$ , the synergy of helium ion irradiation and thermal annealing was studied. Retarded recrystallization due to helium was confirmed with a stronger effect with a maximum increase of recrystallization temperature was  $\sim 500 \text{ K}$ . In addition, the helium concentration dependence of the recovery (the annealing effect happening before recrystallization) was clearly measured for the first time using quasi-in-situ electron scanning microscope.

New phenomena were observed in terms of microscopic changes. Large protrusions termed “thermal ridges” were found in all 111 grains annealed at  $1673 \text{ K}$ , which is suggested to be formed by thermal-driven helium-contained grain boundary migration. Besides, hundred-nanometer-sized holes were frequently observed along grain boundaries in between 100 or 110 grains. Molecular dynamics simulation reveals the critical role of the single edge dislocation or disclination as a preferential channel for helium cluster growth in between 100 or 110 grains, rather than the dislocation junction as discontinuous connection in between 111 grains which is not favourable for helium cluster growth. Furthermore, abnormal oversized helium bubbles ( $> 200 \text{ nm}$  in diameter) in 110 grains annealed at  $1673 \text{ K}$  were observed. Phase field modelling allows the repetition of this size and suggests its formation criterion based on the helium concentration gradient in space.

To summarize, this work clearly demonstrates the synergy of helium ion irradiation and thermal annealing leading to significant changes in both macroscopic and microscopic aspects in tungsten. The results also provide implications for understanding tungsten properties changes in view of thermal/helium-driven microstructure evolution.

### **Fatigue Crack Propagation in Plasma Facing Materials – A case study on ITER grade Tungsten**

Stefan Wurster<sup>1</sup>, Michael Pegritz<sup>1</sup>, Reinhard Pippan<sup>1</sup>, Anton Hohenwarter<sup>2</sup>

<sup>1</sup>Erich Schmid Institute of Materials Science, Austrian Academy of Sciences, Austria; <sup>2</sup>Department of Materials Science, Chair of Materials Physics, Montanuniversität Leoben, Austria.

Tungsten features many interesting physical properties, so it is a very promising choice as

a plasma facing material. One of the drawbacks of tungsten and tungsten-based materials is the presence of a ductile-to-brittle transition temperature. Thus, certain regions of the tungsten-based plasma facing component are likely to be at a temperature below this transition temperature. In addition, periodic heat loads in fusion reactors lead to periodic mechanical loads, which could lead to the propagation of already existing cracks. Cold rolling has already been shown to attenuate the problem of inherent brittleness; this comes at the “cost” of anisotropic fracture and fatigue crack growth propagation properties.

In this contribution, we present recent results on quasi-static fracture and fatigue crack growth properties of pure, uniaxially rolled tungsten material of ITER grade. For accounting the anisotropic mechanical behaviour, specimens are extracted in different orientations in respect to the rolled microstructure, plate respectively, and the influence of microstructure on fracture and fatigue will be discussed. Mode I fracture and fatigue experiments are performed within a custom-built vacuum furnace at temperatures up to 500°C. Quasi-static fracture experiments aid to the interpretation of fatigue crack propagation experiments, where marked changes in the crack propagation rate takes place. Special focus will also be put on the intrinsic as well as extrinsic crack closure mechanisms depending on testing conditions, such as testing temperature or load rate.

POB-96

### **Development of Functionally Graded Copper-Tungsten Composite Coatings Through Collaboration Between IPP Prague and IPP Greifswald**

Jakub Klecka<sup>1</sup>, Joris Fellingner<sup>2</sup>, Frantisek Lukac<sup>1</sup>, Petr Kralicek<sup>1</sup>, Jonas Dudik<sup>1</sup>

<sup>1</sup>Institute of Plasma Physics of the Czech Academy of Sciences, Czech Republic; <sup>2</sup>Max Planck Institute for Plasma Physics, Germany.

Tungsten and tungsten-based materials are currently regarded as some of the most promising materials for plasma-facing components (PFCs) in fusion reactors, including tokamaks and stellarators. Their excellent thermal and mechanical properties, coupled with their resistance to plasma-induced damage, make them ideal candidates for this application. Considering these advantages, a project was initiated to develop a tungsten-based divertor for the Wendelstein 7-X stellarator, which is currently operating with a divertor constructed from carbon-fiber composites (CFC).

To address the challenges arising from tungsten’s inherently demanding machinability, thermal spraying performed in vacuum or protective atmospheres has been identified as a potential solution. This technology offers several benefits, including the ability to prepare advanced feedstock for the deposition of functionally graded composites. Such coatings represent a promising strategy to mitigate issues related to the mismatch in the coefficients of thermal expansion between tungsten coatings and underlying components, which could lead to material failure under operational conditions.

Previous research conducted at the IPP in Prague, Czech Republic, has demonstrated the potential of the RF-ICP (radio-frequency inductively coupled plasma) torch as a viable technology for preparing functionally graded deposits of a stainless steel-tungsten mixture with a pure tungsten top layer. Building on this success, the RF-ICP technology is now being considered for the development of functionally graded coatings of tungsten on copper alloys, required for the new divertor design for the Wendelstein 7-X stellarator.

This contribution will present the latest results of the ongoing collaboration between the two IPPs – Institute of Plasma Physics of the Czech Academy of Sciences in Prague and the Max

Planck Institute for Plasma Physics in Greifswald, Germany. The primary focus will be on the development of copper-tungsten-based functionally graded coatings, which are essential for ensuring the performance of the upgraded divertor. Additionally, the presentation will address other related topics and findings arising from the collaboration.

POB-97

### **Interaction of molten fluoride salts with tungsten-coated structural materials**

Luigi Bana<sup>1</sup>, Davide Vavassori<sup>1</sup>, Nayoung Kim<sup>2</sup>, Weiyue Zhou<sup>2</sup>, Michael Short<sup>2</sup>, David Dellasega<sup>1</sup>, Matteo Passoni<sup>1</sup>

<sup>1</sup>Politecnico di Milano, Italy; <sup>2</sup>Department of Nuclear Science and Engineering, Massachusetts Institute of Technology, United States.

Molten fluoride salt of lithium and beryllium (FLiBe, i.e.  $2\text{LiF}-\text{BeF}_2$ ) has been proposed as blanket material for the ARC reactor to integrate neutron moderation, heat extraction, and tritium breeding [1]. However, the highly reactive nature of molten salts poses significant challenges to the integrity of structural materials, leading to selective dissolution. Effective corrosion mitigation is therefore essential to ensure the longevity and safety of reactor components [2]. Among the multidisciplinary strategies to reach this aim, surface engineering using coatings plays a key role. While oxides are not stable in molten salts, refractory metals such as tungsten and molybdenum have shown good compatibility in metallic form thanks to their noble reduction potential [3].

Here we investigated the applicability of magnetron-sputtered tungsten (W) coatings as protective barriers against molten salt corrosion. The work explored how material degradation proceeds in the presence of a W barrier and evaluated the effectiveness of W coatings with different properties. Corrosion-susceptible substrates (AISI 316L steel) and inert substrates (pure nickel) were coated with W-based layers. We employed advanced deposition techniques, specifically radio-frequency magnetron sputtering (RFMS) and high-power impulse magnetron sputtering (HiPIMS), to tailor coating characteristics e.g., compactness, intrinsic stress, and adhesion. Afterwards, samples were exposed to molten FLiNaK (i.e. an eutectic mixture of LiF, NaF, and KF) as proxy of FLiBe at 650°C in static configuration. Cross-section polishing with ion beam milling was performed and samples were analysed with SEM/EDX to evaluate corrosion morphology.

Our findings reveal localized transgranular corrosion on W-coated steel samples, in contrast to the purely intergranular attack typical of uncoated steel. This suggests that the W coatings alter the corrosion dynamics, probably due to a combination between the presence of tungsten ions in FLiNaK generated by the dissolution of tungsten oxide and galvanic coupling with well-coated regions. Furthermore, the results emphasize the importance of controlling internal stress and adhesion of the coatings, as these characteristics determine the number and distribution of corrosion initiation points. While W demonstrates resistance to dissolution in the molten salt, this work underscores that interface engineering and strict oxygen control are mandatory for realistic application of W-based coatings in molten salt environments.

[1] B. N. Sorbom et al., *Fusion Eng. Des.* 100 (2015) 378–405

[2] R. Ropert et al., *Ann. Nucl. Energy* 169 (2022) 108924

[3] S. Guo et al., *Prog. Mater. Sci.* 97 (2018) 448–487



## Nanosecond laser ablation modelling applied to LIBS diagnostics

Stefano Cipelli<sup>1</sup>, Domenico Aceto<sup>2</sup>, Paolo Francesco Ambrico<sup>2</sup>, Irene Casiraghi<sup>3</sup>, Anna Cremona<sup>3</sup>, Olga De Pascale<sup>2</sup>, Giorgio DiLecce<sup>2</sup>, Arshad Hussain<sup>4</sup>, Laura Laguardia<sup>3</sup>, Matteo Pedroni<sup>3</sup>, Daria Ricci<sup>3</sup>, Dario Ripamonti<sup>5</sup>, Jimmy Scionti<sup>3</sup>, Andrea Uccello<sup>3</sup>

<sup>1</sup>CRF – Università degli Studi di Padova, Padova, Italy; <sup>2</sup>Institute for Plasma Science and Technology, CNR, Bari, Italy;

<sup>3</sup>Istituto per la Scienza e Tecnologia dei Plasmi, CNR, Milano, Italy; <sup>4</sup>Fusion Research Center, University of Padua, Italy;

<sup>5</sup>Institute of Condensed Matter Chemistry and Energy Technologies, CNR, Milan, Italy.

Laser Induced Breakdown Spectroscopy (LIBS) is a powerful diagnostic for the determination of the elemental composition of materials. Its inherent advantages, such as in-situ analysis capability and no need for sample pre-treatment, make LIBS a promising technique for monitoring Plasma-Facing Components after exposure to harsh plasma conditions.

Within this context, determining the depth resolution of the technique and the heat-affected zone remains a challenging issue. To address this, a finite element model was developed using COMSOL Multiphysics to simulate laser ablation of materials predicting crater geometry and ablation rate. Nanosecond pulse duration was considered, as nanosecond LIBS currently represents the most widespread technology in the field of nuclear fusion [1].

The model solves the heat conduction equation assuming gaussian laser heat source. Depending on the fluence and the sample material two different mass removal mechanisms, normal evaporation and phase explosion, were considered. Additionally, the laser intensity reduction caused by the plasma shielding effect was included.

For model validation, three materials were irradiated with nanosecond laser pulses in a low-pressure chamber: the fusion-relevant tungsten and molybdenum, and silicon, chosen for its lower boiling temperature and minimal surface roughness. Laser fluence was varied approximately from 2 J/cm<sup>2</sup> to 90 J/cm<sup>2</sup> and different numbers of consecutive pulses were applied.

Simulations showed an agreement with experimental ablated volumes within 50% for tungsten in the 2–9 J/cm<sup>2</sup> fluence interval, assuming material removal by normal evaporation. For silicon, better agreement (within 13%) was achieved in the 20–90 J/cm<sup>2</sup> fluence range, considering phase explosion and plasma shielding effects. Scanning Electron Microscopy observations confirmed the presence of phase explosion effects in silicon, while no evidences of that were observed for tungsten in the above-mentioned fluence range. An underestimation of simulated ablation rate (up to 1.7 times for silicon and 1.9 for tungsten) was obtained with respect to experiments, probably due to the non-ideal gaussian spatial distribution of pulses. Since a picosecond LIBS is set to be installed on the upgraded-GyM linear device (BiGyM) the model is currently being updated to become valid for this temporal regime. This will require implementing a Two-Temperature Model to account for separate electron and ion heating dynamics.

### Acknowledgements:

Work carried out in the frame of project NEFERTARI – CUP B53C22003070006, funded by the European Union under the National Recovery and Resilience Plan (NRRP) – NextGenerationEU.

### References:

[1] G. S. Maurya, et al., Journal of Nuclear Materials 541, 152417 (2020)

**Detailed analysis of helium and hydrogen isotopes in bubbles formed in tungsten by STEM-EELS**Mitsutaka Miyamoto<sup>1</sup>, Shinsuke Okubo<sup>1</sup>, Mitsutaka Haruta<sup>2</sup><sup>1</sup>Shimane University, Japan; <sup>2</sup>Kyoto University, Japan.

In the ITER DT phase, tungsten plasma facing material will be exposed to the burning plasma with high density helium, produced by fusion reactions, besides hydrogen isotopes. It has been reported that helium atoms in tungsten precipitates as helium bubbles and have a significant effect on hydrogen retention [1,2], although the direct evidence is still scarce. Our previous study using an aberration-corrected scanning TEM combined with electron energy-loss spectrometer (STEM-EELS) showed that hydrogen isotopes are clearly localized and trapped in helium bubbles [3]. In this study, the behaviour of hydrogen isotopes and helium in bubbles under annealing was quantitatively evaluated.

Tungsten thin film samples were pre-irradiated with helium ions at 1573 K and then post-irradiated with deuterium ions at room temperature using In-Situ TEM at Shimane University. The amount and location of helium and deuterium atoms trapped in the tungsten samples were analysed by STEM-EELS at Kyoto University under annealing from room temperature to 673 K.

STEM-EELS analysis revealed that deuterium and helium atoms were localized in the bubbles at nearly equilibrium pressure. In addition, deuterium post-irradiation after helium pre-irradiation resulted in a slight decrease in helium inside the bubbles, and most of the deuterium was trapped by the bubbles. Furthermore, annealing of these samples up to ~500 K caused dissociation of deuterium from the inside of the bubbles and an increase in the helium density in the bubbles. The helium atoms released from the bubble by deuterium post-irradiation are weakly trapped in the matrix and seems to have been re-trapped in the bubble during the annealing.

Acknowledgements: This work is supported by the International Collaborative Research Program of Institute for Chemical Research, Kyoto University (#2024-136), and JSPS KAKENHI Grant No. 22KK0038, 23K25854.

[1] M. Miyamoto, Nucl. Fusion, 49, 065035 (2009)

[2] Y. Sakoi et al., J. Nucl. Mater, 442, S715 (2013)

[3] M. Miyamoto, Nucl. Mater. Energy, 36, 101484 (2023)

POB-100

**Development of Eurofer97 steel powder for additive manufacturing of fusion components**

Xinjiang Hao, Adam Hunt

Globus Metal Powders Ltd, United Kingdom.

Eurofer97 is a high-performance ferritic-martensitic steel, developed primarily for fusion reactor components. Its unique composition delivers excellent mechanical performance while featuring reduced activation—minimising long-term radioactivity for safer, sustainable operation. At Globus Metal Powders, we have achieved ultra-low activation impurity levels—well below 0.01%—through meticulous raw material selection and optimization of atomization and powder handling processes. This poster presents our latest results, including comprehensive powder characterization and mechanical property evaluations of printed components, both in the as-built state and after heat treatment.

# AUTHORS

## INDEX

### A

A. Marques, Nuno 140  
 A. Reis, Sergio 140  
 Abram, Anže 192  
 Abrams, Tyler 136, 117, 95, 181, 158, 143, 113, 73, 71, 114,  
 Aceto, Domenico 199  
 Afanas'ev, Viktor 183  
 Afonin, Aleksandr 48  
 Aiello, Giacomo 96, 44, 69,  
 Aktaa, Jarir 61, 135,  
 Alarcon, Thierry 47  
 Alberti, Gabriele 119  
 Alegre, Daniel 162  
 Alfaazza, Mounir 89  
 Almaviva, Salvatore 37, 149, 51, 38, 103,  
 Alvarez-Diaz, Guillermo 105  
 Alves, Eduardo 122  
 Amarika, Maitane 123  
 Ambrico, Paolo Francesco 199  
 An, Seehon 48  
 Andrew, Philip 63  
 Angot, Thierry 48, 191, 89,  
 Anquetin, Yann 57  
 Antusch, Steffen 104, 44,  
 Anzallo, Viven 47  
 Arnoldbik, Wim 108  
 Asakura, Nobuyuki 120, 65,  
 ASDEX UPGRADE Team, The 182  
 Ashikawa, Naoko 66  
 Aspinall, Garreth 86  
 Assmann, Jochen 63  
 Atikukke, Sahithya 149, 37, 103, 38,  
 Aumayr, Friedrich 73, 56, 42,  
 Avotina, Liga 107  
 Ayres, Charlie 121

### B

B.Correia, José 134  
 Baffie, Thierry 169  
 Bakaev, Alexander 128  
 Balbuena, Juan-Pablo 139  
 Balden, Martin 184, 182, 53, 43, 52,  
 Baldwin, Matt 81, 177, 182, 73, 74, 194,  
 Bana, Luigi 127, 118, 198,  
 Bang, Eunnam 193  
 Banks, Joe 121  
 Baquero-Ruiz, Marcelo 144  
 Baron-Wiechec, Aleksandra 121  
 Barthe, Marie-France 139  
 Baumann, Christoph 184, 41,  
 Beaskoetxea, Gorka 123  
 Beharrell, Paul 156  
 Beidler, Matthew 92  
 Beldishevski, Misha 63  
 Bergstrom, Zachary 95, 114, 136, 96,  
 Bermudez Parra, David 164, 128,  
 Bernard, Elodie 115, 53, 122, 107, 185, 112, 52,  
 Bertoglio, Manon 57  
 Bhattacharya, Arunodaya 96  
 Bin, William 144  
 Bisson, Regis 191, 89, 109, 48, 47, 57,  
 Blatchford, Peter 63  
 Blondel, Sophie 91  
 Boccaccia, Lorenzo 177  
 Boeswirth, Bernd 54, 163, 153, 85,  
 Bogdanovič, Leon 148, 98,  
 Bogdanović Radović, Iva 52, 107,

Boleininger, Max 44  
 Borodin, Dmitriy 122  
 Bousek, Michal 161  
 Bouwmeester, Luc 118  
 Brank, Matic 148, 98,  
 Bräuer, Torsten 49  
 Brezinsek, Sebastijan 38, 41, 51, 77, 149, 121, 63, 39, 103, 142, 147, 37, 58, 40, 111, 122, 180, 170,  
 Brooks, Helen 100  
 Brown, Thomas 158  
 Brucker, Maximilian 110  
 Buchner, Benedikt 64, 84,  
 Bufferand, Hugo 185  
 Bugatti, Marco 127  
 Bushell, Joe 86  
 Bussiahn, René 180  
 Butikova, Jelena 103, 149, 38, 37,  
 Buttenschön, Birger 180  
 Bykov, Igor 92

### C

Cabie, Martiane 107, 160,  
 Cacciotti, Emanuele 155, 97,  
 Cacheris, Alec 113  
 Campos, Andrea 89  
 Cani, Francesco 176  
 Cao, Chengzhi 79  
 Cao, Lei 151  
 Cappelli, Luca 114, 185,  
 Caprin, Eric 47  
 Caprini, Davide 85  
 Carasik, Lane 100  
 Cardella, Antonino 88  
 Cartry, Gilles 89  
 Casali, Livia 148  
 Casiraghi, Irene 143, 144, 125, 199, 176,  
 Castaño Bardawil, David 63

Catarino, Norberto 122  
 Caturla, Maria Jose 139  
 Cerocchi, Marco 155, 85,  
 Chang, Yong Bok 153  
 Chang, Feng-Jen 138  
 Chappuis, Philippe 166  
 Charles, Yann 101  
 Chen, Jie 188  
 Chen, Junling 161  
 Chen, Lei 155, 69,  
 Chen, Zhe 67  
 Chen, Jihui 183  
 Cheng, Long 67, 196,  
 Cho, Hwnag Rae 153  
 Chroeu, Sokay 101  
 Chromiński, Witold 130, 194,  
 Cipciar, Dario 49, 180,  
 Cipelli, Stefano 144, 199,  
 Ciraolo, Guido 57, 185, 116,  
 Ciupiński, Łukasz 194  
 Clancy, Matthews 121  
 Clark, Daniel 96  
 Clement, Antoine 192  
 Coad, Paul 121  
 Coburn, Jonathan 71, 95, 138,  
 73,  
 Coenen, Jan 44, 189, 68, 162,  
 61, 189, 72,  
 Coffey, Ivor 63  
 Corre, Yann 116, 168, 52, 57, 63,  
 109, 47,  
 Costea, Stefan 98, 148,  
 Couëdel, Lenaic 113  
 Crea, Francesco 85, 97,  
 Cremona, Anna 119, 176, 199,  
 Crespillo, Miguel L. 45  
 Cruz, Antonio 138  
 Cui, Xiaoqian 183  
 Cunha, Maria 108, 71, 126,  
 Cupertino Malheiros, Livia 105  
 Cusentino, Mary Alice 73, 71,

## Č

Čížek, Ondřej 136

## D

Daminelli, Giambattista 100  
 Davis, Thomas 96

Davis, James 172  
 De Angeli, Marco 100  
 De Castro, Alfonso 162  
 De Combarieu, Matthieu 47  
 De Luca, Riccardo 85, 97, 155,  
 153,  
 De Pascale, Olga 199  
 De Sano, Gabriele 153  
 Dechelette, Franck 155  
 Dejarnac, Renaud 163, 166,  
 Delaporthé-Mathurin, Remi  
 36  
 Deleau, Amelia 179, 167,  
 Delic, Fahrudin 132  
 Dellasega, David 125, 118, 198,  
 182, 127,  
 Delmas, Etienne 179  
 Demiane, Joey 174  
 Denis, Julien 103, 47, 57, 109,  
 Desgranges, Corinne 109  
 Devynck, Pascal 146  
 Dhamale, Gayatri 182  
 Dhard, Chandra Prakash 49,  
 180,  
 Dhard, Devansh 88  
 Di Bartolomeo, Mariano 155  
 Dias, Marta 134  
 Dias Aleixo, Diogo 169  
 Dickes, Daniel 54  
 Diez, Mathilde 160, 47, 53, 168,  
 116, 115, 107, 179, 52, 122, 185,  
 DiLecce, Giorgio 199  
 Ding, Rui 55, 161, 124, 70,  
 Ding, Hongbin 77  
 Ding, Fang 117, 124,  
 Dittmar, Timo 173, 149, 77, 37,  
 63, 39, 122, 38,  
 Dittrich, Laura 175  
 Djurabekova, Flyura 45  
 Dmitriev, Artem 123  
 Donik, Črtomir 129  
 Donovan, David Christian 113,  
 146, 165,  
 Dorow-Gerspach, Daniel 97,  
 88, 163,  
 Dose, Giacomo 156, 158,

Draksel, Martin 88  
 Du, Juan 72, 189,  
 Duchková, Ester 136  
 Dudarev, Sergei 44  
 Dudik, Jonas 197  
 Dunnell, Kaelyn 57, 36,  
 Dürbeck, Thomas 64  
 Durif, Alan 52, 160, 186,  
 Durovec, Mikulas 166

## d

de Gianni, Ludovica 185  
 de Prado, Javier 130, 97,  
 de Temmerman, Gregory 160

## E

Easley, Davis 113  
 Effenberg, Florian 95, 71, 143,  
 Ehrke, Gunnar 88  
 Ekedahl, Annika 109  
 Eldon, David 148  
 Ellis, Rob 63  
 Eltawila, Mahmoud 100  
 Emdee, Eric 158  
 Ennis, David 180, 181,  
 Entler, Slavomir 161  
 Escourbiac, Frederic 155  
 EUROFUSION TOKAMAK EX-  
 PLOITATION Team, The 63, 182,  
 Evans, Shane 73

## F

Fakhrayi Mofrad, Nima 192  
 Fan, Cuncai 133  
 Favre, Eric 157  
 Fedorczak, Nicolas 116, 146,  
 109, 185,  
 Feichtmayer, Alexander 44  
 Fellinger, Joris 88, 197, 180,  
 Fellinger, Martina 73, 56, 42,  
 Feng, Yühe 159, 157,  
 Feng, Siqing 86  
 Feng, Fan 67, 72,  
 Fernández-Mayo, Pablo 162  
 Ferrero, Gabriele 102  
 Ferro, Yves 103  
 Fevre, Louis 146  
 Figueiredo, João 63

- Firdaouss, Mehdi 54, 168, 169, 179,  
 Flament, Anthony 186  
 Flebbe, Meike 63  
 Flom, Erik 180  
 Fornal, Tomasz 180  
 Fortuna-Zalesna, Elzbieta 121, 100, 52,  
 Fortune, Martin 63  
 Franklin, Trevor 100  
 Frayssines, Pierre-Eric 169  
 Freeman, Davis 91  
 Freitas, Marta 140  
 Friese, Sebastian 63  
 Fu, Wenxue 161  
 Fu, Zhang 98  
 Furno, Ivo 144  
 Furno Palumbo, Maurizio 153
- G**  
 Gaganidze, Ermile 44  
 Gago, Mauricio 166, 104,  
 Galatanu, Andrei 134, 192,  
 Galatanu, Magdalena 192  
 Galende-Pérez, Roberto 82  
 Gall, Grayson 100  
 Gallais, Laurent 186, 160,  
 Gallo, Alberto 57, 47, 109,  
 Gao, Yu 180  
 Gao, Liang 39  
 Gao, Binfu 161  
 García López, Gaston 45  
 Garcia Rosales, Carmen 44, 162,  
 Garcia-Cortés, Isabel 180  
 Gardarein, Jean-Laurent 160  
 Garkusha, Igor 93  
 Garofalo, Andrea 143  
 Garoz, David 164  
 Gąsior, Paweł 38, 103, 90,  
 Gasior, Paweł 149, 37,  
 Gaspar, Jonathan 109, 160, 52, 47,  
 Gaspari, Federico 125  
 Gaspérini, Monique 101  
 Gaston, Derek 100  
 Gautam, Daniel 42, 77, 73,  
 Gerardin, Jonathan 146, 168, 116,  
 Gervasini, Gabriele 109, 63, 47,  
 Geulin, Eleonore 57, 109, 47,  
 Ghidersa, Bradute-Eugen 153  
 Giegerich, Thomas 173  
 Gilbert, Mark 83, 96, 105, 188,  
 Gilson, Erik 78  
 Giorgetti, Francesco 85  
 Giudicelli, Guillaume 100  
 Gleyzes, Hervé 169  
 Goldston, Robert 158  
 Gonda, Tomas 180  
 Gonzalez, Sehila 96  
 Gorelick, Gabriel 74  
 Gorley, Michael 96  
 Goto, Motoshi 78  
 Gradic, Dorothea 180  
 Graening, Tim 59  
 Grammes, Thilo 61  
 Granberg, Fredric 178, 139, 139,  
 Grant, Patrick 61  
 Gray, Travis 59  
 Greuner, Henri 163, 153, 85, 54, 155,  
 Grierson, Brian 156  
 Grigore, Eduard 170, 115, 185,  
 Grisolia, Christian 112  
 Gromelski, Wojciech 38, 149, 116, 37,  
 Grosjean, Alex Thomas 47, 109, 146, 116,  
 Groth, Mathias 147  
 Guillemaut, Christophe 116, 146, 160,  
 Guillermin, Benoit 160, 146,  
 Guittienne, Philippe 144  
 Gunn, Jamie 146, 160, 116,  
 Guterl, Jerome 114  
 Gyergyek, Tomáš 98
- H**  
 Haid, Samuel 91  
 Hájiček, Michal 136  
 Hakola, Antti 115, 122, 182, 122, 47, 149, 109, 184, 53, 63, 38, 185, 52, 37, 107,  
 Halloran, Matthew 68  
 Hamaguchi, Dai 65  
 Hamelin, Cory 96  
 Han, Heung Nam 193  
 Hanada, Kazuaki 120  
 Hao, Xinjiang 201  
 Hao, Sijie 196  
 Harbour, Logan 100  
 Hargreaves, James 94  
 Hargrove, Chase 71  
 Haruta, Mitsutaka 200  
 Harutyunyan, Zori 187  
 Hasegawa, Akira 106  
 Hassanein, Ahmed 117, 68,  
 Hatano, Yuji 65, 106,  
 Havlík, Petr 136  
 Hayakawa, Ayumu 106  
 Hayashi, Takumi 65, 66,  
 Haydon, Imogen 105  
 He, Sicong 74  
 He, Chunyu 161  
 Heikkinen, Samuli 88, 140,  
 Heinola, Kalle 121  
 Heller, Rene 45  
 Herashchenko, Stanislav 93  
 Herfindal, Jeffrey 113, 92,  
 Hernandez, Caroline 179, 167,  
 Hess, Laurin 171  
 Hinoki, Tatsuya 95  
 Hirai, Takeshi 155  
 Hirt, Paul 123  
 Hobrik, Joerg 48  
 Hodille, Etienne 102, 47, 109, 57, 103, 112, 36,  
 Hofer, Christina 83  
 Hohenwarter, Anton 196  
 Hohmann, Tim-Oliver 48  
 Hollmann, Eric 92  
 Hong, Suk-Ho 165, 143,  
 Hood, Ryan 165, 95,  
 Hook, Matt 121  
 Horacek, Jan 161  
 Horachek, Anna 161  
 Hoshino, Yuzuka 106, 190,  
 Hoshino, Kazuo 120

- Houben, Anne 40, 173, 104, 88, 77,  
 Hruby, Jan 161  
 Hruska, Matej 161  
 Hu, Zhiwei 139  
 Hu, Yi 79  
 Hu, Jiansheng 159, 157,  
 Huang, Xiangmei 79  
 Huang, Hao-Xuan 195  
 Huart, Alexis 116  
 Huber, Alexander 63  
 Hunger, Katja 88, 54, 85, 155,  
 Hunt, Adam 201  
 Hunt, Ryan 155  
 Hussain, Arshad 199
- I**  
 lafrati, Matteo 153, 127,  
 lalovega, Mykola 71  
 Icenhour, Casey 100  
 Igitkhanov, Yuri 173  
 Innocente, Paolo 153  
 Inoue, Kazutoshi 83  
 Ipatova, Iuliia 83  
 Iroc, Koray 44  
 Isobe, Kanetsugu 65, 66,  
 Ivashov, Ilia 63  
 Iveković, Aljaž 129, 192, 130, 131,  
 Izaguirre, Ignacio 97, 130,
- J**  
 Jacob, Wolfgang 64  
 Jaehwan, Kim 65  
 Janata, Marek 161  
 Jantunen, Ville 139  
 Järvinen, Aaro 184  
 Jayasundara, Dinusha 110  
 Jenuš, Petra 44, 192, 131, 130,  
 129,  
 Jepu, Ionuț 38, 121, 149, 103, 51,  
 63,  
 Jepu, Ionuț 37  
 JET CONTRIBUTORS Team,  
 The 63  
 Jiang, Xi 63  
 Jílek, Richard 150  
 Jiming, Chen 98, 72,  
 Jin, Xin 45
- Jin, Fanya 72  
 Joffrin, Emmanuel 63  
 Jögi, Indrek 52, 115, 37, 38, 185,  
 149, 103,  
 Johnson, Jack 68  
 Johnson, Curtis A. 146  
 Jones, Nick 37  
 Junghanns, Patrick 155
- K**  
 Kadi, Lyes 144  
 Karhunen, Juuso 149, 37, 184,  
 38, 103,  
 Karimov, Renat 144  
 Karl, Katie 73  
 Karnowska-Peterski, Ilona 121  
 Kasada, Ryuta 106  
 Kasai, Kazuaki 66  
 Kato, Daiji 81  
 Kawan, Christoph 39, 170, 38,  
 37,  
 Kawate, Tomoko 78  
 Kelemen, Mitja 182, 82, 45,  
 Kermouche, Guillaume 186  
 Kesteren, Jort 126, 118, 108,  
 Khan, Aneeqa 126  
 Khodak, Andrei 158  
 Khumthong, Kenneth 156  
 Khvan, Tymofii 130  
 Killer, Carsten 49, 180,  
 Kim, Hyoung Chan 193  
 Kim, Do Yoon 153  
 Kim, Jeongseok 193  
 Kim, Hong-Tack 153  
 Kim, Nayoung 198  
 Kim, Hyeji 59  
 Kinna, David 63  
 Kirka, Michael 59  
 Kirschner, Andreas 41, 58,  
 Klecka, Jakub 197  
 Klein, Alexander 104  
 Klepper, Christopher C. 146  
 Klimenkov, Michael 44  
 Knieps, Alexander 180  
 Knyzhnykova, Diana 131  
 Kolasinski, Robert 190, 138, 106,  
 Končar, Boštjan 88
- Kornejew, Petra 180  
 Kos, Leon 148, 98,  
 Kos, Domagoj 63  
 Kosłowski, Hans Rudolf 173  
 Kosslow, Sean Robert 146  
 Kovačič, Jernej 98  
 Kovacic, Jernej 148  
 Kporha, Faith 178  
 Kralicek, Petr 197  
 Krasikov, Yury 63  
 Krat, Stepan 36  
 Kreter, Arkadi 40, 61, 67, 142,  
 170, 104, 173,  
 Krieger, Karl 122, 63, 182, 184, 43,  
 48, 109, 47,  
 Kriete, David 180, 181,  
 Krimmer, Andreas 63  
 Krychowiak, Maciej 180  
 Kuang, Adam 163  
 Kubásek, Tomáš 150  
 Kumpulainen, Henri 147, 184, 41,  
 Kun, Wang 98  
 Kunkel, Falk 88  
 Kurano, Kazuhiro 83  
 Kurpaska, Łukasz 130  
 Kutilek, Zdenek 161  
 Kwag, Sang Woo 153  
 Kwon, Sungjin 153
- L**  
 Laguardia, Laura 199, 176, 47,  
 63, 153, 109,  
 Lambertz, Horst Toni 63  
 Lang, Eric 73  
 Langenberg, Andreas 180  
 Lasnier, Charles 92  
 Lau, Alexander 189  
 Lavrentiev, Mikhail 137, 110,  
 Lechevalier, Pierre 169  
 Lecis, Nora 118  
 Ledford, Christopher 59  
 Lee, Hyung Ho 153  
 Lee, Jong Man 153  
 Lemetais, Maxime 186  
 Li, Jiangang 70  
 Li, Baizeng 159  
 Li, Yuhao 196, 195,

- Li, Cong 77  
 Li, Hang 145  
 Li, Rongri 105  
 Li, Yu 99  
 Lian, Hui 183  
 Lian, Youyun 67  
 Liang, Linyun 196  
 Lied, Philipp 96  
 Lietz, Amanda 100  
 Likonen, Jari 149, 37, 185, 103, 122, 107, 121, 65, 38, 184, 63, 51, 115,  
 Lin, Qianqian 151  
 Lindblad, Victor 139  
 Linsmeier, Christian 39, 72, 189, 173, 189, 163, 142, 104,  
 Liotti, Enzo 61  
 Lisgo, Steven 160  
 Litnovsky, Andrey 188  
 Liu, Hao-Dong 36  
 Liu, Xiang 72  
 Liu, Peng 86, 154,  
 Liu, Haiqing 183  
 Liu, Zhaodong 72  
 Liu, Yueqiang 92  
 Liu, Mi 67  
 Loarer, Thierry 47, 109, 57,  
 Loarte, Alberto 36  
 Lobanova, Lidia 183  
 Loch, Stuart 181  
 Lombardo, Bruce 156  
 Lopez Perez, Camila 174  
 Lopopolo, Nicolò 79  
 Lorusso, Pierdomenico 85, 155,  
 Losada, Ulises 114, 181,  
 Lu, Guang-Hong 195, 196, 67,  
 Lu, Eryang 45  
 Lukac, Frantisek 197  
 Lunsford, Robert 78  
 Luo, Guangnan 99  
 Lürbke, Robert 131  
 Lvovskiy, Andrey 92
- M**  
 Maddaluno, Giorgio 100  
 Mäenpää, Roni 147  
 Maffini, Alessandro 125, 143,  
 Maier, Hans 163  
 Maingi, Rajesh 158  
 Makhelai, Vadym 93  
 Malec, David 167  
 Manas, Pierre 109, 47, 185,  
 Manchon, Jesus G. 162  
 Manhard, Armin 132, 46,  
 Mao, Yiran 162, 189, 72, 189,  
 Marchuk, Oleksandr 40, 180,  
 Marco, Aitor 123  
 Marian, Jaime 74  
 Marini, Claudio 92  
 Markelj, Sabina 182, 80, 192, 45, 174, 82,  
 Marot, Laurent 123, 79,  
 Martin, Celine 52, 107, 89, 160,  
 Martinez-Loran, Erick 92  
 Martinez-Paneda, Emilio 105  
 Martins, Ricardo 134  
 Marzullo, Domanico 85  
 Mascarenhas, Sean 59  
 Mason, Daniel 44, 139,  
 Masuzaki, Suguru 106, 65, 66, 78,  
 Matějček, Jiří 136  
 Mateus, Rodrigo 122  
 Mathayan, Vairavel 118  
 Mattes, Ray 148  
 Matthieu, Latournerie 191  
 Matveev, Dmitry 36  
 Maviglia, Francesca 94  
 Mayer, Matej 79, 64, 53, 49,  
 McCarthy, Megan 73  
 McCarthy, Kieran Joseph 180  
 McCue, Ian 59  
 McLean, Adam 143, 181,  
 Medina-Roque, Daniel 180  
 Meigs, Andrew 147  
 Menard, Jonathan 158  
 Mendes Reis, Monica 140  
 Meng, Xiancai 196  
 Mertens, Philippe 63  
 Meyer, Ernst 123, 79,  
 Mijatovic, Panto 156  
 Milliot, Marc 91  
 Mingozzi, Simone 157  
 Minissale, Marco 89, 160, 191, 186, 48,  
 Miranda, Francisco 128  
 Miserque, Frédéric 112  
 Mishra, Ashwini Kumar 135, 61,  
 Mitteau, Raphael 168  
 Mittelmann, Steffen 84, 64,  
 Miura, Kenshiro 106  
 Miyamoto, Mitsutaka 65, 200, 177,  
 Mizobuchi, Kazuma 66  
 Möller, Sören 104, 170,  
 Mombelli, Fabio 143, 119,  
 Monteiro, Bernardo 134  
 Monton, Carlos 95, 136,  
 Montupet-Leblond, Floriane 112  
 Moon, Sunwoo 175  
 Moreau, Philippe 109, 47,  
 Morgan, Thomas 79, 108, 157, 94, 118, 93, 126,  
 Morisaki, Tomohiro 78  
 Moser, Lucas 58  
 Motojima, Gen 78  
 Mougénot, Jonathan 89, 101, 36,  
 Mulewska, Katarzyna 130  
 Mummery, Paul 126  
 Murphy, Christopher 143  
 Murtazin, Mark 136  
 Muru, Marta Malin 115  
 Mutzke, Andreas 182, 43,  
 Myra, James 182  
 Młynczak, Krzysztof 63
- N**  
 Nagy, Alexander 78  
 Nakamura, Hirofumi 66, 65,  
 Nallo, Giuseppe Francesco 143  
 Naujoks, Dirk 180, 49,  
 Neisius, Thomas 107  
 Nelson, Nathan 113  
 Nespoli, Federico 78  
 Neu, Rudolf 85, 95, 153, 88, 163, 54, 131,  
 Nguyen-Manh, Duc 188  
 Nicholson, Eric 172



Nicolai, Dirk 142  
 Nishida, Rion 66  
 Nishijima, Daisuke 81, 194, 177,  
 Nogami, Shuhei 44, 60,  
 Noguchi, Yuki 81  
 Norausky, Nikolai 156  
 Nordlund, Kai 45  
 Novak, Saša 131  
 Novak, April 100  
 Novak, Nejc 131  
 Nozawa, Takashi 65  
 Nuckols, Lauren 71

## O

Obata, Yui 66, 65,  
 Odstrcil, Tomas 148  
 Ohno, Noriyasu 120  
 Oishi, Tetsutaro 78  
 Okubo, Shinsuke 200  
 Okumura, Shingo 106  
 OLMAT Team, The 162  
 Olynik, Nicholas 59  
 Oono, Senzai 66  
 Orecchia, Davide 125  
 Orr, Tez 110  
 Otsuka, Teppei 106, 65,  
 Owada, Atushi 66  
 Oya, Yasuhisa 190, 106, 65,  
 Oya, Makoto 120  
 Oyaizu, Makoto 106  
 Oyarzabal, Eider 162

## P

P.Gonçalves, António 134  
 Pablant, Novimir 78, 180,  
 Pacheco Cansino, Jose  
 Miguel 140, 88,  
 Pajuste, Elina 107  
 Pandey, Arun 180  
 Paoletti, Damiano 153  
 Pappalardo, Federica 89, 186,  
 Pardoén, Thomas 128  
 Paris, Peeter 103, 37, 115, 38,  
 185, 149,  
 Park, Soo-Hyeon 153  
 Parkelj, Nejc 80  
 Paschalidis, Konstantinos 170

Passoni, Matteo 182, 119, 125,  
 118, 198, 127, 143,  
 Patino, Marlene 81, 194, 182,  
 Paulin, Irena 131, 129,  
 Pawelec, Ewa 122, 147,  
 Payet, Mickaël 112  
 Pedroni, Matteo 199, 125, 119,  
 Pégourié, Bernard 57  
 Pegritz, Michael 196  
 Pelicon, Primož 82, 182,  
 Pellissier, Francis-Pierre 47  
 Peng, Xuebin 70  
 Peng, Xuebing 86  
 Peng, Jiaguan 196  
 Peterka, Matěj 136, 161,  
 Petersson, Per 175  
 Petráš, Roman 136  
 Petrov, Yurii 93  
 Petty, Craig 143  
 Peyron, Gavriel 87, 88,  
 Piccinelli, Davide 57  
 Pickles, Jim 96  
 Pinghuai, Wang 98  
 Pintsuk, Gerald 163, 192, 44, 96,  
 166, 69,  
 Pippan, Reinhard 196  
 Pitthan, Eduardo 77, 133, 175,  
 42, 73, 56,  
 Pitts, Richard 58, 170, 36, 92,  
 Plechacek, Tomas 161  
 Polli, Gian Mario 85, 153,  
 Popović, Žana 114, 71, 95, 136,  
 Porosnicu, Corneliu 103  
 Prestat, Eric 188, 105,  
 Preuss, Roland 43  
 Prevratil, Jan 161  
 Price, Samuel 59  
 Primetzhofer, Daniel 77, 42, 73,  
 133, 175, 56,  
 Puente, Ricardo 157  
 Puglia, Paulo 47  
 Puig, Jordi 123  
 Punzón-Quijorna, Esther 82,  
 45,  
 Putra, Brian 146

## Q

Qian, Li 98  
 Qin, Ying 67  
 Qin, Yan 157  
 Quadri, Virginia 185

## R

Radež, Miha 98, 148,  
 Rapp, Juergen 182  
 Rasinski, Marcin 118, 173, 61, 170,  
 40, 77,  
 Ratynskaia, Svetlana 170, 100,  
 177, 91, 92, 168,  
 Ray, Tyler 68  
 Rayaprolu, Rahul 37, 38, 51, 142,  
 149, 63,  
 Reali, Luca 44  
 Redl, Andreas 48  
 Reinhart, Michael 142  
 Reiter, Detlev 147  
 Reji, Maria 161  
 Ren, Jun 92, 95, 165,  
 Reux, Cédric 168, 51,  
 Riccardi, Bruno 153  
 Ricci, Daria 176, 144, 199, 125,  
 Richou, Marianne 179, 88, 85,  
 186, 52, 54, 169, 87, 160,  
 Riesch, Johann 189, 54, 163, 95,  
 189, 85, 155,  
 Rieth, Michael 44, 104,  
 Ripamonti, Dario 100, 199,  
 Rispoli, Natale 125  
 Ristkok, Jasper 37, 38, 149, 103,  
 Rivals, Nicolas 185, 116, 146, 47,  
 Rizzi, Tommaso 168  
 Robben, Cas 118, 108,  
 Roccella, Selanna 85, 153, 155,  
 Roche, Hélène 85, 87,  
 Rode, Sebastian 58  
 Rohde, Volker 48  
 Rojas, Julio 59  
 Romazanov, Juri 147, 116, 41,  
 119, 58, 184,  
 Romsy, Tomas 161  
 Ronchi, Gilson 181  
 Rowley, Chris 63  
 Rubel, Marek 66, 42, 65, 121, 77,  
 175,

Rudakov, Dmitry 71, 181, 92, 95,  
Russo, Valeria 125

## **S**

Saari, Samuli 184  
Sackers, Marc 37, 40, 149, 142, 38,  
Sajovic, Miha 80  
Sakamoto, Yoshiteru 120  
Sal, Elisa 162  
Salomon, Eric 48, 191,  
Sammons, Celyn 110  
Sánchez, Maria 97, 130,  
Sanchez, Laura 123  
Sand, Andrea 192  
Santana, Ruben 95, 136,  
Sardo, Margherita 140  
Satriano, Annunziata 85  
Scarisoreanu, Nicu 126  
Schmid, Klaus 41, 36, 43,  
Scholten, John 94  
Schrader, Michael 63  
Schultz, Karl 143  
Schwarz-Selinger, Thomas 64, 80, 45, 194, 174, 171, 110, 74, 182, 39, 46,  
Schwendeman, Brandon 81, 74,  
Scionti, Jimmy 199, 125, 144,  
Sedlacek, Lukas 161  
Sedmidubsky, Vaclav 161  
Sergienko, Gennady 142, 77, 38, 170, 149, 104, 37, 63,  
Sestak, David 166  
Sgrelli, Diana 47  
Shafer, Morgan 165, 143,  
Shams-Latifi, Jila 56  
Shaw, Anthony 147  
Shen, Zeqing 46  
Sherlock, Paul 86  
Shetty, Sanath 90, 103,  
Shevchuk, Pavel 93  
Shibahara, Ryo 83  
Shick, Sophie 162  
Shimada, Masashi 106, 100,  
Shin, Soochaeol 153  
Shiraki, Daisuke 92, 113,

Shoji, Mamoru 78  
Short, Michael 198  
Shu, Rui 189  
Siddiki, Mohammad Faisal 180  
Siketić, Zdravko 107  
Silburn, Scott 122, 63,  
Silva-Solis, Yovany 103  
Simic, Gregor 148  
Simmonds, Michael 74, 81, 194,  
Simon, Pierre-Clément 100  
Sinclair, Gregory 158, 117, 143,  
Sizyuk, Tatyana 117  
Skarlatos, Anastasios 167  
Sobieraj, Damian 188  
Sokulski, Damian 103, 90,  
Sondars, Matiss 107  
Song, Nak Hyong 153  
Soni, Shweta 37, 103, 149, 38,  
Sousa, Tomás 79, 123,  
Sowder, Andrew 96  
Sprouster, David 59  
Staley-Wiggins, Holly 86  
Steinwehr, Ralf 49  
Stollberg, Christine 144  
Stróżyk, Michał 130  
Subba, Fabio 143, 125,  
Sugimoto, Yutaka 66, 65,  
Suman, Guddi 73  
Sun, Yiwon 67  
Sun, Fei 106  
Sureshkumar, Srikanth 185  
Syrocki, Lukasz 180

## **Š**

Šestan Zavašnik, Andreja 45, 192, 174, 80,  
Škapin, Srečo 80

## **T**

Tafalla, David 162  
Tamain, Patrick 185, 57,  
Tamura, Naoki 180  
Tanaka, Hikaru 172  
Tang, Jun 72  
Tang, Shaokai 126  
Tanigawa, Hiroyasu 65  
Tao, Qiang 72  
Tassone, Alessandro 157

Taylor, Chase 106  
Team, HL-3 79  
Teimane, Anete Stine 107  
Tejado, Elena 88, 134, 192,  
Tekavčič, Matej 88  
Terentyev, Dmitry 44, 164, 83, 128,  
Terra, Alexis 58, 63,  
Testoni, Raffaella 102  
Theodorou, Andreas 64  
Theriault, Steven 172  
Thiede, Sebastian 180  
Thomas, Alizée 169  
Tillack, Mark 156  
Timmer, Remco 108  
Tokitani, Masayuki 65, 78,  
Tolias, Panagiotis 168, 100, 177, 170, 92,  
Tomarchio, Valerio 54, 169,  
Tonello, Elena 144  
Torikai, Yuji 65, 66,  
Toupal, Lukáš 150  
Toussaint, Udo von 43, 49,  
Towell, Sophie 137  
Tran, Tuan 42  
Treadwell, Rico 73  
Trelewicz, Jason 59, 163,  
Tretter, Jörg 88  
Tripathi, Jitendra 68  
Tsitrone, Emmanuelle 122, 63, 185, 47, 109, 52, 122, 115, 107,  
Tsui, Cedric 95, 165,  
Tuccari, Carlo 119  
Tyburska-Pueschel, Beata 126, 108, 118,  
Tynan, George 177, 182, 81, 74, 194,

## **U**

Učakar, Aleksander 192  
Uccello, Andrea 199, 119, 176, 143, 144, 125,  
UKAEA RACE Team, The 38, 37, 149,  
Unterberg, Bernhard 104, 173, 142, 166,  
Unterberg, Ezekial A. 146

Ureña, Alejandro 130

## **V**

Vála, Ladislav 136, 150,  
Valadares, Vasco 134  
Valdez-Nava, Zarel 167  
Vano, Lilla 49  
Varadarajan, Naren 185  
Vartarian, Stefane 109, 47, 57,  
Vassallo, Espedito 182  
Vavassori, Davide 127, 198,  
Vavpetič, Primož 82  
Veis, Pavel 149, 38, 103, 37, 90,  
Veis, Matej 90, 103,  
Verbeken, Kim 128  
Verdini, Luigi 85, 155,  
Vernimmen, Jordy 94  
Vesely, Zdenek 161  
Viebke, Holger 49  
Vignal, Nicolas 85  
Vignitchouk, Ladislav 91, 177,  
Villa, Alessio 143, 125,  
Volkova, Yuliia 93  
Von Mueller, Alexander 131, 155,  
Vondracek, Petr 166  
Vrel, Dominique 112  
Vuoriheimo, Tomi 107, 185,

## **v**

van Breemen, Lambert 118  
van Tol, Dane 181  
von Toussaint, Udo 64, 132, 84,

## **W**

W7-X Team, The 180  
Walach, Ulrich 123  
Wampler, William 181  
Wang, Youpeng 123  
Wang, Huiqian 165  
Wang, Dezhen 145, 159,  
Wang, Shouxin 183  
Wang, Hao 67  
Wang, Hanqing 67  
Wang, Ting 67

Wang, Yujian 145  
Wang, Zheng 196  
Wang, Zhongwei 88  
Warkentin, Eduard 173, 40,  
Wauters, Tom 36, 58, 57, 47,  
109,  
Wegner, Thomas 180  
Weisberg, David 156  
Welsh, Austin 148  
Wen, Pan 72  
Widdowson, Anna 47, 65, 121,  
63, 66, 107, 38, 175, 109, 149, 51,  
37, 122,  
Widlund, Ola 88  
Wiesen, Sven 58  
Wilcox, Robert 113, 165,  
Wilkinson, Ute 189  
Wilkinson, Daniel 189  
Wilkison, Daniel 61  
Wilks, Theresa 143  
Wirth, Brian 91  
Wirtz, Marius 69, 192, 166, 163,  
68, 162, 97, 88, 104,  
Wolf, Philipp M. 133, 56,  
Woller, Kevin 174  
Wrobel, Jan 188  
Wu, Jintong 139, 139,  
Wu, Huace 77  
Wurster, Stefan 196  
Wüst, Erik 38, 39, 37, 170, 149,

## **X**

Xiao, Chijin 113  
Xie, Tian 159, 157, 145,  
Xie, Hongxian 196  
Xie, Yanfeng 79  
Xu, Tiejun 70

## **Y**

Y.Pastor, José 134, 192,  
Yajima, Miyuki 66, 65, 78,  
Yan, Rong 183  
Yan, Binyou 67  
Yang, Lin 100

Yang, Xianke 152  
Yanyu, Chen 98  
Yao, Damao 151, 151, 152,  
Yelisyyev, Dmytro 93  
Yi, Rongxing 37, 103, 38, 77, 51,  
149, 63, 104,  
Yin, Hao 67  
Yin, Lei 152  
Yin, Chao 44  
You, Jeong-Ha 88, 155, 94,  
Yu, Hao 106  
Yuan, Yue 67, 196,

## **Z**

Zacha, Pavel 161  
Založnik, Anže 194, 81,  
Zamperini, Shawn 71  
Zaplotnik, Rok 182  
Zavašnik, Janez 80, 174, 45,  
Zayachuk, Yevhen 51  
Zhang, Ling 183  
Zhang, Siyu 135  
Zhang, Qing 117  
Zhang, Wei 159, 157, 145,  
Zhao, Tianyu 72  
Zhengxing, Wei 98  
Zhou, Jun 79  
Zhou, Hongbo 196, 195,  
Zhou, Haishan 99, 124,  
Zhou, Weiyue 198  
Zhu, Xiuli 196  
Zhu, Yi-Wen 99  
Zhu, Dahuan 161  
Zibrov, Mikhail 46  
Zielinski, Witold 100  
Zinovev, Aleksandr 128, 44,  
Zlobinski, Mirosław 63, 51,  
Zoethout, Erwin 118  
Zuo, Guizhong 159, 157,  
Žýka, Jiří 136

## **Ž**

Žužek, Borut 131